STUDIES ON

THE ORBITAL THEORIES FOR OPEN-SHELL SYSTEMS

AND

THE MOLECULAR ELECTRONIC STRUCTURE

HIROSHI NAKATSUJI

KYOTO UNIVERSITY

1970

STUDIES ON

THE ORBITAL THEORIES FOR OPEN-SHELL SYSTEMS

AND

THE MOLECULAR ELECTRONIC STRUCTURE

HIROSHI NAKATSUJI

DEPARTMENT OF HYDROCARBON CHEMISTRY

FACULTY OF ENGINEERING

KYOTO UNIVERSITY

1970

Almost all of the chemical phenomena are governed by the
motions of electrons and nuclei, and the underlying physical laws
necessary to describe these motions are completely known (Dirac,
1929) as a branch of quantum mechanics.   However, since quantum
chemistry deals with an essentially unsoluble many-body problem,
the approximate "concept" which extracts an essence of the physical
reality becomes very important.   Among these approximate concepts,
orbital model (Hartree-Fock theory) have worked very well in the
understandings of the electronic structures of atoms, molecules
and solids.   It is distinguished from other theories by its
physical simplicity and visuality.

However, there are still many things when we go beyond the
Hartree-Fock theory.   These phenomena, which are called collec-
tively as electron-correlation phenomena, offer recent topics in
quantum chemistry.   Among these, spin-correlation is one of the
main interests of the present thesis.   For example, in the open-
shell electronic systems, the simple orbital model breaks down;
the restricted Hartree-Fock (RHF) theory does not take into account
the effect of spin-correlation, and in the unrestricted Hartree-
Fock (UHF) theory, its wavefunction is not an eigenfunction of S^2.
However, an extention of orbital model satisfying both of these
requirements is possible, and is made as the spin-extended Hartree-
Fock (SEHF) theory.

In Part I of this thesis, orbital theories in open-shell
electronic system are studied laying stress on the spin-correlation
problem.   The orbital theories examined are the UHF theory, the

i

projected or annihilated UHF (PUHF) theory and the SEHF theory, and the starting basis is the RHF theory. Firstly, the UHF wavefunction is interpreted in relation to the configuration interaction (CI) method and a first-order relation connecting between the UHF and the PUHF wavefunctions is presented. From this, a simple method is found to separate the UHF or PUHF spin density into contributions due to spin-polarization (SP) and spin-delocalization (SD) mechanisms. These results are applied in Part II to clarify the nature of spin density in doublet radicals. Secondly, perturbation-variation treatment is applied to interconnect these UHF, PUHF and SEHF orbital theories in conjunction with the first-order sum-over-state perturbation method. The accuracy of the expectation values of the one-electron operators using orbital model is also investigated. Through the examination of these results in the light of the physical reality of the correlation phenomena in open-shell electronic systems, it is found out that the orbital model in open-shell electronic system distorts to some extent the real spin-correlation correction, in order to include effectively the correlation correction due essentially to the two-electron correlation phenomena. To overcome this limitation of the orbital model, two methods are suggested for the spin-correlation problem in open-shell electronic system. Thirdly, short examinations of the orbital model in closed-shell spin-correlation problem is given in connection with the finite perturbation theory. This is the background of the treatment given in Part III about the anisotropy of the indirect nuclear spin-spin coupling constant in nuclear magnetic resonance spectra.

In Part II of the present thesis, the electronic structures

of carbonium ions and doublet radicals are studied by the semi-
empirical SCF-MO method for valence electron systems. This method
is also applied to the calculation of force constant of ethylene.

As has been known from the early days of the electronic theory
of chemical valency, valence electrons play essential role in
chemical bindings and in other chemical phenomena. Nevertheless,
it was only recently that the semi-empirical SCF-MO method for
valence electron systems becomes popular (Pople's CNDO method,
1965). The valence-electron SCF-MO method used in Part II is
based on the method presented by Yonezawa, Yamaguchi and Kato.
To apply this method to doublet radicals, extentions are made by
means of the RHF and UHF theories.

Three points should be noted. Firstly, in the studies of
carbonium ions and doublet radicals (especially, their hfs cons-
tants in electron-spin resonance spectra), explicit accounts of
σ-electrons (not like in π-electron theory) and of the electron-
repulsion terms (not like in the extended Hückel theory) are
shown very important. Secondly, the theoretical results of Part
I are applied in the study of doublet radicals, and are proved to
be very useful. Thirdly, the present valence-electron SCF-MO
method is found applicable also to the calculation of force con-
stant after small modification in the core-repulsion term.

In Part III of this thesis, anisotropy of the indirect
nuclear spin-spin coupling constant is studied theoretically.
The information on the order of magnitude of the anisotropy of the
indirect nuclear spin-spin coupling constant is important in the
determination of the molecular geometry from the NMR spectra of
the molecule dissolved in a nematic solvent. Since there has
been no theoretical study on this subject, the author firstly

formulated three mechanisms important to anisotropy by the usual sum-over-state perturbation method. They are Fermi-spin dipolar cross term, spin dipolar term and orbital term. Relative importance of these mechanisms is investigated. Since the indirect coupling constant is due to the spin-correlation phenomena in closed shell electronic systems, the author also applied the finite perturbation theory proved useful in Part I of this thesis. This is the first application of this theory to this problem, except Fermi contact term. The actual calculations are carried out by the INDO method of Pople et al, and the order of magnitude of the anisotropy is calculated for various nuclear pairs. From this and from the detailed examinations on the 'experimental' values of the coupling anisotropy, it is pointed out that the molecular geometry may change from its gas state to the solute state in a nematic solvent. This point will be important in the study on the nature of solvent-solute interaction.

Finally, general conclusions of these investigations are given at the end of this thesis.

ACKNOWLEDGEMENTS

CONTENTS

PART I

STUDIES ON THE ORBITAL THEORIES

IN

THE OPEN-SHELL ELECTRONIC

SYSTEMS

CHAPTER 1

INTRODUCTION

The correlation problem which searches for the gap between the exact wavefunction and the (restricted) Hartree-Fock wavefunction is one of the recent topics in quantum chemistry.[1,2] Some phenomena are there which can never be explained within the restricted Hartree-Fock orbital theory; proton hyperfine splitting constants of the planar π-electron radicals in the electron spin resonance (ESR) spectra, contact shifts and indirect nuclear-spin coupling constants in nuclear magnetic resonance (NMR) spectra, etc.. From theoretical viewpoint, these phenomena are (at least in part) essentially due to the spin-correlation phenomena. Although spin-correlation emerges mainly as the one-electron orbital correction, it is closely related to the two-, three, ---, electron-correlation phenomena.[2]

In Part I of this thesis, orbital theories in open-shell electronic system are studied laying stress on the spin-correlation problem. For example, the restricted Hartree-Fock (RHF) theory[3] does not take into account the effect of spin-polarization, and in the unrestricted Hartree-Fock (UHF) theory[4] its wavefunction is not an eigenfunction of S^2. The spin-extended Hartree-Fock (SEHF) theory[5] is an extention of orbital model satisfying both of these requirements. These orbital theories are interconnected and examined in the light of the physical reality of the correlation phenomena in open-shell electronic systems.

In Chapter 2 (published in Chemical Physics Letters, 2, 454 (1968), and in the Journal of Chemical Physics, 51, 669 (1969)), a method to separate the spin density calculated with the UHF

method into components due to the spin-polarization and spin-delocalization mechanisms is presented, and applied to some doublet and triplet radicals. The results are examined by means of the UHF natural orbitals and of the RHF orbitals, and the validity of the method is confirmed.

In Chapter 3 (published in the Journal of Chemical Physics, 51, 3175 (1969)), the general behavior of the UHF wavefunction is analyzed and interpleted by means of the configuration-interaction (CI) language, and a first-order relation connecting between the UHF and the projected[6] (or annihilated[7]) UHF (PUHF) wavefunctions is presented. The effect of projection (or annihilation) is examined for the expectation values of the one-electron spin-independent and spin-linear operators. From this, the generalization is made on the method for separation of the UHF or PUHF spin density into mechanistic contributions.

In Chapter 4 (under preparation for publication), a perturbation-variation treatment is applied to interconnect the orbital theories in open-shell electronic systems, namely the UHF, PUHF and SEHF theories, in conjunction with the first-order sum-over-state perturbation wavefunction starting from the RHF wavefunction. Interrelation in the spin densities obtained by these four methods is also clarified. The accuracy of the expectation values of the one-electron operators using these orbital models is also investigated for both the closed and open-shell electronic systems. Based on these results, an examination of the orbital model for the spin-correlation problem is carried out in the light of the physical reality of the correlation phenomena in open-shell electronic systems. Two methods are suggested at the end of this study to overcome the limitation of the orbital model in the spin-

2

correlation problem in the open-shell electronic systems.

REFERENCES

1. (a) P. -O. Löwdin, Advan. Chem. Phys. $\underline{2}$, 207 (1959),

   (b) O. Sinanoğlu, ibid. $\underline{6}$, 315 (1964).

   (c) R. Lefebvre and C. Moser ed., "Correlation Effects in Atoms and Molecules," ibid. $\underline{14}$ (1969).

   (d) O. Sinanoğlu and K. A. Brueckner, "Three Approaches to Electron Correlation in Atoms," Yale University Press (1970).

2. (a) O. Sinanoğlu, J. Chem. Phys. $\underline{36}$, 706, 3198 (1962).

   (b) D. F. Tuan and O. Sinanoğlu, ibid. $\underline{38}$, 1740 (1963).

   (c) H. J. Silverstone and O. Sinanoğlu, ibid. $\underline{44}$, 1899, 3608 (1966).

   (d) İ. Öksüz and O. Sinanoğlu, Phys. Rev. $\underline{181}$, 42 (1969).

3. C. C. J. Roothaan, Rev. Mod. Phys. $\underline{32}$, 179 (1960).

4. J. A. Pople and R. K. Nesbet, J. Chem. Phys. $\underline{22}$, 571 (1954).

5. (a) P. -O. Löwdin, Phys. Rev. $\underline{97}$, 1509 (1955).

   (b) K. M. Sando and J. E. Harriman, J. Chem. Phys. $\underline{47}$, 180 (1967).

   (c) J. E. Harriman and K. M. Sando, ibid. $\underline{48}$, 5138 (1968).

6. (a) J. E. Harriman, J. Chem. Phys. $\underline{40}$, 2827 (1964).

   (b) A. Hardisson and J. E. Harriman, ibid. $\underline{46}$, 3639 (1967).

7. T. Amos and L. C. Snyder, J. Chem. Phys. $\underline{41}$, 1773 (1964).

PART I, CHAPTER 2

SPIN DISTRIBUTION MECHANISMS

IN

UNRESTRICTED HARTREE-FOCK THEORY

SPIN POLARIZATION AND SPIN DELOCALIZATION
IN UNRESTRICTED HARTREE-FOCK METHOD

A theory for the separation of the spin density calculated with the unrestricted Hartree-Fock method into the two components due to the spin polarization and spin delocalization mechanisms is given and applied to methyl, ethyl and vinyl radicals.

The unrestricted Hartree-Fock (UHF) method based on a spin polarized self-consistent field single determinant wave function [1] has been widely used for the spin density calculations of many organic and inorganic radicals. However, the unrestricted Hartree-Fock method, compared with the configuration interaction or perturbation methods, does not provide the information about the spin density appearing mechanisms such as the spin polarization (SP) and spin delocalization (SD) mechanisms *. In the present communication, we propose a procedure to separate the spin density calculated with the UHF method and those obtained with the annihilation method [3] into components due to the SP mechanism and to the SD mechanism.

Here we follow closely the results given by Snyder and Amos [4]. The total wave function of the UHF method is written by the p α-spin orbitals and the q β-spin orbitals and we assume $p > q$ without loss of generality. The unitary transformation of the unrestricted molecular orbitals (MO's) gives the corresponding MO's, χ_i and η_i, which are closely related to the natural orbitals, λ, ν and μ:

$$\chi_i = \lambda_i (1 - \Delta_i^2)^{\frac{1}{2}} + \nu_i \Delta_i , \qquad i = 1, \dots, q ;$$

$$\eta_i = \lambda_i (1 - \Delta_i^2)^{\frac{1}{2}} - \nu_i \Delta_i , \qquad i = 1, \dots, q ;$$

$$\chi_i = \mu_i , \qquad i = q + 1, \dots, p ; \quad (1)$$

where

$$\Delta_i = (1 - T_i)^{\frac{1}{2}}/\sqrt{2} , \qquad \int \chi_i \eta_j \, dr = T_i \delta_{ij} .$$

Using eq. (1), we can rewrite the UHF single determinant as the following for doublet radicals ($p = q + 1$)

$$\Psi_{UHF} =$$

$$= C_{\frac{1}{2}}^{rf} \Psi_{\frac{1}{2}}^{rf} + C_{\frac{1}{2}}^{se} \Psi_{\frac{1}{2}}^{se} + C_{\frac{3}{2}}^{se} \Psi_{\frac{3}{2}}^{se} + C_{\frac{1}{2}}^{de} \Psi_{\frac{1}{2}}^{de} + \dots , \quad (2)$$

where

$$\Psi_{\frac{1}{2}}^{rf} = |\lambda_1 \alpha \lambda_1 \beta \lambda_2 \alpha \lambda_2 \beta \dots \lambda_q \alpha \lambda_q \beta \mu_p \alpha| \quad (3)$$

and $\Psi_{\frac{1}{2}}^{se}$ and $\Psi_{\frac{3}{2}}^{se}$ are the sums of the singly excited doublet and quartet configurations resulting from the excitation of an electron from λ_i to ν_i. By assuming $C_{\frac{1}{2}}^{rf} \approx 1 \gg C_{\frac{1}{2}}^{se}$, $C_{\frac{3}{2}}^{se}$, and by neglecting the doubly excited configuration $\Psi_{\frac{1}{2}}^{de}$ and higher terms, the spin density of the UHF method at the position i can be written as *

$$\rho_{UHF}^i \simeq \rho^i(rf\tfrac{1}{2}|rf\tfrac{1}{2}) +$$

$$+ 2C_{\frac{1}{2}}^{se} \rho^i(rf\tfrac{1}{2}|se\tfrac{1}{2}) + 2C_{\frac{3}{2}}^{se} \rho^i(rf\tfrac{1}{2}|se\tfrac{3}{2}) . \quad (4)$$

From the following relations [4]

* The spin density operator and the spin squared operator do not commute.

4

Table 1
Table 1
Spin polarization and spin delocalization in the calculated spin density

Radical	Atomic Orbital	$(\rho_{uhf})_{sp}$	$(\rho_{uhf})_{sd}$	$(\rho_{aa})_{sp}$	$(\rho_{aa})_{sd}$	ρ_{rhf}
Methyl	$2Sc$	0.147(99) *	0.002(1)	0.049(96)	0.002(4)	0.000
	H	-0.028(100)	0.000(0)	-0.009(100)	0.000(0)	0.000
Ethyl	$2Sc_1$	0.159(99)	0.002(1)	0.053(95)	0.002(5)	0.000
	$2Sc_2$	-0.012(100)	0.000(1)	-0.004(100)	0.000(0)	0.000
	H_3	-0.035(100)	0.000(0)	-0.012(100)	0.000(0)	0.000
	H_4	-0.035(100)	0.000(0)	-0.012(100)	0.000(0)	0.000
	$H_5 \cdot H_6$	0.014(26)	0.040(74)	0.005(11)	0.040(89)	0.041
	H_7	-0.002(100)	0.000(0)	-0.001(100)	0.000(0)	0.000
Vinyl	$2Sc\alpha$	0.122(59)	0.083(41)	0.041(33)	0.083(67)	0.081
$\theta = 135^\circ$	$2Sc\beta$	-0.035(111)	0.004(-11)	-0.012(146)	0.004(-46)	0.004
	Hc	0.009(21)	0.035(79)	0.003(8)	0.035(92)	0.036
	Ht	0.026(27)	0.071(73)	0.009(11)	0.071(89)	0.075
	$H\alpha$	-0.042(197)	0.021(-97)	-0.014(-218)	0.021(318)	0.017

* The values in parentheses show the percentages of the contributions. $100 \cdot (\rho^i)_{sp}/\rho^i$ and $100 \cdot (\rho^i)_{sd}/\rho^i$, respectively.

$$\sqrt{2} C_{\frac{1}{2}}^{se} = C_{\frac{3}{2}}^{se}; \qquad \rho^i(rf\tfrac{1}{2}|se\tfrac{3}{2}) = \sqrt{2}\rho^i(rf\tfrac{1}{2}|se\tfrac{1}{2}),$$

eq. (4) reduces to

$$\rho_{UHF}^i = \rho^i(rf\tfrac{1}{2}|rf\tfrac{1}{2}) + 3\sqrt{2}\, C_{\frac{3}{2}}^{se}\rho^i(rf\tfrac{1}{2}|se\tfrac{1}{2}) \quad (5)$$

and similarly, the spin densities after single annihilation (ρ_{asa}) and after annihilation (ρ_{aa}) are [3]

$$\rho_{asa}^i = \rho^i(rf\tfrac{1}{2}|rf\tfrac{1}{2}) + 2\sqrt{2}\, C_{\frac{3}{2}}^{se}\rho^i(rf\tfrac{1}{2}|se\tfrac{1}{2}), \quad (6)$$

$$\rho_{aa}^i = \rho^i(rf\tfrac{1}{2}|rf\tfrac{1}{2}) + \sqrt{2}\, C_{\frac{3}{2}}^{se}\rho^i(rf\tfrac{1}{2}|se\tfrac{1}{2}). \quad (7)$$

Referring to eq. (3), it may be clear that the first terms of eqs. (5)-(7) represent the contributions due to the SD mechanism and the second terms represent approximately those due to the SP mechanism. It may be noteworthy, however, that the unpaired orbital we mean is the natural orbital, μ_i, in eq. (1) and that the $\Psi_{\frac{1}{2}}^{se}$ in eq. (2) includes only the limited configurations like $\lambda_i \cdot \nu_i$, based on the natural orbitals, and does not include those expressed as $\lambda_i \cdot \nu_j$ ($i \neq j$) [3]. The natural orbitals λ, μ and ν are not identical but closely similar to the best restricted orbitals as pointed out by Amos and Snyder [3], and this point will be examined numerically in table 1 by comparing the results obtained with the UHF method to those with the open shell restricted Hartree-Fock (RHF) method [5].

From eqs. (5)-(7), we obtain the results

$$(\rho_{UHF}^i)_{sp} = \tfrac{3}{2}(\rho_{UHF}^i - \rho_{aa}^i), \quad (8)$$

$$(\rho_{asa}^i)_{sp} = \rho_{UHF}^i - \rho_{aa}^i, \quad (9)$$

$$(\rho_{aa}^i)_{sp} = \tfrac{1}{2}(\rho_{UHF}^i - \rho_{aa}^i), \quad (10)$$

where $(\rho_{UHF}^i)_{sp}$ is the SP contribution to the spin density calculated with the UHF method, and $(\rho_{asa}^i)_{sp}$ and $(\rho_{aa}^i)_{sp}$ are those to ρ_{asa}^i and ρ_{aa}^i, respectively. The SD contributions are, therefore, written in common as

$$(\rho^i)_{sd} = \rho^i - (\rho^i)_{sp}. \quad (11)$$

When only the SP mechanism is the source of the spin density as in the case of the σ-type atomic orbitals of the methyl radical, eqs. (8)-(10) give

$$\rho_{UHF}^i = \tfrac{3}{2}\rho_{asa}^i = 3\rho_{aa}^i. \quad (12)$$

as was pointed out by Amos and Snyder.

A semi-empirical unrestricted SCF-MO method for valence electron systems including differential overlap proposed by the present authors [6] gave spin densities listed in table 2. As is well known, the spin densities on the σ-type atomic orbitals of the methyl radical are due only to the SP mechanism and therefore, relation (12) holds fairly satisfactorily.

By using the values shown in table 2, the contributions of the SP and SD mechanisms to spin

Table 2
Spin densities calculated before and after annihilation
of the quartet spin functions

Radical	Atomic Orbital[*]	ρ_{uhf}[**]	ρ_{aa}
Methyl	$2Sc$	0.1487	0.0510
	H	-0.0275	-0.0089
Ethyl	$2Sc_1$	0.1614	0.0555
	$2Sc_2$	-0.0123	-0.0040
	H_3	-0.0345	-0.0111
	H_4	-0.0345	-0.0111
	H_5, H_6	0.0538	0.0442
	H_7	-0.0020	-0.0007
Vinyl	$2Sc_\alpha$	0.2051	0.1240
$\theta = 135^0$ [***]	$2Sc_\beta$	-0.0315	-0.0082
	Hc	0.0438	0.0381
	Ht	0.0974	0.0799
	Hα	-0.0213	0.0064

[*]

$$H_5 \; H_6 \diagdown C_2 - C_1 \diagup H_3 \qquad H_c \diagdown C_\beta - C_\alpha \diagdown H\alpha$$
$$H_7 \diagup \qquad \diagdown H_4 \qquad H_t \diagup \qquad _\theta$$
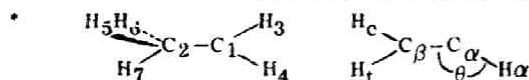
[**] To compare with the experimentally observed proton hyperfine coupling constants. the proportionality constant. 743 gauss. determined by the best fit method is recommended.
[***] The most stable configuration calculated with the present method.

densities are calculated from eqs. (8) - (11) and the results are summarized in table 1. Moreover, the spin density calculated by the RHF method (ρ_{RHF}) may be regarded as a reasonable measure of the validity of the SD contribution obtained by the above method [*], and therefore, the values

[*] Eqs. (8) - (11) are correct only when the contributions due to the higher terms neglected in eq. (4) are negligibly small.

of ρ_{RHF} are given in the last column of table 1. It may be seen that the SD contributions calculated by the UHF method agree reasonable with those obtained by the RHF method. In the ethyl radical. the spin densities on H_5 and H_6 atoms are due to 25 - 10% SP and 75 - 90% SD contributions and those of the other atoms are chiefly due to the SP mechanism. In the vinyl radical. both mechanisms are important, and especially for the α-hydrogen atom, the calculated spin density is the result of the large cancelling contributions of both mechanisms. It may be said based on the present results that extended Hückel type calculations [7,8] of the vinyl radical. where only the SD mechanism is considered. have some doubt as has been mentioned by Dixon [9].

More details of the above method and its extention to the triplet state will be described elsewhere in the near future.

REFERENCES

[1] J. A. Pople and R. K. Nesbet. J. Chem. Phys. 22 (1954) 571.
[2] J. P. Colpa. E. de Boer. D. Lazdins and M. Karplus. J. Chem. Phys. 47 (1967) 3098.
[3] T. Amos and L. C. Snyder. J. Chem. Phys. 41 (1964) 1773.
[4] L. C. Snyder and T. Amos. J. Chem. Phys. 42 (1965) 3670.
[5] C. C. J. Roothaan. Rev. Mod. Phys. 32 (1960) 179.
[6] T. Yonezawa. H. Nakatsuji. T. Kawamura and H. Kato. Bull. Chem. Soc. Japan 40 (1967) 2211: Mol. Phys. 13 (1967) 589.
[7] G. A. Peterson and A. D. McLachlan. J. Chem. Phys. 45 (1966) 628.
[8] R. S. Drago and H. Petersen Jr.. J. Am. Chem. Soc. 89 (1967) 5774.
[9] W. T. Dixon. Mol. Phys. 9 (1965) 201.

Spin Polarization and Spin Delocalization in Unrestricted Hartree–Fock Method

A method to separate the spin density calculated with the unrestricted Hartree–Fock method into components due to spin-polarization and spin-delocalization mechanisms is presented, and applied to some doublet and triplet radicals. The results are examined by means of the UHF natural orbitals and of the open-shell restricted Hartree–Fock orbitals, and the validity of the method is confirmed.

I. INTRODUCTION

The unrestricted Hartree–Fock (UHF) method based on a spin-polarized self-consistent-field single-determinant wavefunction[1] is widely used for spin-density calculations. However, compared with configuration-interaction or perturbation methods,[2,3] the UHF method does not usually provide information about "spin-appearing" mechanisms[4] such as spin-polarization (SP) and spin-delocalization (SD) mechanisms.[5-7]

In a previous communication,[7] we proposed a procedure to separate the spin density calculated with the UHF method (ρ_{UHF}) and that obtained after the annihilation method[8] (ρ_{asa} and ρ_{aa})[9] into components due to the SP mechanism (ρ_{SP}) and to the SD mechanism (ρ_{SD}). For doublet radicals, the results are

$$(\rho_{UHF})_{SP} = \tfrac{3}{2}(\rho_{UHF} - \rho_{aa}),$$

$$(\rho_{asa})_{SP} = \rho_{UHF} - \rho_{aa},$$

$$(\rho_{aa})_{SP} = \tfrac{1}{2}(\rho_{UHF} - \rho_{aa}), \tag{1}$$

where $(\rho_{UHF})_{SP}$ denotes the SP contribution to the spin density calculated with the UHF method and $(\rho_{asa})_{SP}$ and $(\rho_{aa})_{SP}$ are those to ρ_{asa} and ρ_{aa}, respec-

tively. The spin-delocalization contribution is approximated as the difference

$$(\rho)_{SD} = \rho - (\rho)_{SP}. \tag{2}$$

Furthermore, the validity of this approach was confirmed by comparing the SD contributions calculated by Eq. (2) with those obtained by the open-shell restricted Hartree–Fock method.[10]

The separation of the unrestricted spin density into mechanistic contributions is also possible by means of the natural orbitals of the UHF method. Here, we compare the results obtained by the above method with those calculated from the natural orbitals of the UHF method.[8a] In the next section, an extension of the above method to triplet states is described and some assumptions in the formalism are examined. Then, we apply the method to typical doublet and triplet radicals in Sec. III. The conclusion of the present study is given in Sec. IV.

II. THEORY

The total wavefunction of the UHF method is written by a single determinant in which the α-spin orbitals $\{\varphi_i\}$ may be different from the β-spin orbitals $\{\phi_i\}$;

$$\Psi_{UHF} = [(p+q)!]^{-1/2} \det\{\varphi_1(1)\alpha(1)\varphi_2(2)\alpha(2)$$

$$\cdots\varphi_p(p)\alpha(p)\phi_1(p+1)\beta(p+1)\phi_2(p+2)\beta(p+2)$$

$$\cdots\phi_q(p+q)\beta(p+q)\}, \tag{3}$$

where we assume $p \geq q$ without loss of generality. For doublet radicals, $p = q+1$, and for triplet radicals, $p = q+2$. As shown by Amos and Hall[8a] and by Amos and Snyder,[8c] the unitary transformations of the unrestricted molecular orbitals (MO's) $\{\varphi_i\}$ and $\{\phi_i\}$ give the corresponding MO's $\{\chi_i\}$ and $\{\eta_i\}$, respectively. These are closely related to the natural orbitals λ, μ, and ν by the following equations:

$$\chi_i = \lambda_i(1 - \Delta_i^2)^{1/2} + \nu_i\Delta_i, \quad i = 1, \cdots, q,$$

$$\eta_i = \lambda_i(1 - \Delta_i^2)^{1/2} - \nu_i\Delta_i, \quad i = 1, \cdots, q,$$

$$\chi_i = \mu_i, \quad i = q+1, \cdots, p. \tag{4}$$

[1] J. A. Pople and R. K. Nesbet, J. Chem. Phys. 22, 571 (1964).
[2] (a) A. D. McLachlan, Mol. Phys. 3, 233 (1960). (b) S. Aono and J. Higuchi, Progr. Theoret. Phys. 28, 589 (1962). (c) J. P. Malrieu, J. Chem. Phys. 46, 1654 (1967). (d) A. L. H. Chung, ibid. 46, 3144 (1967).
[3] J. P. Colpa and E. de Boer, Mol. Phys. 7, 333 (1964), and the references cited in this paper.
[4] By "spin-appearing" mechanism, we mean the mechanism by which the spin-density distribution occurs.
[5] (a) D. Lazdins and M. Karplus, J. Chem. Phys. 44, 1600 (1966). (b) J. P. Colpa, E. de Boer, D. Lazdins, and M. Karplus, ibid. 47, 3008 (1967).
[6] To avoid confusion [see Ref. 5(b)] we provisionally define the spin delocalization and spin-polarization mechanisms used here. The former means the "spin appearing" mechanism due to the singly occupied orbitals of the best restricted wavefunction, and the latter is defined as that due to correlation between electron spins. This definition of the SP and SD mechanisms is identical with that given by Colpa and de Boer in Ref. 5(b).
[7] T. Yonezawa, H. Nakatsuji, T. Kawamura, and H. Kato, Chem. Phys. Letters 2, 454 (1968).
[8] (a) A. T. Amos and G. G. Hall, Proc. Roy. Soc. (London) A263, 483 (1961). (b) A. T. Amos, Mol. Phys. 5, 91 (1962). (c) T. Amos and L. C. Snyder, J. Chem. Phys. 41, 1773 (1964). (d) L. C. Snyder and T. Amos, ibid. 42, 3670 (1965).
[9] Here we follow the notations used by Amos and Snyder.[8c] The suffixes "asa" and "aa" mean "after single annihilation" and "after annihilation," respectively.

[10] C. C. J. Roothaan, Rev. Mod. Phys. 32, 179 (1960).

where

$$\Delta_i = \frac{(1-T_i)^{1/2}}{\sqrt{2}}, \qquad \int \chi_i \eta_j d\tau = T_i \delta_{ij}.$$

As seen in Eq. (4), the corresponding orbitals of the UHF method are related to the alternant MO's proposed by Löwdin,[11] and the natural orbitals λ and μ are closely related to the restricted MO's, as noted by Amos and Snyder.[3c] In this treatment, we assume that the natural orbitals μ are closely similar to the *unpaired orbitals* of the restricted open-shell method,[12] and this point will be verified later. (See Table VIII.)

Now, we extend the method described previously[7] to the triplet state. As shown by Snyder and Amos,[3d] we can rewrite the UHF single determinant, using Eq. (4), in the following manner for the triplet state ($p=q+2$):

$$\Psi_{\text{UHF}} = C_{2/2}{}^{rt}\Psi_{2/2}{}^{rt} + C_{2/2}{}^{se}\Psi_{2/2}{}^{se} + C_{4/2}{}^{se}\Psi_{4/2}{}^{se} + C_{2/2}{}^{de}\Psi_{2/2}{}^{de} + \cdots, \quad (5)$$

where $\Psi_{2/2}{}^{rt}$ is the normalized restricted function built up of the natural orbitals λ and μ:

$$\Psi_{2/2}{}^{rt} = |\lambda_1\alpha\lambda_1\beta\lambda_2\alpha\lambda_2\beta\cdots\lambda_q\alpha\lambda_q\beta\mu_{q+1}\alpha\mu_{q+2}\alpha|, \quad (6)$$

and its coefficient is given by

$$C_{2/2}{}^{rt} = \prod_{i=1}^{q}(1-\Delta_i^2). \quad (7)$$

$\Psi_{2/2}{}^{se}$ and $\Psi_{4/2}{}^{se}$ are sums of the singly excited triplet and quintet configurations, resulting from excitation from λ_i to ν_i;

$$\Psi_{2/2}{}^{se} = \frac{1}{C_{2/2}{}^{se}}\sum_{i=1}^{q}\Delta_i(1-\Delta_i^2)^{1/2}N_i\frac{1}{\sqrt{2}}[|\cdots\nu_i\lambda_i(\alpha\beta+\beta\alpha)$$
$$\cdots\mu_{q+1}\alpha\mu_{q+2}\alpha| - |\cdots\nu_i\alpha\lambda_i\alpha\cdots\mu_{q+1}\mu_{q+2}(\alpha\beta+\beta\alpha)|],$$
$$(8)$$

$$\Psi_{4/2}{}^{se} = \frac{1}{C_{4/2}{}^{se}}\sum_{i=1}^{q}\Delta_i(1-\Delta_i^2)^{1/2}N_i\frac{1}{\sqrt{2}}[|\cdots\nu_i\lambda_i(\alpha\beta+\beta\alpha)$$
$$\cdots\mu_{q+1}\alpha\mu_{q+2}\alpha| + |\cdots\nu_i\alpha\lambda_i\alpha\cdots\mu_{q+1}\mu_{q+2}(\alpha\beta+\beta\alpha)|],$$
$$(9)$$

where

$$N_i = \prod_{j=1,j\neq i}^{q}(1-\Delta_j^2),$$

and their coefficients are given by

$$C_{2/2}{}^{se} = C_{4/2}{}^{se} = \left(\sum_{i=1}^{q}\Delta_i^2(1-\Delta_i^2)N_i^2\right)^{1/2}. \quad (10)$$

Here we consider the expectation value of the normalized spin-density operator,[13] $\varrho^t = S_z^{-1}\sum_i S_{zi}\delta(r_i - r^t)$. By

assuming $C_{2/2}{}^{rt} \gg C_{2/2}{}^{se}$, $C_{4/2}{}^{se}$ and by neglecting the doubly excited configuration $\Psi_{1/2}{}^{de}$ and higher terms,[14] we obtain

$$\rho_{\text{UHF}}{}^t = (C_{2/2}{}^{rt})^2\rho^t[\text{rf}(2/2) \mid \text{rf}(2/2)]$$
$$+ 2C_{2/2}{}^{rt}C_{2/2}{}^{se}\rho^t[\text{rf}(2/2) \mid \text{se}(2/2)]$$
$$+ 2C_{2/2}{}^{rt}C_{4/2}{}^{se}\rho^t[\text{rf}(2/2) \mid \text{se}(4/2)], \quad (11)$$

where $\rho^t[\text{rf}(2/2) \mid \text{se}(2/2)]$ denotes the matrix element between $\Psi_{2/2}{}^{rt}$ and $\Psi_{2/2}{}^{se}$ with respect to the normalized spin-density operator. From Eq. (10) and from the relation

$$\rho^t[\text{rf}(2/2) \mid \text{se}(2/2)] = \rho^t[\text{rf}(2/2) \mid \text{se}(4/2)],$$

Eq. (11) reduces to

$$\rho_{\text{UHF}}{}^t = (C_{2/2}{}^{rt})^2\rho^t[\text{rf}(2/2) \mid \text{rf}(2/2)]$$
$$+ 4C_{2/2}{}^{rt}C_{2/2}{}^{se}\rho^t[\text{rf}(2/2) \mid \text{se}(2/2)]. \quad (12)$$

Similarly, the spin densities after single annihilation (ρ_{sa}) and after annihilation (ρ_{aa}) are written as

$$\rho_{sa}{}^t = (C_{2/2}{}^{rt})^2\rho^t[\text{rf}(2/2) \mid \text{rf}(2/2)]$$
$$+ 3C_{2/2}{}^{rt}C_{2/2}{}^{se}\rho^t[\text{rf}(2/2) \mid \text{se}(2/2)]$$

and

$$\rho_{aa}{}^t = (C_{2/2}{}^{rt})^2\rho^t[\text{rf}(2/2) \mid \text{rf}(2/2)]$$
$$+ 2C_{2/2}{}^{rt}C_{2/2}{}^{se}\rho^t[\text{rf}(2/2) \mid \text{se}(2/2)]. \quad (13)$$

From the definition given in Ref. 6, the first terms of Eqs. (12) and (13) represent the contributions due to the SD mechanism, and the second terms represent those due to the SP mechanism. Note that $\Psi_{2/2}{}^{se}$ and $\Psi_{4/2}{}^{se}$ given by Eqs. (8) and (9) include only the limited configurations like $|\lambda_i \rightarrow \nu_i|$, the excited configuration, where λ_i is replaced by ν_i, and do not include those expressed by $|\lambda_i \rightarrow \nu_j|$ ($i \neq j$), $|\mu_i \rightarrow \nu_j|$, and $|\lambda_i \rightarrow \mu_j|$, and that the occupation number of μ is unity. [See Eq. (4).] Moreover, Eqs. (12) and (13) show that the annihilation of the lowest contaminating spin state (quintet state in this case) affects only the SP contributions.

From Eqs. (12) and (13), we obtain the results for *triplet radicals*. By using the values of $\rho_{aa}{}^t$, the SP contributions are calculated from

$$(\rho_{\text{UHF}}{}^t)_{\text{SP}} = 2(\rho_{\text{UHF}}{}^t - \rho_{aa}{}^t),$$
$$(\rho_{sa}{}^t)_{\text{SP}} = \frac{3}{2}(\rho_{\text{UHF}}{}^t - \rho_{aa}{}^t),$$
$$(\rho_{aa}{}^t)_{\text{SP}} = \rho_{\text{UHF}}{}^t - \rho_{aa}{}^t, \quad (14)$$

[11] P.-O. Löwdin, Phys. Rev. 97, 1509 (1955).

[12] Strictly speaking, this assumption should be that the *unitarily transformed* natural orbitals μ are closely similar to the unpaired orbitals of the RHF wavefunction.

[13] H. M. McConnell, J. Chem. Phys. 28, 1188 (1958).

[14] This assumption corresponds to neglecting contributions from $\rho^t[\text{se}(2/2) \mid \text{se}(2/2)]$ and $\rho^t[\text{se}(4/2) \mid \text{se}(4/2)]$, etc. In other words, this corresponds to omission of part of the second- and higher-order terms with respect to the spin-correlation perturbation.

and by using $\rho_{\alpha\alpha}{}^i$, from

$$(\rho_{UHF}{}^i)_{SP} = 4(\rho_{UHF}{}^i - \rho_{\alpha\alpha}{}^i),$$

$$(\rho_{\alpha\alpha\alpha}{}^i)_{SP} = 3(\rho_{\alpha\alpha}{}^i - \rho_{\alpha\alpha}{}^i),$$

$$(\rho_{\alpha\alpha}{}^i)_{SP} = 2(\rho_{UHF}{}^i - \rho_{\alpha\alpha}{}^i). \qquad (15)$$

The SD contribution in the triplet state is given by

$$\tfrac{1}{2}[\mid \mu_{q+1}(\mathbf{r}^i) \mid^2 + \mid \mu_{q+2}(\mathbf{r}^i) \mid^2],$$

since the occupation number of μ is unity. But in the present approximation (see Ref. 14), this is given by

$$(\rho^i)_{SD} = (C_{2/2}{}^{\mathbf{r}i})^2 \rho^i[\mathrm{rf}(2/2) \mid \mathrm{rf}(2/2)]$$

$$= \tfrac{1}{2}(C_{2/2}{}^{\mathbf{r}i})^2[\mid \mu_{q+1}(\mathbf{r}^i) \mid^2 + \mid \mu_{q+1}(\mathbf{r}^i) \mid^2], \qquad (16)$$

and is calculated from

$$(\rho)_{SD} = \rho - (\rho)_{SP}, \qquad (17)$$

without a knowledge of the natural orbitals μ_i. When only the SP mechanism is the source of spin density as is the case of spin densities in the σ-type atomic orbitals of the planar $\pi \rightarrow \pi^*$ triplet state of ethylene, Eq. (14) leads to

$$\rho_{UHF}{}^i = \tfrac{4}{3}\rho_{\alpha\alpha}{}^i = 2\rho_{\alpha\alpha}{}^i. \qquad (18)$$

For *doublet radicals*, the results have been reported previously.[7] However, it may be convenient to summarize the results here. The SP contributions to the spin densities are calculated by using ρ_{UHF} and $\rho_{\alpha\alpha}$ from

$$(\rho_{UHF}{}^i)_{SP} = \tfrac{3}{2}(\rho_{UHF}{}^i - \rho_{\alpha\alpha}{}^i),$$

$$(\rho_{\alpha\alpha}{}^i)_{SP} = \rho_{UHF}{}^i - \rho_{\alpha\alpha}{}^i,$$

$$(\rho_{\alpha\alpha}{}^i)_{SP} = \tfrac{1}{2}(\rho_{UHF}{}^i - \rho_{\alpha\alpha}{}^i), \qquad (19)$$

and by using ρ_{UHF} and $\rho_{\alpha\alpha\alpha}$ from

$$(\rho_{UHF}{}^i)_{SP} = 3(\rho_{UHF}{}^i - \rho_{\alpha\alpha\alpha}{}^i),$$

$$(\rho_{\alpha\alpha\alpha}{}^i)_{SP} = 2(\rho_{UHF}{}^i - \rho_{\alpha\alpha\alpha}{}^i),$$

$$(\rho_{\alpha\alpha}{}^i)_{SP} = \rho_{UHF}{}^i - \rho_{\alpha\alpha\alpha}{}^i. \qquad (20)$$

The SD contributions are also given by Eq. (17). When only the SP mechanism is important, the spin densities calculated by the three methods satisfy the following relation:

$$\rho_{UHF}{}^i = \tfrac{3}{2}\rho_{\alpha\alpha}{}^i = 3\rho_{\alpha\alpha}{}^i, \qquad (21)$$

as pointed out by Amos and Snyder.[20]

The separation of the UHF spin densities into mechanistic contributions is also possible by means of the natural orbitals of the UHF method, which is more direct than the above method. In this method, the mechanistic contributions can be calculated directly from Eq. (5) for triplet states, and for doublet radicals from [see Eq. (2) in the previous paper[7]]

$$\Psi_{UHF} = C_{1/2}{}^{\mathbf{r}i}\Psi_{1/2}{}^{\mathbf{r}i} + C_{1/2}{}^{\infty}\Psi_{1/2}{}^{\infty} + C_{3/2}{}^{\infty}\Psi_{3/2}{}^{\infty} + \cdots, \qquad (22)$$

TABLE 1. Comparison of UHF orbitals, UHF natural orbitals, and RHF orbitals of the methyl radical.

Symmetry	Coefficient	T_i
UHF Orbitals		
α-Spin orbitals		
a_1'	$0.7950S + 0.1129(h_2 + h_3 + h_4)$	
e'	$0.4645X - 0.5153(h_3 - h_4)$	
	$0.4645Y + 0.5950h_2 - 0.2975(h_3 + h_4)$	
a_2''	$1.0000Z$	
β-Spin orbitals		
a_1'	$0.6951S + 0.1642(h_2 + h_3 + h_4)$	
e'	$0.4520X - 0.5249(h_3 - h_4)$	
	$0.4520Y + 0.6061h_2 - 0.3030(h_3 + h_4)$	
UHF Natural orbitals		
a_1'	$0.7454S + 0.1386(h_2 + h_3 + h_4)$	0.9979
e'	$0.4582X - 0.5201(h_3 - h_4)$	1.0000
	$0.4582Y + 0.6005h_2 - 0.3002(h_3 + h_4)$	1.0000
a_2''	$1.0000Z$	
RHF Orbitals		
a_1'	$0.7462S + 0.1382(h_2 + h_3 + h_4)$	
e'	$0.4686X - 0.5121(h_3 - h_4)$	
	$0.4686Y + 0.5914h_4 - 0.2957(h_1 + h_4)$	
a_2''	$1.0000Z$	

where the coefficients are given by

$$C_{1/2}{}^{\mathbf{r}i} = \prod_{i=1}^{q} (1 - \Delta_i{}^2)$$

and

$$C_{1/2}{}^{\infty} = (1/\sqrt{2})C_{3/2}{}^{\infty}$$

$$= (\tfrac{2}{3})^{1/2}(\sum_{j=1}^{q} [\Delta_j(1 - \Delta_j{}^2)^{1/2}N_j]^2)^{1/2}. \qquad (23)$$

The SD contribution, which is compared with the one obtained by the above method, is given by Eq. (16) for triplet states, and by the following equation for doublet radicals:

$$(\rho^i)_{SD} = (C_{1/2}{}^{\mathbf{r}i})^2 \mid \mu_{q+1}(\mathbf{r}^i) \mid^2. \qquad (24)$$

On the other hand, the SP contribution may be calculated by applying the spin-density operator to Eq. (5) or to Eq. (22). However, this is rather impractical, since the natural orbital ν_i is given by[20]

$$\nu_i = (\chi_i - \eta_i)/\sqrt{2}(1 - T_i)^{1/2},$$

where T_i is always very close to unity. (For example, see Tables I and II.) A more straightforward way than

TABLE II. Comparison of UHF orbitals, UHF natural orbitals, and RHF orbitals of the $\pi \to \pi^*$ triplet state of planar ethylene.

Symmetry	Coefficient	T_i
	UHF Orbitals	
α-Spin orbitals		
a_g	$0.6014(S_1+S_2)-0.0096(X_1-X_2)-0.0088(h_3+h_4+h_5+h_6)$	
b_{3u}	$0.4987(S_1-S_2)-0.1188(X_1+X_2)+0.2067(h_3+h_4-h_5-h_6)$	
b_{2u}	$0.3396(Y_1+Y_2)+0.3081(h_3-h_4-h_5+h_6)$	
b_{1g}	$0.3240(Y_1-Y_2)+0.4274(h_3-h_4+h_5-h_6)$	
a_g	$-0.0682(S_1+S_2)-0.5069(X_1-X_2)+0.2129(h_3+h_4+h_5+h_6)$	
b_{1u}	$0.6271(Z_1+Z_2)$	
b_{2g}	$0.8283(Z_1-Z_2)$	
β-Spin orbitals		
a_g	$0.5357(S_1+S_2)+0.0242(X_1-X_2)+0.0441(h_3+h_4+h_5+h_6)$	
b_{3u}	$0.4082(S_1-S_2)-0.1258(X_1+X_2)+0.2497(h_3+h_4-h_5-h_6)$	
b_{2u}	$0.3245(Y_1+Y_2)+0.3213(h_3-h_4-h_5+h_6)$	
b_{1g}	$0.3119(Y_1-Y_2)+0.4353(h_3-h_4+h_5-h_6)$	
a_g	$0.0851(S_1+S_2)+0.5014(X_1-X_2)-0.2196(h_3+h_4+h_5+h_6)$	
	UHF Natural orbitals	
a_g	$0.5531(S_1+S_2)-0.0620(X_1-X_2)+0.0472(h_3+h_4+h_5+h_6)$	0.9971
b_{3u}	$0.4537(S_1-S_2)-0.1223(X_1+X_2)+0.2283(h_3+h_4-h_5-h_6)$	0.9977
b_{2u}	$0.3321(Y_1+Y_2)+0.3147(h_3-h_4-h_5+h_6)$	0.9998
b_{1g}	$0.3180(Y_1-Y_2)+0.4313(h_3-h_4+h_5-h_6)$	1.0000
a_g	$-0.1541(S_1+S_2)-0.5003(X_1-X_2)+0.2120(h_3+h_4+h_5+h_6)$	1.0000
b_{1u}	$0.6271(Z_1+Z_2)$	
b_{2g}	$0.8283(Z_1-Z_2)$	
	RHF Orbitals	
a_g	$0.5626(S_1+S_2)-0.0004(X_1-X_2)+0.0259(h_3+h_4+h_5+h_6)$	
b_{3u}	$0.4495(S_1-S_2)-0.1245(X_1+X_2)+0.2294(h_3+h_4-h_5-h_6)$	
b_{2u}	$0.3376(Y_1+Y_2)+0.3099(h_3-h_4-h_5+h_6)$	
b_{1g}	$0.3253(Y_1-Y_2)+0.4266(h_3-h_4+h_5-h_6)$	
a_g	$-0.0905(S_1+S_2)-0.5030(X_1-X_2)+0.2174(h_3+h_4+h_5+h_6)$	
b_{1u}	$0.6271(Z_1+Z_2)$	
b_{2g}	$0.8283(Z_1-Z_2)$	

this is to use the equation

$$(\rho)_{SP} = \rho - (\rho)_{SD}. \qquad (25)$$

In the present paper, we also calculate the mechanistic contributions by this method and compare the results with those obtained with Eqs. (14)–(20). Hereafter we call the method based on Eqs. (14)–(20) as "annihilation method (AN method)" and the one based on Eqs. (16), (24), and (25) as "natural-orbital method (NO method)."

In the formulations of Eqs. (14)–(18) for triplet states and in those of Eqs. (19)–(21) for doublet radicals described previously,[7] we set the following two assumptions: One is that the natural orbitals μ are closely similar to the unpaired orbitals of the *best* restricted molecular orbitals, and the other is that the coefficients in Eq. (5) satisfy the relation $C_{2/2}{}^{r} \gg C_{2/2}{}^{\infty}$, $C_{4/2}{}^{\infty}$. (See also Ref. 14.) Now, we examine these assumptions. In Tables I and II the natural orbitals of the UHF method calculated for the methyl radical and

TABLE III. Comparison of the UHF natural orbitals μ and the RHF unpaired orbitals.[a]

Radical	AO[b]	UHF $\rho^i[\mathrm{rf}(1/2) \mid \mathrm{rf}(1/2)]$	RHF $\rho^i(\mathrm{RHF} \mid \mathrm{RHF})$	Triplet state	AO[b]	UHF $\rho^i[\mathrm{rf}(2/2) \mid \mathrm{rf}(2/2)]$	RHF $\rho^i(\mathrm{RHF} \mid \mathrm{RHF})$
Ethyl	$2P_x(C_1)$	1.000	0.999	H_2CO	$2P_z(C)$	0.525	0.525
	$2P_x(C_2)$	0.000	0.000	$(\pi \rightarrow \pi^*)$	$2P_z(O)$	0.525	0.525
	$5h, 6h$	0.039	0.041				
Vinyl	$2S(C_\alpha)$	0.090	0.081	H_2CO	$2P_y(C)$	0.000	0.000
	$2P_x(C_\alpha)$	0.118	0.125	$(n \rightarrow \pi^*)$	$2P_z(C)$	0.407	0.438
	$2P_y(C_\alpha)$	0.739	0.745		$2P_y(O)$	0.484	0.483
	$2S(C_\beta)$	0.008	0.004		$2P_z(O)$	0.226	0.187
	$2P_x(C_\beta)$	0.001	0.004		h	0.022	0.023
	$2P_y(C_\beta)$	0.000	0.001				
	h_e	0.053	0.037				
	h_t	0.071	0.075				
	h_α	0.020	0.017				

[a] Only the coefficients of the diagonal elements of the AO spin-density matrix are given. (See Ref. 13.)

[b] The values of the AO's other than those given in this table are zero by symmetry.

for the $\pi \rightarrow \pi^*$ triplet state of ethylene are compared[15] with the MO's obtained by the open-shell restricted Hartree–Fock (RHF) method.[10] (The method of calculations and estimations of integral values are described in Ref. 16.) Since the wavefunction obtained with the Roothaan's open-shell method may be regarded as the *best* RHF wavefunction within the approximations introduced in the integral estimations, it provides a good criterion of the restricted configuration [Eq. (6)] included in the UHF wavefunction. As seen in Tables I and II, the natural orbitals of the UHF method accord satisfactorily well with the MO's obtained by the RHF method. Note that, in the cases shown in Tables I and II, the unpaired orbitals are uniquely determined by symmetry requirements. In Table III, the natural orbitals μ of some doublet and triplet radicals are compared with the unpaired orbitals of the RHF method. Generally, they are very close to each other, except some large differences which lie in the h_e AO of the vinyl radical and in the $2P_z(C)$ and $2P_z(O)$ AO's of the $n \rightarrow \pi^*$ triplet state of formaldehyde.

[15] In the cases of the methyl radical and the $\pi \rightarrow \pi^*$ triplet state of planar ethylene each orbital belongs to different symmetry representation except the a_g orbitals in the $\pi \rightarrow \pi^*$ triplet state, so we can compare directly the calculated UHF natural orbitals, having degenerate T_i values, with the MO's obtained by the RHF method.

[16] T. Yonezawa, H. Nakatsuji, T. Kawamura, and H. Kato, "Semi-empirical Unrestricted SCF–MO Treatment for Valence Electron Systems. I. Application to Small Doublet Radicals," Bull. Chem. Soc. Japan (to be published). The methods of estimating the integral values in the present UHF calculations are the same as those in this paper. In the RHF calculations, the two-center σ–π-type exchange repulsion integrals are omitted. Since these integrals are very small in magnitude, they don't affect the SD contributions. Hence, the SD contributions calculated by both methods can be directly compared.

However, the agreement to this order between the UHF natural orbitals and the RHF orbitals is rather surprising, considering the large differences in the variation processes of both methods. This lends support to the first assumption that the natural orbitals μ are closely similar to the unpaired orbitals of the best restricted molecular orbitals. Referring to Tables I and II, we see that the natural-orbital coefficients are always the median in magnitude of those of the α- and β-spin orbitals of the UHF method.

Then, we examine the second assumption: From the T_i values shown in the last column of Tables I and II, the coefficients of the singly excited configurations in Eqs. (5) and (22) are calculated, and they are summarized in Table IV for doublet radicals, while those for triplet states are listed in Table V. Generally speaking, the second assumption that the coefficient of the restricted configuration is much larger than the coefficients of the singly excited configurations is good and the magnitude of error due to this assumption is $\sim (C^{\mathrm{se}})^2/C^{\mathrm{se}}$.[17] As described in Ref. 14, this assumption

[17] The magnitude of error due to this assumption can also be estimated approximately by calculating the weight of mixing of the lowest contaminating spin state into the UHF total wavefunction, and this is calculated for doublet radicals by

$$[C(\text{quartet})/C(\text{doublet})]^2 \simeq (4\langle S^2 \rangle_{\mathrm{UHF}} - 3)/(15 - 4\langle S^2 \rangle_{\mathrm{UHF}})$$

and for triplet states by

$$[C(\text{quintet})/C(\text{triplet})]^2 \simeq (\langle S^2 \rangle_{\mathrm{UHF}} - 2)/(6 - \langle S^2 \rangle_{\mathrm{UHF}}),$$

where $\langle S^2 \rangle_{\mathrm{UHF}}$ is the expectation value of the UHF total wavefunction with respect to the spin-squared operator. These values are 0.00217 and 0.01372 for ethyl and vinyl radicals, and 0.00583 and 0.00472 for the $n \rightarrow \pi^*$ and $\pi \rightarrow \pi^*$ triplet states of formaldehyde. They correspond reasonably well with the values shown in Tables IV and V. See also the succeeding paper (Ref. 16).

TABLE IV. Coefficients in doublet radicals.

Radical	$C_{1/2}{}^{rf}$	$C_{1/2}{}^{oe}$		$C_{3/2}{}^{oe}$	
		$\sigma \rightarrow \sigma^*$ Type	$\pi \rightarrow \pi^*$ Type	$\sigma \rightarrow \sigma^*$ Type	$\pi \rightarrow \pi^*$ Type
Methyl	0.9989	0.0269	...	0.0373	...
Ethyl	0.9984	0.0327	...	0.0464	...
Vinyl	0.9901	0.0260	0.0763	0.0367	0.1079

corresponds to omission of part of the second and higher terms with respect to the spin-correlation perturbation, and the errors in the final results are seen by comparing the SD contributions calculated by the AN and NO methods given in Tables VI–VIII. An examination of this point is discussed more fully in the next section.

III. DISCUSSION OF THE RESULTS

A. Doublet Radicals

In this section, we apply the AN Method to doublet radicals such as ethyl and vinyl radicals (geometries and numberings are illustrated in Fig. 1.) and compare the results with those obtained by the NO method. (About the method of the UHF and RHF calculations and estimations of integral values, see Ref. 16.) The UHF natural orbitals are calculated by means of the method given by Amos and Hall.[8a] The UHF calculations of the spin densities of the ethyl and vinyl radicals were recently reported by Pople, Beveridge, and Dobosh[18] and by Atherton and Hincliffe,[19] respectively, who considered all the valence electrons of the constituent atoms. Here, we also apply the AN method to their results, and compare them with the present ones.

In Table VI, the UHF spin densities and their mechanistic contributions in ethyl radical calculated by the AN method are compared with those obtained by the NO method, and with the values obtained by applying the AN method to the INDO results of Pople, Beveridge, and Dobosh.[18] Since the AN method is derived by assuming $C_{1/2}{}^{rf} \gg C_{1/2}{}^{oe}$, $C_{3/2}{}^{oe}$, the calculated mechanistic contributions include some small errors as seen by the nonzero SD contributions in the $2S(C_1)$

TABLE V. Coefficients in triplet radicals.

Triplet radical		$C_{1/2}{}^{rf}$	$C_{2/2}{}^{oe}$	$C_{4/2}{}^{oe}$
Ethylene	$(\pi \rightarrow \pi^*)$	0.9973	0.0520	0.0520
Formaldehyde	$(n \rightarrow \pi^*)$	0.9942	0.0761	0.0761
	$(\pi \rightarrow \pi^*)$	0.9953	0.0684	0.0684

[18] J. A. Pople, D. L. Beveridge, and P. A. Dobosh, J. Chem. Phys. **47**, 2026 (1967).

[19] N. M. Atherton and A. Hincliffe, Mol. Phys. **12**, 349 (1967).

and $2P_z(C_2)$ AO's, which must be zero by symmetry. Nevertheless, the SD contributions calculated by the AN method agree fairly well with those obtained by means of the NO method and of the RHF method (the fourth column of Table III). This is a direct proof that the natural orbital of the UHF method is closely similar to the unpaired orbital of the restricted open-shell method, and that the contributions to spin densities from part of the second- and higher-order terms with respect to the spin-correlation perturbation[14] are negligibly small. The UHF spin densities on the atomic orbitals, where the NO method gives zero spin density, are due only to the SP mechanism. Hence, in these positions, the relation [Eq. (21)] $\rho_{UHF} = 3\rho_{ss}$ holds fairly satisfactorily, and this is also true for the INDO calculations.[18]

The UHF spin densities on the H_5 and H_6 protons obtained before annihilation are due to 26% SP and 74% SD contributions in the present calculation, and the mechanistic separation of the INDO results predicts 47% SP and 53% SD contributions. Anyway, the SP mechanism contributes much to the spin densities on these protons. Lazdins and Karplus[5a] pointed out
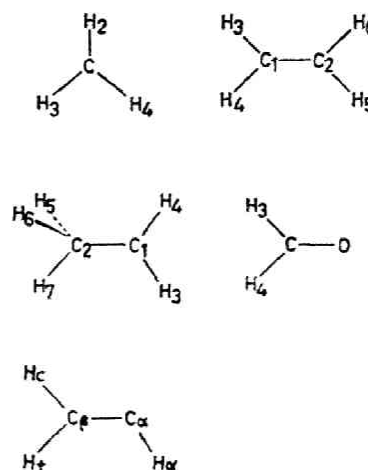

FIG. 1. Geometries [L. E. Sutton (Ed.), Chem. Soc. (London), Spec. Publ. 11 (1956); 18 (1965)]. For methyl radical, C–H = 1.079 Å; for ethyl, C–C = 1.50 Å, C(1)–H = 1.079 Å, C(2)–H = 1.09 Å; for vinyl, C–C = 1.34 Å, C–H = 1.07 Å, ∠CCH(a) = 135°; for ethylene triplet radical, C–C = 1.337 Å, C–H = 1.086 Å, ∠HCH = 117.3°; for formaldehyde, C–H = 1.12 Å, C–O = 1.21 Å, ∠HCH = 118°.

TABLE VI. SP and SD mechanism in ethyl radical.[a]

| Atom | AO | AN Method | | | | | | NO Method |
| | | Before annihilation | | | After annihilation | | | |
		$\langle\rho\rangle_{UHF}$	$(\rho)_{SP}$	$(\rho)_{SD}$	$\langle\rho\rangle_{AA}$	$(\rho)_{SP}$	$(\rho)_{SD}$	$(\rho)_{SD}$
		A. Present						
		$\langle S^2\rangle=0.7565$			$\langle S^2\rangle=0.7500$			
C_1	$2S$	0.161	0.159	0.002	0.055	0.053	0.002	0.000
	$2P_x$	0.042	0.042	0.000	0.014	0.014	0.000	0.000
	$2P_y$	0.015	0.015	0.000	0.005	0.005	0.000	0.000
	$2P_z$	1.000	0.002	0.998	0.999	0.001	0.998	0.997
C_2	$2S$	−0.012	−0.012	0.000	−0.004	−0.004	0.000	0.000
	$2P_x$	−0.047	−0.048	0.001	−0.015	−0.016	0.001	0.000
	$2P_y$	0.000	0.000	0.000	0.000	0.000	0.000	0.000
	$2P_z$	−0.013	−0.013	0.000	−0.004	−0.004	0.000	0.000
	$3h$	−0.035	−0.035	0.000	−0.011	−0.012	0.000	0.000
	$4h$	−0.035	−0.035	0.000	−0.011	−0.012	0.000	0.000
	$5h, 6h$	0.054	0.014	0.040	0.044	0.005	0.040	0.039
	$7h$	−0.002	−0.002	0.000	−0.001	−0.001	0.000	0.000
		B. Pople, Beveridge, and Dobosh[b]						
		$\langle S^2\rangle=0.7573$			$\langle S^2\rangle=0.7500$			
C_1	$2S$	0.049	0.048	0.001	0.017	0.016	0.001	...
	$2P_x$	0.028	0.028	0.000	0.009	0.009	0.000	...
	$2P_y$	0.030	0.030	0.000	0.010	0.010	0.000	...
	$2P_z$	0.926	0.010	0.916	0.919	0.003	0.916	...
C_2	$2S$	−0.015	−0.015	0.000	−0.005	−0.005	0.000	...
	$2P_x$	−0.033	−0.033	0.000	−0.011	−0.011	0.000	...
	$2P_y$	−0.013	−0.012	0.001	−0.005	−0.004	0.001	...
	$2P_z$	−0.046	−0.048	0.002	−0.014	−0.016	0.002	...
	$3h$	−0.037	−0.037	0.000	−0.012	−0.012	0.000	...
	$4h$	−0.038	−0.038	0.000	−0.013	−0.013	0.000	...
	$5h, 6h$	0.075	0.035	0.040	0.051	0.012	0.040	...
	$7h$	0.003	0.003	0.000	0.001	0.001	0.000	...

[a] Geometry and numbering are illustrated in Fig. 1. [b] Reference 18.

this fact in the valence-bond languages.[bb] Some attention was also given to this point by Colpa and de Boer[3] and by Pople, Beveridge, and Dobosh,[18] but they estimated the SP contribution to the methyl-proton spin density from the one on the H_7 atom in the configuration illustrated in Fig. 1. Since there is no reason[20]

to believe that the SP mechanism has no angular dependence on the rotation about the C–C single bond, this kind of estimation of the SP mechanism is certainly erronious and leads to too small values.[21]

From Table VI, we notice that the INDO results are rather similar, except for the SP contribution in the $2S(C_1)$ AO, to those of the present authors. This is

[bb] The SP mechanism also shows a large angular dependence, and the manner of dependence is written to a good approximation as $(\rho)_{SP} = (\rho^0)_{SP} + (\rho^1)_{SP}\cos^2\theta$. This point will be discussed more fully in the near future.

[21] Colpa and de Boer[3] estimated about 3% SP contribution, and Pople, Beveridge, and Dobosh[18] estimated 7% SP contribution from the results quoted in Table VI.

TABLE VII. SP and SD mechanisms in vinyl radical.[a]

| Atom | AO | AN Method | | | | | | NO Method |
| | | Before annihilation | | | After annihilation | | | |
		$\langle\rho\rangle_{UHF}$	$(\rho)_{SP}$	$(\rho)_{SD}$	$\langle\rho\rangle_{aa}$	$(\rho)_{SP}$	$(\rho)_{SD}$	$(\rho)_{SD}$
		A. Present ($\angle CCH_a = 130°$)[b]						
		$\langle S^2\rangle = 0.7892$			$\langle S^2\rangle = 0.7503$			
C_a	$2S$	0.205	0.122	0.083	0.124	0.041	0.083	0.088
	$2P_x$	0.153	0.026	0.127	0.136	0.009	0.127	0.116
	$2P_y$	0.748	0.017	0.731	0.737	0.006	0.731	0.724
	$2P_z$	0.196	0.188	0.008	0.070	0.063	0.007	0.000
C_β	$2S$	−0.031	−0.035	0.004	−0.008	−0.012	0.004	0.008
	$2P_x$	−0.028	−0.033	0.005	−0.006	−0.011	0.005	0.001
	$2P_y$	−0.012	−0.014	0.002	−0.003	−0.005	0.002	0.000
	$2P_z$	−0.193	−0.198	0.005	−0.061	0.066	0.005	0.000
	h_s	0.044	0.009	0.035	0.038	0.003	0.035	0.052
	h_t	0.097	0.026	0.071	0.080	0.009	0.071	0.070
	h_a	−0.021	−0.042	0.021	0.006	−0.014	0.021	0.020
		B. Atherton and Hincliffe ($\angle CCH_a = 160°$)[c]						
		$\langle S^2\rangle = 0.7634$			$\langle S^2\rangle = 0.7501$			
C_a	$2S$	0.031	−0.006	0.037	0.035	−0.002	0.037	···
	$2P_x$	0.027	−0.007	0.034	0.031	−0.002	0.033	···
	$2P_y$	0.766	0.017	0.749	0.755	0.006	0.749	···
	h_s	0.115	0.055	0.060	0.079	0.018	0.060	···
	h_t	0.174	0.079	0.095	0.121	0.026	0.095	···
	h_a	0.028	0.011	0.017	0.020	0.004	0.016	···

[a] Geometry is given in Fig. 1.
[b] Reference 22.
[c] Reference 19.

very interesting, considering the large differences of these two methods. (See Refs. 16 and 18.)

Now, we discuss the spin densities of the vinyl radical.[22] In Table VII, the UHF spin densities and their mechanistic contributions calculated by the AN method are compared with those obtained from the NO method. As seen from the values given in the last two columns, the SD contributions calculated by these two methods agree satisfactorily except the ones in the h_s AO. The differences in these two set of values are attributed to the assumption $C_{1/2}^r \gg C_{1/2}^{\infty}$, $C_{3/2}^{\infty}$, and are nearly $100 \times (C^{\infty})^2/(C^{r\infty})$ % of the value of $\langle\rho\rangle_{UHF}$. (See Table IV.) Referring to Table III, the SD contributions calculated by the AN method agree satis-

factorily well with those obtained by the RHF wavefunction. Hence, the errors due to the two assumptions set in the previous section almost cancel in this case.

In the lower part of Table VII, the SP and SD contributions in the CNDO/2 results of Atherton and Hincliffe[19] are calculated by means of the AN method. Although the SD contributions obtained by both authors are rather similar, the SP contributions are quite different, especially in the AO's near the radical center atom. The most remarkable differences exist in the $2S(C_a)$ and h_a AO's, and both results differ even in sign. The most probable reason of these differences is that in the CNDO/2 method the one-center exchange repulsion integrals are neglected, while in the present method the one-center (and part of the two-center) σ–π-type exchange repulsion integrals, which are important to the SP mechanism, are included. (See Ref. 16.) Since, referring to Table III, the natural

[22] In the succeeding paper,[24] the angular configuration of vinyl radical is examined. The most probable configuration expected from both the potential curve and the calculated hfs constants is $\angle CCH_a = 135°$. (See Fig. 1.)

14

TABLE VIII. Normalized spin densities[a] and their SP and SD contributions in triplet state.[b]

Triplet state	Atom	AO	AN Method						NO Method
			Before annihilation			After annihilation			
			$\langle\rho\rangle_{UHF}$	$(\rho)_{SP}$	$(\rho)_{SD}$	$\langle\rho\rangle_{AA}$	$(\rho)_{SP}$	$(\rho)_{SD}$	$(\rho)_{SD}$
C_2H_4			$\langle S^2\rangle = 2.0109$			$\langle S^2\rangle = 2.0001$			
$(\pi\to\pi^*)^3$	C	$2S$	0.077	0.075	0.002	0.040	0.038	0.002	0.000
		$2P_x$	0.002	0.002	0.000	0.001	0.001	0.000	0.000
		$2P_y$	0.009	0.009	0.000	0.005	0.005	0.000	0.000
		$2P_z$	0.540	0.001	0.539	0.539	0.000	0.539	0.537
		h	−0.020	−0.020	0.000	−0.010	−0.010	0.000	0.000
H_2CO			$\langle S^2\rangle = 2.0188$			$\langle S^2\rangle = 2.0001$			
$(\pi\to\pi^*)^3$	C	$2S$	0.072	0.070	0.002	0.037	0.035	0.002	0.000
		$2P_z$	−0.009	−0.011	0.002	−0.003	−0.005	0.002	0.000
		$2P_y$	0.007	0.007	0.000	0.003	0.003	0.000	0.000
		$2P_x$	0.525	0.002	0.523	0.524	0.001	0.523	0.520
	O	$2S$	0.090	0.088	0.002	0.047	0.045	0.002	0.000
		$2P_z$	0.015	0.014	0.001	0.008	0.007	0.001	0.000
		$2P_y$	0.008	0.008	0.000	0.004	0.004	0.000	0.000
		$2P_x$	0.525	0.002	0.523	0.524	0.001	0.523	0.520
		h	−0.028	−0.028	0.000	−0.014	−0.014	0.000	0.000
H_2CO			$\langle S^2\rangle = 2.0232$			$\langle S^2\rangle = 2.0001$			
$(n\to\pi^*)^3$	C	$2S$	0.052	0.049	0.003	0.027	0.024	0.003	0.000
		$2P_x$	−0.013	−0.017	0.004	−0.005	−0.009	0.004	0.000
		$2P_y$	−0.006	−0.006	0.000	−0.003	−0.003	0.000	0.000
		$2P_z$	0.407	0.002	0.405	0.406	0.001	0.405	0.402
	O	$2S$	0.113	0.108	0.005	0.059	0.054	0.005	0.000
		$2P_z$	0.025	0.023	0.002	0.014	0.012	0.002	0.000
		$2P_y$	0.484	0.003	0.481	0.482	0.001	0.481	0.478
		$2P_z$	0.226	0.002	0.224	0.225	0.001	0.224	0.223
		h	0.017	−0.006	0.023	0.020	−0.003	0.023	0.022

[a] Reference 13.   [b] Geometries are given in Fig. 1.

orbital μ and the unpaired orbital of the RHF wavefunction are mainly composed of the $2P_z(C_\alpha)$ and $2P_y(C_\alpha)$ AO's, inclusion of these integrals is essential even in the σ-electron radicals like the vinyl radical, as in the π-electron radicals.[16]

B. Triplet State

The "spin-appearing" mechanisms in triplet states are very similar[23] as in doublet radicals, and the definition of these mechanisms is completely the same as in doublet radicals. (See Ref. 6.) Here, we apply the AN method to the UHF spin densities of some triplet

[23] A. D. McLachlan, Mol. Phys. 5, 53 (1962).

radicals such as the $\pi\to\pi^*$ triplet states of ethylene and formaldehyde and the $n\to\pi^*$ triplet state of formaldehyde. (The geometries are illustrated in Fig. 1.)

In Table VIII, the mechanistic contributions to the UHF spin densities in the triplet state calculated by the AN method are summarized and compared with the SD contributions calculated from the NO method. By comparing the SD contributions calculated by these two methods, the validity of the assumption $(C_{2/2}{}^{rf} \gg C_{2/2}{}^{ne}, C_{4/2}{}^{ne})$ is examined. The largest error is 0.005 in the $2S(O)$ AO in the $n\to\pi^*$ triplet state of formaldehyde, and is 4% of the value of $\langle\rho\rangle_{UHF}$. Moreover, the UHF spin densities in the AO's, where zero SD contributions are expected from the symmetry

requirement, satisfy the relation [Eq. (18)] $\rho_{UHF}{}^i = 2\rho_{a\,s}{}^i$ to good approximation.

In the present calculation of triplet states, their ground-state geometries are consistently used. Since the excited-state configurations are quite different[24] from the ground-state ones in the cases of ethylene and formaldehyde, the spin densities reported here do not correspond to the real ones. Nevertheless, the spin densities in the $\pi \rightarrow \pi^*$ triplet state of ethylene in the planar configuration has foremost importance in the study of $\pi \rightarrow \pi^*$ triplet states of conjugated hydrocarbons. The situation is very similar to that of the methyl radical in the study of conjugated radicals. Close similarities are found between the $\pi \rightarrow \pi^*$ triplet state of ethylene and the π-electron radical such as ethyl radical. Referring to Tables VI and VIII, we see that the ratios of the spin densities, $\rho_{2S(C)}/\rho_{2P_z(C)}$ and $\rho_h/\rho_{2P_z(C)}$, in the $\pi \rightarrow \pi^*$ triplet state of ethylene are closely similar to $\rho_{2S(C_1)}/\rho_{2P_z(C_1)}$ and $\rho_h/\rho_{2P_z(C_1)}$, in ethyl radical.

The unpaired orbitals of the $n \rightarrow \pi^*$ triplet state of formaldehyde are calculated by the RHF method to be

$$\psi_n = 0.9828 P_y(O) + 0.0206 P_y(C) - 0.2139(h_3 - h_4)$$

and

$$\psi_{\pi^*} = 0.8220 P_z(O) - 0.4173 P_z(C).$$

The n-type orbital is mainly localized on the $2P_y(O)$ AO and lies in the molecular plane, while the π^* orbital has its node in this plane. This situation is very interesting, namely, the $n \rightarrow \pi^*$ triplet state of formaldehyde

in this configuration has both characteristic features of the σ- and π-electron radicals, and may be regarded as the starting point for a study of the $n \rightarrow \pi^*$ triplet state of heteroconjugated molecules. A prominent difference between the spin densities of the planar $\pi \rightarrow \pi^*$ and $n \rightarrow \pi^*$ triplet states of formaldehyde exists in their proton spin densities. That of the former is negative in sign and that of the latter is positive in sign, and they are comparable in magnitude. The positive proton spin density in the $n \rightarrow \pi^*$ triplet state of formaldehyde is due to the delocalization of the n-type unpaired orbital ψ_n above.

IV. CONCLUSION

As seen in the previous sections, the validity of the AN method, proposed to separate the UHF spin densities into mechanistic contributions, is confirmed. Since the SP and SD mechanisms are quite different and very important origins of the spin density, the present method to calculate their contributions is very useful in order to clarify the nature of spin density. Note that, when the lowest contaminating spin state in the UHF wavefunction is annihilated to improve the spin density,[8] the information about the "spin-appearing" mechanisms is obtained at the same time by means of the AN method. The generalization of the method to any multiplicity is simple.[25] Some applications of the method to doublet radicals are given in the succeeding paper.[16]

[24] G. Herzberg, *Molecular Spectra and Molecular Structure* (D. Van Nostrand Co., Inc., New York, 1966), Vol. 3.

[25] H. Nakatsuji, H. Kato, and T. Yonezawa, "On the Unrestricted Hartree–Fock Wavefunction," J. Chem. Phys. (to be published).

PART I, CHAPTER 3

STUDIES ON

THE UNRESTRICTED

HARTREE-FOCK WAVEFUNCTION

On the Unrestricted Hartree-Fock Wavefunction

The unrestricted Hartree-Fock (UHF) wavefunction is analyzed and interpreted in configuration-interaction (CI) language. The results of the present study are as follows. (i) The UHF wavefunction includes only one type of the singly excited configurations [Eq. (20)], and thus the correlation effects included are very limited ones, compared with the usual CI treatment. (ii) The weight of the lowest contaminating spin function, included in the UHF wavefunction, decreases with increasing spin multiplicity. (iii) The annihilation of the lowest contaminating spin function little affects the electron density distributions and other physical quantities, the operators of which commute with the annihilation operator. (iv) In the UHF method, the "spin-appearing" (spin-polarization and spin-delocalization) mechanisms are clearly divided, and an approximate method to separate these contributions is generalized, and some discussions about spin annihilation are made.

I. INTRODUCTION

The unrestricted Hartree-Fock (UHF) method,[1] which takes account of correlation effects between electrons with different spins, has been extensively applied in the study of spin properties. Amos, Hall, and Snyder[2] examined the UHF wavefunction and connected it with the alternant molecular-orbital method and with the configuration-interaction method. Since the UHF wavefunction is not an eigenfunction of a spin-squared operator S^2, they proposed to annihilate the lowest contaminating spin function after energy minimization.[2] However, the validity of annihilation after energy minimization is still questionable,[3] and Sando and Harriman[4] compared the spin densities associated with the various SCF methods.

Here, the UHF wavefunction is analyzed and interpreted in configuration-interaction language by means of the natural orbitals of the UHF wavefunction.[2a] The charge-density and spin-density properties of the UHF wavefunction are studied and the generalization of the previous results,[5] which provides a useful procedure to separate the UHF spin densities into components due to the mechanistic contributions (spin-polarization and spin-delocalization contributions), are carried out. Some discussions about spin annihilation are made in the last section.

II. BASIC THEORY

The unrestricted single-determinantal wavefunction built up of the p α-spin and q β-spin orbitals is written as

$$\Psi_{UHF}=[(p+q)!]^{-1/2}\det\{\varphi_1\alpha\varphi_2\alpha\cdots\varphi_p\alpha\phi_1\beta\phi_2\beta\cdots\phi_q\beta\},$$

(1)

where φ_i and ϕ_i may be different, and we assume $p\geq q$ without loss of generality. The wavefunction (1) is an eigenfunction of an operator S_z, and its eigenvalue is $\frac{1}{2}s$ ($s=p-q$) in $\hbar$ units,

$$S_z\Psi_{UHF}=\frac{1}{2}s\Psi_{UHF}.$$

(2)

As shown by Amos and Hall,[2a] the unitary transformations of the unrestricted molecular orbitals (MO's) $\{\varphi_i\}$ and $\{\phi_i\}$ lead to the corresponding orbitals $\{\chi_i\}$ and $\{\eta_i\}$ which are orthonormal in each sets but have overlap between them when $i=j$,

$$\int \chi_i\eta_j d\tau = T_i\delta_{ij}.$$

(3)

By means of these corresponding orbitals, the UHF wavefunction is rewritten as[4c]

$$\Psi_{UHF}=[(p+q)!]^{-1/2}\det\{\chi_1\alpha\chi_2\alpha\cdots\chi_p\alpha\eta_1\beta\eta_2\beta\cdots\eta_q\beta\}.$$

(4)

where we omitted the unimportant constant factor introduced by the unitary transformation. Furthermore, these corresponding orbitals are connected with the natural orbitals λ, μ, and ν, of the UHF wavefunction by the following equations[2a]:

$$\chi_i=a_i\lambda_i+b_i\nu_i, \qquad i=1,\cdots,q,$$

$$\eta_i=a_i\lambda_i-b_i\nu_i, \qquad i=1,\cdots,q,$$

$$\chi_{q+i}=\mu_i, \qquad i=1,\cdots,s, \qquad (5)$$

[1] J. A. Pople and R. K. Nesbet, J. Chem. Phys. 22, 571 (1954).
[2] (a) A. T. Amos and G. G. Hall, Proc. Roy. Soc. (London) A263, 483 (1961); (b) A. T. Amos, Mol. Phys. 5, 91 (1962); (c) T. Amos and L. C. Snyder, J. Chem. Phys. 41, 1773 (1964); (d) L. C. Snyder and T. Amos, ibid. 42, 3670 (1965).
[3] W. Marshall, Proc. Phys. Soc. (London) A78, 113 (1961).
[4] (a) K. M. Sando and J. E. Harriman, J. Chem. Phys. 47, 180 (1967); (b) J. E. Harriman and K. M. Sando, ibid. 48, 5138 (1968); (c) see also J. E. Harriman, ibid. 40, 2827 (1964).
[5] (a) T. Yonezawa, H. Nakatsuji, T. Kawamura, and H. Kato, Chem. Phys. Letters 2, 454 (1968). (b) T. Yonezawa, H. Nakatsuji, T. Kawamura, and H. Kato, J. Chem. Phys. 51, 669 (1969).

where

$$a_i = [\tfrac{1}{2}(1+T_i)]^{1/2},$$
$$b_i = [\tfrac{1}{2}(1-T_i)]^{1/2}. \qquad (6)$$

These natural orbitals are orthogonal to each other and diagonalize the reduced density matrix[2a]

$$\rho(1\mid 2) = \sum_i^q (1+T_i)\lambda_i{}^*(1)\lambda_i(2)$$

$$+ \sum_i^q (1-T_i)\nu_i{}^*(1)\nu_i(2) + \sum_i^s \mu_i{}^*(1)\mu_i(2). \quad (7)$$

Note that the natural orbitals are not changed by projection. Only the occupation numbers are changed by projection.[4c] Moreover, the natural orbitals λ_i and μ_i are similar[2c,5] to the restricted Hartree–Fock MO's.[6]

By using Eq. (5), the UHF wavefunction [Eq. (4)] may be expanded in the form of the limited configuration interaction,[2c,7]

$$\Psi_{\mathrm{UHF}} = C_{s/2}{}^{\mathrm{rf}}\Psi_{s/2}{}^{\mathrm{rf}} + C^{\mathrm{se}}\Psi^{\mathrm{se}} + C^{\mathrm{de}}\Psi^{\mathrm{de}} + C^{\mathrm{te}}\Psi^{\mathrm{te}}\cdots, \quad (8)$$

where $\Psi_{s/2}{}^{\mathrm{rf}}$ is the normalized restricted function with eigenvalue of S^2, $\tfrac{1}{2}s(\tfrac{1}{2}s+1)$,

$$\Psi_{s/2}{}^{\mathrm{rf}} = \mid \lambda_1\alpha\lambda_1\beta\cdots\lambda_q\alpha\lambda_q\beta\mu_1\alpha\mu_2\alpha\cdots\mu_s\alpha \mid \quad (9)$$

and its coefficient is given by

$$C_{s/2}{}^{\mathrm{rf}} = \prod_{i=1}^q a_i{}^2. \quad (10)$$

Ψ^{se} and Ψ^{de} are the sums of the normalized singly excited and doubly excited configurations,

$$C^{\mathrm{se}}\Psi^{\mathrm{se}} = \sum_{i=1}^q C^{\mathrm{se}}(ii^*)\Psi^{\mathrm{se}}(ii^*), \quad (11)$$

$$C^{\mathrm{se}}(ii^*) = \sqrt{2}N_i a_i b_i,$$

$$\Psi^{\mathrm{se}}(ii^*) = \mid \lambda_1\alpha\lambda_1\beta\cdots\nu_i\lambda_i(1/\sqrt{2})$$
$$\times (\alpha\beta+\beta\alpha)\cdots\lambda_q\alpha\lambda_q\beta\mu_1\alpha\mu_2\alpha\cdots\mu_s\alpha \mid, \quad (12)$$

and

$$C^{\mathrm{de}}\Psi^{\mathrm{de}} = \sum_{i<j}^q \sum_j^q C^{\mathrm{de}}(ii^*;jj^*)\Psi^{\mathrm{de}}(ii^*;jj^*)$$

$$+ \sum_i^q C_{s/2}{}^{\mathrm{de}}(ii^*)\Psi_{s/2}{}^{\mathrm{de}}(ii^*), \quad (13)$$

$$C^{\mathrm{de}}(ii^*;jj^*) = 2a_i b_i a_j b_j N_{ij},$$

$$\Psi^{\mathrm{de}}(ii^*;jj^*) = \mid \lambda_1\alpha\lambda_1\beta\cdots\nu_i\lambda_i(1/\sqrt{2})(\alpha\beta+\beta\alpha)\cdots\nu_j\lambda_j$$
$$\times (1/\sqrt{2})(\alpha\beta+\beta\alpha)\cdots\lambda_q\alpha\lambda_q\beta\mu_1\alpha\cdots\mu_s\alpha \mid, \quad (14)$$

$$C_{s/2}{}^{\mathrm{de}}(ii^*) = b_i{}^2 N_i,$$

$$\Psi_{s/2}{}^{\mathrm{de}}(ii^*) = \mid \lambda_1\alpha\lambda_1\beta\cdots\nu_i\alpha\nu_i\beta\cdots\lambda_q\alpha\lambda_q\beta\mu_1\alpha\cdots\mu_s\alpha \mid,$$

[6] C. C. J. Roothaan, Rev. Mod. Phys. **32**, 179 (1960).
[7] R. Lefebvre, H. H. Dearman, and H. M. McConnell, J. Chem. Phys. **32**, 176 (1960).

where

$$N_i = \prod_{m=1(m\neq i)}^q a_m{}^2 = a_i{}^2 N_{ij},$$

$$N_{ij} = \prod_{m=1(m\neq i,j)}^q a_m{}^2.$$

The higher-order terms in Eq. (8) are written in the same manner as above. Note that the singly and doubly excited configurations given above are not eigenfunctions of the spin-squared operator S^2, except $\Psi_{s/2}{}^{\mathrm{de}}(ii^*)$.

III. SPIN FUNCTIONS INCLUDED IN THE UHF WAVEFUNCTION

As shown previously,[5b] the b_i values in Eq. (6) are very small and then the relation, $C_{s/2}{}^{\mathrm{rf}} > C^{\mathrm{se}} > C^{\mathrm{de}}\cdots$, may be expected in Eq. (8). Therefore, the correlation effects included in the UHF wavefunction may be attributed mainy to the singly excited configurations expressed by Eqs. (11) and (12). This was certainly true in the cases previously studied.[8] Here, we analyze this configuration and divide it into eigenfunctions with respect to the spin-squared operator S^2.

We rewrite the singly excited configuration as

$$\Psi^{\mathrm{se}}(ii^*) = \mid \lambda_1\alpha\lambda_1\beta\cdots\nu_i\lambda_i(1/\sqrt{2})$$
$$\times (\alpha\beta+\beta\alpha)\cdots\lambda_q\alpha\lambda_q\beta\mu_1\alpha\mu_2\alpha\cdots\mu_s\alpha \mid$$
$$= \mid \nu_i\lambda_i(1/\sqrt{2})(\alpha\beta+\beta\alpha)\mu_1\alpha\mu_2\alpha\cdots\mu_s\alpha \mid \quad (15)$$

for brevity. It includes $s+2$ singly occupied orbitals, and is the eigenfunction of the operator S_z with eigenvalue $\tfrac{1}{2}s$. This configuration $\Psi^{\mathrm{se}}(ii^*)$ may be expressed as

$$\Psi^{\mathrm{se}}(ii^*) = \zeta\Psi_{s/2}{}^{\mathrm{se}}(ii^*) + \xi\Psi_{(s/2)+1}{}^{\mathrm{se}}(ii^*), \quad (16)$$

where the functions satisfy the following eigenvalue problems:

$$S^2\Psi_{s/2}{}^{\mathrm{se}}(ii^*) = \tfrac{1}{2}s(\tfrac{1}{2}s+1)\Psi_{s/2}{}^{\mathrm{se}}(ii^*),$$

$$S_z\Psi_{s/2}{}^{\mathrm{se}}(ii^*) = \tfrac{1}{2}s\Psi_{s/2}{}^{\mathrm{se}}(ii^*), \quad (17)$$

$$S^2\Psi_{(s/2)+1}{}^{\mathrm{se}}(ii^*) = (\tfrac{1}{2}s+1)(\tfrac{1}{2}s+2)\Psi_{(s/2)+1}{}^{\mathrm{se}}(ii^*),$$

$$S_z\Psi_{(s/2)+1}{}^{\mathrm{se}}(ii^*) = \tfrac{1}{2}s\Psi_{(s/2)+1}{}^{\mathrm{se}}(ii^*). \quad (18)$$

Obviously, there is only one function which satisfies the relation (18). It is expressed as

$$\Psi_{(s/2)+1}{}^{\mathrm{se}}(ii^*) = (s+2)^{-1/2} \mid \nu_i\lambda_i\mu_1\cdots\mu_s$$

$$\times \{(\alpha\beta+\beta\alpha)\alpha\cdots\alpha + \alpha\alpha \sum_{j=1}^s \alpha\cdots\alpha\beta\alpha\cdots\alpha\} \mid, \quad (19)$$

where the second term in the braces means the sum

$$\sum_{j=1}^s \alpha\cdots\alpha\beta\alpha\cdots\alpha = \beta\alpha\alpha\cdots\alpha + \alpha\beta\alpha\cdots\alpha$$

$$+ \alpha\alpha\beta\cdots\alpha + \cdots + \alpha\alpha\alpha\cdots\beta.$$

[8] For example, see Tables IV and V of Ref. 5(b).

Now, we determine the function which satisfies Eq. (17). There are $s+1$ such functions. Note that *all* of these $s+1$ functions are considered in the usual CI treatment. However, as shown in the Appendix, *only one* function among them satisfies Eq. (16) and it is given by

$$\Psi_{s/2}{}^{se}(ii^*)$$

$$= (s+2)^{-1/2} \mid \nu_i\lambda_i\mu_1\cdots\mu_s\{(\tfrac{1}{2}s)^{1/2}(\alpha\beta+\beta\alpha)\alpha\cdots\alpha$$

$$- (2/s)^{1/2}\alpha\alpha \sum_i^s \alpha\cdots\alpha\beta\alpha\cdots\alpha\} \mid. \quad (20)$$

From Eqs. (19) and (20), the coefficients in Eq. (16) are given by

$$\zeta = [s/(s+2)]^{1/2}, \qquad \xi = [2/(s+2)]^{1/2}, \quad (21)$$

as shown in the Appendix. Then Eq. (16) becomes

$$\Psi^{se}(ii^*) = [s/(s+2)]^{1/2}\Psi_{s/2}{}^{se}(ii^*)$$

$$+ [2/(s+2)]^{1/2}\Psi_{(s/2)+1}{}^{se}(ii^*). \quad (22)$$

Equations (19), (20), and (22) show the nature of the correlation effects and of the contaminating spin function included in the UHF wavefunction: The correlation effect included in the UHF wavefunction is a very limited one, compared with the usual CI treatment. First, the UHF wavefunction includes only that type of singly excited configuration which is expressed by the transitions from λ_i to ν_i.[2e] Second, only one spin function [Eq. (20)] among the $s+1$ spin functions [see Eq. (A1) in Appendix] is considered in the UHF wavefunction.

Note the following two limiting cases; when $s=0$ (singlet case), Eq. (22) reduces to

$$\Psi^{se}(ii^*) = \Psi_1{}^{se}(ii^*), \quad (23)$$

which shows that the singly excited configurations included in the UHF wavefunction are *all* due to the contaminating (triplet) spin function. Pople, McIver, and Ostlund[9] exploited this fact in their finite perturbation methods. (Note that the spin-density operator and the spin-squared operator do not commute.) When $s = \infty$,

$$\Psi^{se}(ii^*) = \Psi_{s/2}{}^{se}(ii^*),$$

which shows that the singly excited configurations in the UHF wavefunction *do not* include the contaminating spin function. Since $\Psi_{s/2}{}^{rf}$ in Eq. (8) is the eigenfunction of S^2 with the eigenvalue $\tfrac{1}{2}s(\tfrac{1}{2}s+1)$, a conclusion is that the weight of the lowest contaminating spin state in the UHF wavefunction decreases with increasing spin multiplicity, $s+1$. However, as s increases, so decrease the correlation effects included in the UHF wavefunction, compared with the usual CI treatment. Of course, these discussions are valid only when the

[9] J. A. Pople, J. W. McIver, Jr., and N. S. Ostlund, J. Chem. Phys. 49, 2960, 2965 (1968).

singly excited configurations are important, as in the actual calculations reported previously.[5] However, for the spin-density calculations, only the singly excited configuration expressed by Eq. (20) is important, and the other s spin functions and the doubly excited and higher-order configurations in Eq. (8) do not contribute to the first-order approximation of a perturbation theory (see Appendix).

To the first-order approximation of a perturbation theory, the coefficient $C^{se}(ii^*)$ of Eq. (11) may be written as[2d]

$$C^{se}(ii^*) = \sqrt{2}N_ia_ib_i$$

$$= [s/(s+2)]^{1/2}$$

$$\times \frac{\langle \Psi_{s/2}{}^{rf} \mid \mathfrak{K} \mid \Psi_{s/2}{}^{se}(ii^*) \rangle}{E^{rf} - [s/(s+2)]E_{s/2}{}^{se}(ii^*) - [2/(s+2)]E_{(s/2)+1}{}^{se}},$$

$$(24)$$

where $\mathfrak{K}$ is a Hamiltonian operator. Note that in the calculation of the spin densities of the σ-type atomic orbitals of the π-electron radicals, the numerator of Eq. (24) reduces to the $\sigma-\pi$-type electron repulsion integrals.

IV. DENSITY

Here, we discuss the density properties of the UHF wavefunction. The UHF electron density at position $\mathbf{r}$ is calculated by applying the density operator

$$\mathbf{q}(\mathbf{r}) = \sum_k \delta(\mathbf{r}_k - \mathbf{r})$$

to Eq. (8),

$$q_{UHF}{}^r = \langle \Psi_{UHF} \mid \mathbf{q}(\mathbf{r}) \mid \Psi_{UHF} \rangle$$

$$= (C_{s/2}{}^{rf})^2 \langle \Psi_{s/2}{}^{rf} \mid \mathbf{q}(\mathbf{r}) \mid \Psi_{s/2}{}^{rf} \rangle$$

$$+ 2C^{se}C_{s/2}{}^{rf}\langle \Psi_{s/2}{}^{rf} \mid \mathbf{q}(\mathbf{r}) \mid \Psi^{se} \rangle$$

$$+ (C^{se})^2\langle \Psi^{se} \mid \mathbf{q}(\mathbf{r}) \mid \Psi^{se} \rangle + \cdots. \quad (25)$$

The second term in Eq. (25) is calculated by using Eqs. (9) and (12),

$$C^{se}\langle \Psi_{s/2}{}^{rf} \mid \mathbf{q}(\mathbf{r}) \mid \Psi^{se} \rangle$$

$$= \sum_i^q C^{se}(ii^*) \langle \Psi_{s/2}{}^{rf} \mid \mathbf{q}(\mathbf{r}) \mid \Psi^{se}(ii^*) \rangle$$

$$= \tfrac{1}{2} \sum_i^q C^{se}(ii^*) \{\lambda_i(\mathbf{r})\nu_i(\mathbf{r}) - \lambda_i(\mathbf{r})\nu_i(\mathbf{r})\}$$

$$= 0.$$

Similarly, all the off-diagonal elements included in the expansion (25) are zero. This is obvious from Eq. (7). Thus, Eq. (25) reduces to

$$q_{UHF}{}^r = (C_{s/2}{}^{rf})^2\langle \Psi_{s/2}{}^{rf} \mid \mathbf{q}(\mathbf{r}) \mid \Psi_{s/2}{}^{rf} \rangle$$

$$+ (C^{se})^2\langle \Psi^{se} \mid \mathbf{q}(\mathbf{r}) \mid \Psi^{se} \rangle + \cdots, \quad (26)$$

which includes only the diagonal elements.

19

As shown previously,[5b,8] the relation, $(C_{s/2}{}^{rl})^2 \gg (C^{\infty})^2$ holds fairly satisfactorily in the actual calculations. Therefore, Eq. (26) shows that the annihilation of the lowest contaminating spin function in the UHF wavefunction little affects the electron density distribution. This point was suggested by Amos,[2b] Harriman,[4c] and by the present authors.[10] Referring to Eq. (7), the above approximation, $(C_{s/2}{}^{rl})^2 \gg (C^{\infty})^2$, corresponds to omitting the second term in Eq. (7).

Note that the above conclusion is obtained more elegantly only from the knowledge that the charge-density operator commutes with the annihilation operator. This is easily generalized. Namely, all the UHF expectation values of the physical quantities, the operators of which commute with the annihilation operator, do not change much by annihilation, if $(C_{s/2}{}^{rl})^2 \gg [C_{(s/2)+1}{}^{\infty}(\hat{u}^*)]^2$.

V. SPIN DENSITY

The UHF method is frequently applied to the spin-density calculations. Especially in π-electron radicals the correlation effects are essential to interpret the observed ESR hfs constants. The UHF spin density at the position $\mathbf{r}$ is calculated by applying the following normalized spin-density operator[12]:

$$\varrho(\mathbf{r}) = S_z^{-1} \sum_k S_{zk}\delta(\mathbf{r}_k - \mathbf{r}),$$

which do not commute with the annihilation operator, to Eq. (8). The result is

$$\rho_{UHF}{}^r = \langle \Psi_{UHF} \mid \varrho(\mathbf{r}) \mid \Psi_{UHF}\rangle$$
$$= (C_{s/2}{}^{rl})^2 \langle \Psi_{s/2}{}^{rl} \mid \varrho(\mathbf{r}) \mid \Psi_{s/2}{}^{rl}\rangle$$
$$+ 2C^{\infty}C_{s/2}{}^{rl}\langle \Psi_{s/2}{}^{rl} \mid \varrho(\mathbf{r}) \mid \Psi^{\infty}\rangle$$
$$+ (C^{\infty})^2\langle \Psi^{\infty} \mid \varrho(\mathbf{r}) \mid \Psi^{\infty}\rangle + \cdots. \quad (27)$$

From Eqs. (4) and (5), $\rho_{UHF}{}^r$ is also written as

$$\rho_{UHF}{}^r = \frac{2}{S_z}\sum_{i=1}^{s} a_i b_i \lambda_i(\mathbf{r})\nu_i(\mathbf{r}) + (2S_z)^{-1}\sum_{i=1}^{s}\mu_i(\mathbf{r})^2. \quad (28)$$

Equation (28) is very simple and has clear physical meaning about the "spin-appearing" mechanisms.[5] The first term represents the contributions due to the "spin-polarization" (SP) mechanism, and the second term represents those due to the "spin-delocalization" (SD) mechanism. (The definitions of these terminologies were given previously.[13]) By calculating the terms in Eq. (27), we obtain the following descriptions

[10] See Table III of Ref. 11.
[11] T. Yonezawa, H. Nakatsuji, T. Kawamura, and H. Kato, Bull. Chem. Soc. Japan 42, No. 9 (1969).
[12] H. M. McConnell, J. Chem. Phys. 28, 1188 (1958).
[13] See Footnote 6 of Ref. 5(b).

for each of the mechanistic contributions:

$$(\rho_{UHF}{}^r)_{SD} = (2S_z)^{-1}\sum_{i=1}^{s}\mu_i(\mathbf{r})^2$$
$$= (C_{s/2}{}^{rl})^2\rho^r(rf\tfrac{1}{2}s \mid rf\tfrac{1}{2}s) + (C^{\infty})^2\rho^r(se \mid se)$$
$$+ (C^{de})^2\rho^r(de \mid de) + \cdots, \quad (29)$$

which contains only diagonal elements, and

$$(\rho_{UHF}{}^r)_{SP} = \frac{2}{S_z}\sum_{i=1}^{s}a_i b_i \lambda_i(\mathbf{r})\nu_i(\mathbf{r})$$
$$= 2C^{\infty}C_{s/2}{}^{rl}\rho^r(rf\tfrac{1}{2}s \mid se) + 2C^{de}C^{\infty}\rho^r(se \mid de)$$
$$+ 2C^{de}C^{te}\rho^r(de \mid te) + \cdots, \quad (30)$$

which contains only off-diagonal elements. $\rho^r(rf\tfrac{1}{2}s \mid se)$ is the matrix element between $\Psi_{s/2}{}^{rl}$ and Ψ^{∞} with respect to the normalized spin-density operator $\varrho(\mathbf{r})$.

VI. SPIN-APPEARING MECHANISMS

Here we derive the approximate equations which serve a useful procedure in the separation of the UHF spin densities into mechanistic (spin-polarization and spin-delocalization) contributions. For the special cases of doublet and triplet radicals, the results have already been reported.[5]

First, we assume that the second and higher terms in Eqs. (29) and (30) are negligibly small,

$$(\rho_{UHF}{}^r)_{SD} = (C_{s/2}{}^{rl})^2\rho^r(rf\tfrac{1}{2}s \mid rf\tfrac{1}{2}s), \quad (31a)$$
$$(\rho_{UHF}{}^r)_{SP} = 2C^{\infty}C_{s/2}{}^{rl}\rho^r(rf\tfrac{1}{2}s \mid se), \quad (31b)$$
$$\rho_{UHF}{}^r = (\rho_{UHF}{}^r)_{SD} + (\rho_{UHF}{}^r)_{SP}. \quad (31c)$$

By using Eq. (22), Eq. (8) is rewritten as

$$\Psi_{UHF} = C_{s/2}{}^{rl}\Psi_{s/2}{}^{rl} + C_{s/2}{}^{\infty}\Psi_{s/2}{}^{\infty} + C_{(s/2)+1}{}^{\infty}\Psi_{(s/2)+1}{}^{\infty}, \quad (32)$$

where

$$C_{s/2}{}^{\infty} = [s/(s+2)]^{1/2}C^{\infty},$$
$$C_{(s/2)+1}{}^{\infty} = [2/(s+2)]^{1/2}C^{\infty}. \quad (33)$$

From Eqs. (9), (19), and (20), the equation

$$\rho^r[rf\tfrac{1}{2}s \mid se(\tfrac{1}{2}s+1)] = (2/s)^{1/2}\rho^r(rf\tfrac{1}{2}s \mid se\tfrac{1}{2}s) \quad (34)$$

is obtained. By using Eqs. (32)–(34), the UHF spin density $(\rho_{UHF}{}^r)$ is written as

$$\rho_{UHF}{}^r = (C_{s/2}{}^{rl})^2\rho^r(rf\tfrac{1}{2}s \mid rf\tfrac{1}{2}s)$$
$$+ 2[1 + (2/s)]C_{s/2}{}^{rl}C_{s/2}{}^{\infty}\rho^r(rf\tfrac{1}{2}s \mid se\tfrac{1}{2}s). \quad (35)$$

Similarly, by assuming that the renormalization constant associated with the annihilation of the lowest contaminating spin function is very close to unity, the spin densities obtained after single annihilation (asa) and after annihilation (aa)[2] are given by

$$\rho_{asa}{}^r = (C_{s/2}{}^{rl})^2\rho^r(rf\tfrac{1}{2}s \mid rf\tfrac{1}{2}s)$$
$$+ 2(1 + s^{-1})C_{s/2}{}^{rl}C_{s/2}{}^{\infty}\rho^r(rf\tfrac{1}{2}s \mid se\tfrac{1}{2}s)$$

TABLE I. Ratios of $(\rho_{UHF})_{SP} : (\rho_{asa})_{SP} : (\rho_{aa})_{SP}$.

	Singlet $s=0$	Doublet $s=1$	Triplet $s=2$	Quartet $s=3$	Qunitet $s=4$	$\cdots$	$s=s$
$(\rho_{UHF})_{SP}$	2	3	4	5	6	$\cdots$	$s+2$
$(\rho_{asa})_{SP}$	1	2	3	4	5	$\cdots$	$s+1$
$(\rho_{aa})_{SP}$	0	1	2	3	4	$\cdots$	s

and

$$\rho_{aa}{}^r = (C_{s/2}{}^{rf})^2 \rho^r (rf\tfrac{1}{2}s \mid rf\tfrac{1}{2}s)$$
$$+ 2C_{s/2}{}^{rf}C_{s/2}{}^{se} \rho^r (rf\tfrac{1}{2}s \mid se\tfrac{1}{2}s). \quad (36)$$

By comparing Eqs. (35) and (36) with Eq. (31), the mechanistic contributions are derived. The *SP contribution* is given by using ρ_{UHF} and ρ_{aa} as

$$(\rho_{UHF})_{SP} = \tfrac{1}{2}s[1 + (2/s)](\rho_{UHF} - \rho_{aa}),$$
$$(\rho_{asa})_{SP} = \tfrac{1}{2}s(1 + s^{-1})(\rho_{UHF} - \rho_{aa}),$$
$$(\rho_{aa})_{SP} = \tfrac{1}{2}s(\rho_{UHF} - \rho_{aa}), \quad (37)$$

or, by using ρ_{UHF} and ρ_{asa} as

$$(\rho_{UHF})_{SP} = s[1 + (2/s)](\rho_{UHF} - \rho_{asa}),$$
$$(\rho_{asa})_{SP} = s(1 + s^{-1})(\rho_{UHF} - \rho_{asa}),$$
$$(\rho_{aa})_{SP} = s(\rho_{UHF} - \rho_{asa}). \quad (38)$$

The *SD contribution* is calculated from Eq. (31c) as

$$(\rho)_{SD} = \rho - (\rho)_{SP}. \quad (39)$$

Note the fact that the SP contributions to the spin densities associated with the various stages of annihilation satisfy the relation,

$$(\rho_{UHF})_{SP} : (\rho_{asa})_{SP} : (\rho_{aa})_{SP} = (s+2):(s+1):s \quad (40)$$

and

$$(\rho_{UHF})_{SD} = (\rho_{asa})_{SD} = (\rho_{aa})_{SD}. \quad (41)$$

Table I shows the above relation [Eq. (40)] for some examples.

For special case of $s=0$ (singlet state), Eqs. (37) and (38) cannot be applied. However, in this case, from Eq. (23), the spin densities are all due to the contaminating (triplet) spin function and are due only to the SP mechanism. By the similar procedure as above, the spin densities obtained at various stages of annihilation are shown to hold the relation,

$$\rho_{UHF} : \rho_{asa} : \rho_{aa} = 2:1:0. \quad (42)$$

This is the special case of Eq. (40).

VII. DISCUSSION

As may be noticed, Eq. (5) is very similar to the starting point of alternant molecular-orbital (AMO) method. λ_i and ν_i correspond to the bonding and antibonding AMO partners, respectively. Therefore, all the results obtained by the present study apply to the *unprojected* AMO method. The extensive studies of the AMO method were given by Löwdin, de Heer, and Pauncz.[14]

Now, we discuss the approximate method obtained in Sec. VI. Since the spin densities in the σ-type atomic orbitals of the π-electron radicals are due only to the SP mechanism, the approximate relation (40) holds for the total spin densities. Moreover, this relation may be used to check the validity of the approximations introduced in Sec. VI.[5,11] For example, in the "π-quartet" state of the allyl radical,[15] the values of

TABLE II. Spin density[a] in the "π-quartet" state of the allyl radical.[b]

Atom	AO	ρ_{UHF}	ρ_{aa}	ρ_{aa} from Eqs. (40), (41)
C_1, C_3	$2S$	0.051	0.031	0.031
	$2Px$	0.000	0.000	0.000
	$2Py$	0.003	0.002	0.002
	$2Pz$	0.355	0.354	0.355
C_2	$2S$	0.054	0.033	0.033
	$2Px$	0.000	0.000	0.000
	$2Py$	0.005	0.003	0.003
	$2Pz$	0.377	0.376	0.377
H_4, H_8	$1S$	−0.013	−0.008	−0.008
H_5, H_7	$1S$	−0.012	−0.007	−0.007
H_6	$1S$	−0.018	−0.010	−0.010

[a] About the method of calculation, see Ref. 13.
[b] Numbering of atoms is as follows:
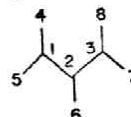
The geometry is C–C = 1.40 Å, C–H = 1.08 Å, and $\angle$HCH = $\angle$HCC = $\angle$CCC = 120°.

[14] (a) P.-O. Löwdin, Phys. Rev. 97, 1509 (1955); (b) R. Pauncz, J. de Heer, and P.-O. Löwdin, J. Chem. Phys. 36, 2247 (1962), and the succeeding papers; (c) R. Pauncz, *Alternant Molecular Orbital Method* (W. B. Saunders and Co., Philadelphia, Pa., 1967).
[15] Note that in the "π-quartet" state of the allyl radical, the order of the proton spin densities (absolute values) is $H_6 > H_4 > H_5$, but, on the other hand, in the doublet allyl radical, it is $H_5 > H_4 > H_6$ and is reverse to the above. (Ref. 11.)

ρ_{aa} are compared with those calculated by Eqs. (40) and (41) from ρ_{UHF} (Table II). They agree very satisfactorily. For some doublet and triplet radicals, the examination of the method described in Sec. VI is carried out more rigorously in the previous reports.[5]

Equations (40) and (41) show approximately the theoretical relations existing among ρ_{UHF}, ρ_{aaa}, and ρ_{aa}. Thus, at present, we think it almost meaningless to discuss theoretically whether the annihilation of the lowest contaminating spin function "improves" the spin-density properties. For example, in the methyl radical, the spin densities in the σ-type atomic orbitals are due only to the SP mechanism,[5a,11] then the relation,

$$\rho_{UHF}:\rho_{aaa}:\rho_{aa}=3:2:1,$$

can be expected transcendentally. The computational examination of the validity of projection after energy minimization is carried out by Harriman and Sando.[4] They reported that the spin densities obtained by the spin-extended SCF calculations are generally (but not always) closer to the unrestricted values.[4]

Another important aspect of the spin-density calculations (especially in the semiempirical ones) lies in their agreement with experiments. From the above standpoint and from Eq. (24), the problem, "which stages of annihilation are best recommended," depends very much on the choice of the integral values (especially on the choice of the $\sigma-\pi$-type electron repulsion integrals).[16] In the conventional (semiempirical) calculations of the hfs constants (a), it may be approved to consider A of the following equation:

$$a=A\rho,$$

as a proportionality constant determined by "best fitting" the calculated spin densities with the observed hfs constants.[11,17] However, from Eqs. (24), (40), and (41), we think it very difficult to determine both the values of A_{UHF} and A_{aa}, which reproduce satisfactorily the observed hfs constants from ρ_{UHF} and ρ_{aa}, respectively. A good example is the ethyl radical. Its methylene-group proton spin density is due only to the SP mechanism, and thus $(\rho_{UHF})_{CH_2}=3(\rho_{aa})_{CH_2}$,[11,18] while its methyl-group proton spin density (assuming free rotation) is due to both (SP and SD) mechanisms, and thus, $(\rho_{UHF})_{CH_3}\simeq1.2(\rho_{aa})_{CH_3}$ in our calculation[11] and $(\rho_{UHF})_{CH_3}\simeq1.4(\rho_{aa})_{CH_3}$ in the Pople, Beveridge, and Dobosh's calculation.[18] This example shows that if one adjusts the semiempirical ($\sigma-\pi$-type) repulsion integrals[16] so as to obtain a good correlation of the

[16] See the paragraph which includes Eq. (24).
[17] (a) J. A. Pople, D. L. Beveridge, and P. A. Dobosh, J. Am. Chem. Soc. 90, 4201 (1968); (b) D. L. Beveridge and P. A. Dobosh, J. Chem. Phys. 48, 5532 (1968).
[18] J. A. Pople, D. L. Beveridge, and P. A. Dobosh, J. Chem. Phys. 47, 2026 (1967).

UHF spin densities with the observed hfs constants, then only A_{UHF} is acceptable in the least-mean-square sense (and vice versa).[11]

For some doublet and triplet radicals, the method stated in Sec. VI has been applied in order to clarify the "spin-appearing" mechanisms, and threw a new light on the nature of spin density.[5,11]

APPENDIX

Here we determine the spin function which satisfies Eq. (17). There are $s+1$ such functions. The spin parts of them may be written as[19]

$$\Theta_{\frac{1}{2}s,\frac{1}{2}s;1}=(1/\sqrt{2})(\alpha\cdots\alpha\beta\alpha-\alpha\cdots\alpha\alpha\beta),$$

$$\Theta_{\frac{1}{2}s,\frac{1}{2}s;2}=6^{-1/2}(2\alpha\cdots\beta\alpha\alpha-\alpha\cdots\alpha\beta\alpha-\alpha\cdots\alpha\alpha\beta),$$

$$\vdots$$

$$\Theta_{\frac{1}{2}s,\frac{1}{2}s;s}=[s(s+1)]^{-1/2}(s\alpha\beta\alpha\cdots\alpha-\alpha\alpha\beta\cdots\alpha-\cdots$$
$$-\alpha\cdots\beta\alpha\alpha-\alpha\cdots\alpha\beta\alpha-\alpha\cdots\alpha\alpha\beta),$$

$$\Theta_{\frac{1}{2}s,\frac{1}{2}s;s+1}=[(s+1)(s+2)]^{-1/2}[(s+1)\beta\alpha\alpha\cdots\alpha-\alpha\beta\alpha\cdots\alpha$$
$$-\cdots-\alpha\cdots\beta\alpha\alpha-\alpha\cdots\alpha\beta\alpha-\alpha\cdots\alpha\alpha\beta]. \quad (A1)$$

Among the above functions, we need only the functions which satisfy the following two demands: (a) The first two terms must have the form, $(\alpha\beta+\beta\alpha)\alpha\cdots\alpha$, except for a constant factor, (b) it must satisfy Eq. (16) with Eq. (19). From demand (a) only the last two functions are important. By taking linear combinations of these two functions, we obtain

$$[s/2(s+1)]^{1/2}\Theta_{s/2,s/2;s}-[(s+2)/2(s+1)]^{1/2}\Theta_{s/2,s/2;s+1}$$
$$=1/\sqrt{2}(\alpha\beta-\beta\alpha)\alpha\cdots\alpha \quad (A2)$$

and

$$[(s+2)/2(s+1)]^{1/2}\Theta_{s/2,s/2;s}+[s/2(s+1)]^{1/2}\Theta_{s/2,s/2;s+1}$$
$$=(s+2)^{-1/2}[(\tfrac{1}{2}s)^{1/2}(\alpha\beta+\beta\alpha)\alpha\cdots\alpha$$
$$-(2/s)^{1/2}\alpha\alpha\sum_{j}\alpha\cdots\alpha\beta\alpha\cdots\alpha]. \quad (A3)$$

Between the above two functions, only the second satisfies the demands (a) and (b). Then, Eq. (20) follows.

From Eqs. (19) and (20), the coefficients ζ and ξ in Eq. (16) are determined. By comparing Eq. (16) with Eqs. (19) and (20), we obtain the following two relations:

$$(s+2)^{-1/2}[\xi+(\tfrac{1}{2}s)^{1/2}\zeta]=1/\sqrt{2},$$

and

$$(s+2)^{-1/2}[\xi-(2/s)^{1/2}\zeta]=0,$$

Thus, Eq. (21) follows.

[19] See, for example, M. Kotani, A. Amemiya, E. Ishiguro, and T. Kimura, *Tables of Molecular Integrals* (Maruzen Co., Ltd., Tokyo, Japan, 1963), p. 5.

PART I, CHAPTER 4

STUDIES ON

THE ORBITAL MODEL

IN

THE SPIN-CORRELATION PROBLEM

Studies on the Orbital Model in the Spin-Correlation

Problem

I. INTRODUCTION

There are several methods which stand essentially on the orbital model and which are used to calculate spin-correlation effects in open-shell electronic structure. Among these, the unrestricted, the projected (or annihilated) unrestricted, and the spin-extended Hartree-Fock theories are the representstive.[1] The unrestricted Hartree-Fock (UHF) wavefunction is a single determinant in which different orbitals are allowed for different spins. However objections can be raised to spin-density calculations with this method since its wavefunction is not an eigenfunction of S^2. The projected (or annihilated) unrestricted Hartree-Fock (PUHF) wavefunction is the spin-projected (or spin-annihilated) function of the UHF wavefunction after energy minimization. Then, this wavefunction does not satisfy the variation condition. The spin-extended Hartree-Fock (SEHF) wavefunction is the function which minimize the energy after spin-projection of a single determinant. Thus, the SEHF method is the best among these three methods.

In the previous paper,[2] we analyzed the UHF wavefunction in configuration-interaction (CI) language to first order and showed a simple relation existing between the UHF and the PUHF wavefunctions. From this, we found a simple method to separate the spin density calculated with the UHF method into contributions due to spin-polarization and spin-delocalization mechanisms.[2, 3a] Because of the physical symplicity and visuality of each mechanism, more profound understandings than before on the nature of spin

23

density have become possible.[3b]

In the present study, our aim is to clarify the theoretical features of these orbital models of the open-shell electronic structure and to examine their applicabilities (or limitations) in the spin-correlation problem, refering the physical reality of the correlation phenomena in open-shell electronic systems.[4]

In the following two sections, we present the perturbation-variational description of the UHF and the SEHF wavefunctions to first order, taking the restricted Hartree-Fock (RHF) wavefunction[5] as a starting point. These results on the orbital models are compared in Section IV with the first-order perturbation theory. The interconnection of the UHF, PUHF and SEHF orbital theories for open-shell electronic systems becomes clear in conjunction with the first order sum-over-state perturbation theory starting from the RHF wavefunction. Interrelation in the spin densities obtained from these four orbital theories is also given. In Section V, the accuracy of the expectation values of the one-electron operators using these orbital models is investigated for both closed and open-shell electronic systems. Then, in Section VI, the examination of orbital model for the spin-correlation problem is carried out in the light of the physical reality of the correlation phenomena in open-shell electronic systems. Lastly in Section VII, two methods are suggested to overcome the limitation of the orbital model for the spin-correlation problem in open-shell electronic systems.

II. PERTURBATION-VARIATIONAL DESCRIPTION OF THE UHF WAVEFUNCTION

The starting wavefunction of the present study is the RHF single determinant built up from q closed orbitals and s (= p-q) open orbitals,

$$^s\Psi_0 = |\,\psi_1\bar\psi_1 \cdots \psi_k\bar\psi_k \cdots \psi_q\bar\psi_q\,\psi_{q+1} \cdots \psi_m \cdots \psi_p\,| \qquad (1)$$

which is an eigenfunction of the operators S^2 and S_z with eigenvalues $\frac{s}{2}\left(\frac{s}{2}+1\right)$ and $\frac{1}{2}s$, respectively. In the followings, k,l refer to closed orbitals, m, n to open orbitals, t, u to vacant orbitals and i,j to general orbitals. The important feature of the RHF wavefunction given in Eq. (1) is the following Brillouin theorem. Consider the one-electron excited functions of the forms;

$$^s\Psi_k{}^t(1) = |\,\psi_1\bar\psi_1 \cdots \psi_t\psi_k\tfrac{1}{\sqrt2}(\alpha\beta-\beta\alpha) \cdots \psi_q\bar\psi_q\,\psi_{q+1} \cdots \psi_p\,|,$$

$$^s\Psi_k{}^m = |\,\psi_1\bar\psi_1 \cdots \psi_k\bar\psi_m \cdots \psi_q\bar\psi_q\,\psi_{q+1} \cdots \psi_p\,|, \qquad (2)$$

$$^s\Psi_m{}^t = |\,\psi_1\bar\psi_1 \cdots \psi_q\bar\psi_q\,\psi_{q+1} \cdots \psi_{m-1}\psi_t\psi_{m+1} \cdots \psi_p\,|,$$

then, the Hamiltonian matrix elements between $^s\Psi_0$ and the configurations given in Eq.(2) becomes zero:

$$\langle\,^s\Psi_0|\,\mathcal{H}\,|\,^s\Psi_k{}^t(1)\rangle = 0,$$

$$\langle\,^s\Psi_0|\,\mathcal{H}\,|\,^s\Psi_k{}^m\rangle = 0, \qquad (3)$$

$$\langle\,^s\Psi_0|\,\mathcal{H}\,|\,^s\Psi_m{}^t\rangle = 0.$$

The UHF single determinant built up from p α-spin and q ß-spin orbitals is written as

$$\Psi_{UHF} = |\,\phi_1^\alpha\bar\phi_1^\beta \cdots \phi_k^\alpha\bar\phi_k^\beta \cdots \phi_q^\alpha\bar\phi_q^\beta\,\phi_{q+1}^\alpha \cdots \phi_m^\alpha \cdots \phi_p^\alpha\,|, \qquad (4)$$

which is an eigenfunction of S_z with eigenvalue $\frac{s}{2}$, but not an eigenfunction of S^2. Note that Ψ_{UHF} is independent of the unitary transformations within the α-spin and ß-spin orbitals except an unimportant constant factor. This stands also for the RHF wave-

25

function of Eq. (1) for the unitary transformations within the closed and open orbitals. After relevant unitary transformations, the difference between UHF and RHF orbitals becomes very small.[6] We set these differences as $f_i{}^\alpha$ and $f_i{}^\beta$.

$$\phi_i{}^\alpha = \psi_i + f_i{}^\alpha ; \qquad i = 1, \text{---} , p;$$
$$\phi_i{}^\beta = \psi_i + f_i{}^\beta ; \qquad i = 1, \cdots , q. \qquad (5)$$

In the treatment below, it is more convenient to substitute,

$$\Delta_k = \tfrac{1}{2}(f_k{}^\alpha + f_k{}^\beta),$$
$$\pi_k = \tfrac{1}{2}(f_k{}^\alpha - f_k{}^\beta), \qquad k = 1, \cdots, q. \qquad (6)$$

Then, Eq. (5) becomes

$$\phi_k{}^\alpha = \psi_k + \pi_k + \Delta_k ,$$
$$\phi_k{}^\beta = \psi_k - \pi_k + \Delta_k , \qquad k = 1, \cdots, q \qquad (7)$$
$$\phi_m{}^\alpha = \psi_m + f_m{}^\alpha ,$$

where π_k represents the polarization correction to orbital ψ_k.

In the UHF method, the total energy expressed by

$$E_{UHF} = \langle \Psi_{UHF} | \mathcal{H} | \Psi_{UHF} \rangle / \langle \Psi_{UHF} | \Psi_{UHF} \rangle \qquad (8)$$

is minimized to all orders of the independent orbital corrections $f_k{}^\alpha$ and $f_k{}^\beta$ and therefore, to all orders of the independent corrections π_k, Δ_k and $f_m{}^\alpha$. The treatment given below in this section is similar to that used by Ditchfield et al.[7] in the analysis of the finite perturbation theory.[8]

Since our main interest of the present paper lies in the spin-correlation correction which comes chiefly from the first-oder correction to the RHF wavefunction, it may be sufficient to minimize the energy correct to second order in π_k, Δ_k and $f_m{}^\alpha$.[9] Inserting Eq. (7) to Eq. (6) and expanding it up to second order,

we obtain the expression except normalization factor,

$$\Psi_{UHF} = {}^{s}\Psi_0 + \sum_{k}^{c} | \psi_1 \bar{\psi}_1 \cdots \pi_k \psi_k (\alpha\beta + \beta\alpha) \cdots \psi_{\zeta} \bar{\psi}_{\zeta} \psi_{\zeta+1} \cdots \psi_P |$$

$$+ \sum_{k}^{c} | \psi_1 \bar{\psi}_1 \cdots \Delta_k \psi_k (\alpha\beta - \beta\alpha) \cdots \psi_{\zeta} \bar{\psi}_{\zeta} \psi_{\zeta+1} \cdots \psi_P |$$

$$+ \sum_{m}^{0} | \psi_1 \bar{\psi}_1 \cdots \psi_{\zeta} \bar{\psi}_{\zeta} \psi_{\zeta+1} \cdots f_m^{\alpha} \cdots \psi_P |$$

$$+ \sum_{k}^{c} \Big\{ | \psi_1 \bar{\psi}_1 \cdots \Delta_k \bar{\Delta}_k \cdots \psi_{\zeta} \bar{\psi}_{\zeta} \psi_{\zeta+1} \cdots \psi_P | - | \psi_1 \bar{\psi}_1 \cdots \pi_k \bar{\pi}_k \cdots \psi_{\zeta} \bar{\psi}_{\zeta} $$
$$\times \psi_{\zeta+1} \cdots \psi_P | \Big\}$$

$$+ \sum_{k}^{c} | \psi_1 \bar{\psi}_1 \cdots \pi_k \Delta_k (\alpha\beta + \beta\alpha) \cdots \psi_{\zeta} \bar{\psi}_{\zeta} \psi_{\zeta+1} \cdots \psi_P |$$

$$+ \sum_{k<\ell}^{c}\sum^{c} \Big\{ | \psi_1 \bar{\psi}_1 \cdots \pi_k \psi_k (\alpha\beta + \beta\alpha) \cdots \pi_{\ell} \psi_{\ell} (\alpha\beta + \beta\alpha) \cdots \psi_{\zeta} \bar{\psi}_{\zeta} \psi_{\zeta+1} \cdots \psi_P | $$
$$+ | \psi_1 \bar{\psi}_1 \cdots \Delta_k \psi_k (\alpha\beta - \beta\alpha) \cdots \Delta_{\ell} \psi_{\ell} (\alpha\beta - \beta\alpha) \cdots \psi_{\zeta} \bar{\psi}_{\zeta} \psi_{\zeta+1} \cdots \psi_P | \Big\}$$

$$+ \sum_{k}^{c}\sum_{\ell(\neq k)}^{c} | \psi_1 \bar{\psi}_1 \cdots \pi_k \psi_k (\alpha\beta + \beta\alpha) \cdots \Delta_{\ell} \psi_{\ell} (\alpha\beta - \beta\alpha) \cdots \psi_{\zeta} \bar{\psi}_{\zeta} \psi_{\zeta+1} \cdots \psi_P |$$

$$+ \sum_{k}^{c}\sum_{m}^{0} \Big\{ | \psi_1 \bar{\psi}_1 \cdots \pi_k \psi_k (\alpha\beta + \beta\alpha) \cdots \psi_{\zeta} \bar{\psi}_{\zeta} \psi_{\zeta+1} \cdots f_m^{\alpha} \cdots \psi_P | $$
$$+ | \psi_1 \bar{\psi}_1 \cdots \Delta_k \psi_k (\alpha\beta - \beta\alpha) \cdots \psi_{\zeta} \bar{\psi}_{\zeta} \psi_{\zeta+1} \cdots f_m^{\alpha} \cdots \psi_P | \Big\}$$

$$+ \sum_{m<n}^{0}\sum^{0} | \psi_1 \bar{\psi}_1 \cdots \psi_{\zeta} \bar{\psi}_{\zeta} \psi_{\zeta+1} \cdots f_m^{\alpha} \cdots f_n^{\alpha} \cdots \psi_P |$$

$$+ \text{(higher order term)}. \tag{9}$$

Now, let's expand the orbital corrections π_k, Δ_k and f_m^{α} by means of the complete set of the RHF orbitals $\{\psi_i\}$. From the anti-symmetric property of determinant, the expansions become;

$$\pi_k = \sum_{t}^{V} a_{kt} \psi_t, \qquad \Delta_k = \sum_{t}^{V} b_{kt} \psi_t, \qquad f_m^{\alpha} = \sum_{t}^{V} c_{mt} \psi_t \tag{10}$$

where t runs over the vacant orbitals. Insertion of Eq. (10) into Eq. (9) gives the UHF wavefunction correct to second order in orbital corrections, which is given in Eq. (A-1) of Appendix. Among the first-order configurations, Ψ_k^t, ${}^{s}\Psi_k^{t}{}^{(1)}$ and ${}^{s}\Psi_m^t$ given in Appendix, the most important configuration Ψ_k^t given by

27

$$\Psi_k^t = | \psi_1 \bar{\psi}_1 \cdots \psi_t \psi_k (\alpha\beta + \beta\alpha)/\sqrt{2} \cdots \psi_g \bar{\psi}_g \psi_{g+1} \cdots \psi_p | \quad (11)$$

is not an eigenfunction of S^2, and can be rewritten as the sum of the spin-eigenfunctions,[2]

$$\Psi_k^t = \left(\frac{s}{s+2}\right)^{1/2} {}^s\Psi_k^t(2) + \left(\frac{2}{s+2}\right)^{1/2} {}^{s+2}\Psi_k^t, \quad (12)$$

where the configurations, ${}^s\Psi_k^t(2)$ and ${}^{s+2}\Psi_k^t$ satisfies

$$S^2 \, {}^s\Psi_k^t(2) = \frac{s}{2}\left(\frac{s}{2}+1\right) {}^s\Psi_k^t(2), \qquad S^2 \, {}^{s+2}\Psi_k^t = \left(\frac{s}{2}+1\right)\left(\frac{s}{2}+2\right) {}^{s+2}\Psi_k^t \quad (13)$$

and is given by

$${}^s\Psi_k^t(2) = (s+2)^{-1/2} | \psi_t \psi_k \psi_{g+1} \cdots \psi_p \{ \left(\tfrac{s}{2}\right)^{1/2}(\alpha\beta + \beta\alpha)\alpha \cdots \alpha - \left(\tfrac{2}{s}\right)^{1/2}\alpha\alpha \sum_d^{\frac{s}{2}} \alpha \cdots \alpha\beta\alpha\cdots\alpha \} |, \quad (14\text{-}a)$$

$${}^{s+2}\Psi_k^t = (s+2)^{-1/2} | \psi_t \psi_k \psi_{g+1} \cdots \psi_p \{ (\alpha\beta + \beta\alpha)\alpha \cdots \alpha + \alpha\alpha \sum_d^{s} \alpha\cdots\alpha\beta\alpha\cdots\alpha \} | \quad (14\text{-}b)$$

In Eq. (16), we used the abbreviations like;

$$| \psi_1 \bar{\psi}_1 \cdots \psi_t \psi_k (\alpha\beta + \beta\alpha) \cdots \psi_g \bar{\psi}_g \psi_{g+1} \cdots \psi_p | \equiv | \psi_t \psi_k \psi_{g+1} \cdots \psi_p (\alpha\beta + \beta\alpha)\alpha \cdots \alpha | .$$

Note that the configuration (14-b) is the main spin-contaminating configuration of the UHF wavefunction. Then the effects of spin-annihilation and spin-projection[11] on the UHF spin density can be analyzed approximately by starting from Eq. (14).[2]

The UHF total energy correct to second order in π_k, Δ_k and f_m^α is obtained from Eq. (8) by using Eq. (11) and the Brillouin theorem shown in Eq. (3). The final result is given in Eq. (A-3) of Appendix. From the variation theorem, we can require the expansion coefficients, a_{kt}, b_{kt} and c_{mt}, which make the second order energy given in (A-3) stationary. Firstly, by differentiating this with respect to a_{kt}, we obtain

$$\frac{1}{2}\frac{d^{(2)}E_{UHF}}{d\,a_{kt}} = 2a_{kt}\left\{ \left[\frac{s}{s+2} {}^sE_k^t(2) + \frac{2}{s+2} {}^{s+2}E_k^t \right] - E_0 - K_{kt} \right\}$$

$$- \sum_m^0 (mt \mid km)$$

$$+ \sum_{\ell(\neq k)}^{c} a_{\ell t} \left[\sum_{m}^{0} (km|\ell m) - (k\ell|tt) - (kt|\ell t) \right]$$

$$+ \sum_{u(\neq t)}^{V} a_{ku} \left[\sum_{m}^{0} (tm|um) - (tu|kk) - (tk|uk) \right]$$

$$- \sum_{\ell(\neq k)}^{c} \sum_{u(\neq t)}^{V} a_{\ell u} \left[(tu|\ell k) + (ku|\ell t) \right]$$

$$+ b_{kt} \sum_{m}^{0} (K_{mk} - K_{mt})$$

$$+ \sum_{\ell(\neq k)}^{c} b_{\ell t} \left[\sum_{m}^{0} (km|\ell m) \right] - \sum_{u(\neq t)}^{V} b_{ku} \left[\sum_{m}^{0} (tm|um) \right]$$

$$+ \sum_{m}^{0} c_{mt} \left[\sum_{n}^{0} (mn|kn) - (mk|tt) - (kt|mt) \right]$$

$$- \sum_{m}^{0} \sum_{u(\neq t)}^{V} c_{mu} \left[(tu|mk) + (ku|mt) \right]$$

$$= 0 \tag{16}$$

Secondly, by differeratiating with respect to b_{kt}, we obtain,

$$\frac{1}{2} \frac{d^{(2)}E_{UHF}}{d b_{kt}} = 2 b_{kt} \left\{ {}^{S}E_{k}{}^{t}{}_{(1)} - E_{0} + K_{kt} \right\}$$

$$+ \sum_{\ell(\neq k)}^{c} b_{\ell t} \left[\sum_{m}^{0} (km|\ell m) - (k\ell|tt) + 3(t\ell|kt) \right]$$

$$+ \sum_{u(\neq t)}^{V} b_{ku} \left[\sum_{m}^{0} (tm|um) - (tu|kk) + 3(kt|uk) \right]$$

$$+ \sum_{\ell(\neq k)}^{c} \sum_{u(\neq t)}^{V} b_{\ell u} \left[4(tk|\ell u) - (tu|\ell k) - (ku|\ell t) \right]$$

$$+ a_{kt} \sum_{m}^{0} (K_{mk} - K_{mt})$$

$$+ \sum_{\ell(\neq k)}^{c} a_{\ell t} \left[\sum_{m}^{0} (\ell m|km) \right] - \sum_{u(\neq t)}^{V} a_{ku} \left[\sum_{m}^{0} (um|tm) \right]$$

$$+ \sum_{m}^{0} c_{mt} \left[\sum_{n}^{0} (mn|kn) - (mk|tt) + 3(kt|mt) \right]$$

$$+ \sum_{m}^{0} \sum_{u(\neq t)}^{V} c_{mu} \left[4(tk|mu) - (tu|mk) - (mt|ku) \right]$$

$$= 0 \tag{17}$$

Thirdly, by differentiating with respect to c_{mt}, we obtain,

$$\frac{d^{(2)}E_{uHF}}{d\,c_{mt}} = 2\,C_{mt}\,({}^{s}E_m^t - E_0)$$

$$+ \sum_{n(\neq m)}^{0} c_{nt}\left[\frac{1}{2}\sum_i^{0}(im|in) - (mn|tt) + (mt|nt)\right]$$

$$+ \sum_{u(\neq t)}^{V} c_{mu}\left[\frac{1}{2}\sum_n^{0}(nt|un) - (tu|mm) + (mt|mu)\right]$$

$$+ \sum_{n(\neq m)}^{0}\sum_{u(\neq t)}^{V} c_{nu}\left[2(mt|nu) - (mn|tu) - (mu|nt)\right]$$

$$+ 2\sum_k^{c} a_{kt}\left[\sum_n^{0}(mn|kn) - (mk|tt) - (kt|mt)\right]$$

$$- 2\sum_k^{c}\sum_{u(\neq t)}^{V} a_{ku}\left[(tu|mk) - (kt|mu)\right]$$

$$+ 2\sum_k^{c} b_{kt}\left[\sum_n^{0}(mn|kn) - (mk|tt) + 3(kt|mt)\right]$$

$$+ 2\sum_k^{c}\sum_{u(\neq t)}^{V} b_{ku}\left[4(ku|mt) - (tu|mk) - (mu|kt)\right]$$

$$= 0 \qquad\qquad\qquad (18)$$

In the above equation,

$$(ij|k\ell) = \iint \psi_i^*(1)\,\psi_j(1)\,1/r_{12}\,\psi_k^*(2)\,\psi_\ell(2)\,d\tau_1\,d\tau_2 ,$$

and E_0, ${}^{s}E_k^t(1)$, ${}^{s}E_k^t(2)$, ${}^{s+2}E_k^t$ and ${}^{s}E_m^t$ are the energies correspond-ing to the configurations ${}^{s}\Psi_0$, ${}^{s}\Psi_k^t(1)$, ${}^{s}\Psi_k^t(2)$, ${}^{s+2}\Psi_k^t$ and ${}^{s}\Psi_m^t$, respectively.

By using the coefficients obtained from Eqs. (16), (17) and (18), the UHF wavefunction correct to first order in orbital correc-tion is given by

$$\Psi_{uHF} = {}^{s}\Psi_0 + \sqrt{2}\sum_k^{c}\sum_t^{V} a_{kt}\Psi_k^t + \sqrt{2}\sum_k^{c}\sum_t^{V} b_{kt}\,{}^{s}\Psi_k^t(1) + \sum_m^{0}\sum_t^{V} c_{mt}\,{}^{s}\Psi_m^t .$$

$$(19)$$

Eqs. (16), (17) and (18) are the coupled equations. In order to solve these equations, SCF process becomes necessary. This situation is very similar to that appeared in the coupled Hartree-

30

Fock perturbation theory.[12]   As in this theory, the uncoupling of
these equations makes the problem very simple.   The uncoupled
equations of Eqs. (16), (17) and (18) are

$$a_{kt} = \frac{\frac{1}{2} \sum_m^0 (mt \mid km)}{\left(\frac{s}{s+2} \, {}^s E_k^t{}_{(2)} + \frac{2}{s+2} \, {}^{s+2}E_k^t\right) - E_0 - K_{kt}} , \qquad (20)$$

$$b_{kt} = 0 , \qquad\qquad (21)$$

$$c_{mt} = 0 . \qquad\qquad (22)$$

Namely, in the uncoupled approximation, the orbital corrections Δ_k
and f_m^{α} are zero as expected from the Brillouin theorem, although
they are not necessarily zero in the coupled equations (See Eq.
(19).).   Then, in the uncoupled approximation, the UHF wavefunction
is written to first order as

$$\Psi_{UHF} = {}^s\Psi_0 + \sqrt{2} \sum_k^C \sum_t^V a_{kt} \Psi_k^t . \qquad (23)$$

Note firstly that the numerator of Eq. (20` comes from the
matrix element $\langle {}^s\Psi_0 \mid \mathcal{H} \mid \Psi_k^t \rangle = -\frac{1}{\sqrt{2}} \sum_m^0 (mt \mid km)$, and secondly that
the term ${}^{s+2}E_k^t$ in the denominator comes from the spin-contaminating
configuration ${}^{s+2}\Psi_k^t$ appearing in Eq. (12), and thirdly that the
term K_{kt} in the denominator comes from the matrix element $\langle {}^s\Psi_0 \mid \mathcal{H} \mid {}^s\Psi_{kk}^{tt} \rangle$
in which ${}^s\Psi_{kk}^{tt}$ is usually the most important configuration in the
electron-correlation corrections[13](See Eq. (A-2) in Appendix).
By using the following relation,

$${}^s E_k^t{}_{(2)} - {}^{s+2}E_k^t = \frac{s+2}{2s} \sum_m^0 (K_{mk} + K_{mt}), \qquad (24)$$

Eq. (20) is rewritten as

$$a_{kt} = \frac{\frac{1}{2} \sum_m^0 (mt \mid km)}{{}^s E_k^t{}_{(2)} - E_0 - \frac{1}{s} \sum_m^0 (K_{mk} + K_{mt}) - K_{kt}} \qquad (20)'$$

III. PERTURBATION-VARIATIONAL DESCRIPTION OF THE SEHF WAVEFUNCTION

In this section, we consider on the SEHF wavefunction along the same line to the treatment of the previous section. In the SEHF method, the single determinant of the same form as the UHF function of Eq. (4) is first spin-projected and then its orbital is varied to minimize the energy.

$$E_{SEHF} = \langle O_s \Psi_{UHF} | \mathcal{H} | O_s \Psi_{UHF} \rangle / \langle O_s \Psi_{UHF} | O_s \Psi_{UHF} \rangle \qquad (25)$$

where O_s is the projection operator[14] having the property,

$$S^2 O_s = \tfrac{1}{2} s (1 + \tfrac{s}{2}) O_s .$$

Firstly, let's examine the effect of the projection operator on the UHF wavefunction expressed by Eq. (A-1) in Appendix. Among the configurations expressed in Eq. (A-2) of Appendix, only that configurations which are not eigenfunctions of S^2 suffer change. They are the configurations 1), 6)$\sim$9) and 11). More-over, in the energy expression of Eq. (A-3), the configurations 6) $\sim$9) and 11) appears only in the form, $\langle {}^S \Psi_0 | \mathcal{H} | \Psi_{6\sim 9 \, or \, 11} \rangle$, since here we consider the energy correct only to second order in orbital corrections. Thus, from the equality,

$$\langle {}^S \Psi_0 | \mathcal{H} | \Psi_{6\sim 9 \, or \, 11} \rangle = \langle {}^S \Psi_0 | \mathcal{H} | O_s \Psi_{6\sim 9 \, or \, 11} \rangle ,$$

we have only to consider the effect of projection operator on Ψ_k^t in the energy expression of Eq. (A-3) in Appendix. This effect appears only in the matrix element, $2 \sum_k^c \sum_{\ell}^c \sum_t^V \sum_u^V a_{kt} a_{\ell u} \langle \Psi_k^t | \mathcal{H} | \Psi_{\ell}^u \rangle$ and in the normalization term coming from $\sum_k^c \sum_t^V (a_{kt})^2 \langle \Psi_k^t | \Psi_k^t \rangle$. They are calculated easily by using the relation,

$$O_s \Psi_k^t = (\tfrac{s}{s+2})^{1/2} \, {}^s \Psi_k^t (12)$$

obtained from Eq. (12). The final expression of the total energy

for the SEHF wavefunction is given in Eq. (A-4) in Appendix.

Thus, the orbital corrections in the SEHF wavefunction,

$$\pi_k' = \sum_t^V a_{kt}' \psi_t \, , \qquad \Delta_k' = \sum_t^V b_{kt}' \psi_t \, , \qquad f_m^{\alpha'} = \sum_t^V c_{mt}' \psi_t \, , \qquad (26)$$

are easily calculated as before by varying the SEHF energy correct
to second order with respect to a_{kt}', b_{kt}' and c_{mt}'. The results
for a_{kt}' is given by

$$\frac{1}{2} \frac{d^{(2)}E_{SEHF}}{d a_{kt}'} = 2 a_{kt}' \left\{ \frac{s}{s+2} [\, ^sE_k^t {}_{(2)} - E_0] - K_{kt} \right\}$$

$$- \sum_m^0 (mt \mid km)$$

$$+ \sum_{\ell(\neq k)}^c a_{\ell t}' \left[\frac{s+1}{s+2} \sum_m^0 (km \mid \ell m) - \frac{s}{s+2} (k\ell \mid tt) - (kt \mid \ell t) \right]$$

$$+ \sum_{u(\neq t)}^V a_{ku}' \left[\frac{s+1}{s+2} \sum_m^0 (mt \mid um) - \frac{s}{s+2} (tu \mid kk) - (kt \mid ku) \right]$$

$$- \sum_{\ell(\neq k)}^c \sum_{u(\neq t)}^V a_{\ell u}' \left[\frac{s}{s+2} (tu \mid \ell k) + (ku \mid t\ell) \right]$$

$$+ b_{kt}' \sum_m^0 (K_{mk} - K_{mt})$$

$$+ \sum_{\ell(\neq k)}^c b_{\ell t}' \left[\sum_m^0 (km \mid \ell m) \right] - \sum_{u(\neq t)}^V b_{ku}' \left[\sum_m^0 (tm \mid um) \right]$$

$$+ \sum_m^0 c_{mt}' \left[\sum_n^0 (mn \mid kn) - (mk \mid tt) - (kt \mid mt) \right]$$

$$- \sum_m^0 \sum_{u(\neq t)}^V c_{mu}' \left[(tu \mid mk) + (ku \mid mt) \right]$$

$$= 0 \qquad\qquad\qquad (27)$$

The results for b_{kt}' and c_{mt}' have exactly the same forms as those
given in Eqs. (17) and (18) except that a_{kt}, b_{kt} and c_{mt} appearing
in these equations change to a_{kt}', b_{kt}' and c_{mt}'. By using these
coefficients obtained from Eq.(27) and the SEHF correspondences of
Eqs. (17) and (18), the SEHF wavefunction correct to first order

in orbital correction is given by,

$$^S\Psi_{SEHF} = {}^S\Psi_0 + \sqrt{\frac{2S}{S+2}} \sum_k^c \sum_t^V a_{kt}' \, {}^S\Psi_k^t(2) + \sqrt{2} \sum_k^c \sum_t^V b_{kt}' \, {}^S\Psi_k^t(1)$$

$$+ \sum_m^0 \sum_t^V c_{mt}' \, {}^S\Psi_m^t \qquad (28)$$

As seen in the previous section, the uncoupling of those equations giving a_{kt}', b_{kt}' and c_{mt}' leads to the following simple equations.

$$a_{kt}' = \frac{\frac{1}{2}\sum_m^0 (mt \mid km)}{\frac{S}{S+2}\left({}^S E_k^t(2) - E_0 \right) - K_{kt}} \quad , \qquad (29)$$

$$b_{kt}' = 0, \qquad (30)$$

$$c_{mt}' = 0. \qquad (31)$$

That is, in the uncoupled approximation, the orbital corrections a_k' and $f_m^{\alpha}{}'$ are zero as expected from the Brillouin theorem, and the SEHF wavefunction becomes to first order as

$$^S\Psi_{SEHF} = {}^S\Psi_0 + \sqrt{\frac{2S}{S+2}} \sum_k^c \sum_t^V a_{kt}' \, {}^S\Psi_k^t(2). \qquad (32)$$

Comparing Eq. (29) to Eq. (20), note that in the denominator of Eq. (29) the term K_{kt} still appears, although the term due to spin-contamination is projected out in Eq. (29).

34

IV. COMPARISON WITH THE SUM-OVER-STATE PERTURBATION THEORY

In this section, we compare the results for the UHF and SEHF wavefunctions obtained in the previous sections, and the result for the PUHF wavefunction reported previously[2] to the first-order sum-over-state perturbation (FO-SOSP) wavefunction based on the RHF wavefunction as in the previous section.

Considering the Brillouin theorem for the RHF wavefunction, there are s one-electron excited spin-functions which interact with the RHF wavefunction ${}^s\Psi_0$ of Eq. (1).[2] They are all built up from the excitation from the closed orbital k to the open orbital t. However, since our present interest lies in the spin-correlation problem, we have only to consider the configuration ${}^s\Psi_k^t(2)$ of Eq. (14-a) among these s spin-functions.

From the first order perturbation theory,

$$^s\Psi_{SOS} = {}^s\Psi_0 + \sqrt{2} \sum_k^c \sum_t^V a_{kt}^{SOS} \, {}^s\Psi_k^t(2), \qquad (33)$$

where the coeffecient a_{kt}^{SOS} is given by

$$a_{kt}^{SOS} = \frac{\frac{1}{2} \sum_m^0 (mt \mid km)}{\left(\frac{s}{s+2}\right)^{1/2} ({}^sE_k^t(2) - E_0)} . \qquad (34)$$

Since the FO-SOSP coefficient of Eq. (34) is essentially the uncoupled one, we compared it in Table I to the UHF, PUHF and SEHF ones obtained by the uncoupled approximation. In Table I the coefficients are defined by the equation,

$$\Psi = {}^s\Psi_0 + \sum_k^c \sum_t^V a_{kt}^s \, {}^s\Psi_k^t(2) + \sum_k^c \sum_t^V a_{kt}^{s+2} \, {}^{s+2}\Psi_k^t , \qquad (35)$$

where the last configuration is the spin-contaminating configuration (See Eq. (12).). Refering Table I, note firstly that the term, $\frac{1}{s} \sum_m^0 (K_{mk} + K_{mt})$ in the denominators of the UHF and PUHF methods comes from the spin-contaminating configuration ${}^{s+2}\Psi_k^t$ (See Eq. (12).),

35

Table I. First-order coefficients in the uncoupled approximation.[a]

Method	a^s_{kt}	a^{s+2}_{kt}
FO-SOSP	$$\dfrac{\sqrt{\tfrac{1}{2}}\ \sum\limits_m^0 (mt\mid km)}{\sqrt{\tfrac{s}{s+2}}\ (^sE^t_k{}_{(2)} - E_0)}$$	0
UHF[b]	$$\dfrac{\sqrt{\tfrac{1}{2}}\ \sum\limits_m^0 (mt\mid km)}{\sqrt{\tfrac{s+2}{s}}\left[^sE^t_k{}_{(2)} - E_0 - \tfrac{1}{s}\sum\limits_m^0 (K_{mk}+K_{mt}) - K_{kt}\right]}$$	$$\dfrac{\sqrt{\tfrac{1}{2}}\ \sum\limits_m^0 (mt\mid km)}{\sqrt{\tfrac{s+2}{2}}\left[^sE^t_k{}_{(2)} - E_0 - \tfrac{1}{s}\sum\limits_m^0 (K_{mk}+K_{mt}) - K_{kt}\right]}$$
PUHF[b]	$$\dfrac{\sqrt{\tfrac{1}{2}}\ \sum\limits_m^0 (mt\mid km)}{\sqrt{\tfrac{s+2}{s}}\left[^sE^t_k{}_{(2)} - E_0 - \tfrac{1}{s}\sum\limits_m^0 (K_{mk}+K_{mt}) - K_{kt}\right]}$$	0
SEHF	$$\dfrac{\sqrt{\tfrac{1}{2}}\ \sum\limits_m (mt\mid km)}{\sqrt{\tfrac{s}{s+2}}\ (^sE^t_k{}_{(2)} - E_0) - \sqrt{\tfrac{s+2}{s}}\ K_{kt}}$$	0

[a] The coefficients are defined by

$$\Psi = {}^s\Psi_0 + \sum_k^c \sum_t^V a^s_{kt}\ {}^s\Psi_k^t{}_{(2)} + \sum_k^c \sum_t^V a^{s+2}_{kt}\ {}^{s+2}\Psi_k^t \ .$$

[b] The energy ${}^{s+2}E^t_k$ of the spin-contaminating configuration ${}^{s+2}\Psi_k^t$, appearing in the denominator, is given by

$$^{s+2}E^t_k = {}^sE^t_k{}_{(2)} - \frac{s+2}{2s}\sum_m^0 (K_{mk}+K_{mt}).$$

and secondly that the exchange integral K_{kt} common to the denominators of the three orbital models, UHF, PUHF and SEHF methods, but missing in the FO-SOSP method, comes from the two-electron excited configuration ${}^s\Psi_{kk}^{tt}$ which is usually the most important configuration in the electron-correlation corrections[13] (See Eq. (A-2) in Appendix). This point is more fully discussed in Sec. VI in the light of the physical visuality of the Sinanoğlu's meny electron theory.[4,13]

Since spin density gives a good measure of the spin-correlation effects in the open-shell electronic structure, it is convenient to compare these four methods by means of this measure. By applying the normalized spin-density operator[15]

$$\rho(\mathbf{r}) = \langle S_z \rangle^{-1} \sum_k S_{zk} \, \delta(\mathbf{r}_k - \mathbf{r})$$

to Eq. (37), and by using the relation[2]

$$\langle {}^s\Psi_0 | \rho(\mathbf{r}) | {}^{s+2}\Psi_k^t \rangle = \left(\tfrac{2}{s}\right)^{1/2} \langle {}^s\Psi_0 | \rho(\mathbf{r}) | {}^s\Psi_k^t(2) \rangle,$$

We obtain the following equations for the first-order spin density,

$$\rho = \rho_{SD} + \rho_{SP}, \qquad\qquad (36)$$

where

$$\rho_{SD} = \langle {}^s\Psi_0 | \rho(\mathbf{r}) | {}^s\Psi_0 \rangle,$$

$$\rho_{SP} = \sum_k^c \sum_t^V \left(a_{kt}^s + \left(\tfrac{2}{s}\right)^{1/2} a_{kt}^{s+2} \right) \langle {}^s\Psi_0 | \rho(\mathbf{r}) | {}^s\Psi_k^t(2) \rangle.$$

In Eq. (36), ρ_{SD} is the spin density due to the spin-delocalization (SD) mechanism and ρ_{SP} is the one due to the spin-polarization (SP) mechanism.[2,3] As seen from Eq. (37), ρ_{SD} is the same for these FO-SOSP, UHF, PUHF and SEHF methods in the uncoupled approximation. However, ρ_{SP} is different for different methods and gives a good measure of the spin-correlation effects included in

37

these methods.   In Table II, ρ_{SP} obtained in the uncoupled appro-
ximation of the UHF, PUHF and SEHF methods are compared to that
obtained from the FO-SOSP method.   Note that, in the UHF method,
ρ_{SP} includes also the contribution due to the spin-contaminating
configuration $^{s+2}\Psi_k{}^t$, although it is easily picked out by projec-
tion or by the method reported previously (See Table I of Ref. 2.).

From Table II, we first notice that the differences in ρ_{SP}
among the FO-SOSP, UHF and SEHF methods lie in their denominators.
Since the exchange integrals K_{mk}, K_{mt} and K_{kt} are always positive,
the relations;

$$|(\rho_{SOS})_{SP}| < |(\rho_{UHF})_{SP}|,$$

$$\tag{38}$$

$$|(\rho_{SOS})_{SP}| < |(\rho_{SEHF})_{SP}|,$$

are expected in the first-order uncoupled approximation.   The
relative magnitude between $(\rho_{UHF})_{SP}$ and $(\rho_{SEHF})_{SP}$ depends on the
relative magnitude between $\sum_m^0 (K_{mk} + K_{mt})$ and $2K_{kt}$.   Generally
speaking, the more similar the orbitals i and j are, the larger the
exchange integral K_{ij}.   Since the similality between orbitals i
and j is closely related to the level splitting between orbitals
i and j, we can expect the relation, $K_{mk} + K_{mt} > 2 K_{kt}$ for the
ground state radicals like alternant hydrocarbon radicals.   Since
s is always larger than unity (s = 1, for doublet radicals), the
following relation may be expected.

$$\sum_m^0 (K_{mk} + K_{mt}) > 2 K_{kt} \tag{39}$$

Thus,

$$|(\rho_{SEHF})_{SP}| < |(\rho_{UHF})_{SP}| \tag{40}$$

However, if the symmetry representation of the orbitals k, t are
the same but different from that of the orbital m, the relation (39)

38

Table II. ρ_{SP} in the uncoupled approximation.

Method	ρ_{SP}
FO-SOSP	$\dfrac{2}{S}\sum_{k}^{c}\sum_{t}^{v}\dfrac{\sum_{m}^{0}(mt\mid km)}{{}^{s}E_{k}^{t}{}_{(2)}-E_{0}}\;\psi_{k}(r)\,\psi_{t}(r)$
UHF	$\dfrac{2}{S}\sum_{k}^{c}\sum_{t}^{v}\dfrac{\sum_{m}^{0}(mt\mid km)}{{}^{s}E_{k}^{t}{}_{(2)}-E_{0}-\frac{1}{S}\sum_{m}^{0}(K_{mk}+K_{mt})-K_{kt}}\;\psi_{k}(r)\,\psi_{t}(r)$
PUHF[a]	$\dfrac{S}{S+2}\cdot(\rho_{UHF})_{SP}$
SEHF	$\dfrac{2}{S}\sum_{k}^{c}\sum_{t}^{v}\dfrac{\sum_{m}^{0}(mt\mid km)}{{}^{s}E_{k}^{t}{}_{(2)}-E_{0}-(1+\frac{2}{S})K_{kt}}\;\psi_{k}(r)\,\psi_{t}(r)$

[a] See Table I of Ref. 2.

and therefore (40) do not necessarily correct (e.g. π-electron spin density in the planar H_2CO anion).

For the relative magnitude between $(\rho_{UHF})_{SP}$ and $(\rho_{PUHF})_{SP}$, the relation obtained previously[2] is useful. For the usual doublet (s=1), triplet(s=2) and quartet(s=3) radicals, the value of $(\rho_{PUHF})_{SP}$ obtained from the relation[2],

$$(\rho_{PUHF})_{SP} \simeq \frac{s}{s+2} (\rho_{UHF})_{SP} \qquad (41)$$
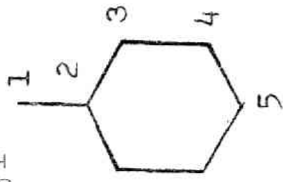
is expected to be much smaller than $(\rho_{UHF})_{SP}$ and even than $(\rho_{SEHF})_{SP}$ and $(\rho_{SOS})_{SP}$, considering the magnitude of the exchange integrals appearing in the denominators given in Table II. Therfore, we can expect finally the following relation,

$$|(\rho_{PUHF})_{SP}| < |(\rho_{SOS})_{SP}| < |(\rho_{SEHF})_{SP}| < |(\rho_{UHF})_{SP}| \qquad (42)$$

in the first-order uncoupled approximation. Note that the relation (40) stands on the assumed inequality (39), and therefore can reverse in certain cases.

To verify the relation (42) in the actual calculations, we summarized in Table III the spin densities calculated by these methods.[1,16] All the values are calculated by the PPP method with the same integral values. Among these, the values for FO-SOSP method are obtained by the present author. As seen in the positions of negative spin density, where only the SP mechanism is important, the relation (42) holds satisfactorily. However, for the positions where both of the SP and SD mechanisms are important, the relation expected from Eq. (42) and from the equality of ρ_{SD} for these four methods does not always holds. This is perhaps due to the crudeness of the uncoupled approximation. Note that the last relation $\rho_A = \frac{1}{4} (\rho_{UHF} + 3\rho_{PUHF})$ proposed by Amos and Woodward[16] from the exa-

Table III. Spin densities calculated by the various methods.[a,b]

Doublet Radical	Position	Full CI	FO-SCSF	SEHF	UHF	PUHF	$\frac{1}{4}(\rho_{UHF} + 3\rho_{PUHF})$[b]
Allyl	1	0.578	0.584	0.584	0.651	0.547	0.573
	2	-0.156	-0.167	-0.167	-0.302	-0.093	-0.145
Pentadienyl	1	0.413	0.405	0.452	0.545	0.389	0.422
	2	-0.140	-0.127	-0.159	-0.307	-0.094	-0.147
	3	0.452	0.444	0.415	0.524	0.422	0.443
Benzyl[c]	1	0.715	----	0.602	0.771	0.718	0.731
	2	-0.110	----	-0.134	-0.189	-0.060	-0.092
	3	0.185	----	0.279	0.254	0.157	0.181
	4	-0.070	----	-0.143	-0.158	-0.050	-0.077
	5	0.165	----	0.260	0.225	0.128	0.152

a J. E. Harriman and K. M. Sando, J. Chem. Phys. 43, 5138 (1965).

b T. Amos and M. Woodward, J. Chem. Phys. 50, 119 (1969); A. T. Amos and B. L. Burrows, ibid. 52, 3072 (1970).

c The values for the PUHF method in benzyl radical are obtained by the single annihilation of the spin-contaminating quartet state.

41

mination of the numerical results obtained for the several alter-
nant hydrocarbon radicals can be rewritten by using Eq. (41) as,

$$P_A = \frac{1}{4}(P_{UHF} + P_{PUHF}) \simeq (P_{UHF})_{SD} + \frac{1}{2}(P_{UHF})_{SP} \qquad (43)$$

which states that, at least in the alternant hydrocarbon radicals,
the spin density calculated by the Full CI method with the PPP
approximation can generally be approximated by taking half of the
SP contribution of the UHF spin density. However, this relation
seems not to hold generally. See, for example the data given by
Meyer.

V. ACCURACY OF THE EXPECTATION VALUES OF ONE-ELECTRON OPERATORS USING ORBITAL MODEL

In this section, we examine the order of magnitude of the
residual errors of the expectation values of one-electron operators
calculated by using orbital model. Although there have been many
studies on this subject,[18] almost all of them are concerned with
the accuracy of the expectation values of the spin-independent one
electron operators using the RHF wavefunction for closed-shell
electronic systems. In the followings, we first examine the
errors of the orbital model in the closed-shell electronic systems.
Our main interest lies in the finite perturbation theory (FPT).[7,8]
Then, we proceed to examine the errors in the SEHF method. The
physical meaning of the result is disscussed in the next section.

To begin with, let us write the true wavefunction ψ as

$$\psi = (\phi_0 + \mu\chi)/(1 + 2\mu\langle\phi_0|\chi\rangle + \mu^2\langle\chi|\chi\rangle)^{1/2}, \qquad (44)$$

where ϕ_0 is the approximate wavefunction and χ is the correction term to it. Here, χ is taken to be nonorthogonal to ϕ_0 for generality. Then, the expectation value of an arbitrary operator A is given by

$$\langle \psi | A | \psi \rangle = A_{ext}$$

$$= \frac{\langle \phi_0 | A | \phi_0 \rangle + 2\mu \langle \phi_0 | A | \chi \rangle + \mu^2 \langle \chi | A | \chi \rangle}{1 + 2\mu \langle \phi_0 | \chi \rangle + \mu^2 \langle \chi | \chi \rangle}, \tag{45}$$

which is rewritten as the followings correct to second order in μ,

$$A_{ext} = A_{00} + 2\mu \langle \phi_0 | A - A_{00} I | \chi \rangle$$
$$+ \mu^2 \{ \langle \chi | A | \chi \rangle - 4 \langle \phi_0 | \chi \rangle \langle \phi_0 | A | \chi \rangle$$
$$+ (4 \langle \phi_0 | \chi \rangle^2 - \langle \chi | \chi \rangle) A_{00} \}$$
$$+ O(\mu^3) \cdots \cdots \tag{46}$$

where $A_{00} = \langle \phi_0 | A | \phi_0 \rangle$ and I is the identity operator. Thus, if $\langle \phi_0 | A - A_{00} I | \chi \rangle$ vanishes, the expectation value of A calculated from the approximate wavefunction ϕ_0 is correct to second order in μ.

V-1. Examination for Closed-Shell Electronic System

In FPT, the Hamiltonian under consideration is

$$\mathcal{H}^R = H + \lambda \sum_{\nu} f(r_{\nu}) + \sum_{\mu > \nu} \sum 1/r_{\mu\nu} \tag{47}$$

$$\mathcal{H}^U = H + \lambda \sum_{\nu} f(r_{\nu}) S_{z\nu} + \sum_{\mu > \nu} \sum 1/r_{\mu\nu} \tag{48}$$

where H denotes the core-Hamiltonian due to the kinetic plus nuclear attraction energy. In Eq. (47), the spin-independent one-electron perturbation, $\lambda \sum_{\nu} f(r_{\nu})$, exert to the system. In Eq. (48), it is spin-linear[20], and then spin-correlation do occur in this closed-

shell system.[19]   Since $[S^2, \mathcal{H}^u] \neq 0$, the wavefunction correspond-
ing to $\mathcal{H}^u$ need not to be an eigenfunction of S^2, although it must
be an eigenfunction of S_z, since $[S_z, \mathcal{H}^u] = 0$.

The present interest is the accuracy of the expectation values
of another one-electron operators, $\sum_\nu \acute{f}(\nu_\nu)$ and $\sum_\nu \acute{f}(\nu_\nu) \delta_{z\nu}$, calculated
from the RHF and UHF wavefunctions, $^R\Phi_0$ and $^U\Phi_0$ corresponding to the
Hamiltonians (47) and (48), respectively.   The Brillouin theorem
for the RHF and UHF wavefunction is given by

$$ RHF; \quad \langle\, ^R\Phi_0 |\, \mathcal{H}^R |\, ^R\Phi_k{}^{\nu} \rangle = 0, \qquad (\text{See } Eq. \ (3).) \qquad\qquad (49) $$

$$ UHF; \quad \langle\, ^U\Phi_0 |\, \mathcal{H}^U |\, ^U\Phi_{k_\alpha}{}^{t_\alpha} \rangle = 0; \quad \langle\, ^U\Phi_0 |\, \mathcal{H}^U |\, ^U\Phi_{k_\beta}{}^{t_\beta} \rangle = 0, \quad (50) $$

where $^U\Phi_{k_\alpha}{}^{t_\alpha}$ is the one-electron excited configuration obtained from
$^U\Phi_0$ by changing the occupied orbital ϕ_k^α to the vacant orbital ϕ_t^α.
Eqs. (49) and (50) states that the correlation correction χ in Eq.
(44) begins from the two-electron excited configurations for both
RHF and UHF wavefunctions.   Since A in Eq. (48) is here the one-
electron operator and since χ is here orthogonal to ϕ_0 , the
matrix element $\langle \phi_0 |A - A_{00} I|\chi\rangle$ vanishes for both the RHF and UHF wavefunc-
tions.   Thus, the second-order property calculated by using FPT
is correct to second order in the correlation correction for both
the spin-independent and spin-linear operators.   Since, in the
small perturbation limit, FPT is equivalent to the coupled Hartree-
Fock perturbation method,[12] the above statement applies also to
this method.

V-2. Examination for the SEHF Method in Open-Shell Electronic System
     In the SEHF method, the correction term χ in Eq. (44) may be
witten as

$$\chi = \sum_i \sum_a c_{ia}\, O_s \Phi_i^a + \sum_{i>j} \sum_{a \neq b} C_{ij}^{ab}\, O_s \Phi_{ij}^{ab} + \cdots \cdots , \qquad (51)$$

where Φ_i^a is a single determinant obtained by changing the i-th occupied spin-orbital of the single determinant Φ_0 of the SEHF wavefunction $O_s \Phi_0$ to the vacant spin-orbital φ_a. φ_a is chosen such that

$$\langle \varphi_a | \varphi_i \rangle = 0 , \qquad (52)$$

where φ_i runs over the all occupied orbitals in Φ_0. Φ_{ij}^{ab} is the two-electron excited determinant similarly defined as Φ_i^a. The ϕ_0 in Eq. (44) is here $O_s \Phi_0$, the normalization facter of which is omitted here for brevity. Note that the overlaps $\langle O_s \Phi_0 | O_s \Phi_i^a \rangle$ and $\langle O_s \Phi_0 | O_s \Phi_{ij}^{ab} \rangle$ are not necessarily zero even if the orbitals satisfy Eq. (52).[21]

As shown by Kaldor,[22] the generalized Brillouin theorem applying to the SEHF wavefunction is

$$\langle O_s \Phi_i^a | \mathcal{H} - E I | O_s \Phi_0 \rangle = 0 , \qquad (53)$$

where E is the SEHF energy, and I the identity operator. From the first-order perturbation theory making use of the expansion in terms of the arbitrary complete set,[9] the coefficient c_{ia} in Eq. (51) is written to first order as

$$C_{ia} = - \sum_j \sum_b \langle O_s \Phi_j^b | \mathcal{H} - E I | O_s \Phi_0 \rangle \Big/ \langle O_s \Phi_i^a | \mathcal{H} - E I | O_s \Phi_j^b \rangle ,$$

which vanishes from Eq. (53). Thus, the correction term χ of Eq. (51) may be rewritten as

$$\chi = \sum_{i>j} \sum_{a \neq b} C_{ij}^{ab} \Phi_{ij}^{ab} + \cdots \cdots . \qquad (54)$$

As seen from Eq. (46), if $\langle O_s \Phi_0 | A - A_{00} I | \chi \rangle$ vanishes, the expectation value of the operator A calculated from the SEHF wavefunc-

tion is correct to second order in μ. However, $\langle 0_s \Phi_0 | A - A_{00} I | 0_s \Phi_{ij}^{ab} \rangle$ does not necessarily vanish even if A is a one-electron operator (spin-independent or spin-linear) and the spin-orbitals φ_a and φ_b satisfies Eq. (52). This comes from the fact that the overlap between two space parts of α-spin and β-spin orbitals does not necessarily vanish. Therefore, the expectation values calculated from the SEHF wavefunction include errors to first order in μ. Note however that the meaning of μ used for the SEHF wavefunction in the open-shell electronic system is utterly different from that used for the wavefunctions obtained by the FPT or the coupled Hartree-Fock theory in the closed-shell electronic systems, discussed in the previous paragraph. Although, in the closed-shell systems, the physical meaning of μ was clear as the correlation correction due mainly to the binary "collision" of two electrons[13], that for the SEHF wavefunction becomes vague since it includes partly the effect of "Coulomb hole" <u>within</u> the orbital model. This point is the main subject of the next section.

Lastly we note that it is nonsence to discuss the accuracy of the expectation value of the spin-linear operator, obtained from the UHF and PUHF wavefunctions, because of their defects stated in Sec. I.[2] For the expectation value of the spin-independent operator, we discussed previously.[2]

VI. EXAMINATION OF ORBITAL MODEL FOR THE SPIN-CORRELATION PROBLEM IN OPEN-SHELL ELECTRONIC SYSTEM

In this section, the features of orbital model of the open-shell electronic structure are examined in the light of the physical visuality of the Sinanoğlu's many-electron theory.[4,13]

46

Our starting point is the RHF wavefunction.

Electron has two attributes, namely charge and spin. In the closed-shell electronic structure, orbitals are determined by the average coulombic field, where the effect of spin appears only to modify this field. However, in the open-shell electronic structure such as in the doublet and triplet states, the effects of spins are not canceled out. Thus there arises two fields, spin field and charge field (or Coulomb field). The first is spin selective, although the second isn't, and these two fields always accompany. In the restricted orbital model, two electrons of different spins are forced on the same orbital, neglecting the spin-selective character of the spin field. Thus, in the electron-correlation problem in open-shell electronic system, two correlation effects becomes important, namely $\hat{f}_i$ and $\hat{u}_{ij}'$. [13] $\hat{f}_i$ represents mainly the orbital spin-polarization effects τ_k in Eq. (7) (spin-origin) in the present study. Δ_k and f_i^α are also included in $\hat{f}_i$, but are expected to be very small from the Brillouin theorem. $\hat{u}_{ij}'$ is the sum

$$\hat{u}_{ij}' = \hat{f}_i \hat{f}_j + \hat{u}_{ij} = \circ \; \circ \;\; + \;\; \circ\!\!-\!\!\circ \;\; , \qquad (55)$$

where the first term $\hat{f}_i \hat{f}_j$ (that is, the unlinked cluster $\circ \; \circ$ in Sinanoğlu's notation) is mainly the "coupling" of orbital polarization and the second term $\hat{u}_{ij}$ ($\circ\!\!-\!\!\circ$) represent chiefly the effect due to the binary "collision" of two electrons (charge-origin). [13] Note that in the closed-shell electronic systems, $\hat{f}_i$ (orbital correction) is very small due to the Brillouin theorem. It comes out only from the third order correction. However, in the open-shell electronic system, $\hat{f}_i$ is usually very important and is the origin of spin-correlation effects. $\hat{u}_{ij}$ plays an impor-

tant role mainly to improve total energy (or the expectation values of the more-than-two electron operator). $\hat{f}_i$ is not so important energetically.[4b]

In the orbital model which is, in other words, the orbital-constrained variation method, one introduces first rather formally the orbital correction $\hat{f}_i$ as in Eq. (5) and makes it optimum from the variational standpoint. However, since the first-order correction to the wavefunction is determined by varying the energy correct to second order,[9] there comes out the coupling term $\hat{f}_i\hat{f}_j$ in the energy expression. This is seen in Eqs. (A-3) and (A-4) in Appendix. Among these, the most important is $\hat{f}_i\hat{f}_i$ which gives the configurations $\sum_k^c \sum_t^v (a_{kt})^2 \, ^s\Psi_{kk}^{tt}$ and $\sum_k^c \sum_{t\neq u}^v a_{kt} a_{ku} \, ^s\Psi_{kk}^{tu}(l)$ in Eq.(A-1). However, these configurations, $^s\Psi_{kk}^{tt}$ and $^s\Psi_{kk}^{tu}(l)$ are also important in describing the "collision" term $\hat{u}_{ij}$. In other words, these two-electron excited configuration of desired spin-multiplicity is also used to describe the correlation term $\hat{u}_{ij}$, by giving free variation parameter like $\sum_k^c \sum_t^v C_{kk}^{tt} \, ^s\Psi_{kk}^{tt}$, which is not constrained as the product of orbital corrections like $\sum_k^c \sum_t^v (a_{kt})^2 \, ^s\Psi_{kk}^{tt}$. Therefore, by the variation of the energy correct to second-order in orbital correction, the effect of the binally "collision" $\hat{u}_{ij}$ is included effectively through the constrained form $\hat{f}_i\hat{f}_j$. It is well known that, like this, we can explain about 85 % of the π-electron correlation energy of benzene by means of the alternant molecular orbital method.[23,24] However, this is not so grateful in the open-shell electronic systems, since the real orbital polarization $\hat{f}_i$ is distorted by the effective inclusion of $\hat{u}_{ij}$. In other words, if we write the orbital polarization obtained by the orbital model as $\hat{f}_i^{orb}$, it is distorted like, say, $\hat{f}_i^{orb} = \hat{f}_i + \sum_j \sqrt{u_{ij}}$ by the orbital-constrained variation. Since the configuration

48

${}^{S}\Psi_{kk}^{tt}$ is very important also in μ , it appears even in the uncoupled equations (20) and (29) as K_{kt} in the denominator ($\langle \Psi_0 | \mathcal{H} | {}^{S}\Psi_{kk}^{tt} \rangle$ = K_{kt}). For example, as seen in Eq. (42), the spin density due to the SP mechanism in the SEHF method is always larger than that calculated by the FO-SOSP method. This point is also seen numerically even if we compare the values of $(\rho_{SEHF})_{SP}$ with those calculated by the full CI method. (See Table III.) Moreover, that the error in the expectation value of one-electron operator begins with the first order term in μ , which is proved rather formally in the previous section for the SEHF method, seems to support the above disscussions.

Note lastly that, in the closed-shell electronic systems, the effect purely due to $\hat{f_k}$ is very small even in the alternant molecular orbital method. This point may be clear from the fact that all the singly excited configuration constructed by introducing $\hat{f_k}$ is completely projected out by the projection operator.[24]

VII. Discussions

As shown in the previous sections, the orbital model in open-shell electronic system sacrifices to some extent the orbital polarization correction $\hat{f_k}$ in order to include effectively the correlation effect due to binary "collision" $\hat{u}_{ij}$. Since both of these corrections, $\hat{f_k}$ and $\hat{u}_{ij}$, are important in open-shell electronic systems, it seems necessary for the future theories of spin-correlation to include both of these corrections explicitly in a reasonable way, or to exclude reasonably the effect due to the correlation $\hat{u}_{ij}$.

In order to keep $\hat{f_k}$ from the effect of $\hat{u}_{ij}$, Meyer[17] dropped

49

out from the projected function of Eq. (A-1) in Appendix the confi-
gurations ${}^s\Psi_{kk}^{tt}$ and ${}^s\Psi_{kk}^{tu}(l)$ coming from the coupling term $\hat{f}_i\hat{f}_i$ and
considered only the polarization interaction term $\Psi_{kl}^{tu}(l)$. .
Although he considered only the correction π_k' in Eq. (26) in an
approximate way, his results were satisfactory in the calculations
of the hfs constants of the first-low atoms. Since in atoms, the
main correlation effect is the intra-shell correlation effect in $\hat{u}_{ij}$,
his treatment may be justified. However, we doubt wether the con-
figurations ${}^s\Psi_{kk}^{tt}$ and ${}^s\Psi_{kk}^{tu}(l)$ are purely $\hat{u}_{ij}$ origin and can be
omitted completely. Moreover, from the general treatment presented
here, we found that many other terms than $\Psi_{kl}^{tu}(l)$ arises. The rela-
tive importance between them and the relative weight in their ori-
gins between $\hat{f}_i$ and $\hat{u}_{ij}$ must also be examined if we adhere to
the orbital model.

Taking account of the considerations given hitherto, we may
rather set up more direct method which covers both correlation
effects $\hat{f}_i$ and $\hat{u}_{ij}$ in the possible simplest, but unconstrained
framework. This point is the problem succeeded by future study.
However, it is expected that the multi-configurational SCF treatment
will be hopeful, since, by this method, the expectation value of one-
electron operator is correct to second order in μ defined by Eq. (44).

Insertion of Eq. (10) into Eq. (9) gives the unnormalized UHF wavefunction correct to second order in orbital correction,

$$
\begin{aligned}
\Psi_{UHF} &= {}^{s}\Psi_{0} + \sqrt{2}\sum_{k}^{c}\sum_{t}^{v} a_{kt}\Psi_{k}^{t} + \sqrt{2}\sum_{k}^{c}\sum_{t}^{v} b_{kt}\,{}^{s}\Psi_{k}^{t}(1) + \sum_{m}^{d}\sum_{n}^{o} C_{mt}\,{}^{s}\Psi_{m}^{t} \\
&+ \sum_{k}^{c}\sum_{t}^{v}\{(b_{kt})^{2} - (a_{kt})^{2}\}\,{}^{s}\Psi_{kk}^{tt} + \sqrt{2}\sum_{k}^{c}\sum_{t<u}^{v} (b_{kt}b_{ku} - a_{kt}a_{ku})\,{}^{s}\Psi_{kk}^{tu}(1) \\
&+ \sqrt{2}\sum_{k}^{c}\sum_{t}^{v}\sum_{u(\neq t)}^{v} a_{kt}b_{ku}\Psi_{kk}^{tu} + 2\sum_{k<\ell}^{c}\sum_{t}^{v}(a_{kt}a_{\ell t} - b_{kt}b_{\ell t})\Psi_{k\ell}^{tt}(1) \\
&+ 2\sum_{k<\ell}^{c}\sum_{t}^{v}\sum_{u(\neq t)}^{v} a_{kt}a_{\ell u}\Psi_{k\ell}^{tu}(1) + 2\sum_{k<\ell}^{c}\sum_{t}^{v}\sum_{u(\neq t)}^{v} b_{kt}b_{\ell u}\Psi_{k\ell}^{tu}(2) \\
&+ 2\sum_{k}^{c}\sum_{\ell(\neq k)}^{c}\sum_{t}^{v} a_{kt}b_{\ell t}\Psi_{k\ell}^{tt}(3) + 2\sum_{k}^{c}\sum_{\ell(\neq k)}^{c}\sum_{t}^{v}\sum_{u(\neq t)}^{v} a_{kt}b_{\ell u}\Psi_{k\ell}^{tu}(3) \\
&+ \sqrt{2}\sum_{k}^{c}\sum_{m}^{o}\sum_{t}^{v}(a_{kt}C_{mt} - b_{kt}C_{mt})\,{}^{s}\Psi_{km}^{tt}(1) + \sqrt{2}\sum_{k}^{c}\sum_{m}^{o}\sum_{t}^{v}\sum_{u(\neq t)}^{v} a_{kt}C_{mu}\Psi_{km}^{tu}(2) \\
&+ \sqrt{2}\sum_{k}^{c}\sum_{m}^{o}\sum_{t}^{v}\sum_{u(\neq t)}^{v} b_{kt}C_{mu}\,{}^{s}\Psi_{km}^{tu}(1) + \sum_{m}^{o}\sum_{n}^{o}\sum_{t}^{v}\sum_{u(\neq t)}^{v} C_{mt}C_{nu}\,{}^{s}\Psi_{mn}^{tu} \\
&+ \cdots\cdots, \qquad\qquad\qquad (A-1)
\end{aligned}
$$

where

0) ${}^{s}\Psi_{0} = |\,\psi_{1}\bar{\psi}_{1}\cdots\cdots\psi_{k}\bar{\psi}_{k}\cdots\cdots\psi_{q}\bar{\psi}_{q}\,\psi_{q+1}\cdots\cdots\psi_{m}\cdots\cdots\psi_{p}\,|$

1) $\Psi_{k}^{t} = |\,\psi_{1}\bar{\psi}_{1}\cdots\cdots\psi_{t}\psi_{k}\,(\alpha\beta + \beta\alpha)/\sqrt{2}\cdots\cdots\psi_{q}\bar{\psi}_{q}\,\psi_{q+1}\cdots\cdots\psi_{p}\,|$

2) ${}^{s}\Psi_{k}^{t}(1) = |\,\psi_{1}\bar{\psi}_{1}\cdots\cdots\psi_{t}\psi_{k}\,(\alpha\beta - \beta\alpha)/\sqrt{2}\cdots\cdots\psi_{q}\bar{\psi}_{q}\,\psi_{q+1}\cdots\cdots\psi_{p}\,|$

3) ${}^{s}\Psi_{m}^{t} = |\,\psi_{1}\bar{\psi}_{1}\cdots\cdots\psi_{q}\bar{\psi}_{q}\,\psi_{q+1}\cdots\cdots\psi_{m-1}\,\psi_{t}\,\psi_{m+1}\cdots\cdots\psi_{p}\,|$

4) ${}^{s}\Psi_{kk}^{tt} = |\,\psi_{1}\bar{\psi}_{1}\cdots\cdots\psi_{t}\bar{\psi}_{t}\cdots\cdots\psi_{q}\bar{\psi}_{q}\,\psi_{q+1}\cdots\cdots\psi_{p}\,|$

5) ${}^{s}\Psi_{kk}^{tu}(1) = |\,\psi_{1}\bar{\psi}_{1}\cdots\cdots\psi_{t}\psi_{u}\,(\alpha\beta - \beta\alpha)/\sqrt{2}\cdots\cdots\psi_{q}\bar{\psi}_{q}\,\psi_{q+1}\cdots\cdots\psi_{p}\,|$

6) $\Psi_{kk}^{tu} = |\,\psi_{1}\bar{\psi}_{1}\cdots\cdots\psi_{t}\psi_{u}\,(\alpha\beta + \beta\alpha)/\sqrt{2}\cdots\cdots\psi_{q}\bar{\psi}_{q}\,\psi_{q+1}\cdots\cdots\psi_{p}\,|$

7) $\Psi_{k\ell}^{tu}(1) = |\psi_1 \bar{\psi}_1 \cdots \psi_t \psi_k (\alpha\beta + \beta\alpha)/\sqrt{2} \cdots \psi_u \psi_\ell (\alpha\beta + \beta\alpha)/\sqrt{2} \cdots \psi_g \bar{\psi}_g \psi_{g+1} \cdots \psi_p|$

8) $\Psi_{k\ell}^{tu}(2) = |\psi_1 \bar{\psi}_1 \cdots \psi_t \psi_k (\alpha\beta - \beta\alpha)/\sqrt{2} \cdots \psi_u \psi_\ell (\alpha\beta - \beta\alpha)/\sqrt{2} \cdots \psi_g \bar{\psi}_g \psi_{g+1} \cdots \psi_p|$

9) $\Psi_{k\ell}^{tu}(3) = |\psi_1 \bar{\psi}_1 \cdots \psi_t \psi_k (\alpha\beta + \beta\alpha)/\sqrt{2} \cdots \psi_u \psi_\ell (\alpha\beta - \beta\alpha)/\sqrt{2} \cdots \psi_g \bar{\psi}_g \psi_{g+1} \cdots \psi_p|$

10) $^s\Psi_{km}^{tu}(1) = |\psi_1 \bar{\psi}_1 \cdots \psi_t \psi_k (\alpha\beta - \beta\alpha)/\sqrt{2} \cdots \psi_g \bar{\psi}_g \psi_{g+1} \cdots \psi_{m-1} \psi_u \psi_{m+1} \cdots \psi_p|$

11) $\Psi_{km}^{tu}(2) = |\psi_1 \bar{\psi}_1 \cdots \psi_t \psi_k (\alpha\beta + \beta\alpha)/\sqrt{2} \cdots \psi_g \bar{\psi}_g \psi_{g+1} \cdots \psi_{m-1} \psi_u \psi_{m+1} \cdots \psi_p|$

12) $^s\Psi_{mn}^{tu}(1) = |\psi_1 \bar{\psi}_1 \cdots \psi_g \bar{\psi}_g \psi_{g+1} \cdots \psi_{m-1} \psi_t \psi_{m+1} \cdots \psi_{n-1} \psi_u \psi_{n+1} \cdots \psi_p|$

$$(A-2)$$

The configurations 1)$\sim$3) are the one-electron excited first-order configurations and those of 4)$\sim$12) are the two-electron excited second-order configurations. The superscript s denotes that it is an eigenfunction of S^2 with eigenvalue, $\frac{s}{2}(1+\frac{s}{2})$.

The UHF total energy correct to second order in orbital corrections is calculated from Eq. (8) by using Eq. (A-1) and the Brillouin theorem shown in Eq. (3). Note that in the energy expression, the configurations 6) and 9) do not contribute since $\langle ^s\Psi_0|\mathcal{H}|\Psi_{kk}^{tu}\rangle$ = $\langle ^s\Psi_0|\mathcal{H}|\Psi_{k\ell}^{tu}(3)\rangle$ = 0 . After some manipulations, the energy correct to second order in orbital correction is given by,

$$^{(2)}E_{UHF} = \langle \Psi_{UHF}|\mathcal{H}|\Psi_{UHF}\rangle / \langle \Psi_{UHF}|\Psi_{UHF}\rangle$$

$$= E_0 + 2\sum_k^c \sum_t^v \left((a_{kt})^2 \left\{ \left[\frac{s}{s+2} {}^sE_k^t{}_{(2)} + \frac{s}{s+2} {}^{s+2}E_k^t \right] - E_0 - K_{kt} \right\} \right.$$

$$\left. - a_{kt} \left[\sum_m^0 (mt|km) \right] \right)$$

$$+ 2\sum_k^c \sum_t^v \sum_{u(\neq t)}^v a_{kt} a_{ku} \left[\sum_n^0 (nt|un) - (tu|kk) - (kt|ku) \right]$$

52

$$+ 2 \sum_{k}^{c} \sum_{\ell(\neq k)}^{c} \sum_{t}^{v} a_{kt} \, a_{\ell t} \left[\sum_{n}^{0} (kn|\ell n) - (k\ell|tt) - (kt|\ell t) \right]$$

$$- 2 \sum_{k}^{c} \sum_{\ell(\neq k)}^{c} \sum_{t}^{v} \sum_{u(\neq t)}^{v} a_{kt} \, a_{\ell u} \left[(tu|\ell k) + (ku|t\ell) \right]$$

$$+ 2 \sum_{k}^{c} \sum_{t}^{v} (b_{kt})^2 \left[(\,^{s}E_{k}^{t}(1) - E_0) + K_{kt} \right]$$

$$+ 2 \sum_{k}^{c} \sum_{t}^{v} \sum_{u(\neq t)}^{v} b_{kt} \, b_{ku} \left[\sum_{n}^{0} (tn|un) + 3(tk|uk) - (kk|tu) \right]$$

$$+ 2 \sum_{k}^{c} \sum_{\ell(\neq k)}^{c} \sum_{t}^{v} b_{kt} \, b_{\ell t} \left[\sum_{n}^{0} (kn|\ell n) + 3(t\ell|kt) - (k\ell|tt) \right]$$

$$+ 2 \sum_{k}^{c} \sum_{\ell(\neq k)}^{c} \sum_{t}^{v} \sum_{u(\neq t)}^{v} b_{kt} \, b_{\ell u} \left[4(tk|\ell u) - (tu|\ell k) - (ku|\ell t) \right]$$

$$+ \sum_{m}^{0} \sum_{t}^{v} (c_{mt})^2 \, (\,^{s}E_{m}^{t} - E_0)$$

$$+ \sum_{m}^{0} \sum_{t}^{v} \sum_{u(\neq t)}^{v} c_{mt} \, c_{mu} \left[\tfrac{1}{2} \sum_{n}^{0} (nt|un) - (mm|tu) + (mt|um) \right]$$

$$+ \sum_{m}^{0} \sum_{n(\neq m)}^{0} \sum_{t}^{v} c_{mt} \, c_{nt} \left[\tfrac{1}{2} \sum_{i}^{0} (in|im) - (mn|tt) + (mt|nt) \right]$$

$$+ \sum_{m}^{0} \sum_{n(\neq m)}^{0} \sum_{t}^{v} \sum_{u(\neq t)}^{v} c_{mt} \, c_{nu} \left[2(mt|nu) - (mn|tu) - (mu|nt) \right]$$

$$+ 2 \sum_{k}^{c} \sum_{t}^{v} a_{kt} \, b_{kt} \sum_{n}^{0} (K_{nk} - K_{nt})$$

$$- 2 \sum_{k}^{c} \sum_{t}^{v} \sum_{u(\neq t)}^{v} a_{kt} \, b_{ku} \sum_{m}^{0} (tm|um) \;+\; 2 \sum_{k}^{c} \sum_{\ell(\neq k)}^{c} \sum_{t}^{v} a_{kt} \, b_{\ell t} \sum_{m}^{0} (km|\ell m)$$

$$+ 2 \sum_{k}^{c} \sum_{m}^{0} \sum_{t}^{v} a_{kt} \, c_{mt} \left[\sum_{n}^{0} (mn|kn) - (mk|tt) - (kt|mt) \right]$$

$$- 2 \sum_{k}^{c} \sum_{m}^{0} \sum_{t}^{v} \sum_{u(\neq t)}^{v} a_{kt} \, c_{mu} \left[(tu|mk) + (ku|mt) \right]$$

$$+ 2 \sum_{k}^{c} \sum_{m}^{0} \sum_{t}^{v} b_{kt} \, c_{mt} \left[\sum_{n}^{0} (mn|kn) + 3(kt|mt) - (mk|tt) \right]$$

$$+ 2 \sum_{k}^{c} \sum_{m}^{0} \sum_{t}^{v} \sum_{u(\neq t)}^{v} b_{kt} \, c_{mu} \left[4(kt|mu) - (tu|mk) - (mt|ku) \right]$$

$$+ \cdots \cdots \; . \hspace{4cm} (A\text{-}3)$$

53

The energy expression for the SEHF wavefunction is obtained from Eq. (25). As discussed in the text, this is easily calculated by using the following relation obtained from Eq. (12),

$$O_S \Psi_k^t = \left(\frac{S}{S+2}\right)^{1/2} {}^S\Psi_k^t(2).$$

The final expression is different from Eq. (A-3) only in the terms in which the coefficients are the product of two a's, except that all coefficients change to a_{kt}', b_{kt}' and c_{mt}' in the SEHF expression. Then, in the following expression, only the first four terms different from Eq. (A-3) is given, the others are formally the same as Eq. (A-3).

$$
{}^{(2)}E_{SEHF} = \langle O_S \Psi_{UHF} | \mathcal{H} | O_S \Psi_{UHF} \rangle / \langle O_S \Psi_{UHF} | O_S \Psi_{UHF} \rangle
$$

$$
= E_0 + 2 \sum_k^C \sum_t^V \left((a_{kt}')^2 \left\{ \frac{S}{S+2} ({}^S E_k^t(2) - E_0) - K_{kt} \right\} \right.
$$
$$
\left. - a_{kt}' \sum_m^0 (mt|km) \right)
$$

$$
+ 2 \sum_k^C \sum_t^V \sum_{u(\neq t)}^V a_{kt}' a_{ku}' \left[\frac{S+1}{S+2} \sum_n^0 (tn|un) - \frac{S}{S+2}(tu|kk) - (kt|ku) \right]
$$

$$
+ 2 \sum_k^C \sum_{\ell(\neq k)}^C \sum_t^V a_{kt}' a_{\ell t}' \left[\frac{S+1}{S+2} \sum_n^0 (kn|\ell n) - \frac{S}{S+2}(k\ell|tt) - (kt|\ell t) \right]
$$

$$
- 2 \sum_k^C \sum_{\ell(\neq k)}^C \sum_t^V \sum_{u(\neq t)}^V a_{kt}' a_{\ell u}' \left[\frac{S}{S+2}(tu|\ell k) + (ku|t\ell) \right]
$$

$$
+ \cdots\cdots\cdots\cdots . \tag{A-4}
$$

54

REFERENCES

1. (a) J. E. Harriman and K. M. Sando, J. Chem. Phys. 48, 5138
   (1968).

   (b) K. M. Sando and J. E. Harriman, J. Chem. Phys. 47, 180 (1967).

2. H. Nakatsuji, H. Kato and T. Yonezawa, J. Chem. Phys. 51, 3175
   (1969) (included in this volume, Part I, Chap.3).

3. (a) T. Yonezawa, H. Nakatsuji, T. Kawamura and H. Kato, J. Chem.
   Phys. 51, 669 (1969); Chem. Phys. Letters 2, 454 (1968) (included
   in this volume, Part I, Chap. 2).

   (b) T. Yonezawa, H. Nakatsuji, T. Kawamura and H. Kato, Bull.
   Chem. Soc. Jap. 42, 2437 (1969) (included in this volume, Part II,
   Chap. 3).

   (c) H. Nakatsuji, H. Kato and T. Yonezawa, ibid. 43, 698 (1970)
   (included in this volume, Part II, Chap. 3).

4. (a) H. J. Silverstone and O. Sinanoğlu, J. Chem. Phys. 44, 1899,
   3608 (1966).

   (b) İ. Öksüz and O. Sinanoğlu, Phys. Rev. 181, 42 (1969).

5. C. C. J. Roothaan, Rev. Mod. Phys. 32, 179 (1960).

6. Generally, the UHF orbitals ϕ_i^α and ϕ_i^β in Eq. (5) are the corres-
   ponding orbitals proposed by Amos and Hall (Proc. Roy. Soc.
   (London), A263, 483 (1961)), and the RHF orbital ψ_i in Eq. (5)
   is the unitarily transformed one of the RHF orbital which dia-
   gonalize the Roothaan's open-shell RHF operator.[5]

7. R. Ditchfield, N. S. Ostlund, J. N. Murrel and M. A. Turpin,
   Mol. Phys. 18, 433 (1970).

8. H. D. Cohen and C. C. J. Roothaan, J. Chem. Phys. 43, S34 (1965);
   J. A. Pople, J. W. McIver, and N. S. Ostlund, J. Chem. Phys. 49,
   2960 (1968).

9. J. O. Hirschfelder, W. Byers-Brown and S. T. Epstein, **Advan.** Quant. Chem. 1, 255 (1964).

10. (a) A. T. Amos and G. G. Hall, Proc. Roy. Soc. (London), A263, 483 (1961).

    (b) A. T. Amos, Mol. Phys. 5, 91 (1962).

    (c) T. Amos and L. C. Snyder, J. Chem. Phys. 41, 1773 (1964); 42, 3670 (1965).

11. (a) J. E. Harriman, J. Chem. Phys. 40, 2827 (1964).

    (b) A. Hardisson and J. E. Harriman, ibid. 46, 3639 (1967).

12. For example, see (a) R. M. Stevens, R. M. Pitzer, and W. N. Lipscomb, J. Chem. Phys. 38, 550 (1963); (b) P. W. Langhoff, M. Karplus and R. P. Hurst, J. Chem. Phys. 44, 505 (1966).

13. (a) O. Sinanoğlu, J. Chem. Phys. 36, 706, 3198 (1962).

    (b) D. F. Tuan and O. Sinanoğlu, ibid. 38, 1740 (1963).

    (c) O. Sinanoğlu, Advan. Chem. Phys. 6, 315 (1964).

14. P. -O. Löwdin, Phys Rev. 97, 1509 (1955).

15. H. M. McConnell, J. Chem. Phys. 28, 1188 (1958).

16. (a) T. Amos and M. Woodward, **J**. Chem. Phys. 50, 119 (1969).

    (b) A. T. Amos and B. L. Burrows ibid. 52, 3072 (1970).

17. W. Meyer, J. Chem. Phys. 51, 5149 (1969).

18. (a) E. Eckert, Phys. Rev. 36, 878 (1930).

    (b) J. Goodisman and W. A. Klemperer, J. Chem. Phys. 38, 721 (1963).

    (c) M. H. Alexander, ibid. 51, 5650 (1969), and the references therein.

19. M. Barfield, J. Chem. Phys. 44, 1836 (1966); 49, 2145 (1968).

20. In Eq. (48), we can choose the spin-linear operator as $\sum_{y} f(r_{y}) S_{zy}$ in spite of $\sum_{y} f(r_{y}) S_{y}$, without loss of generality.

21. F. E. Harris, Advan. Quant. Chem. 3, 61 (1967).

22. U. Kaldor, J. Chem. Phys. 48, 835 (1968).

23. (a) T. Itoh and H. Yoshizumi, J. Phys. Soc. Jap. 10, 201 (1955).

   (b) H. Yoshizumi and T. Itoh, J. Chem. Phys. 23, 412 (1955).

24. R. Pauncz, "Alternant Molecular Orbital Method", (W. B. Saunders and Co., Philadelphia, Pa., 1967).

25. (a) A. Veillard and E. Clementi, Theoret. chim. Acta (Berl.) 7, 133 (1967).

   (b) J. Hinze and C. C. J. Roothaan, Prog. Theoret. Phys. (Kyoto), 40, S37 (1967).

   (c) B. Levy and G. Berthier, Intern. J. Quant. Chem. 2, 307 (1968).

CHAPTER 5

CONCLUSION

In Part I of this thesis, orbital theories in open-shell electronic system are studied laying stress on the spin-correlation problem.

In Chapter 2, a method is proposed for separating the spin density calculated by the UHF method into components due to spin-polarization and spin delocalization mechanisms, and the validity of the method is confirmed. By using this method, more profound understandings than before on the nature of spin density may be gained because of the physical simplicity and visuality of each mechanism. This will be exemplified in the actual applications given in Part II, Capter 4. Moreover, since these two mechanisms depend on the different type of integrals, the estimation of these integral values and the examination of the computational scheme becomes more easy. The author believes that this general trearment has put an end to the previous confusions seen on this subject.

From the study given in Chapter 3, an interconnection between UHF and PUHF wavefunctions is clarified. Moreover, some of the general properties of the UHF wavefunction have revealed. Firstly, the weight of the lowest contaminating spin function included in the UHF wavefunction decreases with increasing spin multiplicity. Secondly, the annihilation of the lowest contaminating spin function little affects on the electron density distribution and on the other physical quantities, the operators of which commute with the annihilation operator. Thirdly, in the UHF method, the "spin-appearing mechanisms" (spin-polarization and spin-delocalization) are clearly divided, and the generalization of the method to

58

separate these contributions is carried out.

From the study given in Chapter 4, an interconnection between UHF and SEHF theories are clarified. Thus, together with the results given in Chapter 3, the three orbital thories (UHF, PUHF and SEHF theories) for open-shell electronic systems are interconnected in conjunction with the first-order sum-over-state perturbation wavefunction starting from the RHF wavefunction. The accuracy of the expectation values of one-electron operators calculated from these wavefunctions is also clarified for both the closed and open-shell electronic systems. These results mean physically that the orbital model in open-shell electronic system sacrifices to some extent the spin-polarization correction in order to include effectively the correlation correction due essentially to the two-electron correlation phenomena. Since both of the spin-correlation and the two-electron correlation corrections are important in open snell electronic systems, it seems necessary for the future theories of spin-correlation to include both of these corrections explicitly in a reasonable way, or to exclude reasonably the effect due to the two-electron correlation corrections.

PART II

STUDIES ON

THE ELECTRONIC STRUCTURE OF

CARBONIUN IONS

AND

DOUBLET RADICALS

AND

THE CALCULATION OF FORCE CONSTANTS

CHAPTER 1

INTRODUCTION

As has been known from the early days of the electronic theory of chemical valency, valence electrons play essential role in chemical bindings and in other chemical phenomena. Nevertheless, it was only recently that the semi-empirical SCF-MO method for valence electron systems have become popular in various studies of chemistry: After the extended Hückel theory (Hoffmann, 1963)[1] for valence electron systems, the first attempt to extend valence electron theory to the SCF scheme[2] was firstly made by Pople, Santry and Segal (1965) as CNDO method,[3] which has now become popular in various studies of molecular electronic structure. This method is based on the zero-differential overlap approximation which was widely used in the π-electron theories, such as in the Pariser-Parr-Pople's method.[4] On the other hand, the valence electron SCF-MO method including differential overlap was firstly developed by Yonezawa, Yamaguchi and Kato in 1967[5] although an application of this method appeared already in 1966.[6]

The first purpose of this part is to extend the applicability of the above method to various molecular properties, and the second is to show in actual calculations the usefulness of the method proposed in Part I, Chapter 2 to separate the UHF spin density into its mechanistic components. The method of calculation and the values of integrals used in the following chapters are due basically to the study given in Ref. 5. Small modifications added to the original method are given in each chapter. Extention to the open-shell electronic systems[7] by means of the UHF theory will be described in Chapter 3.

In Chapter 2 (published in the Journal of the American Chemical Society, $\underline{90}$, 1239 (1968), and in the Bulletin of the Cemical Society of Japan, $\underline{39}$, 2788 (1966)), the electronic structures of carbonium ions are studied by the semi-empirical SCF-MO method for valence electron systems. The carbonium ions studied are alkyl cations and some protonated hydrocarbons. It is found out that the explicit inclusions of σ-electrons (not like in π-electron theory) and of the electron-repulsion terms (not like in the extended Hückel theory) are very important for the electron-deficient species like carbonium ions. The change of the σ and π electron populations with the structural change in alkyl cations, and the π-type conjugation seen in cyclopropylmethyl cation are also investigated.

In Chapter 3, two studies on the electronic structure of doublet radicals are summarized. The main interest lies in their spin densities, and the method proposed in Part I, Chapter 2 is successfully applied.

In Chapter 3, Section 1 (published in the Bulletin of the Chemical Society of Japan, $\underline{42}$, 2437 (1969), and in Molecular Physics, $\underline{13}$, 589 (1967)), an extention of the original valence-electron SCF-MO method[5] to the open-shell electronic system is made by means of the unrestricted Hartree-Fock method,[7] and this is applied to the study of the electronic structure of small doublet radicals. By the inclusion of all the valence electrons, the empirical McConnell relation for the π-electron radicals becomes unnecessary, and direct calculation of the hfs constant becomes possible. Generally, the calculated proton hfs constants agree satisfactorily with experiments. Furthermore, by separating the calculated spin densities into mechanistic contributions, the

spin-polarization mechanism is shown important even in the cases where the spin-delocalization mechanism has been considered dominant (e.g. ethyl and vinyl radicals). The structure dependence of the hfs constants and their mecanistic contributions are also examined. Lastly, the preferable structure of the hydrogenated pyridine is studied by examining both of the total energy and the hfs constants.

In Chapter 3, Section 2 (published in the Bulletin of the Chemical Society of Japan, 43, 698 (1970)), the angular dependence of the methyl group hfs constants is studied, laying stress on the behavior of the spin-polarization mechanism, since this mechanism is found very important by the study given in Section 1. Origin of the angular dependence is also investigated by applying the theory given in Part I, Chapter 3.

In Chapter 4 (published in the Journal of Chemical Physics, 53, 1305 (1970)), the present valence electron SCF-MO method is applied to the calculation of force constant of ethylene after a small modification in the core-repulsion energy. All the diagonal quadratic force constants in the internal symmetry coordinate system are calculated and compared with those obtained from vibrational spectra. It is noticeable that this method can reproduce reasonable potential curves even for the stretching coordinate.

REFERENCES

1. R. Hoffmann, J. Chem. Phys. 39, 1397 (1963).

2. C. C. J. Roothaan, Rev. Mod. Phys. 23, 69 (1951).

3. J. A. Pople, D. P. Santry and G. A. Segal, J. Chem. Phys. 43, S129 (1965); J. A. Pople and G. A. Segal, ibid. 43, S136 (1965).

4. (a) R. Pariser and R. G. Parr, J. Chem. Phys. 21, 466, 767 (1953) (b) J. A. Pople, Trans. Faraday Soc. 49, 1375 (1953).

5. T. Yonezawa, K. Yamaguchi and H. Kato, Bull. Chem. Soc. Jap. 40, 536 (1967); see also H. Kato, H. Konishi and T. Yonezawa, ibid. 40, 1017, 2761 (1967).

6. T. Yonezawa, H. Nakatsuji and H. Kato, Bull. Chem. Soc. Jap. 39, 2788 (1966) (included in this volume, Part II, Chapter 3).

7. See also, T. Yonezawa, H. Nakatsuji, T. Kawamura and H. Kato, Bull. Chem. Soc. Jap. 40, 2211 (1967).

PART II, CHAPTER 2

ELECTRONIC STRUCTURE

OF

CARBONIUM IONS

The Electronic Structure of Carbonium Ions.
Alkyl Cations and Protonated Hydrocarbons

Abstract: The electronic structure of alkyl cations and some protonated hydrocarbons has been studied by a semi-empirical SCF MO treatment for valence electron systems. It is found that the inclusion of electron repulsion and core repulsion terms is essential for the successful investigation of charged species. Good agreements of calculated ionization potentials of alkyl radicals with experiments are obtained. The electronic excitation energies and oscillator strengths of some alkyl cations are presented; the energy changes in some ionic reactions are calculated, and the results compare satisfactorily with experiment. The change of σ and π electron populations with structural change in alkyl cations is investigated, and the comparison of the electronic structure of CH_5^+ and CH_5^- is carried out. The stable configurations of $C_2H_5^+$ and $C_2H_3^+$ are also examined.

The chemistry of carbonium ions has been developed extensively in recent years. Until recently, one of the most general features of carbonium ions was their transient character. But recently, it has been possible to capture carbonium ions in the form of stable salts with very strong acids.[1]

Theoretical studies of carbonium ions have been largely limited to conjugated cations and thereby the behavior of σ electrons, perhaps essential for the study of positively charged species, was left unsolved.

Recently, Hoffmann developed the extended Hückel theory[2] and applied it to some carbonium ions.[3] This was the first attempt to treat carbonium ions extensively, considering all valence electrons of the constitutent atoms, and was very instructive. But one of the shortcomings of this treatment was that the electron

interaction and nuclear repulsion terms were not taken into account explicitly.

In the present work, the electronic structures of some carbonium ions have been studied with our newly developed semiempirical ASMO SCF method for valence electron systems.[4] The carbonium ions investigated are some alkyl cations, such as methyl, ethyl, n-propyl, isopropyl, isobutyl, and t-butyl cations, and some protonated hydrocarbons, such as protonated methane, protonated ethylene, and protonated acethylene. We also examined the electronic structures of some alkyl anions and CH_5^- as a reference.

One of the main purposes of this study is to examine the effects of the electron repulsion term in charged species. It has been found that the inclusion of electron

(1) (a) N. C. Deno, *Progr. Phys. Org. Chem.*, **2**, 129 (1964); (b) G. A. Olah and C. U. Pittman, *Advan. Phys. Org. Chem.*, **4**, 305 (1966).
(2) R. Hoffmann, *J. Chem. Phys.*, **39**, 1397 (1963).
(3) R. Hoffmann, *ibid.*, **40**, 2480 (1964).

(4) T. Yonezawa, K. Yamaguchi, and H. Kato, *Bull. Chem. Soc. Jap.*, **40**, 536 (1967). In these calculations, one-center exchange integrals are further considered. See also H. Kato, H. Konishi, and T. Yonezawa, *ibid.*, **40**, 1017, 2761 (1967).

repulsion is essential especially for the successful investigation of orbital energies.

Method and Parameters

The molecular orbitals (MO's), φ_i's, are taken as a linear combination of all valence atomic orbitals (AO's), χ_r's, centered on the various atoms of the molecule. Roothaan's SCF equation[5] for a closed shell molecule is

$$\sum_r C_{ir}(F_{rs} - S_{rs}\epsilon_i) = 0 \qquad (s = 1, 2, \cdots) \qquad (1)$$

where

$$F_{rs} = H_{rs} + \sum_{tu} P_{tu}[(rs|tu) - \tfrac{1}{2}(rt|su)] \qquad (2)$$

$$S_{rs} = \int \chi_r \chi_s \, d\tau \qquad (3)$$

$$(rs|tu) = \int \chi_r(\mu)\chi_s(\mu) \frac{e^2}{r_{\mu\nu}} \chi_t(\nu)\chi_u(\nu) \, d\tau_\mu d\tau_\nu \qquad (4)$$

The atomic integrals appearing in the above equations are evaluated by the approximations previously reported.[4]

The additional improvement introduced in the present calculations is the inclusion of one-center exchange integrals with the approximations[6]

$$(2s,2p\sigma|2s,2p\sigma) = (2s,2p\pi|2s,2p\pi)$$
$$= 0.200(2s,2s|2p\sigma,2p\sigma) \qquad (5)$$

and

$$(2p\sigma,2p\pi|2p\sigma,2p\pi) = (2p\pi,2p\bar{\pi}|2p\pi,2p\bar{\pi})$$
$$= 0.0604(2p\sigma,2p\sigma|2p\pi,2p\pi) \qquad (6)$$

The Wolfsberg–Helmholtz parameter, K, introduced[4] in the calculations of off-diagonal elements of H_{rs}[7] in eq 2 is set at 1.1 and 1.08.[8]

The total electronic energy (E) of the valence electrons is written as

$$E = \tfrac{1}{2}\sum_{rs} P_{rs}(H_{rs} + F_{rs}) \qquad (7)$$

and the total energy (W) of the molecule is obtained by

$$W = E + \sum_{A>B}\sum Z_A Z_B / R_{AB} \qquad (8)$$

in which the nuclear repulsion energy $\sum_{A>B}\sum Z_A Z_B / R_{AB}$ is calculated by the hole approximation[9]

$$\sum_{A>B}\sum Z_A Z_B / R_{AB} = \sum_{A>B}\sum Z_A Z_B(2S_A,2S_A|2S_B,2S_B) \qquad (9)$$

where Z_A and $2S_A$ are the core charge and the 2S AO of the atom, A, respectively.

In the present calculations, it is assumed that the cationic carbon of alkyl cation is in the trigonal state,[10]

(5) C. C. J. Roothaan, *Rev. Mod. Phys.*, 23, 69 (1951).
(6) H. Hinze and H. H. Jaffé, *J. Chem. Phys.*, 38, 1834 (1963).
(7) The invariance of the Wolfsberg-Helmholtz approximation to rotation of the basis set in space is easily seen in eq 6 and 7 in ref 4, representing that H_{rr}'s for 2p$_x$, 2p$_y$, and 2p$_z$ AO's on the same atom become equal regardless of their orientation in space.
(8) The results obtained by adjusting K to 1.08 are almost parallel with those obtained by $K = 1.1$, so that we will show only the results obtained by $K = 1.1$.
(9) G. Del Re and R. G. Parr, *Rev. Mod. Phys.*, 35, 604 (1963).
(10) Recently, Olah, *et al.*, substantiated the planar sp²-hybridized structure of the simple alkyl cations in solution: G. A. Olah, E. B. Baker, J. C. Evans, W. S. Tolgyesi, J. S. McIntyre, and I. J. Bastien, *J. Amer. Chem. Soc.*, 86, 1360 (1964).

and that the bond distance between the sp^2 and sp^3 carbons is 1.50 Å. The bond distances between a carbon and a hydrogen atom and between sp^3 carbons are taken to be 1.09 and 1.54 Å, respectively.

Results and Discussion

In the present paper, we will discuss first the general results on the orbital energies and the electronic transitions of carbonium ions, and then enter into details of the electronic structures of alkyl cations and protonated hydrocarbons.

Orbital Energies. Carbonium ions are electron-deficient species compared with radicals or neutral molecules. Therefore, the destabilization due to the electron repulsion decreases in these species. Hence, the neglect of electron interaction and parametrization for neutral molecules will lead to too high orbital energies in carbonium ions. This is the case for the treatment of carbonium ions by the extended Hückel method. The orbital energies calculated for ethyl cation and staggered ethane by the extended Hückel method and the present method are compared in Table I. The ionization potentials (IP's) of ethyl cation and

Table I. Orbital Energies of Ethyl Cation and Staggered Ethane

	C₂H₅⁺ Hoffmann	C₂H₅⁺ Present, $K = 1.1$	Stag. C₂H₆ Hoffmann	Stag. C₂H₆ Present, $K = 1.1$
LV	-10.482	-8.696	3.212	13.917
HO	-13.744	-19.899	-13.763	-12.088
	-14.316	-20.222	-13.763	-12.589
	-15.295	-20.690	-14.126	-12.589
	-16.070	-22.677	-15.871	-14.918
	-21.231	-26.765	-15.871	-14.918
	-26.860	-30.563	-21.873	-19.757
			-26.711	-23.001

ethane calculated by the extended Hückel method are 13.74 and 13.76 eV, respectively, and those calculated by the present method are 19.90 eV for $K = 1.1$, 19.42 eV for $K = 1.08$, and 12.09 eV for $K = 1.1$, 11.42 eV for $K = 1.08$, respectively. The IP of ethyl cation has never been reported, so far as we know, but it may be expected to be much larger than that of neutral molecule, which is compatible with the present results. On the other hand, the orbital energies of ethane calculated by the two different methods do not differ as much as in the case of the ethyl cation, and the IP calculated by our method agrees reasonably with the experimental value,[11] 11.65 eV. It seems therefore that the extended Hückel method may be approximately valid in the calculations of the neutral molecules, but invalid in those of the charged molecules such as cations and anions, where the term representing the electron interaction in eq 2 cannot be neglected.

The orbital energies of methyl cation, methyl anion, and methane are compared in Table II. The changes of orbital energies are remarkable and their trends seem reasonable, for the lowest vacant (LV) and the highest occupied (HO) orbital energies correspond to the electron affinity and the IP of the referring molecules, respectively.

(11) K. Watanabe, *J. Chem. Phys.*, 26, 542 (1957).

Table II. Orbital Energies of Methyl Cation, Methane, and Methyl Anion

	CH_3^+, $K = 1.1$	CH_4, $K = 1.1$	CH_3^-, $K = 1.1$
LV	−9.661	11.740	18.878
HO	−21.618	−12.671	−0.290
	−21.618	−12.671	−3.371
	−29.053	−12.671	−3.371
		−20.137	−10.260

The ionization potential of a radical may be set approximately equal to the electron affinity of the corresponding cation.[12]

$$IP_{radical} = -\epsilon^{LV}_{cation} \qquad (10)$$

But, in the above approximation, a further investigation should be required to adopt the energy of the LV orbital, since the LV orbital is not included in the SCF procedure.

An IP of a radical can also be calculated by

$$IP_{radical} = W_{cation} - W_{radical} \qquad (11)$$

which is essentially a better approximation of the IP of a radical than eq 10, and may be used to check the validity of the LV orbital energy. The term, $W_{radical}$, appearing in eq 11 denotes the total energy of the referring radical and is calculated by the relation[13]

$$W_{radical} = W_{anion} + IP_{anion} \qquad (12)$$

The IP's of the alkyl radicals calculated by the above two methods are compared with the experimental values in Table III, where the IP's calculated by eq 11 and 12

Table III. IP's of Alkyl Radicals and Cations

	IP of radical $K = 1.1$	Exptl[a]	*IP* of cation, $K = 1.1$
CH_3	9.661 (9.643)[b]	9.95	21.168
C_2H_5	8.696 (8.712)	8.78	19.899
n-C_3H_7	8.377	8.69	18.826
i-C_3H_7	7.410 (7.436)	7.90	19.423
i-C_4H_9	8.155	8.35	18.523
t-C_4H_9	5.885	7.42	19.513

[a] A. Streitwieser, Jr., *Progr. Phys. Org. Chem.*, 1, 1 (1963). [b] The values in parentheses are calculated by eq 11.

are shown in parentheses. It is seen that the IP values calculated by both methods are very close and agree fairly well with experiments, and, hence, the validity of the LV orbital energies in SCF procedure may be assured.

Further, the calculated IP values of the alkyl cations are summarized in Table III. The IP's of alkyl cations seem not to have been observed and these values should be checked by experiment.

The Electronic Transitions. Some calculated transition energies and transition moments of various alkyl cations are shown in Table IV. It is seen from the table that the lowest transitions of alkyl cations are excitations of the $\sigma \to \pi^*$ type and their intensity will be rather small.

(12) N. S. Hush and J. A. Pople, *Trans. Faraday Soc.*, 51, 901 (1955).
(13) In these calculations, the geometries of cations and anions are assumed to be the same.

Table IV. Calculated Transition Energies (ΔE) and Transition Moments (Q) of Alkyl Cations

Cation	Type of transition[a]	$K = 1.1$ $^3\Delta E$, eV	$K = 1.1$ $^1\Delta E$, eV	$K = 1.1$ Q, Å	$K = 1.08$ $^3\Delta E$, eV	$K = 1.08$ $^1\Delta E$, eV	$K = 1.08$ Q, Å
CH_3^+	$\sigma-\pi^*$	2.06	2.47	0.0	1.56	1.95	0.0
$C_2H_5^+$	$\sigma_1-\pi^*$	3.91	4.07	0.110	3.51	3.63	0.103
	$\sigma_2-\pi^*$	2.27	3.28	0.179	1.78	2.39	0.188
	$\pi-\pi^*$	4.88	6.04	0.684	4.16	5.07	0.684
n-$C_3H_7^+$	$\sigma_1-\pi^*$	4.06	4.23	0.095	3.14	3.26	0.040
	$\pi-\pi^*$	4.99	5.55	0.526	4.44	4.85	0.451
	$\sigma_2-\pi^*$	4.91	5.06	0.170	4.33	4.50	0.181
i-$C_3H_7^+$	$\sigma_1-\pi^*$	4.52	4.79	0.098	3.34	3.65	0.085
	$\sigma_2-\pi^*$	4.89	5.17	0.162	3.94	4.24	0.179
	$\pi-\pi^*$	6.41	7.24	0.849	5.32	6.03	0.786
i-$C_4H_9^+$	$\sigma_1-\pi^*$	4.57	4.64	0.052	3.69	3.77	0.091
	$\sigma_2-\pi^*$	4.71	5.06	0.271	4.01	4.35	0.233
	$\pi-\pi^*$	5.28	6.39	0.718	4.28	5.34	0.704
t-$C_4H_9^+$	$\sigma_1-\pi^{*b}$	6.26	6.56	0.002	4.73	5.05	0.010
	$\sigma_2-\pi^*$	7.73	7.79	0.002	6.33	6.37	0.001
	$\pi-\pi^*$	8.51	9.22	0.779	6.91	7.54	0.739

[a] π^* orbital is LV orbital in every case. σ_1 and σ_2 denote the highest and the next highest σ-type orbitals, respectively. [b] The HO orbital is doubly degenerate.

Table V. Some Orbitals of Ethyl Cation Calculated with $K = 1.1$

(A) HO orbital of ethyl cation[a]
 $-0.294\pi'_{C1} + 0.562\pi'_{C2} - 0.236(h_3 - h_4) - 0.395(h_5 - h_6)$
(B) LV orbital of ethyl cation[b]
 $0.992\pi_{C1} - 0.174\pi_{C2} + 0.119(h_5 + h_6) - 0.239h_7$
(C) Highest π-type orbital of ethyl cation[c]
 $0.200\pi_{C1} + 0.573\pi_{C2} - 0.226(h_5 + h_6) + 0.452h_7$

[a] π and π' denote the $p\pi$ AO in and out of the molecular plane, respectively, and the numbering of the constituent atoms are shown in Table VII. [b] The geometry chosen for ethyl cation causes additional terms due to hyperconjugation, and these are: $-0.002s_{C1} - 0.003\sigma_{C1} + 0.001s_{C2} + 0.001(h_3 + h_4)$. [c] The additional terms due to hyperconjugation are: $0.002s_{C1} + 0.003\sigma_{C1} - 0.002s_{C2} + 0.001\sigma_{C2} - 0.001(h_3 + h_4)$.

These circumstances may be understood by referring to the natures of HO and LV orbitals of alkyl cations. As an example, the HO and LV orbitals of ethyl cation are listed in Table V. As will be seen in this example, the HO orbitals of alkyl cations are the σ-type orbitals consisting of AO's lying in the molecular plane, and, on the other hands, the LV orbitals of alkyl cations are the π-type orbitals which are almost localized on the cationic carbon atom.

Referring to Table IV, the strong transitions in alkyl cations which are expected to be found in the rather short wavelength region may be due to the excitation of a electron from the highest π-type orbitals to the LV orbitals. The highest π-type orbitals of mono-, di-, and trimethylcarbonium ions are constructed chiefly by the pseudo-π and -$p\pi$ AO's of the hyperconjugative methyl groups, as is shown by the example of ethyl cation in Table V.

Measurements of electronic spectra of alkyl cations have been made by several investigators but decisive assignments of the observed spectra to alkyl cations seem not to have been completed.[14] However, the

(14) The ultraviolet absorption of alkyl cations was observed by J. Rosenbaum and M. C. R. Symons (*Mol. Phys.*, 3, 205 (1960)) in concentrated sulfuric acid and they reported that isopropyl and *t*-butyl cations have the absorption maxima at 296 and 293 mμ (ϵ_{max} 6.4 × 10^3), respectively. (The intensity of absorption was later corrected to be <2000; see ref 1b.) But Deno[1c] held a different view and suggested that they are entirely due to a mixture of cyclopentenyl and cyclohexenyl cations.

present calculations may suggest that the observed spectra of isopropyl cation at 296 mμ (4.19 eV) and of t-butyl cations at 293 mμ (4.25 eV) are assigned to the $\sigma \rightarrow \pi^*$ transition.

As shown in the previous paper,[4] the LV orbital energy depends comparatively on the Wolfsberg–Helmholtz parameter, K, and the greater the value of K, the higher the LV energy. Therefore, the calculated transition energy for K = 1.1 is larger than those for K = 1.08.[15] But the calculated transition moment is little influenced by this parameter, as is seen in Table IV.

Alkyl Cations. The total electronic energies, nuclear repulsion energies, and total energies calculated for alkyl cations are summarized in Table VI. It is seen in the table that the structural isomerizations of alkyl cations cause only small changes in total energies, in spite of the rather large changes in total electronic energies and nuclear repulsion energies.

Table VI. Total Electronic Energies (E), Nuclear Repulsion Energies (NRE), and Total Energies (W) of Alkyl Cations

Cation	E, K = 1.1	NRE	W, K = 1.1
CH₃⁺ a	−287.79	128.67	−159.11
CH₃⁺ b	−288.03	129.54	−158.50
C₂H₆⁺	−802.84	475.38	−327.46
n-C₃H₇⁺	−1493.10	986.80	−506.29
i-C₃H₇⁺	−1482.95	976.58	−506.37
i-C₄H₉⁺	−2352.73	1657.08	−695.65
t-C₄H₉⁺	−2328.43	1632.48	−695.95

a Trigonal configuration. b Tetrahedral configuration.

Further, it may be noted that the experimentally observed order of stability between isomers (i-C₃H₇⁺ and t-C₄H₉⁺ are more stable than n-C₃H₇⁺ and i-C₄H₉⁺, respectively) should reflect those of the nuclear repulsion energy. Since the resultant isomerization energies seem rather small compared with experiment, a further improvement in the present treatment seems necessary.

The calculated populations of some alkyl cations and, for comparison, those of methane and staggered ethane are presented in Table VII. It is seen in Table VII that the charge of the cationic carbon distributes chiefly on the hydrogens of the adjacent methyl or methylene groups, and even to those of the terminal methyl group of the n-propyl cation. The average net charges of the hydrogen atom in methyl groups of isopropyl and t-butyl cations are +0.153 and +0.146 for K = 1.1 and these parallel the observed[10] chemical shifts of −5.06 and −4.35 ppm from tetramethylsilane, respectively. The population of the C–H bond lying in the plane perpendicular to the molecular plane is the smallest in every case, and it is expected that next fission of a hydrogen may occur at this bond. It is to be noted that the bonds between α-carbon and β-carbon are generally the weakest ones in the molecule, and that the bond population between the cationic carbon and α-carbon is exceptionally

Olah, et al.,[10] also observed a single weak absorption maximum around 290 mμ with a low extinction coefficient in antimony pentafluoride solution of some alkyl fluorides, and they assigned it to $\sigma \rightarrow \pi^*$ transition. But Olah and Pittman corrected their conclusion in their recent review[1b] and stated that this absorption is not due to alkyl cation but to impurity ions.

(15) From the calculations carried out for neutral molecules, the transition energies calculated by K = 1.1 may be recommended for the small molecules and those calculated by K = 1.08 for the large molecules, such as isobutyl and t-butyl cations (see ref 4).

Table VII. Atom Bond Populations of Alkyl Cations Calculated with K = 1.1

Alkyl cation	Atom	Population (Atom)	Bond	Population (Bond)
Methyl				
(i) the sp² form	C	+0.261	C–H	0.724
	H	+0.246		
(ii) the sp³ form	C	+0.231	C–H	0.714
	H	+0.256		
Ethyl	1	+0.339	1–2	0.809
	2	−0.198	1–3	0.802
	3	+0.180	2–5	0.790
	5	+0.154	2–7	0.740
	7	+0.192		
n-Propyl	1	+0.372	1–2	0.897
	2	−0.142	2–3	0.714
	3	−0.212	1–4	0.822
	4	+0.152	1–5	0.812
	5	+0.153	2–6	0.769
	6, 7 a	+0.175	3–10	0.813
	8, 9, 10 a	+0.108		
Isopropyl	1	+0.362	1–2	0.866
	2	−0.209	1–4	0.840
	4	+0.135	2–5	0.795
	5	+0.137	2–6	0.790
	6	+0.180	2–7	0.746
	7	+0.143		
Isobutyl	1	+0.379	1–2	0.944
	2	−0.064	2–3	0.717
	3	−0.206	1–5	0.823
	5	+0.136	2–7	0.780
	7	+0.172	3–8	0.816
	8, 9, 10 a	+0.108		
t-Butyl	1	+0.382	1–2	0.891
	2	−0.231	2–5	0.794
	5	+0.134	2–7	0.749
	7	+0.170		
Methane	C	−0.167	C–H	0.788
	H	+0.042		
Stag. ethane	C	−0.113	C–C	0.681
	H	+0.064	C–H	0.823

a Average value.

large, compared with that of the ethane C–C bond. These parallel the experimentally observed[10] bond-stretching frequencies of C–C and C–H bonds of the simple alkyl cations. In these, the small bond populations between the α- and β-carbons of n-propyl and isobutyl cations interpret the well-known β-fission rule.[16]

The change in charge at the cationic carbons with increasing number of methyl groups attached is of special interest. They are +0.261, +0.345, +0.362, and +0.382 for methyl, ethyl, isopropyl, and t-butyl cations, respectively.[17] More detailed analyses of these values are shown in Table VIII,[18] which also includes those of the populations on α-carbons. It is seen in Table VIII that the π population at the cationic carbon increases with increasing number of methyl groups linked to it. This is the same trend as that obtained by Muller and

(16) For example, see B. S. Greensfelder in "The Chemistry of Petroleum Hydrocarbons," Vol. 4, B. T. Brook, et al., Ed., Reinhold Publishing Corp., New York, N. Y., 1954, Chapter 27.

(17) The corresponding values calculated by Hoffmann were +0.609, +0.571, +0.611, and +0.692, respectively, and their changes were not monotonous (see ref 3).

(18) We gave preliminary results on the electronic structure of cyclopropylmethyl cations calculated by the method which does not include one-center exchange terms in eq 5 and 6. Therefore, the values presented here differ a little from those in our earlier paper: T. Yonezawa, H. Nakatsuji, and H. Kato, Bull. Chem. Soc. Jap., 39, 2788 (1966).

Table VIII. AO Populations at Cationic Carbons and α-Carbons

Cation	Cationic carbon, $K = 1.1$			α-Carbon, $K = 1.1$		
	σ^a	π	$\sigma + \pi$	σ^a	π	$\sigma + \pi$
CH_3^+	3.739	0.0	3.739			
$C_2H_5^+$	3.512	0.150	3.661	3.152	1.046	4.198
$n\text{-}C_3H_7^+$	3.412	0.216	3.628	3.098	1.044	4.142
$i\text{-}C_3H_7^+$	3.342	0.296	3.638	3.143	1.066	4.209
$i\text{-}C_4H_9^+$	3.359	0.262	3.621	3.060	1.004	4.064
$t\text{-}C_4H_9^+$	3.225	0.393	3.618	3.140	1.093	4.232
Stag. C_2H_6				3.153	1.039	4.192

^{a} σ-AO's in this table are the sums of s, pσ, and pπ' AO's of the referring carbon atom.

Mulliken,[19] so that these delocalization of π electrons may be attributed to the hyperconjugative effect of the methyl group. On the other hand, σ electrons behave conversely compared with π electrons, namely, the σ population at the cationic carbon decreases with increasing number of methyl groups attached to it. This behavior of σ electrons is reasonable, since an increase of π-population due to hyperconjugation will cause a decrease of σ population owing mainly to the one-center electron repulsion terms in eq 2.

The behavior of the AO populations at cationic carbon with increasing number of methyl groups attached is illustrated in Figure 1, which shows that, in spite of large changes in σ and π populations, the change of total population is surprisingly small. The trend of total population reflects that of the σ population, but is the inverse of that of the π population. Hence it may be stressed that the usual approximation of σ–π separation is inadequate in alkyl cations.

Further, Table VIII may indicate that the σ population of the "trigonal" carbon atom is larger than that of the adjacent sp³ carbon atom. This would be the consequence of larger electronegativity of an sp² carbon than an sp³ carbon.[20] However, interestingly, the AO population of the α-carbon in an alkyl cation suffers little change from those of the sp³ carbon in ethane (Table VIII), so that the comparatively large σ population of the sp² carbon is due chiefly to the supply from hydrogens in the molecule. The σ and π populations at the cationic carbon of the n-propyl cation are between those of ethyl and isopropyl cations, and those of the isobutyl cation are between those of n-propyl and isopropyl cations. These facts may suggest the order of the electronic effect of alkyl substituents on the cationic carbon atom.

The π AO bond populations between cationic carbon and α-carbon calculated with $K = 1.1$ are 0.094, 0.090, and 0.081 for $C_2H_5^+$, $i\text{-}C_3H_7^+$, and $t\text{-}C_4H_9^+$, respectively, which shows that the π-bond population decreases with increasing number of methyl groups linked to the cationic carbon. Further, those of $n\text{-}C_3H_7^+$ and $i\text{-}C_4H_9^+$ are calculated with $K = 1.1$ to be 0.120 and 0.133, respectively.

Protonated Hydrocarbons. Proton Affinities and Heat of Reactions in Some Ionic Reactions. A protonated hydrocarbon is a proton adduct of a hydrocarbon, and the energy which is released in this process is the proton affinity of a hydrocarbon. The calculated total energies of protonated hydrocarbons are listed in

(19) N. Muller and R. S. Mulliken, *J. Amer. Chem. Soc.*, **80**, 3489 (1958).
(20) W. Moffitt, *Proc. Roy. Soc.* (London), A202, 534, 538 (1950).
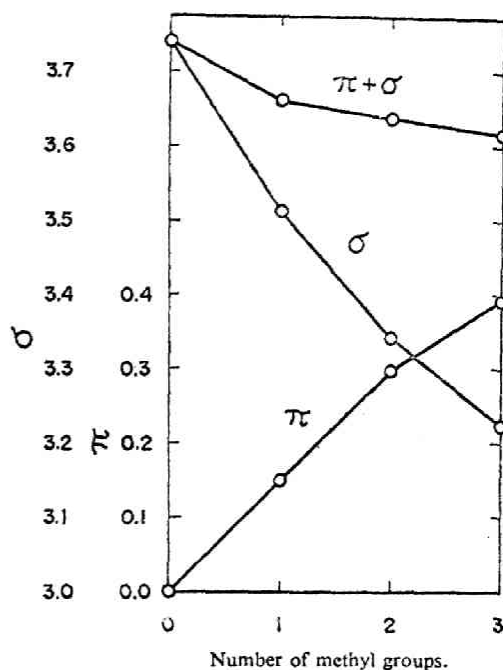
Figure 1. Changes of AO populations at the cationic carbon with increasing number of methyl groups attached.

Table IX, which also includes those of the parent hydrocarbons. Calculated proton affinities of CH_4, C_2H_4, and C_2H_2 are shown in Table X, together with the calculated energy changes for the reactions

$$CH_5^+ \longrightarrow CH_3^+ + 2H$$
$$CH_4 \longrightarrow CH_3^+ + H$$

and

$$C_2H_6 \longrightarrow C_2H_5^+ + H$$

Table IX. Calculated Total Energies of Protonated Hydrocarbons and Their Parent Hydrocarbons

Species	$K = 1.1$	Species	$K = 1.1$
CH_5^+	−192.07	CH_4	−186.15
$C_2H_7^+$		C_2H_2	−285.53
A form	−327.48	C_2H_4	−320.31
A' form	−328.00	C_2H_6	−356.79
B form	−326.86		
$C_2H_5^+$			
A form	−290.68		
B form	−291.19		

Table X. Calculated Energy Changes for Some Reactions

Reaction	Exptl	Calcd, $K = 1.1$
$CH_4 \longrightarrow CH_3^+ + H + e$	14.39^a	13.44
$CH_5^+ \longrightarrow CH_3^+ + 2H$	≥5.7^a	5.76
$CH_5^+ \longrightarrow CH_4 + H^+$	4.95 ~ 5.58^b	5.92
$C_2H_3^+ \longrightarrow C_2H_2 + H^+$	5.93^c	5.67
$C_2H_5^+ \longrightarrow C_2H_4 + H^+$	6.6^d	7.68
$C_2H_6 \longrightarrow C_2H_5^+ + H + e$	12.9^e	15.19

^{a} Reference 21. ^{b} Reference 25. ^{c} Estimated value from ΔH_f $(C_2H_3^+) = 283$ kcal/mol.[30] ^{d} Reference 16. ^{e} J. L. Franklin and H. E. Lumpkin, *J. Chem. Phys.*, **20**, 745 (1952).

In calculating the values shown in Table X, we used the total energy of the most stable conformation expected for

the referring cation, which will be discussed below. The agreement with experiment seems satisfactory, and the more detailed discussions about Table X will be seen in the corresponding sections which follow.

Protonated Methane and Its Negative Isomer. The assumed geometry of protonated methane is a trigonal bipyramid with a carbon–hydrogen bond of 1.05 Å.[21] · This model may be considered as an adduct of two hydrogen atoms on both ends of the vacant π AO of the methyl cation. The calculated atom bond populations are shown in Table XI, which indicates that the three hydrogens (H_a's) of the parent methyl group are bound more tightly than the other two hydrogens (H_b's). Interestingly, the charge of the central carbon is more negative than that of methane, and the net charge of this cation is completely distributed to hydrogens in molecule.

Table XI. Atom Bond Populations of Protonated Hydrocarbons Calculated with $K = 1.1$

Protonated hydrocarbon	Atom	Population		
			Bond	
Protonated methane				
	1	−0.348	1–a	0.702
	a	+0.231	1–b	0.613
	b	+0.328		
Protonated ethylene				
(i) the A form[a]	1	+0.060	1–2	0.885
	3	+0.162	1–3	0.823
	7	+0.233	1–7	0.313
(ii) the A' form[b]	1	+0.028	1–2	0.801
	3	+0.168	1–3	0.817
	7	+0.274	1–7	0.423
(iii) the B form[a]	1	+0.034	1–2	0.862
	3	+0.170	1–3	0.815
	7	+0.252	1–7	0.310
Protonated acetylene				
(i) the A form	1	+0.120	1–2	1.478
	3	+0.238	1–3	0.775
	5	+0.285	1–5	0.278
(ii) the B form	1	+0.248	1–2	1.288
	2	+0.062	1–3	0.743
	3	+0.268	2–4	0.752
	4	+0.211		
Ethylene	C	−0.155	C–C	1.225
	H	+0.078	C–H	0.827
Acetylene	C	−0.135	C–C	1.828
	H	+0.135	C–H	0.794

[a] The distance between H₋ and the center of the C–C bond is 1.2 Å. [b] The distance between H_7 and the center of the C–C bond is 0.8 Å.

The nature of the carbon–hydrogen bond in protonated methane is of special interest, and we summarized the calculated AO and AO-bond populations of CH_5^+ in Table XII, which also includes those of methane, ethylene, and acetylene. The value of the ratio of the AO-bond populations, $(p\sigma_C–h)/(s_C–h)$, in Table XII, which may be considered to represent the hybridized state of the referring carbon atom, undergoes a great change from methane to ethylene, and from

(21) (a) J. R. Hoyland and F. W. Lampe, *J. Chem. Phys.*, **37**, 1066 (1962); (b) J. Higuchi, *ibid.*, **31**, 563 (1959).

Table XII. AO and AO-Bond Populations in CH_4, C_2H_4, C_2H_2, CH_5^+, and CH_5^{-a}

Species	$s_C–h$	$p\sigma_C–h$	C–H bond population	H atom population	$(p\sigma_C–h)/(s_C–h)$
CH_4	0.207	0.581	0.788	0.958	2.81
C_2H_4	0.285	0.542	0.827	0.922	1.90
C_2H_2	0.376	0.418	0.794	0.865	1.11
CH_5^+					
H_a	0.164	0.538	0.702	0.769	3.28
H_b	0.186	0.427	0.613	0.672	2.29
CH_5^-					
H_a	0.272	0.533	0.805	1.175	1.96
H_b	0.049	0.417	0.466	1.405	8.51

[a] The values in this table are calculated with $K = 1.1$.

ethylene to acetylene. These values of the C–H_a and C–H_b bonds in CH_5^+ are remarkably different from each other, although the assumed bond lengths are 1.05 Å for both bonds, and it may be concluded that the s character of C–H_b bond is greater than that of the C–H_a bond.

The LV orbital of CH_5^+ calculated with $K = 1.1$ is[22]

$$\varphi^{LV}_{CH_5^+} = 0.100 s_C + 0.552(h_{a1} + h_{a2} + h_{a3}) - 0.889(h_{b1} + h_{b2})$$

This is bonding between s_C and h_a AO's but antibonding between s_C and h_b AO's. The orbital energy calculated with $K = 1.1$ is −1.429 eV and is extraordinarily higher than the LV orbital energies of usual alkyl cations and protonated hydrocarbons (−6 ~ −10 eV; see also Table III). Also the electron affinity of CH_5^+ may be expected to be very small,[23] and will be the order of magnitude of those in neutral molecules.[24] We examined further the occupied orbitals of CH_5^+ and found that all the occupied orbitals are bonding between the C–H_b bond.

The proton affinity of methane was observed[25] to be in the range 4.95–5.58 eV, and the present calculation gave 5.92 eV by $K = 1.1$ and 4.68 eV by $K = 1.08$ as shown in Table X.

We also calculated the electronic structure of CH_5^-, which may be assumed to be a model compound resembling the transition state of the S_N2 reaction. The calculated AO and AO-bond populations and the ratio, $(p\sigma_C–h)/(s_C–h)$, are also summarized in Table XII. It may be noted that the difference between the bond populations of the C–H_a and C–H_b bonds increases remarkably from CH_5^+ to CH_5^-. This means that the C–H_b bond becomes much weaker than the C–H_a bond in CH_5^-. Further, the $s_C–h$ bond population is nearly zero in CH_5^-, indicating that the C–H_b bond in CH_5^- is formed by almost pure p AO of the central carbon atom. Thus, the H_b–C–H_b bond of CH_5^- may properly be called a three-center bond. The ratio, $(p\sigma_C–h)/(s_C–h)$, of the C–H_a bond in CH_5^- approaches to the value of ethylene.

(22) The appropriateness of this LV orbital may be checked by the HO orbital of CH_5^- (see below).
(23) The electron affinity of CH_5^+ calculated by eq 11 is 1.446 eV and agrees fairly well with the estimated value (1.429 eV) from the LV orbital energy of CH_5^+.
(24) For example, the observed electron affinity of methyl radical is 1.1 eV. See also H. O. Pritchard, *Chem. Rev.*, **52**, 529 (1953), and N. S. Hush and J. A. Pople, *Trans. Faraday Soc.*, **51**, 600 (1955).
(25) V. L. Tal'rose and E. L. Frankevitch, *J. Amer. Chem. Soc.*, **80**, 2344 (1958).

The HO orbital of CH_5^- which corresponds to the LV orbital of CH_5^+ is

$$\varphi^{HO}_{CH_5^-} = 0.059s_C + 0.560(h_{a1} + h_{a2} + h_{a3}) - 0.884(h_{b1} + h_{b2})$$

and its energy is $+6.367$ eV, which is very large and is extraordinarily higher than that of the usual anions, since the HO orbital energy of an anion may be set approximately equal to the electron affinity of the corresponding radical.[24] Further, because of the instability of the HO orbital of CH_5^- the total energy of CH_5^- (-87.148 eV) is larger than that of CH_5^+ (-192.069), and this is also exceptional, referring to those of alkyl cations and anions.

Protonated Ethylene. Protonated ethylene is an isomer of ethyl cation and is sometimes postulated to represent the true configuration of $C_2H_5^+$.[26] In order to study the stable configuration, we calculated the total energies of protonated ethylenes with some configurations which are shown in Table XI. In the A form in Table XI, the proton adds symmetrically to planar ethylene. In the B form, the terminal carbon–hydrogen bonds are bent in the tetrahedral angle; in both cases, the C—C bond lengths are assumed to be 1.44 Å. As a first step, the distance from the adding proton to the center of the C=C bond is assumed to be 1.2 Å[3] and the results with $K = 1.1$ and $K = 1.08$ predict that the A form will be more stable than the B form by 0.61 and 0.52 eV, respectively. When this length in the A form is varied, the total energy minimum is obtained about 0.8 Å (the A' form in Table XI) by $K = 1.1$. But this value may be rather small, and may not represent the real configuration of protonated ethylene, since the approximation introduced in eq 9 may underestimate the nuclear repulsion energy when the interatomic distance becomes small.

Comparing the total energy of the A' form with that of ethyl cation of the geometry shown in Table VII, the present calculation may suggest that the stable configuration of $C_2H_5^+$ will be protonated ethylene type of the A' form.

The atom bond populations of the A, A', and B forms are illustrated in Table XI. The charge of the adding proton is well distributed, and the bond population between this proton and carbon atom is relatively large. The π-AO population of the carbon atom is 0.790 in the A' form and is remarkably small, compared with the value 1.00 for ethylene. Further, the C–C bond population of ethylene calculated by $K = 1.1$ is 1.225. This bond in protonated ethylene is considerably weakened by protonation.

The proton affinity of ethylene and the heat of formation of $C_2H_5^+$ from ethane, which are shown in Table X, are calculated based on the A' form which is expected to be the most stable form of $C_2H_5^+$. The appearance potentials of CH_3^+ from CH_4 and of $C_2H_5^+$ from C_2H_6 were observed to be 14.39 and 12.9 eV, respectively, and the stabilization energy[27] of $C_2H_5^+$ relative to CH_3^+ was

(26) L. G. Connell and R. W. Taft, Jr., *J. Amer. Chem. Soc.*, 78, 5812 (1956).

(27) See Table X, footnote *e*.

expected to be 1.5 eV. But we failed in calculating the stabilization energy of $C_2H_5^+$, and this is due to the overestimation of off-diagonal core Hamiltonian matrix elements (Hrs in eq 2) by the weight K.[4,28]

Protonated Acetylene. Protonated acetylenes of two configurations, symmetrical and unsymmetrical, illustrated in Table XI are considered. In the A form, the distance between the adding proton and the center of the C–C bond of acetylene is assumed to be 1.20 Å, in the B form, one of the terminal carbons is assumed to be in the sp^2 state, and C–C bond lengths of both forms are assumed to be 1.27 Å. As shown in Table IX, the B form which may be regarded as the product of the dehydride reaction of ethylene is expected to be more stable than the A form by 0.514 eV, and this is the same trend as reported by Hoffmann.[3] However, both methods involve some approximations, and further investigations would be necessary to draw a final conclusion.

The atom bond populations of protonated acetylene are shown in Table XI, which shows also that the net charge of the adding proton distributes in the molecule. Further, the atom population of the sp carbon in the B form is remarkably small and this is due to the small value (0.115 by $K = 1.1$) of the π'-AO population of this carbon atom.

The LV and next LV orbitals of the B form are[29]

LV

$$0.995\pi'_{C1} - 0.114\pi'_{C2} - 0.248(h_4 - h_5)$$

Next LV

$$0.742\pi_{C1} - 0.902\pi_{C2}$$

and their orbital energies are -8.58 and -7.05 eV,[30] respectively. These results may suggest that the protonated acetylene of the B form has two stable unoccupied orbitals, one of which lies in the molecular plane and the other lies in the plane perpendicular to the molecular plane.

The proton affinity of acetylene estimated from the observed[30] heat of formation of $C_2H_3^+$ is 5.93 eV and is less than the observed value for ethylene. The calculated proton affinity of acetylene, based on the B form, is 5.67 eV and is also less than the calculated value of ethylene, as shown in Table X. The agreement of the calculated value with the estimated values is excellent.

(28) By improving the overestimation of off-diagonal core Hamiltonian matrix element, we succeeded in calculating the stabilization energy. Namely, the appearance potentials of CH_3^+ from CH_4 and of $C_2H_5^+$ from C_2H_6 are calculated by the improved method as 13.43 and 12.40 eV, respectively. More details about this improvement will be published in the near future.

(29) In the LV orbital, the group orbital ($h_4 - h_5$) is antibonding with π'_{C1}, and bonding with π'_{C2}.

(30) The *IP* of the vinyl radical was observed to be 9.45 eV: A. G. Harrison and F. P. Lossing, *J. Amer. Chem. Soc.*, 82, 519 (1960). But the observed configuration of vinyl radical is different from that of the B form in the present calculation: R. W. Fessenden and R. H. Schuler, *J. Chem. Phys.*, 39, 2147 (1963).

The π-Type Conjugation in the Cyclopropylmethyl Cation

The high conjugative ability of the cyclopropyl group with an adjacent π orbital has been established experimentally[1] and theoretically.[2-4] For the cyclopropyl derivatives, Walsh predicted that this conjugation would be most effective when these compounds were in a "bisected" conformation (I in Fig. 1). Recently his prediction has been confirmed by Pittman and Olah through their NMR measurements.[1]

In the present paper, we will treat quantitatively the electronic structures of the two conformers, "bisected" (I) and "non-bisected" (II) (see Fig. 1), of the cyclopropylmethyl cation with our newly-developed semi-empirical ASMO-SCF method.[5] The geometry chosen for the cyclopropyl group is the same as that in cyclopropane, while the C_1–C_5 bond distance (in Fig. 1) is assumed to be 1.50 Å.
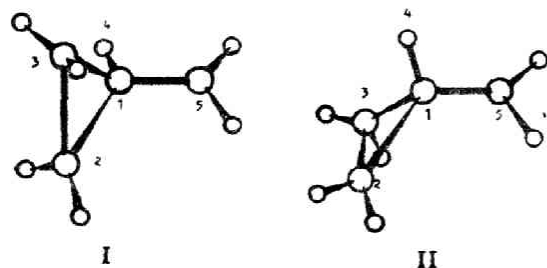

Fig. 1. The configurations of "bisected" (I) and "non-bisected" (II) conformers. In the I form, the atoms H_4, C_1 and the terminal CH_2 group are on the same plane, and in the II form the C_1–H_4 bond is perpendicular to the plane of the terminal CH_2 group.

TABLE I. THE ATOM AND AO BOND POPULATIONS IN CYCLOPROPYL GROUP

Compound	C_1–C_2	p_1–p_2	C_1–H_4	$p_{\sigma 1}$–h
Bisected (I)	0.585	0.309	0.847	0.523
Non-bisected (II)	0.650	0.378	0.785	0.464
Cyclopropane	0.651	0.367	0.839	0.539

1) C. U. Pittman, Jr., and G. A. Olah, J. Am. Chem. Soc., 87, 5123 (1965).
2) A. D. Walsh, Trans. Faraday Soc., 45, 179 (1949).
3) C. A. Coulson and W. E. Moffitt, Phil. Mag., 40, 1, (1949).
4) R. Hoffmann, J. Chem. Phys., 40, 2840 (1964); Tetrahedron Letters, 43, 3819 (1965).
5) T. Yonezawa, K. Yamaguchi and H. Kato, This Bulletin, to be published; Abstract of the Symposium on Molecular Structure, Osaka (1966), p. 49.
* In Ref. 1 it is stated that the energy difference between these two conformers might be larger than 8 - 10 kcal./mol.

The calculated total energies show that the I form is more stable than the II form by 0.813 eV. The π atomic orbital (AO) population of the C_5 atom is 0.443 in I and 0.280 in II. As to the atom bond population between the C_1 and C_5 atoms, the values are 1.015 in I and 0.924 in II, while the π AO bond populations are 0.203 in I and 0.113 in II; other π AO bond values obtained by the same method include 0.425 in ethylene, 0.114 in the ethyl cation, and -0.022 in ethane. Accordingly, it may be concluded that the π-conjugation in the I form is quite strong and that it contributes greatly to the stabilization of the I form.

The atom bond populations of C_1–C_2 and C_1–H_4 are collected in Table I, together with the corresponding values in cyclopropane. The table implies that the values of C_1–C_2 in the II form and of C_1–H_4 in the I form do not suffer much change, compared with the values in the cyclopropane, while remarkable changes do occur in C_1–C_2 in I and in C_1–H_4 in II. Further, in Table I, the sum of the AO bond populations between the three p AO's belonging to the C_1 and C_2 atoms, denoted by p_1–p_2 in Table I, and the value between the pσ AO of the C_1 atom and the 1s AO of the H_4 atom ($p_{\sigma 1}$–h) are also indicated. Hence, the following conclusion may be drawn; the large changes in the atom bond population of C_1–C_2 in I and of C_1–H_4 in II are mainly caused by the changes in p_1–p_2 in I and in $p_{\sigma 1}$–h in II. As may be seen in Fig. 1, the p AO of the C_1 atom conjugating with the vacant π AO of the C_5 atom also participates in the C–C bonding in the I form and in the C–H bonding in the II form. Accordingly, the above-mentioned changes are largely due to the interactions between the p AO of the C_1 atom and the vacant π AO.

From the above discussions, it is clear that the stabilization in the I form arises mainly from π-type interaction between the vacant π AO of the sp^2 carbon and the π-like AO's in the ring carbons.

The transition energies for the first excitation may be evaluated as 6.60 eV. and 5.04 eV., and the oscillator strengths as 0.054 and 0.015, for I and II respectively. These transitions may be attributed to the intramolecular charge transfer from the cyclopropane ring to the vacant π AO of the sp^2 carbon.

PART II, CHAPTER 3

ELECTRONIC STRUCTURE OF DOUBLET RADICALS

BY THE UNRESTRICTED HARTREE-FOCK METHOD

SECTION 1

ELECTRONIC STRUCTURE

OF

DOUBLET RADICALS

Semi-empirical Unrestricted SCF-MO Treatment for Valence Electron Systems. I. Application to Small Doublet Radicals

A semi-empirical SCF method for valence electron systems including a differential overlap previously prepared by the present authors is here extended to molecules with an open-shell structure. The unrestricted Hartree-Fock method is applied, and the one-centre and part of two-centre $\sigma-\pi$-type exchange repulsion integrals, playing an essential role in spin-density calculations, are included in the calculations. The calculated spin densities are divided into the mechanistic (spin-polarization and spin-delocalization) contributions. The spin-polarization mechanism is shown to be important even in cases where the spin delocalization mechanism has usually been considered to be dominant (e. g., ethyl and vinyl radicals). The calculated spin densities of π-electron radicals (methyl, ethyl, allyl, and trans-butadienyl anion radicals) and of σ-electron radicals (vinyl, formyl, NO_2, CO_2^-, CN) are discussed. Their hfs constants and mechanistic contributions are calculated; for the methyl and vinyl radicals these are shown to be strongly angular-dependent. The calculated potential curve and the hfs constants of the vinyl radical lead to the CCH$_\alpha$ angle, $\theta \simeq 135°$; furthermore, the H$_\alpha$ and C$_\beta$ hfs constants are shown to be negative. Generally, the calculated proton hfs constants agree satisfactorily with the experimental data and with other calculations except in the case of the formyl radical. The atomic dipoles of some σ-electron radicals are calculated, and some interesting features common to all the σ-electron radicals studied are found.

Recently semi-empirical SCF methods for valence electron systems have been generally applied[1-5] to calculations of certain physical and chemical properties of molecules. We have previously proposed a semi-empirical SCF method including differential overlaps for valence electron systems and applied it to various closed-shell molecules.[4] Here, we extend this method to molecules with an open-shell structure. As in the preliminary reports,[5] the unrestricted Hartree-Fock (UHF) method[6] is applied. Since the UHF wave function is not an eigenfunction of the spin-squared operator, S^2, the lowest contaminating spin functions are annihilated[7] after energy minimization.

The spin density calculated by the UHF method originates from two main mechanisms,[8] the spin-polarization (SP) and spin-delocalization (SD) mechanisms. In order to clarify the nature of the spin-density, these mechanistic contributions are

1) a) J. A. Pople, D. P. Santry and G. A. Segal, J. Chem. Phys., 43, 3129 (1965). b) J. A. Pople and G. A. Segal, ibid., 44, 3289 (1966). c) J. A. Pople, D. L. Beveridge and P. A. Dobosh, ibid., 47, 2026 (1967). d) J. A. Pople, D. L. Beveridge and P. A. Dobosh J. Am. Chem. Soc., 90, 4201 (1968).

2) N. M. Atherton and A. Hinchliffe, Mol. Phys., 12, 349 (1967).

3) T. Yonezawa, H. Konishi and H. Kato, This Bulletin, 41, 1031 (1968).

4) a) T. Yonezawa, K. Yamaguchi and H. Kato, ibid., 40, 535 (1967). b) T. Yonezawa, H. Konishi and H. Kato, ibid., 40, 1071 (1967). c) H. Kato, H. Konishi, H. Yamabe and T. Yonezawa, ibid., 40, 2761 (1967). d) T. Yonezawa, H. Nakatsuji and H. Kato, J. Am. Chem. Soc., 90, 1239 (1968).

5) a) T. Yonezawa, H. Nakatsuji, T. Kawamura and H. Kato, This Bulletin, 40, 2211 (1967). b) T. Yonezawa, H. Nakatsuji T. Kawamura and H. Kato, Mol. Phys., 13, 589 (1967).

6) J. A. Pople and R. K. Nesbet, J. Chem. Phys., 22, 571 (1954).

7) a) T. Amos and G. G. Hall, Proc. Roy. Soc. (London), A263, 483 (1961). b) A. T. Amos, Mol. Phys., 5, 91 (1962). c) T. Amos and L. C. Snyder, J. Chem. Phys., 41, 1773 (1964). d) L. C. Snyder and T. Amos, ibid., 42, 3670 (1965).

separated by the method reported previously.[5] In π-electron radicals, the SP mechanism is dominant and is reduced to small σ-π-type electron repulsion integrals. In the present calculation, the one-center and part of two-center σ-π-type exchange repulsion integrals are included, although the latter was neglected previously.[5]

The method is applied mainly to the spin-density calculations of π-electron radicals, such as the methyl, ethyl, allyl, and s-*trans*-butadienyl anion radicals, and of some σ-electron radicals, such as vinyl, formyl, NO_2, CO_2^- and CN radicals. The mechanistic contributions to the spin density are separated, and some interesting features of spin density are revealed. Lastly, the dipole moments of the σ-electron radicals are analyzed.

Method

An unrestricted wavefunction for a system with p α-spin and q β-spin electrons has the form:

$$\psi_{uhf} = |\varphi_1^\alpha(1)\alpha(1)\cdots\varphi_p^\alpha(p)\alpha(p)\varphi_1^\beta(p+1)\beta(p+1)\cdots$$

$$\varphi_q^\beta(n)\beta(n)|, \qquad (1)$$

where $n=p+q$. For the doublet radicals considered here $p=q+1$. The molecular orbital is expanded as a linear combination of all the valence atomic orbitals (VAO's), χ_r, of the constituent atoms:

$$\varphi_i^\alpha = \sum_r C_{ir}^\alpha \chi_r$$

and:

$$\varphi_i^\beta = \sum_r C_{ir}^\beta \chi_r. \qquad (2)$$

The unrestricted SCF equations of the LCAO approximation are:

$$F^\alpha C_i^\alpha = \varepsilon_i^\alpha S C_i^\alpha$$

and:

$$F^\beta C_i^\beta = \varepsilon_i^\beta S C_i^\beta \qquad (3)$$

in the usual notations.[6]

Estimation of Integral Values. One of the main features of the unrestricted SCF theory is its inclusion of spin correlation, thus enabling us to calculated negative spin densities. In the case of π-electron radicals, the spin densities appearing in the σ-type AO's are due to the σ-π-type spin-polarization mechanism.[9,10] In order to study these radicals, the following exchange integrals are considered in the calculations:

(a) The one-center exchange repulsion integrals[*2] are evaluated by the approximate relations:[4c]

$$(pp'sp) = 0.045Z_A(ss|pp)$$

and:

$$(pp'|pp') = 0.011Z_A(pp|pp), \qquad (4)$$

where s denotes the 2s AO.

(b) A part of the two-center σ-π-type exchange repulsion integrals is approximated by the following semi-empirical estimation:

$$(h\pi_X|h\pi_X)_{\text{semi-empirical}} = k(h\pi_X|h\pi_X)_{\text{Slater}}$$

$$(\mu_X\bar\pi_{X'}|\mu_X\bar\pi_{X'})_{\text{semi-empirical}} = k(\mu_X\bar\pi_{X'}|\mu_X\bar\pi_{X'})_{\text{Slater}} \qquad (5)$$

$$(\mu_X\nu_{X'}|\mu_Y\nu_{Y'}) = \{(\mu_X\nu_{X'}|\mu_X\nu_{X'})\cdot(\mu_Y\nu_{Y'}|\mu_Y\nu_{Y'})\}^{1/2}$$

where h is a hydrogen 1s AO, where μ is a 2s, 2pσ or 2pπ AO, and where X and Y denote the first-row elements of the periodic table. The value of the parameter, k, is chosen so that the calculated proton spin densities of the methyl and ethyl radicals obtained before annihilation may reasonably be compared with the experimental results; the value is equal to 0.58 throughout these calculations.[*3] For the 2s AO spin density of the carbon atom, the above two-center σ-π-type exchange repulsion integrals are not so important as are those for the proton spin density.[*4]

Note that many other two-center σ-π-type electron repulsion integrals are omitted. However, the parameter k, introduced in Eq. (5), may effectively include these neglected integrals for the proton-spin density in the C–H bond;[*5] this assumption will, however, break down for heteropolar cases such as for the N–H and O–H bonds,

9) a) H. M. McConnell, *J. Chem. Phys.*, **24**, 764 (1956). b) H. M. McConnell and D. B. Chesnut, *ibid.*, **27**, 984 (1957); **28**, 107 (1958). c) H. M. McConnell, *ibid.*, **28**, 1188 (1958). d) S. I. Weissman, *ibid.*, **25**, 890 (1956).

10) M. Karplus and G. K. Fraenkel, *J. Chem. Phys.*, **35**, 1312 (1961).

*2 The inclusion of one-center exchange repulsion integrals destroys the invariance[1a] of the Mulliken approximation, since $(pp|p'p') = (pp|pp) - 2(pp'|pp')$. Therefore, the one-center exchange repulsion integrals are included in the method after the Mulliken approximation for $(rs|tu)$ is completed, and the term $-2(pp'|pp')$ is introduced as a correction to $(pp|p'p')$. Thus, the present method is invariant to rotation around local atomic axis.

*3 The ratios of the adopted one-center exchange integrals to the theoretical values calculated from Slater AO's are 0.51 for $(pp'|pp')$ and 0.58 for $(sp|sp)$.

*4 For the methyl radical, the contributions of the one- and the two-center σ-π-type exchange repulsion integrals are -0.0787 and -0.0512 for the proton-spin density, and 0.1788 and -0.0301 for the carbon 2s AO spin-density (before annihilation).

*5 The contribution of the σ-π-type ionic integrals is zero if the C–H bond is assumed to be homopolar. For example, the configuration interaction treatment of the methyl radical, using the simple MO's based on the hybrid orbitals, showed that the contribution due to the two center σ-π-type ionic integrals amounts to only 6% of the total proton spin density.

8) a) T. Yonezawa, H. Nakatsuji, T. Kawamura and H. Kato, *Chem. Phys. Letters*, **2**, 454 (1968). b) T. Yonezawa, H. Nakatsuji, T. Kawamura and H. Kato, *J. Chem. Phys.*, in press. c) H. Nakatsuji, H. Kato and T. Yonezawa, *ibid.*, in press.

where the omitted $\sigma-\pi$ type ionic integrals may become important.

The method of estimating all the other integral values is the same as has been previously reported.[4-6]

Spin-polarization and Spin-delocalization Contributions. As has been shown in previous papers,[8] the spin-polarization (SP) contribution to the calculated spin density at the i position is given by the following equations for doublet radicals:

$$(\rho_{ba}^i)_{SP} = \frac{3}{2} (\rho_{ba}^i - \rho_{aa}^i),$$

$$(\rho_{aa}^i)_{SP} = \frac{1}{2} (\rho_{ba}^i - \rho_{aa}^i). \qquad (6)$$

$(\rho_{ba}^i)_{SP}$ is the SP contribution to the spin density, ρ_{ba}^i, calculated by the UHF method, and $(\rho_{aa}^i)_{SP}$ is the SP contribution to the spin density, ρ_{aa}^i, obtained after annihilation.[*6] The spin-delocalization (SD) contributions are the same for both stages (ba and aa) and are approximated[8] by:

$$(\rho^i)_{SD} = \rho^i - (\rho^i)_{SP}. \qquad (7)$$

Estimation of the Isotropic hfs Constants. The isotropic proton hfs constant, a, is expressed approximately by: $a_H = A_H \rho_H$,[9c] while the values for the first-row nuclei of the periodic table are given as the sum of the $2s$ contribution ($A_{2s(N)} \cdot \rho_{2s(N)}$) and of the inner $1s$ contribution.

In the present calculations, A_H is regarded as a proportionality constant determined by "best fitting" the calculated spin densities (before annihilation) to the observed hfs constants. A_H is set equal to 743 gauss throughout this paper. The $2s$ contribution to the hfs constant of the ^{13}C nucleus is calculated by setting $A_{2s(C)} = 1110$ gauss.[11] However, the present method does not give the quite important contributions to hfs constants by

---

[*6] Hereafter, the spin densities calculted befor and after annihilation will be wyitten as $\langle\rho\rangle_{ba}$ and $\langle\rho\rangle_{aa}$, and the charge densties, as $\langle q\rangle_{ba}$ anb $\langle q\rangle_{aa}$, $\langle\rho\rangle_{ba}$ has the same meaning as the ρ_{uhf} in the previous paper.[8]

[*7] For the proton, the hfs constants calculated only from $(\rho_h)_{ba}$ are compared with the experimental results. The reasons for this are as follows: As may be seen from Eq. (6), the SP contributions satisfy the relation: $(\rho_{ba}^i)_{SP} = 3(\rho_{aa}^i)_{SP}$, while the SD contributions satisfy $(\rho_{ba}^i)_{SD} = (\rho_{aa}^i)_{SP}$. For example, in the ethyl radical, the spin density of the H_7 atom is due to both mechanisms, while that of the H_3 atom is due only to the SP mechanism. (See Fig. 1 and Table 4.) Thus, $\rho_{ba} \simeq 1.2\rho_{aa}$ for the H_7 atom and $\rho_{ba} \simeq 3\rho_{aa}$ for the H_3 atom. This example shows that, if the $\sigma-\pi$-type electron repulsion integrals are so adjusted that ρ_{ba} correlates well with the experimental values, then ρ_{aa} correlates poorly with the observed values in the least-mean-square's sense. For a comparison of the spin densities calculated by the various methods, see the article by Harriman and Sando (*J. Chem. Phys.*, **48**, 5138 (1968)).

11) J. R. Morton, *Chem. Revs.*, **64**, 453 (1964).

12) A. L. H. Chung, *J. Chem. Phys.*, **46**, 3144 (1967).

---

inner $1s$ AO's.[10,12] These contributions are opposite in sign to those of the $2s$ AO's.[10,12]

Application of the Method

In this section we will present the results obtained by applying the above method to three types of radicals: 1) organic π-electron radicals, such as methyl, ethyl, allyl, and *trans*-butadienyl anion radicals; 2) organic σ-electron radicals, such as vinyl and formyl radicals, and 3) inorganic σ-electron radicals, such as NO_2, CO_2^-, and CN radicals. The geometries and the numberings are illustrated in Fig. 1. In this section we will first show the general features common to the three types of radicals. Secondly, the characteristic features of each type of radical will be compared with the experimental results, and lastly, the dipole moments of the σ-electron radicals will be analyzed.

General Features. The calculated ionization potentials and electron affinities are given in Table 1, together with the experimental values. The calculated ionization potentials are generally larger than the observed values.

Table 2 gives the expectation values of the spin-squared operator, S^2, before and after the annihilation of the quartet spin function. The annihilation of the lowest contaminating spin state yields a sufficiently pure eigenstate of S^2. If the sextet and higher spin states are neglected, the UHF wavefunction for doublet radicals may be written as:

$$\psi_{uhf} = C_{1/2}\psi_{1/2} + C_{3/2}\psi_{3/2},$$

and the relative weight, $(C_{3/2})^2/(C_{1/2})^2$, may be calculated by:[7]

$$(C_{3/2})^2/(C_{1/2})^2 = \frac{4\langle S^2\rangle_{uhf}-3}{15-4\langle S^2\rangle_{uhf}}. \qquad (8)$$

In the last column of Table 2, these values are given for various radicals; they are less than 0.04 for all the cases studied here.

That annihilation of the lowest contaminating spin state weakly influences the total charge densities[7b] is shown in Table 3 for the methyl and NO_2 radicals. This fact can be deduced generally.[8c] However, the annihilation causes large changes in the spin-density distributions, as will be shown below.

Organic π-Electron Radicals. *i) Methyl Radical.* The geometry, hfs constants, and some other properties of the methyl radical have been examined theoretically[1,10,12,13] and experimental-

13) a) M. Karplus, *J. Chem. Phys.*, **30**, 15 (1959). b) D. M. Schrader and M. Karplus, *ibid.*, **40**, 1593 (1964). c) D. M. Schrader, *ibid.*, **46**, 3895 (1967). d) K. Morokuma, L. Pedersen and M. Karplus, *ibid.*, **48**, 4801 (1968). e) D. L. Beveridge and K. Miller, *Mol. Phys.*, **14**, 401 (1968).

C-H = 1.079 A

C-C = 1.40 A, C-H = 1.08 A
∠HCH = ∠HCC = ∠CCC = 120°

C-C = 1.50 A
C(1)-H = 1.079 A, C(2)-H = 1.09 A

C(1)-C(2) = 1.337 A, C-H = 1.08 A
C(2)-C(3) = 1.483 A

C-C = 1.34 A, C-H = 1.07 A

C-O = 1.198 A, C-H = 1.08 A
∠HCO = 119.5°

N-O = 1.2 A
∠ONO = 134°

C-O = 1.188 A
∠OCO = 134°

C-N = 1.1718 A
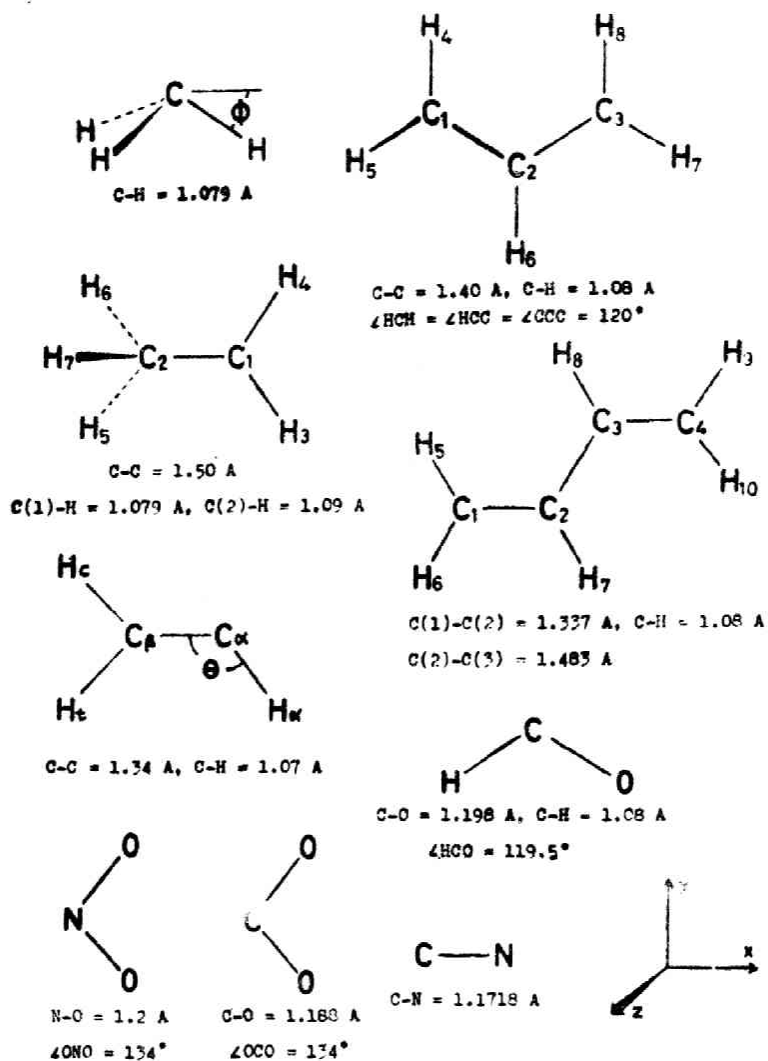
Fig. 1. Geometries (L. E. Sutton Ed., "Tables of Interatomic Distances and Configuration in Molecules and Ions," Chem. Soc. (London), (1956) and (1965)).

TABLE 1. IONIZATION POTENTIAL (IP) AND ELECTRON AFFINITY (EA) (eV)

| Radical | IP | | EA | |
	Exptl.	Calcd	Exptl.	Calcd
CH_3	9.86,[a] 9.95[a]	10.310	1.1,[d] 1.4[e]	−0.813
C_2H_5	8.67,[a] 8.78[a]	10.062	0.9,[d] 0.94[e]	−0.690
C_3H_5	8.16,[a] 8.755[a]	9.202	2.1,[d] 2.21[e]	0.050
$C_4H_6^-$	−0.34[b]	−0.164	—	−7.728
C_2H_3	9.45[c]	10.223	—	−0.665
HCO	9.82,[a] 9.88[a]	9.854	—	0.200
NO_2	11.3,[a] 9.78[a]	11.967	2.34,[f] 1.62[d]	2.18
CO_2^-	—	1.820	—	−8.041
CN	14.55,[a] 15.13[a]	11.307	3.21[e]	0.445

a) R. W. Kiser, "Tables of Ionization Potentials", United States Atomic Energy Commission, TID-6142 (1960).

b) The value cited is the calculated EA of trans-butadiene: N. S. Hush and J. A. Pople, Trans. Faraday Soc., 51, 600 (1955).

c) F. W. McLafferty, "Mass Spectrometry of Organic Ions," Academic Press Inc., New York (1963), p. 240.

d) H. O. Pritchard, Chem. Revs., 52, 529 (1953); H. O. Pritchard and H. A. Skinner, ibid., 55, 745 (1955).

e) F. M. Page, Symp. Combust. 9-th, Pasadena, Calif., 1960, p 160.

f) D. F. C. Morris, J. Inc. Nucl. Chem., 6, 295 (1958).

g) J. T. Herron and V. H. Dibeler, J. Am. Chem. Soc., 82, 1555 (1960).

75

TABLE 2. THE EXPECTATION VALUES OF $\langle S^2 \rangle$ BEFORE AND AFTER ANNIHILATION OF THE QUARTET SPIN FUNCTION

Radical	$\langle S^2 \rangle$		$\frac{(C_{3/2})^{2\,a)}}{(C_{1/2})^2}$
	Before annihilation	After annihilation	
Methyl			
$\phi = 0.0°$	0.7544	0.7500	0.0014
6.0°	0.7542	0.7500	0.0014
12.0°	0.7537	0.7500	0.0012
19.47°	0.7529	0.7500	0.0010
Ethyl	0.7564	0.7500	0.0021
Allyl	0.8584	0.7510	0.0399
(t-Butadiene)⁻	0.7828	0.7502	0.0113
Vinyl			
$\theta = 120°$	0.7880	0.7502	0.0132
135°	0.7892	0.7503	0.0137
150°	0.7906	0.7504	0.0142
180°	0.7922	0.7506	0.0148
Formyl	0.7713	0.7502	0.0071
NO_2	0.7563	0.7500	0.0021
CO_2^-	0.7529	0.7500	0.0009
CN	0.7562	0.7500	0.0020

a) See Eq. (8).

TABLE 3. TOTAL CHARGE DENSITIES OF THE CH_3 AND NO_2 RADICALS CALCULATED BEFORE AND AFTER ANNIHILATION

	CH_3			NO_2		
Atomic orbital	$\langle q \rangle_{ba}$	$\langle q \rangle_{aa}$		Atomic orbital	$\langle q \rangle_{ba}$	$\langle q \rangle_{aa}$
$2s$	1.1152	1.1126		$2s(N)$	1.4906	1.4900
$2p_x, 2p_z$	0.4200	0.4200		$2p_x(N)$	1.0690	1.0686
$2p_y$	1.0000	1.0000		$2p_y(N)$	0.2588	0.2578
h	0.7611	0.7602		$2p_z(N)$	0.7605	0.7603
				$2s(O)$	2.0238	2.0239
				$2p_x(O)$	1.5712	1.5712
				$2p_y(O)$	1.1459	1.1454
				$2p_z(O)$	1.4142	1.4141

ly[14] in great detail. In this paper we examine its structure, force constant, and *hfs* constants.

In Fig. 2, the calculated potential curve for the out-of-plane bending of the methyl radical is shown. The present calculation predicts a planar configura-
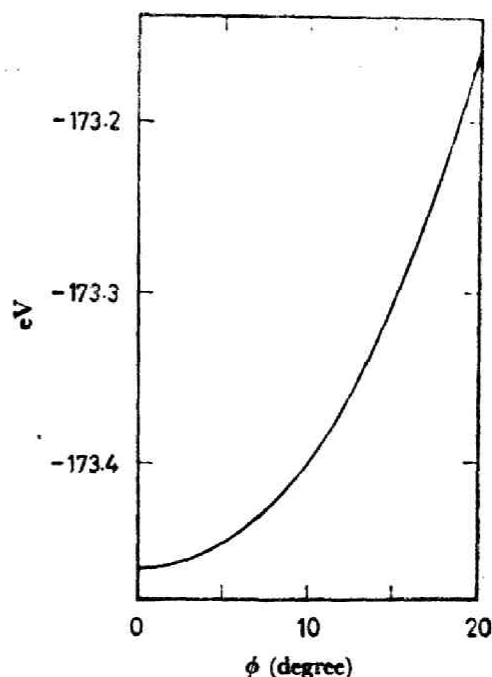
14) a) T. Cole, H. O. Pritchard, N. R. Davidson and H. M. McConnell, *Mol. Phys.*, **1**, 406 (1958). b) G. Herzberg and J. Shoosmith, *Can. J. Phys.*, **34**, 523 (1956). c) G. Herzberg, *Proc. Roy. Soc. (London)*, **A262**, 291 (1961). d) R. W. Fessenden and R. H. Schuler, *J. Chem. Phys.*, **39**, 2147 (1963). e) R. W. Fessenden, *J. Phys. Chem.*, **71**, 74 (1967). f) W. L. S. Andrews and C. C. Pimentel, *J. Chem. Phys.*, **44**, 2527 (1966). g) D. E. Milligan and M. E. Jacox, *ibid.*, **47**, 5146 (1967).

Fig. 2. Potential curve for out-of-plane bending of the methyl radical.

tion[14] and gives a force constant of 0.183 mdyn/A, which is comparable with the experimental values, 0.2527 in a solid-argon matrix[14f] and 0.177 in a nitrogen matrix.[14g]

Recently, the isotope effects on the *hfs* constants of the methyl radicals have been reported by Fessenden;[14e] the spin densities on both the proton and the carbon nuclei have been seen to increase with an increase in the angle ϕ of Fig. 1. Here, we will examine the angular dependence of the spin densities in order to clarify the mechanism of these angular dependencies. The results are summarized in Table 4, while those for the carbon $2s$ AO are illustrated in Fig. 3. They predict reasonably well the angular dependences of the spin densities on both the hydrogen $1s$ and the carbon $2s$ AO's, which is in accordance with the experiments. Note that as the angle ϕ increases, the $(\rho_{2s(c)})_{SD}$ value increases, and that this increase exceeds the decreasing tendency of $(\rho_{2s(c)})_{SP}$, vis. Fig. 3. For the proton-spin density, the observed tendency may be explained by the increasing contribution of the SD mechanism with an increase in the angle. Note that the SP contribution is almost constant over the angular range considered and that the SD contribution is very small, even in the tetrahedral configuration.

In Table 5, these isotope effects of the methyl radicals are summarized and compared with the experimental values,[14e] the temperature effects[13] are neglected and the calculated *hfs* constants are averaged over the zero-point vibration, and the force constant of the CH_3 radical obtained by Milligan and Jacox[14g] is used for all the isotopical-

TABLE 4. SPIN DENSITIES IN THE METHYL RADICAL.

Geometry ϕ	Atomic orbital	Before annihilation			After annihilation		
		$\langle\rho\rangle_{\text{UA}}$	$(\rho)_{\text{SP}}$	$(\rho)_{\text{SD}}$	$\langle\rho\rangle_{\text{UA}}$	$(\rho)_{\text{SP}}$	$(\rho)_{\text{SD}}$
0°	$2s(C)$	0.1487	0.147	0.002[a]	0.0510	0.049	0.002[a]
	$2p_x(C), 2p_z(C)$	0.0115	0.012	0.000	0.0038	0.004	0.000
	$2p_y(C)$	1.0000	0.000	1.000	0.9990	0.000	0.999
	h	−0.0275	−0.028	0.000	−0.0089	−0.009	0.000
6°	$2s(C)$	0.1523	0.143	0.009	0.0570	0.048	0.009
	$2p_x(C), 2p_z(C)$	0.0117	0.012	0.000	0.0039	0.004	0.000
	$2p_y(C)$	0.9909	0.001	0.990	0.9897	0.000	0.990
	h	−0.0270	−0.028	0.001	−0.0084	−0.009	0.001
12°	$2s(C)$	0.1622	0.132	0.030	0.0739	0.044	0.030
	$2p_x(C), 2p_z(C)$	0.0126	0.013	0.000	0.0042	0.004	0.000
	$2p_y(C)$	0.9653	0.003	0.962	0.9635	0.001	0.962
	h	−0.0258	−0.028	0.002	−0.0071	−0.009	0.002
19.47°[b]	$2s(C)$	0.1812	0.114	0.067	0.1052	0.038	0.067
	$2p_x(C), 2p_z(C)$	0.0145	0.015	0.000	0.0049	0.005	0.000
	$2p_y(C)$	0.9164	0.004	0.912	0.9138	0.001	0.912
	h	−0.0241	−0.029	0.005	−0.0050	−0.010	0.005

a) This value must be zero by symmetry, and the error results from the approximation used to derive Eq. (7) (See Ref. 8).
b) Tetrahedral angle.
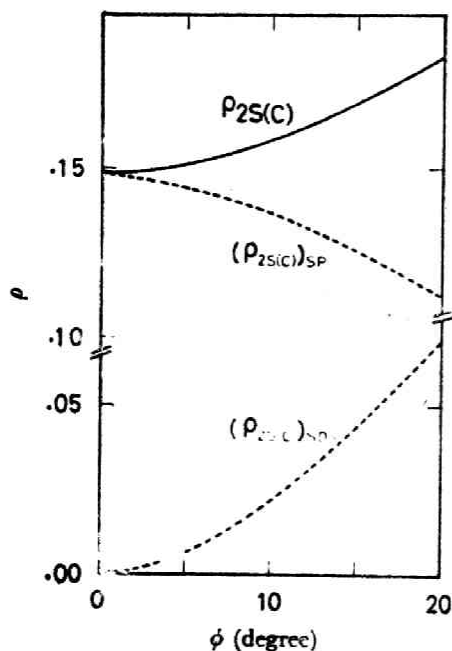
Fig. 3. $\langle\rho_{2s(c)}\rangle_{\text{ua}}$ and its mechanistic contributions *versus* the bending angle ϕ in the methyl radical. Only the curves obtained before annihilation are given, but the characteristic features are the same in both stages.

ly-substituted methyl radicals. As Table 5 shows, the rate of the change in the calculated *hfs* constants with an increase in the number of the deuterium atom is less than that required to explain the observed *hfs* constants; this has also been noted by Morokuma, Pedersen and Karplus.[13d] The vibrational corrections to the spin density are +0.0004 (0.29 gauss) and +0.0156 ∼ +0.0052 (17.31∼5.77 gauss) for the hydrogen $1s$ AO and for the carbon $2s$ AO respectively. (See also Table 7.)

ii) Ethyl, Allyl and Butadienyl Anion Radicals. In this section, the spin densities of the ethyl, allyl, and *s-trans*-butadienyl anion radicals are discussed. The calculated spin densities and their mechanistic contributions are summarized in Table 6, while the proton *hfs* constants calculated from $\langle\rho_h\rangle_{\text{ua}}$ are shown in Table 7.

Previously,[8] the methyl proton *hfs* constants of the ethyl radical have been shown to be due to a major SD contribution and a minor SP contribution. When we assume the experimentally observed relation[15] for the methyl proton *hfs* constant, $a_H = B_0 + B_1\cos^2\theta$, where θ is the rotational angle about the C–C single bond, the values of B_0 and B_1 may be calculated as −1.49 and 55.28 gauss respectively.** The average a_H value over the rotational angle, θ, is 26.15 gauss, which may be compared with the observed value,[14d] 26.87 gauss.

15) a) C. Heller and H. M. McConnell, *J. Chem. Phys.*, 32, 1535 (1960). b) A. Horsfield, J. R. Morton and D. H. Whiffen, *Mol. Phys.*, 4, 425 (1961).

** B_0 is calculated from the results previously reported (Ref. 8).

TABLE 5. ISOTOPE EFFECTS FOR THE hfs CONSTANT (gauss)

Radical	$\langle \rho_h \rangle_{ba}$	a_B Calcd	a_B Exptl.[b]	Radical	$\langle \rho_{2s(C)} \rangle$ ba	$\langle \rho_{2s(C)} \rangle$ aa	$\Delta a(^{13}C)$[a] Calcd ba	$\Delta a(^{13}C)$[a] Calcd aa	$\Delta a(^{13}C)$[a] Exptl.[b]
$^{12}CH_3$	-0.0271_3	20.15	23.038	$^{13}CH_3$	0.1518_0	0.0562_3	0.00	0.00	0.00
$^{12}CH_2D$	-0.0271_5	20.17	23.10	$^{13}CH_2D$	0.1515_6	0.0558_7	-0.24	-0.41	-0.52
$^{12}CHD_2$	-0.0271_8	20.19	23.21	$^{13}CHD_2$	0.1513_5	0.0554_7	-0.50	-0.85	-1.28
$^{12}CD_3$	-0.0272_1	20.22	23.29[c]	$^{13}CD_3$	0.1511_0	0.0550_4	-0.78	-1.33	-2.36

a) $\Delta a(^{13}C) = a(^{13}C) - a(^{13}C$ in $^{13}CH_3)$
b) Ref. 14c.
c) The relation, $a_B = 6.514 a_D$, is used.

TABLE 6. SPIN DENSITIES IN THE ETHYL, ALLYL, AND $trans$-BUTADIENYL ANION RADICALS

Radical	Atomic orbital	Before annihilation $\langle \rho \rangle_{ba}$	$(\rho)_{SP}$	$(\rho)_{SD}$	After annihilation $\langle \rho \rangle_{aa}$	$(\rho)_{SP}$	$(\rho)_{SD}$
Ethyl	$2s(C_1)$	0.1614	0.159	0.002[a]	0.0555	0.053	0.002[a]
	$2p_s(C_1)$	1.0001	0.002	0.998	0.9985	0.001	0.998
	$2s(C_2)$	-0.0123	-0.012	0.000	-0.0040	-0.004	0.000
	$2p_s(C_2)$	-0.0130	-0.013	0.000	-0.0042	-0.004	0.000
	h_3, h_4	-0.0345	-0.035	0.000	-0.0111	-0.011	0.000
	h_5, h_6	0.0165	0.003	0.013	0.0142	0.001	0.013
	h_7	0.0524	0.020	0.052	0.0593	0.007	0.052
Allyl	$2s(C_1)$	0.0988	0.099	0.000	0.0335	0.034	0.000
	$2p_s(C_1)$	0.6840	0.173	0.511	0.5686	0.058	0.511
	$2s(C_2)$	-0.0534	-0.054	0.000	-0.0175	-0.018	0.000
	$2p_s(C_2)$	-0.3414	-0.356	0.015[a]	-0.1043	-0.119	0.015[a]
	h_4, h_6	-0.0188	-0.019	0.000	-0.0061	-0.006	0.000
	h_5, h_7	-0.0191	-0.019	0.000	-0.0062	-0.006	0.000
	h_8	0.0049	0.005	0.000	0.0016	0.002	0.000
Butadienyl Anion	$2s(C_1)$	0.0674	0.067	0.000	0.0228	0.022	0.000
	$2p_s(C_1)$	0.5022	0.095	0.407	0.4387	0.032	0.407
	$2s(C_2)$	0.0157	0.016	0.000	0.0053	0.005	0.000
	$2p_s(C_2)$	0.1330	-0.094	0.227	0.1957	-0.031	0.227
	h_9, h_{10}	-0.0132	-0.013	0.000	-0.0043	-0.004	0.000
	h_6, h_9	-0.0125	-0.013	0.000	-0.0041	-0.004	0.000
	h_7, h_8	-0.0070	-0.007	0.000	-0.0023	-0.002	0.000

a) See Ref. a) of Table 4.

The allyl radical has been extensively studied[16] using the π-approximation method. The π-spin densities calculated by the UHF method by Berthier[16a] are 0.812 for $2p_s(C_1)$ and -0.619 for $2p_s(C_2)$ AO, and the projected values[16b] are 0.609 and -0.185 respectively. The corresponding values obtained by the present method are given in Talbe 6. The SP contribution to the spin density in the $2p_s(C_1)$ AO is as great as 10—25%.[16d] The spin densities on the $2p_s(C_2)$ and the h_8 AO's are calculated to be negative and positive in sign respectively, which is in agreement with earlier theoretical works.[16]

The electron-spin resonance study by Fessenden and Schuler[14a] of the allyl radical in a liquid medium showed a slight difference in the hfs constants for the two methylene protons (H_1 and H_5 in Fig. 1). Obviously, McConnell's relation,[16b] $a_H = Q_H \rho_c^\pi$, can not interpret this observed difference. However, the present valence electron treatment yields a small difference in the spin densities on the H_4 and H_5 nuclei. Therefore, the observed hfs constants of 13.93 and 14.83 gauss may be assigned

16) a) G. Berthier, J. chim. Phys., 52, 141 (1955).
b) H. M. McConnell, J. Chem. Phys., 29, 244 (1958).
c) C. Heller and T. Cole, ibid., 37, 243 (1962). d) D. Lazdins and M. Karplus, ibid., 44, 1600 (1966).

Radical	Position	hfs Constant (gauss)	
		Calcd[a]	Exptl.[b]
Methyl ($\phi=0$)	H	−20.43	(−) 23.04
Ethyl	H(CH₃)	−25.63	(−) 22.38
	H(CH₃)	26.15[c]	(+) 26.87
Allyl	H_4, H_6	−13.97	(−) 13.93
	H_5, H_7	−14.19	(−) 14.83
	H_9	3.64	(+) 4.06
t-Butadienyl Anion	H_5, H_{10}	−9.8?	(−) 7.62
	H_6, H_9	−9.29	(−) 7.62
	H_7, H_8	−5.21	(−) 2.79
Vinyl ($\theta=135°$)	H_c	32.54	(+) 34
	H_t	72.37	(+) 68
	H_a	−15.83	(−) 16, (−) 13.4
Formyl	H	38.63	(+) 137.0

TABLE 7. ISOTROPIC PROTON hfs CONSTANTS

a) Calculated from $\langle\rho\rangle_{ba}$. See footnote **.
b) Refs. 14e, 18, and 22.
c) The relation, $a_H = B_0 + B_1 \cos^2\theta$, is assumed.

to the H_4 (H_6) and H_5 (H_7) nuclei respectively. This assignment is the same as the one previously reported.[5a] However, the recent calculations by Hincliffe and Atherton[17] and by Pople, Beveridge, and Dobosh[14] gave an assignment opposite to that reported here. Further experime... ...rk is necessary to settle this point.**

The proton hfs constants of the butadienyl anion radical have been observed by Levy and Myers.[18] The calculated values, assuming the s-trans configuration, are shown in Table 6. The CH_2 protons of butadiene are ron-equivalent and different hfs constants are predictd; this is in contrast to the observed identical hfs constants for these protons.[18]

As is well known, the spin densities in the σ-type AO's of planar π-electron radicals and in the $2p_z(C_2)$ AO of the allyl radical are due only to the SP mechanism. Therefore, the $\langle\rho\rangle_{ba} = 3 \langle\rho\rangle_{aa}$ relation,[7c,8] is fairly satisfactory, except for the $2p_z(C_2)$ AO of the allyl radical.*10

Organic σ-Electron Radicals. i) Vinyl Radical. The hfs constants of the vinyl radical have recently been observed,[14d,14e,19] and its structure and the sign of the hfs constant of its α-proton have

been intensely investigated.[2,5a,19,20] Previously,[5] we suggested that the hfs constant of the α-proton is negative in sign. Here, we will examine theoretically the structure*11 and the hfs constants of this radical.

The calculated potential curve with respect to the bending of the θ angle of Fig. 1 is illustrated in Fig. 4. The minimum in the potential curve appears near 135°, the calculated barrier to inversion:

$$\underset{H}{\overset{H}{\diagdown}}C{-}\overset{\diagup H}{\underset{}{C}}\cdot \;\rightleftharpoons\; \underset{H}{\overset{H}{\diagdown}}C{-}\overset{}{\underset{\diagdown H}{C}}\cdot$$

is 1.6 kcal/mol, which is comparable with the value, ~2 kcal/mol, estimated by the ESR technique.[14d]

One of the main features of the present method lies in its consistent applicability to the spin-density calculations of both σ- and π-electron radicals. Good examples in which the σ–π-type SP mechanism, the "bulk" SP mechanism, and the SD mechanism are all competing with one another are the spin densities on the α-hydrogen and the α- and β-carbon atoms of the vinyl radical. None of these mechanisms can be ignored. This may be understood from the fact that the unpaired orbital of this radical
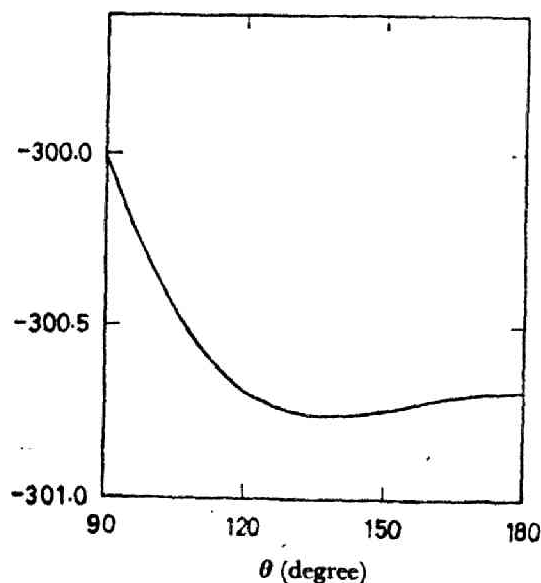
Fig. 4. Total energy (eV) on bending of CCH_2 in the vinyl radical.
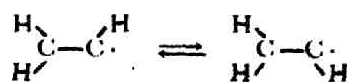
17) A. Hincliffe and H. M. Atherton, Mol. Phys., 13, 89 (1967).
** Recent experiments by Kochi and Krusic (J. Am. Chem. Soc., 90, 7157 (1968)) support the present assignment.
18) D. H. Levy and R. J. Myers, J. Chem. Phys., 41, 1062 (1964).
*10 This exception may be attributed to the rather large value of $(C_2/_3)^2/(C_1/_2)^2$ shown in Table 2, since the assumption used to derive Eq. (6) is not ... ... in this case (see Ref. 9b).

19) E. L. Cochran, F. J. Adrian and V. A. Bowers, J. Chem. Phys., 40, 213 (1964).
20) a) W. T. Dixon, Mol. Phys., 9, 201 (1965). b) G. A. Peterson and A. D. McLachlan, J. Chem. Phys., 45, 628 (1966). c) R. S. Drago and H. Petersen, Jr., J. Am. Chem. Soc., 89, 5774 (1967). d) A. Hinchliffe, Theoret. chim. Acta (Berl.), 8, 300 (1967). e) Y. Ellinger, A. Rassat, R. Subra and G. Berthier, ibid., 10, 289 (1968).
*11 The present method predicts the angular geometry of ethylene in fair agreement with the experiment; this will be reported in detail at a later date.

at $\theta = 135°$, calculated with the open-shell restricted Hartree-Fock (RHF) method,[*12] is

$$\varsigma_{rhf} = 0.2848(2s(C_\alpha)) + 0.3542(2p_x(C_\alpha))$$
$$+ 0.8630(2p_y(C_\alpha)) - 0.0609(2s(C_\beta))$$
$$-0.3564(2p_x(C_\beta)) + 0.0368(2p_y(C_\beta))$$
$$-0.1910(h_c) + 0.2737(h_t) - 0.1519(h_a)$$

and is mainly localized in the $2p_x(C_\alpha)$ and $2p_y(C_\alpha)$ AO's.

The spin densities and their mechanistic contributions are given in Table 8 for various configurations of the vinyl radical. The dependence of the carbon $2s$ AO spin density on the θ angle is illustrated in Fig. 5, while that of the proton spin density is illustrated in Fig. 6.

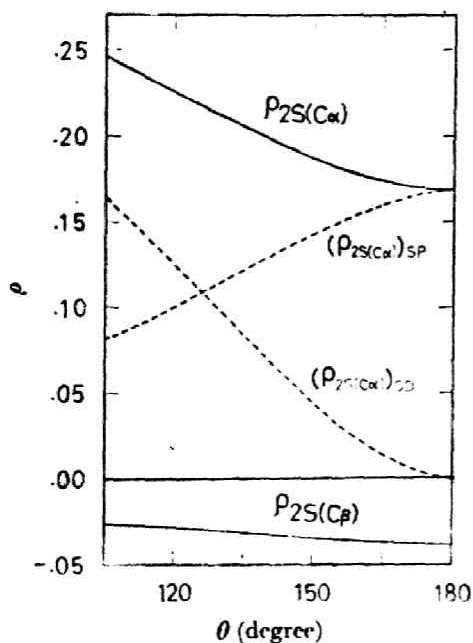Fig. 5. $2s$ AO spin densities of carbon atoms *versus* the bending of CCH$_\alpha$ in the vinyl radical. Only the curves obtained before annihilation are shown, but the characteristic features are the same in both stages.

Figure 5 shows that the angular dependence of the SD contribution to the α-carbon $2s$ AO spin density is opposite to that of the SP contribution, and that it determines the dependence of the total spin density. At $\theta = 135°$, $\rho_{2s}(C_a)$ is due to the 41–67% SD and 59–33% SP contributions. For the β-carbon atom, the angular dependence is exceptionally small and its $2s$ AO spin density is always negative.

Figure 6 shows that the spin density on the α-proton is the sum of the negative SP and the positive

*12 C. C. J. Roothaan, *Rev. Mod. Phys.*, **32**, 179 (1960). The estimations of the integral values are the same as for the present UHF calculations, except that the two center $\sigma-\pi$-type exchange repulsion integrals are not included in the RHF calculation.
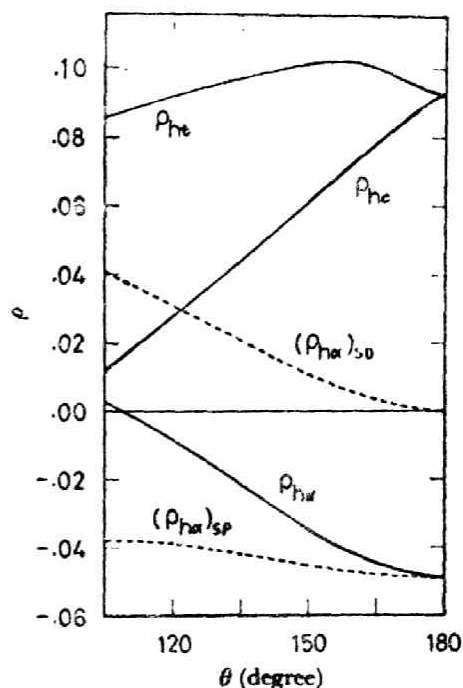
Fig. 6. Proton spin densities (ba) *versus* bending of CCH$_\alpha$ in vinyl radical.

SD contributions. They depend oppositely on the angle θ, and at $\theta = 135°$, where the minimum potential lies, the α-proton spin density is due to the 97% SD and -197% SP contributions. For the cis- and trans-protons, their spin densities also show a large angular dependence, and they are also due to both the SD and SP mechanisms. At $\theta = 135°$, the spin density of the trans-proton is due to the 73% SD and 27% SP contributions, while that of the cis-proton is due to the 80% SD and 20% SP contributions.

The calculated proton hfs constants at the minimum potential $(\theta = 135°)$ are $a_{Hc} = 32.54$, $a_{Ht} = 72.37$, and $a_{Ha} = -15.83$ gauss (Table 7). These values agree satisfactorily with the experimental values. Moreover, as may be seen in Table 8 and Fig. 6, the calculated proton hfs constants obtained near $\theta = 135°$ agree most reasonably with the experimental values, thus lending support to the vinyl radical configuration with $\theta = 135°$.

Note that the calculated hfs constant of the α-proton is negative in sign.[5a] However, recent INDO calculations by Pople, Beveridge and Dobosh[1d] have predicted the opposite sign. Further experimental work, such as with isotope effects,[14e] will be necessary to settle this point. Figures 5 and 6 will be very useful when one experimentally determines the sign of the α-proton hfs constant. When the α-proton is replaced by deuterium, a smaller hfs constant (except for a constant factor $g_H/g_D = 6.514$) should be observed if a_{Ha} is negative, and *vice versa*.

Let us now comment on the recent theoretical spin-density studies of the vinyl radical, in which

TABLE 8. SPIN DENSITIES IN THE VINYL RADICAL

Geometry θ	Atomic orbital	Before annihilation			After annihilation		
		$\langle \rho \rangle_{AA}$	$(\rho)_{SP}$	$(\rho)_{SD}$	$\langle \rho \rangle_{AA}$	$(\rho)_{SP}$	$(\rho)_{SD}$
120°	$2s(C_\alpha)$	0.2251	0.100	0.125	0.1581	0.033	0.125
	$2s(C_\beta)$	−0.0286	−0.033	0.004	−0.0063	−0.011	0.004
	h_c	0.0286	0.005	0.024	0.0255	0.002	0.024
	h_t	0.0913	0.024	0.067	0.0752	0.008	0.067
	h_a	−0.0083	−0.039	0.031	0.0175	−0.013	0.031
135	$2s(C_\alpha)$	0.2051	0.122	0.083	0.1240	0.041	0.083
	$2s(C_\beta)$	−0.0315	−0.035	0.004	−0.0082	−0.012	0.004
	h_c	0.0438	0.009	0.035	0.0381	0.003	0.035
	h_t	0.0974	0.026	0.071	0.0799	0.009	0.071
	h_a	−0.0213	−0.042	0.021	0.0064	−0.014	0.021
150°	$2s(C_\alpha)$	0.1870	0.143	0.044	0.0917	0.048	0.044
	$2s(C_\beta)$	−0.0348	−0.037	0.002	−0.0102	−0.012	0.002
	h_c	0.0614	0.013	0.048	0.0525	0.004	0.048
	h_t	0.1013	0.027	0.074	0.0832	0.009	0.074
	h_a	−0.0345	−0.045	0.011	−0.0042	−0.015	0.011
180°	$2s(C_\alpha)$	0.1690	0.166	0.003[a]	0.0583	0.055	0.003[a]
	$2s(C_\beta)$	−0.0384	−0.038	0.000	−0.0125	−0.013	0.000
	h_c, h_t	0.0926	0.023	0.070	0.0774	0.008	0.070
	h_a	−0.0487	−0.050	0.001[a]	−0.0153	−0.017	0.002[a]

a) See Ref. a) of Table 4.

only the SD contribution was taken into account.[20b,20c] For instance, if the SP mechanism is neglected, the α-proton spin density will be about +0.021 $((\rho_{Ha})_{SD}$ shown in Table 8), which is of the same magnitude, but of the opposite sign, as the present result, −0.0213. Thus, even if the SP contribution is neglected, a value which is apparently reasonable in magnitude can be obtained for the α-proton spin density. Furthermore, neglect of the SP contribution leads to serious errors in the calculation of the spin densities even of other protons and of the carbon 2s AO's, as is shown in Table 8, Fig. 5, and Fig. 6. This is probably true for other σ-electron radicals as well; namely, one should not neglect the spin polarization mechanism even in σ-electron radicals, especially in AO's near the radical-center atom.[8b,20a]

ii) Formyl Radical. Recently, the results of a non-empirical UHF calculation of the formyl radical *hfs* constants have been reported by Hincliffe and Cook[21] to be in good agreement with the experimental values.[22] However, most of the semi-empirical MO calculations[1,2,20b,20c] have

failed to yield such a large proton *hfs* constant as was experimentally observed value, 137.0 gauss.[22] As may be seen in Table 9, the present result for the proton *hfs* constant is also disappointing. It is necessary to examine the present result to determine its failing by comparing it with the result of the non-empirical calculation.

From the $(\rho)_{SD}$ shown in Table 9 we can see that the unpaired orbital consists mainly of the $2p_y(C)$ and $2p_y(O)$ AO's. This implies that the SP mechanism is very important to the *hfs* constant of this radical. The nonempirical calculation of the proton *hfs* constant gave 154.58 gauss before annihilation and 133.95 gauss after single annihilation. The SP and SD contributions calculated from these values (see Eq. (20) of the previous report.[8b]) are 61.89 and 92.69 gauss before annihilation. In the present calculations, they are −5.94 and 44.58 gauss respectively. Very large differences exist in both contributions. The SP contributions of both methods differ especially even in sign. The reason for this is perhaps that σ–π-type exchange repulsion integrals other than those included in the present calculation (especially the two center σ–π-type ionic integrals which make a positive contribution to the proton *hfs* constant) can not be neglected in this case.

Inorganic σ-Electron Radicals. We chose here, as sample calculations for the inorganic σ-electron radicals, the isoelectronic NO_2 and CO_2^- radicals, where the spin densities on the VAO's

21) A. Hincliffe and D. B. Cook, *Chem. Phys. Letters*, 1, 217 (1967).
22) a) F. J. Adrian, E. L. Cochran and V. A. Bowers, *J. Chem. Phys.*, 36, 1661 (1962). b) J. A. Brivati, N. Keen and M. C. R. Symons, *J. Chem. Soc.*, 1962, 237. c) F. J. Adrian, E. L. Cochlan and V. A. Bowers, *J. Chem. Phys.*, 44, 4626 (1966)

TABLE 9. SPIN DENSITIES IN THE FORMYL RADICAL

Atomic orbital	Before annihilation			After annihilation		
	$\langle\rho\rangle_{ba}$	$(\rho)_{SP}$	$(\rho)_{SD}$	$\langle\rho\rangle_{aa}$	$(\rho)_{SP}$	$(\rho)_{SD}$
$2s(C)$	0.1603	0.029	0.131	0.1409	0.010	0.131
$2p_x(C)$	−0.0169	−0.021	0.004	−0.0029	−0.007	0.004
$2p_y(C)$	0.5028	−0.014	0.517	0.5124	−0.005	0.517
$2p_z(C)$	−0.1118	−0.114	0.002	−0.0356	−0.038	0.002
h	0.0522	−0.008	0.060	0.0574	−0.003	0.060
$2s(O)$	0.1106	0.109	0.002	0.0378	0.036	0.002
$2p_x(O)$	0.0593	0.020	0.039	0.0457	0.007	0.039
$2p_y(O)$	0.4802	0.012	0.468	0.4725	0.004	0.468
$2p_z(O)$	0.1310	0.128	0.003	0.0457	0.043	0.003

a) See Ref. a) of Table 4.

TABLE 10. SPIN DENSITIES IN NO_2, CO_2^-, AND CN RADICALS

Radical	Atomic orbital	$\langle\rho\rangle_{ba}$	$\langle\rho_{SP}\rangle_{ba}$	$\langle\rho_{SD}\rangle_{ba}$	$\langle\rho\rangle_{aa}$	Experimental
NO_2	$2s(N)$	0.1900	0.057	0.133	0.1522	0.106, 0.097
	$2p_x(N)$	0.4576	0.001	0.457	0.4570	0.452, 0.371
	$2p_z(N)$	0.0497	0.049	0.000	0.0169	0.019
	$2s(O)$	0.0505	0.048	0.003	0.0185	———
	$2p_x(O)$	0.3495	0.012	0.337	0.3412	———
	$2p_z(O)$	−0.0250	−0.025	0.000	−0.0082	———
CO_2^-	$2s(C)$	0.2652	0.012	0.253	0.2571	0.14
	$2p_x(C)$	0.5421	−0.006	0.548	0.5460	0.66
	$2p_z(C)$	0.0131	0.013	0.000	0.0044	0.08
	$2s(O)$	0.0641	0.056	0.008	0.0271	———
	$2p_x(O)$	0.2746	0.008	0.267	0.2690	———
	$2p_z(O)$	−0.0080	−0.008	0.000	−0.0026	———
CN	$2s(C)$	0.0884	−0.026	0.115	0.1060	———
	$2p_x(C)$	0.3377	−0.003	0.341	0.3398	———
	$2p_y(C), 2p_z(C)$	−0.0494	−0.050	0.001	−0.0162	———
	$2s(N)$	0.0876	0.054	0.034	0.0515	———
	$2p_x(N)$	0.4994	0.006	0.493	0.4956	———
	$2p_y(N), 2p_z(N)$	0.0563	0.056	0.000	0.0191	———

a) Ref. 23a.

are assumed from the anisotropy of the ESR parameters[23] and the CN radical, which is especially interesting in its dipole moment. Table 10 summarizes the spin densities calculated on the various VAO's of these radicals, along with those estimated from the experiments.[23] The NO_2 spin densities theoretically calculated by McEwen[24a] and by Green and Linnett[24b] gave small magnitudes (0.263 and 0.222 respectively) for the spin density on the $2p_x(N)$ AO, but the present method gave $\rho_{2px(N)} = 0.457$, which is in closer agreement with the experimental estimations.

Table 10 shows that the present calculation qualitatively predicts almost all features of the spin densities of the isoelectronic NO_2 and CO_2^- radicals. For example, the spin density on the $2p_x(N)$ AO of NO_2 is smaller than that on the $2p_x(C)$ AO of CO_2^-, the delocalization of the unpaired spin to oxygens is greater in NO_2 than in CO_2^-, etc.

23) a) P. W. Atkins, N. Keen and M. C. R. Symons, J. Chem. Soc., 1962, 2873. b) H. Zeldes and R. Livingston, J. Chem. Phys., 35, 563 (1961). c) H. Zeldes and R. Livingston, ibid., 37, 3017 (1962). d) D. W. Ovenall and D. H. Whiffen, Proc. Chem. Soc., 1960, 420. e) D. W. Ovenall and D. H. Whiffen, Mol. Phys., 4, 135 (1961). f) J. A. Brivati, N. Keen, M. C. R. Symons and P. A. Trevalion, Proc. Chem. Soc., 1961, 66.

24) a) K. L. McEwen, J. Chem. Phys., 32, 1801 (1960). b) M. Green and J. W. Linnett, Trans. Faraday Soc., 57, 1 (1961).

Note that the 2s spin densities shown in the last column of Table 10 are estimated from the observed values without paying any attention to the inner 1s contributions. Hence, these 2s contributions cannot be compared directly with the calculated contributions.

Analyses of Dipole Moments of σ-Electron Radicals. The dipole moment of a neutral molecule may be expressed approximately as the sum of the atomic dipole (μ_{AD}) and the charge dipole (μ_{CD}). The atomic dipole (x-direction) of the first-row atoms of the periodic table is given by:

$$\mu_{AD}(x) = -7.3370\sum_A(P^A_{xp(x)}/\zeta_A)$$

in debye units, and the charge dipole is:

$$\mu_{CD}(x) = 4.8029\sum_A(Z_A-N_A)x_A,$$

if we adopt the Mulliken approximation:

$$(\chi_r|x|\chi_s) = \frac{1}{2}S_{rs}\{(\chi_r|x|\chi_r)+(\chi_s|x|\chi_s)\}.$$

ζ_A is the Slater exponent, and N_A is the atomic population of the A atom. $P^A_{SP(x)}$ is the off-diagonal density matrix element between the 2s and $2p_x$ AO's of the A atom.

The analyses of the dipole moment of vinyl, formyl, NO_2, and CN radicals are given in Table 11; they were obtained by using the values obtained before annihilation. μ^α_{AD} and μ^β_{AD} are the contributions to the atomic dipole from all the occupied α- and β- spin orbitals respectively. These contributions may be further divided into those due to the first-row atoms in the molecule. As is shown in the forth and fifth columns of the table, μ^α_{AD} due

to the radical center atom (e.g., C_α in vinyl) surpasses the μ^α_{AD} due to the other atoms and the μ^α_{AD} values of all the constituent atoms. The values of μ^α_{AD} (HO) in the sixth column give contributions to the atomic dipole only from the highest occupied (HO) α-spin orbital. Note that the μ^α_{AD} (HO) at the radical-center atom makes the dominant contribution to μ^α_{AD} and even to μ_{AD}. Thus, the most unstable HO orbital of the σ-electron radical extends considerably out of the molecule from the radical center atom. The direction of the $-\mu^\alpha_{AD}$ (HO) of the vinyl radical is 113 from the C_α-C_β bond.

In NO_2 and CN radicals, the contributions due to the charge dipole cancel those due to the atomic dipole. In the CN radical especially, these two contributions are almost the same in magnitude, but reverse in direction, so the resultant dipole moment is very small. This should be compared with the well-known example of the CO molecule, where its atomic dipole surpasses its charge dipole and makes it a powerful ligand in the chemistry of metal complexes. The calculated dipole moment of NO_2 is -1.301 debye, which is too large if compared with the oserved value, -0.29 debye. However, the above qualitative discussion will not be altered by more rigorous calculations.

Summary and Conclusions

As has been seen in the previous sections, the semi-empirical method for valence electron systems including differential overlap can be satisfactorily extended to systems with open-shell structures.

TABLE 11. ANALYSES OF DIPOLE MOMENTS OF σ-ELECTRON RADICALS (in debye units)

Radical	Atom	Direction	Analyses of atomic dipole				Total
			μ^α_{AD}[a]	μ^β_{AD}	μ^α_{AD}(HO)[b]	μ_{AD}[c]	
Vinyl ($\theta=135°$)	C_α	x	-0.36	0.06	-0.31	-0.31	$\mu_{AD}=0.68$
		y	-0.85	0.16	-0.71	-0.69	$\mu_{CD}=0.52$
	C_β	x	0.16	0.09	-0.02	0.24	$\mu=1.19$
		y	0.01	0.01	-0.01	0.02	
Formyl	C	x	0.31	0.36	-0.13	0.67	$\mu_{AD}=1.42$
		y	-1.58	-0.36	-1.09	-1.93	$\mu_{CD}=3.07$
	O	x	-0.36	-0.55	0.01	-0.91	$\mu=3.16$
		y	0.23	0.30	0.04	0.53	
NO_2[d]	N	x	1.17	0.32	0.59	-1.49	$\mu_{AD}=0.52$
	O	x	-0.17	-0.31	0.02	-0.48	$\mu_{CD}=-1.83$
							$\mu=-1.30$
CN	C	x	1.87	0.90	1.03	2.77	$\mu_{AD}=1.13$
	N	x	-1.01	-0.63	-0.31	-1.64	$\mu_{CD}=-1.18$
							$\mu=-0.05$

a) μ^α_{AD} denotes the contribution to atomic dipole (μ_{AD}) from all the occupied α-spin orbitals.

b) μ^α_{AD}(HO) denotes the contribution to atomic dipole from the highest occupied α-spin orbital.

c) $\mu_{AD} = \mu^\alpha_{AD} + \mu^\beta_{AD}$.

d) The experimental value is -0.29 debye; C. H. Townes and A. L. Schawlow, "Microwave Spectroscopy," McGraw-Hill Book Co., New York (1955).

The results of the present study are as follows:

(1) The separation of the mechanistic contributions to spin density makes it possible to enter into detailed discussions of the nature of the spin density; e.g., the spin-polarization mechanism is shown to be very important even when the spin-delocalization mechanism has hitherto been considered dominant (e.g., ethyl and vinyl radicals).

(2) A good correlation between the calculated *hfs* constants and the configurations of radicals is found for methyl and vinyl radicals. The geometry of the vinyl radical is predicted to be $\theta \simeq 135°$ from both the potential curve and the calculated *hfs* constants. Since there are many radicals with known *hfs* constants, but with unknown configurations, the agreement between the configuration expected from the calculated potential curve and that expected from the calculated *hfs* constants is ideal for a reliable prediction of the configuration of the radical from the theoretical point of view.

(3) The analyses of the atomic dipole moments of the σ-electron radicals revealed some interesting features. For example, the highest occupied orbitals of these σ-electron radicals make decisive contributions to the total atomic dipole.

The calculations were carried out on a HITAC 5020 E computer at the computation center of the University of Tokyo.

84

Notes on the E.S.R. spectrum of hydrogenated pyridine

The E.S.R. spectrum of irradiated pyridine has recently been reported by different authors [1, 2]. David *et al.* and Tsuji *et al.* obtained almost the same spectra for irradiated pyridine in solid state and confirmed that three kinds of radicals were produced. The triplet spectrum observed at 77°K was assigned by both authors to the pyridine cation radical produced by the removal of one electron from the nitrogen lone pair. The singlet spectrum observed at 221°K is identified by Tsuji *et al.* as the pyridyl radical. The spectrum observed at about 200°K, however, was assigned to different species of hydrogenated pyridine; namely, David *et al.* assigned to N-hydrogenated pyridine (N–Py), and on the other hand, Tsuji *et al.* to 3-hydrogenated pyridine (C–Py).
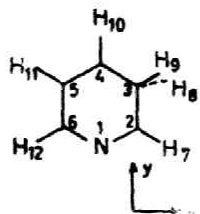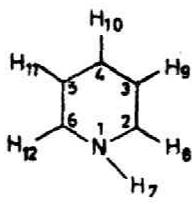
In order to settle this problem, we have calculated the electronic structures for both N–Py and C–Py radicals. The calculation was carried out by the semi-empirical unrestricted SCF–MO method, all the valence electrons being considered. The evaluation of matrix elements was made by the method developed by the present authors [3, 4], except for the off-diagonal core Hamiltonian matrix elements [5]. In actual calculation, we assumed that the hydrogen attaches to the 3-carbon atom or the nitrogen atom of pyridine with the tetrahedral angle and with the C–H bond distance of 1·09 Å and the N–H bond distance of 1·032 Å for C–Py and N–Py, respectively.

The total energy was calculated to be −932·25 and −935·66 ev for C–Py and N–Py, respectively†, and the calculated hyperfine coupling constants of both hydrogenated pyridines are summarized in the table. The observed coupling constant (24 G) was assigned by David *et al.* to 1-hydrogen of N–Py, and by Tsuji *et al.* to 8-hydrogen of C–Py. The present calculations seem to support the assignment by David *et al.* The coupling constants calculated for N–Py are in good agreement with the observed values. The hyperfine coupling constant, 54·6 G calculated for 8-hydrogen of C–Py is almost consistent with the observed [8] and calculated [9, 10] results for the cyclohexadienyl radical.

We may conclude from the above two reasons (total energy and calculated hyperfine coupling constants) that the E.S.R. spectrum of the irradiated pyridine observed at about 200°K may be due to the N-hydrogenated pyridine radical.

It may be interesting to discuss here the electronic structure of N–Py briefly. The highest occupied orbital (singly occupied orbital in the sense of restricted MO

---

† The single determinant used in unrestricted Hartree-Fock method is not generally the eigenfunction of the total spin angular momentum operator, S^2, but it might not lead to serious error for the comparison of the total energy of two molecules composed of the same number of electrons [6].

Radical	Position	a, obsd. (G)	a, calcd. (G)	
(1) C-Py	N	—	$2\cdot13$†	—
	7	12	$-11\cdot2$	$(-10\cdot0)$‡
	8	24	$56\cdot4$	—
	10	12	$-15\cdot2$	$(-11\cdot7)$
	11	—	$8\cdot13$	$(4\cdot91)$
	12	12	$-15\cdot2$	$(-11\cdot9)$
(2) N-Py	N	12	$9\cdot37$	—
	7	24	$24\cdot4$	—
	8	12	$-8\cdot64$	$(-8\cdot08)$
	9	—	$5\cdot59$	$(3\cdot45)$
	10	12	$-13\cdot2$	$(-10\cdot3)$

† The proton hyperfine coupling constants are calculated by multiplying 508 G to the spin density on hydrogen atom, and the nitrogen hyperfine coupling constants are calculated by the empirical relation obtained by Ward [7].

‡ The values in parentheses are calculated from the spin densities on the carbon π-AO's using the McConnell relation ($a_H = -23\cdot04\ \rho_{c_\pi}$).

Calculated hyperfine coupling constants (a's) of C-Py and N-Py radicals.

method) of N-Py is;

$$0\cdot11S_N - 0\cdot30P_{yN} - 0\cdot41P_{zN} + 0\cdot53(P_{z2c} + P_{z6c})$$
$$+ 0\cdot11(P_{z3c} + P_{z5c}) - 0\cdot58P_{z4c} - 0\cdot24h_7 + 0(0\cdot01),$$

where, $0(0\cdot01)$ denotes the smaller term, the coefficients of which are in the range of $0\cdot01 \sim 0\cdot09$.

The remarkable π-type conjugation is assured between the sp^3-type AO's on the nitrogen atom and the π-type AO's of the carbon skeletons of N-Py. Further, the π-bond population of the C-N bonds in N-Py and pyridine are calculated to be 0·056 and 0·216, respectively. This shows that the double bond character of the C-N bonds in N-Py radical decreases remarkably. The C_2-C_3 bond in N-Py is, however, strengthened compared with that in pyridine; the π-bond population of C_2-C_3 bond in N-Py and pyridine are calculated to be 0·292 and 0·243, respectively.

The details of this study will be published in the near future.

REFERENCES

[1] DAVID, D., GEUSKENS, G., VELHASSELT, A., JULG, P., and OTH, J. G. M., 1966, Molec. Phys., 11, 257.
[2] TSUJI, K., YOSHIDA, H., and HAYASHI, K., 1966, J. chem. Phys., 45, 2894.
[3] YONEZAWA, T., YAMAGUCHI, K., and KATO, H., 1967, Bull. chem. Soc. Japan, 40, 536.
[4] YONEZAWA, T., NAKATSUJI, H., KAWAMURA, H., and KATO, H., 1967, Bull. chem. Soc. Japan, 40, 2211.
[5] KATO, H., KONISHI, H., and YONEZAWA, T., 1967, Bull. chem. Soc. Japan, 40, 1017.
[6] AMOS, A. T., and HALL, G. G., 1961, Proc. R. Soc. A, 263, 483.
[7] WARD, R. L., 1962, J. Am. chem. Soc., 84, 332.
[8] FESSENDEN, R. W., and SCHULER, R. H., 1963, J. chem. Phys., 38, 773.
[9] FISCHER, H., 1962, J. chem. Phys., 37, 1094.
[10] INGALLS, R. B., and KIVELSON, D., 1963, J. chem. Phys., 37, 1907.

PART II, CHAPTER 3

SECTION 2

ANGULAR DEPENDENCE

OF THE METHYL GROUP

HYPERFINE SPLITTING CONSTANT

Semi-empirical Unrestricted SCF-MO Treatment for Valence Electron Systems. II. The Angular Dependence of the Methyl Group *hfs* Constants

Since the spin-polarization contribution to the methyl-group *hfs* constant of the ethyl radical has been recognized to be important, the angular dependence of the β-proton *hfs* constants is re-examined for various radicals. Thus, the observed relation, $Q(\theta) = B_0 + B_1 \cos^2 \theta$, is interpreted as being the sum of the following two equations.

$$Q_{SD}(\theta) = (B_1)_{SD} \cos^2 \theta$$
$$Q_{SP}(\theta) = (B_0)_{SP} + (B_1)_{SP} \cos^2 \theta.$$

where SD and SP denote the spin delocalization and spin polarization contributions respectively. θ is the rotational angle about C–C single bond. A molecular orbital description of the above angular dependences is also given.

The methyl-group proton *hfs* constants of aliphatic and aromatic hydrocarbon radicals have been extensively studied from both experimental[1] and theoretical[2] points of view. The theoretical studies of the methyl proton spin densities have been carried out mainly by two different methods, namely by the valence bond (VB) and molecular orbital (MO) methods,[3] and an interesting view of the spin-appearing mechanisms was presented by Lazdins and Karplus.[2g] They stated that the methyl-group proton spin density in the ethyl radical is due to nearly 60% "exchange polarization" and nearly 40% "electron transfer" contributions. In a previous MO study[4b] it was shown that the methyl-

proton spin density is due to 74% "spin delocalization (SD)" and 26% "spin polarization (SP)" contributions.[5]

The angular dependence of the β-proton *hfs* constant on the rotation about the C_α–C_β single bond has been well established experimentally and is explained by the relation[1]:

$$a_\beta^H = Q(\theta)\rho_C^\pi, \tag{1}$$

where ρ_C^π is the spin density in the $2p_{C_\alpha}$ atomic orbital of the contiguous π-carbon atom, and where $Q(\theta)$ is expressed as:

$$Q(\theta) = B_0 + B_1 \cos^2\theta, \tag{2}$$

where θ is the angle between the axis of the $2p_{C_\alpha}$ orbital and the C_β–H bond, both projected on a plane perpendicular to the C_α–C_β bond. Aono and Higuchi[2c] studied the angular dependence of the β-proton *hfs* constant theoretically by considering only the spin delocalization (spin-hyperconjugation) mechanism; they successfully derived the $Q(\theta) = B_1 \cos^2\theta$ relation, where B_1 is a constant. However, since the β-proton spin density is in large part due to the SP mechanism, it seems necessary to examine the angular dependence of the SP contribution in order to interpret the observed relation (2).

In the present study, the methyl-proton *hfs* constants of the various doublet radicals (ethyl, *n*-propyl, methyl-substituted allyl radicals, and toluene ion-radicals) are calculated by the unrestricted Hartree-Fock (UHF) method reported

1) a) C. Heller and H. M. McConnell, *J. Chem. Phys.*, **32**, 1535 (1960). b) A. Horsfield, J. R. Morton and D. H. Whiffen, *Mol. Phys.*, **4**, 425 (1961). c) J. R. Bolton, A. Carrington and A. D. McLachlan, *ibid.*, **5**, 31 (1962). d) J. R. Bolton, A. Carrington, A. Forman and L. E. Orgel, *ibid.*, **5**, 43 (1962). e) A. Horsfield, J. R. Morton and D. H. Whiffen, *ibid.*, **5**, 115 (1962).

2) a) A. D. McLachlan, *ibid.*, **1**, 233 (1958). b) P. G. Lykos, *J. Chem. Phys.*, **32**, 625 (1960). c) S. Aono and J. Higuchi, *Progr. Theor. Phys.* (Kyoto), **28**, 589 (1962). d) E. W. Stone and A. H. Maki, *J. Chem. Phys.*, **37**, 1326 (1962). e) K. Morokuma and K. Fukui, This Bulletin, **36**, 534 (1963). f) J. P. Colpa and E. de Boer, *Mol. Phys.*, **7**, 333 (1964). g) D. Lazdins and M. Karplus, *J. Chem. Phys.*, **44**, 1600 (1966). h) Z. Luz, *ibid.*, **48**, 4186 (1968).

3) T. H. Brown and M. Karplus, *ibid.*, **46**, 870 (1967).

4) a) T. Yonezawa, H. Nakatsuji, T. Kawamura and H. Kato, *Chem. Phys., Letters*, **2**, 454 (1968). b) T. Yonezawa, H. Nakatsuji, T. Kawamura and H. Kato, *J. Chem. Phys.*, **51**, 669 (1969).

5) J. P. Colpa, E. de Boer, D. Lazdins and M. Karplus, *J. Chem. Phys.*, **47**, 3098 (1967).

Semi-empirical Unrestricted SCF-MO Treatment for Valence Electron Systems. II

TABLE 1. THE METHYL PROTON SPIN DENSITY IN THE ETHYL RADICAL

Angle θ	UHF spin density						AA ρ_{aa}
	ρ_{uhf}	From Eq. (2)	$(\rho)_{SP}$	From Eq. (3)	$(\rho)_{SD}$	From Eq. (4)	
0	0.072	(0.072)	0.020	(0.020)	0.053	(0.053)	0.059
15	0.067	0.067	0.018	0.018	0.050	0.049	0.055
30	0.054	0.053	0.014	0.014	0.039	0.039	0.044
45	0.035	0.035	0.009	0.009	0.026	0.026	0.029
60	0.017	0.017	0.003	0.003	0.013	0.013	0.014
75	0.003	0.003	0.000	0.000	0.004	0.004	0.003
90	−0.002	(−0.002)	−0.002	(−0.002)	0.000	0.000	−0.001

in a previous study of this series,[6] and the mechanistic contributions to the *hfs* constants are diveded by means of the method previously proposed by the present authors.[7,4] The conclusions are that the SP contribution to the methyl-proton *hfs* constant has the angular dependence expressed by:

$$Q_{SP}(\theta) = (B_0)_{SP} + (B_1)_{SP} \cos^2\theta \qquad (3)$$

and that the observed relation (2) is to be understood as the sum of the angular dependence of the SD contribution.

$$Q_{SD}(\theta) = (B_1)_{SD} \cos^2\theta \qquad (4)$$

and that of the SP contribution (Eq. (3)). Thus, the constants, B's, in Eq. (2) are expressed as:

$$B_0 = (B_0)_{SP}$$

and:

$$B_1 = (B_1)_{SP} + (B_1)_{SD}. \qquad (5)$$

Moreover, for the isotropic γ-carbon *hfs* constants, one may expect the same dependences as those for the methyl-proton *hfs* constants. This is certainly true for the $2s$ AO spin density of the γ-carbon atom of the *n*-propyl radical.

In the last section, a molecular orbital description of the above angular dependences is given. It is shown that the intrinsic restriction of the UHF method, compared with the configuration interaction method, does not much affect the above conclusions.

Results and Discussion

Angular Dependence. In Table 1 the methyl-proton spin densities in the ethyl radical are given for the various angles, and then they are illustrated in Fig. 1. For the total spin density, ρ_{uhf}, the relation (2) holds fairly satisfactorily, while for the SP and SD contributions Eqs. (3) and (4) excellently represent their angular dependences. The curves obtained from Eqs. (2), (3), and (4) almost overlap with the corresponding curves shown in Fig. 1.

6) T. Yonezawa, H. Nakatsuji, T. Kawamura and H. Kato, This Bulletin, **42**, 2437 (1969).

7) H. Nakatsuji, H. Kato and T. Yonezawa, *J. Chem. Phys.*, **51**, 3175 (1969).
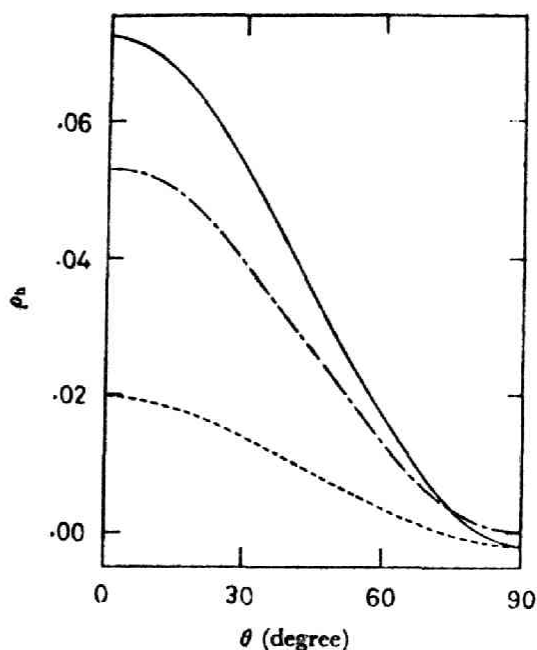

Fig. 1. Angular dependence of the methyl proton spin density in the ethyl radical.
——, ρ_{uhf}; -·-, $(\rho_{uhf})_{SD}$; -----, $(\rho_{uhf})_{SP}$

The coefficients, B, calculated from the results shown in Table 1, are given in Table 2.

For the *n*-propyl radical, the situation is very similar to that of the ethyl radical. For the β-proton spin density, the dependences of ρ_{uhf}, $(\rho_{uhf})_{SP}$, and $(\rho_{uhf})_{SD}$ on the rotational angle, θ, is illustrated in Fig. 2. The relation (2) deviates only slightly from the calculated dependence; this deviation is mainly due to the SD contribution. The constants, B, in Eqs. (2), (3), and (4) were obtained by fitting the calculated curves; they are given in Table 2.

For the isotropic γ-carbon *hfs* constants of the *n*-propyl radical, one may expect the same dependences as those for the methyl proton *hfs* constants in the ethyl radical. This is certainly true for the $2s$ AO spin density of the γ-carbon atom. The angular dependences of the $2s$ AO spin density and of the mechanistic contributions are illustrated in Fig. 3. The curves of this figure are very well represented by $\rho_{uhf} = -0.001 + 0.018 \cos^2\theta$, $(\rho_{uhf})_{SD} =$
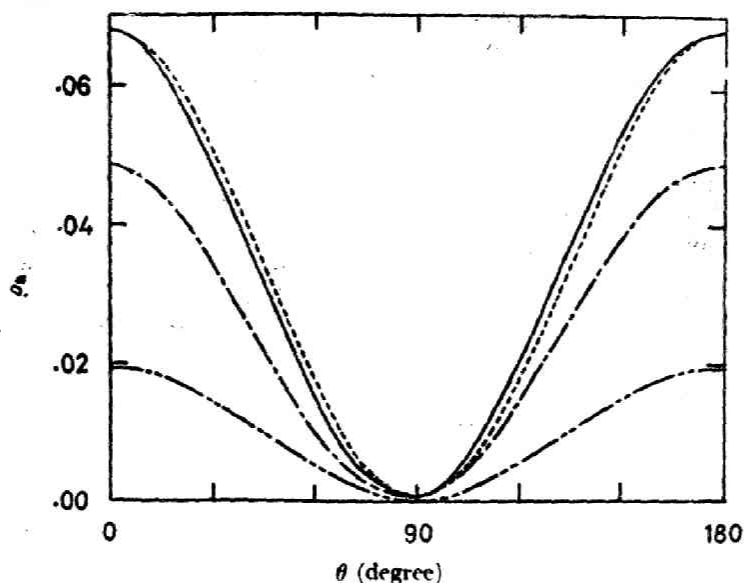
88

Fig. 2. Angular dependence of the β-proton spin density of the n-propyl radical.

——, ρ_{uhf}; -·—, $(\rho_{uhf})_{SD}$; ·—·—. $(\rho_{uhf})_{SP}$; -----, ρ calculated from Eq. (2)

TABLE 2. ANGULAR DEPENDENCE OF THE MECHANISTIC CONTRIBUTIONS[a]

Radical	B_0[b]	B_1	$(B_1)_{SP}$	$(B_1)_{SD}$	ρ_C^π
Ethyl	−1.5	55.4	16.0	39.4	1.000
i-Propyl	0.6	50.0	13.7	36.3	1.000
cis-1-Methylallyl	−0.5	49.2	21.4	27.9	0.689
$trans$-1-Methylallyl	−0.5	50.7	21.7	29.0	0.694
2-Methylallyl	1.6	44.1	44.1	0.0	−0.545
Toluene anion	4.1	39.1	39.1	0.0	−0.135
Toluene cation	−1.0	63.4	23.8	39.6	0.383

a) The values of B are given in gauss unit.
b) $B_0 = (B_0)_{SP}$

0.005 $\cos^2\theta$, and $(\rho_{uhf})_{SP} = -0.001 + 0.013 \cos^2\theta$.

Among the methyl-substituted allyl radicals, the 2-methylallyl radical is of great interest. Since the singly-occupied π-orbital of this radical has a node on the C_2 atom, the spin density of the methyl group is expected to be due only to the SP mechanism and to be negative in sign. This is certainly true, as Tables 2 and 3 show. Thus, the angular dependence of the methyl proton spin density of the 2-methylallyl radical is well represented *only* by

TABLE 3. THE METHYL PROTON SPIN DENSITY OF THE 2-METHYLALLYL RADICAL

Angle	UHF spin density				AA
θ	ρ_{uhf}	$(\rho)_{SP}$	$(\rho)_{SD}$	From Eq.(2)or(3)	ρ_{AA}
0	−0.020	−0.020	0.000	(−0.020)	−0.006
30	−0.016	−0.016	0.000	−0.016	−0.005
60	−0.006	−0.006	0.000	−0.006	−0.002
90	−0.001	−0.001	0.000	(−0.001)	0.000
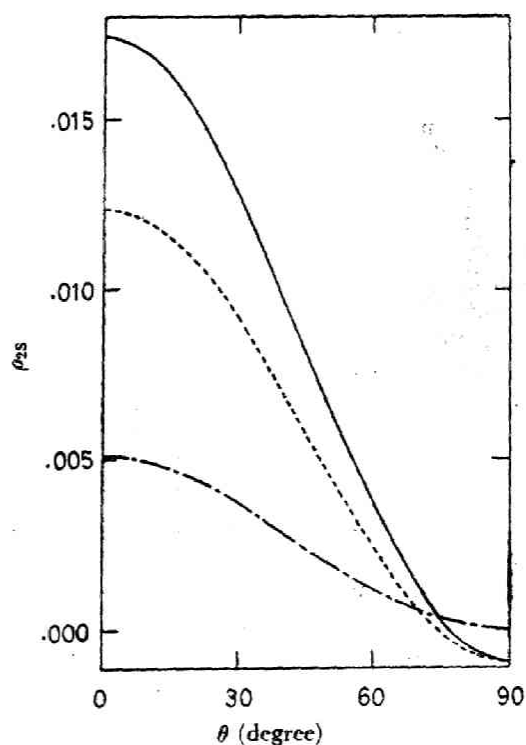
Fig. 3. Angular dependence of the $2s$ AO spin density of the γ-carbon atom of the n-propyl radical.

——, ρ_{uhf}; -·—, $(\rho_{uhf})_{SD}$; -----, $(\rho_{uhf})_{SP}$

Eq. (3), as is shown in Table 3.

For the other methyl-substituted allyl radicals (cis-1-methylallyl and $trans$-1-methylallyl), the situations are similar to that of the ethyl radical. The SD contributions to the methyl proton spin densities of these radicals are nearly 60%, small compared with those of the ethyl radical (See Table 2). Much

TABLE 4. THE METHYL PROTON SPIN DENSITY OF THE TOLUENE ION-RADICALS

Species	Angle θ	UHF spin density						AA ρ_{AA}
		ρ_{uhf}	From Eq. (2)	$(\rho)_{SP}$	From Eq. (3)	$(\rho)_{SD}$	From Eq. (4)	
Anion	0	−0.008	(−0.008)	−0.008	(−0.008)	0.000	0.000	−0.003
	30	−0.006	−0.006	−0.006	−0.006	0.000	0.000	−0.002
	45	−0.004	−0.005	−0.004	−0.005	0.000	0.000	−0.001
	60	−0.003	−0.003	−0.003	−0.003	0.000	0.000	0.001
	90	0.001	(−0.001)	−0.001	(−0.001)	0.000	0.000	0.000
Cation	0	0.033	(0.033)	0.012	(0.012)	0.021	(0.021)	0.025
	30	0.024	0.025	0.009	0.009	0.015	0.016	0.018
	45	0.016	0.016	0.006	0.006	0.010	0.010	0.012
	60	0.007	0.008	0.002	0.003	0.005	0.005	0.006
	90	−0.001	(−0.001)	−0.001	(−0.001)	0.000	0.000	0.000

as with the above examples, the angular dependences of the SP and SD contributions are well represented by Eqs. (3) and (4). The values of B in these equations are given in Table 2.

The methyl-proton spin densities of the toluene-ion radicals are summarized in Table 4. Although the toluene ions have nearly degenerate symmetric and antisymmetric electronic states with respect to the C_s operation, only their ground electronic states (the symmetric electronic state for the cation and the antisymmetric state for the anion) are calculated for the present purposes. For the antisymmetric state of the anion radical, its singly-occupied π-orbital has a node on the 1-carbon (the carbon to which the methyl group is attached); therefore, the spin density of the methyl proton is due only to the SP mechanism and is negative, similar to that of the 2-methylallyl radical. By referring to Table 4, Eq. (3) is found to apply satisfactorily. For the symmetric state of the cation radical, the SD contribution to the methyl proton spin density is nearly 60%. As is shown in Table 3, Eqs. (2), (3), and (4) hold very satisfactorily. The values of B in these equations are given in Table 2. Note that the B_1 values of the anion and cation differ greatly.

One conclusion from Table 2 is that the methyl proton spin densities are composed of a major (60—75%) SD contribution and of a minor (25—40%) SP contribution, except for the special cases of the 2-methylallyl radical and the antisymmetric state of the toluene anion. Note that the B values of the 2-methylallyl and toluene anion radicals, in which only the SP mechanism is important, deviate greatly from the average B values. Another conclusion of the present study is that the observed relation, (2), can be interpreted as the sum of Eqs. (3) and (4), and that this relation may also hold for the $2s$ AO spin density of the γ-carbon atom (as is shown in the case of the n-propyl radical).

hfs Constants. The proton hfs constants[8]

8) Proton hfs constants are calculated by multiplying ρ_{uhf} by 743 gauss.

calculated by assuming the free rotation of the methyl group are compared with the experimental results in Tables 5 and 6. Although the toluene ions have nearly degenerate electronic states, the calculated values given in Table 5 correspond only to the lower electronic states (the symmetric state for the cation and the antisymmetric state for the anion). For a more rigorous discussion of the hfs constants, the thermal and vibronic coupling effects must be considered,[14] as Purins and Karplus did recently.[9] Note, however, that the inclusion of

TABLE 5. CALCULATED PROTON hfs CONSTANTS

Radical	Position	hfs constant	
		Calcd.[a]	Exptl.
Ethyl	α-H	−25.6	(−)22.38[b]
	β-H	26.2	(+)26.87[b]
n-Propyl	α-H	−25.3	(−)22.08[b]
	β-H	25.6	(+)33.2[b]
	γ-H	−1.8	(−)0.38[b]
Toluene anion[c]	o-H	−9.0	(−)5.12[d]
	m-H	−9.6	(−)5.45[d]
	p-H	−0.1	(−)0.59[d]
	$H(CH_3)$	−3.2	(+)0.79[d]
Toluene cation[e]	o-H	−2.7	—
	m-H	−1.1	—
	p-H	−9.1	—
	$H(CH_3)$	11.8	—

a) The calculated values are obtained by assuming free rotation of the methyl group about the C–C single bond.

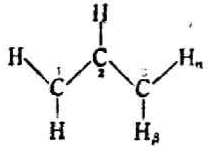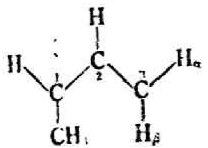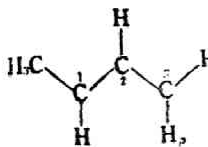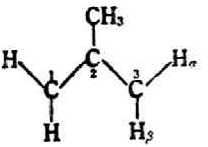b) R. W. Fessenden and R. H. Schuler, *J. Chem. Phys.*, **39**, 2147 (1963).

c) Only the antisymmetric electronic state is calculated.

d) J. R. Bolton, A. Carrington, A. Forman and L. E. Orgel, *Mol. Phys.*, **5**, 43 (1962).

e) Only the symmetric electronic state is calculated.

9) a) D. Purins and M. Karplus, *J. Chem. Phys.*, **50**, 241 (1969). b) D. Purins and M. Karplus, *J. Amer. Chem. Soc.*, **90**, 6275 (1968).

Radical	Position	hfs constant	
		Calcd.[a]	Exptl.[b]
Allyl	$H_{1,3\alpha}$	−14.19	(−) 14.81
	$H_{1,3\beta}$	−13.97	(−) 13.90
	H_2	3.64	(+) 4.06
cis-1-Methylallyl	$H(CH_3)$	16.80	(+) 14.01
	$H_{1\alpha}$	−18.87	(−) 14.17
	H_2	4.49	(+) 3.83
	$H_{3\alpha}$	−13.89	(−) 14.94
	$H_{3\beta}$	−13.64	(−) 13.52
trans-1-Methylallyl	$H(CH_3)$	17.22	(+) 16.43
	$H_{1\beta}$	−18.99	(−) 13.83
	H_2	3.97	(+) 3.85
	$H_{3\alpha}$	−14.12	(−) 14.78
	$H_{3\beta}$	−13.91	(−) 13.83
2-Methylallyl	$H(CH_3)$	− 7.89	(−) 3.19
	$H_{1,3\alpha}$	−13.97	(−) 14.68
	$H_{1,3\beta}$	−13.74	(−) 13.82

a) The calculated values are obtained by assuming free rotation of the methyl group about the C–C single bond.
b) J.K. Kochi and P.J. Krusic, *J. Amer. Chem. Soc.*, **90**, 7157 (1968).

these effects, which are expressed by the weighted mean of the hfs constants of the symmetric and antisymmetric electronic states, will improve the calculated hfs constants of the toluene anion.[10]

Since Fessenden and Schuler[11] observed the different hfs constants for the terminal methylene protons of the allyl radical, the observed hfs constants have been assigned theoretically by several investigators.[6,12–14] This finding was of particular interest since the well-known McConnell rule cannot interpret the observed difference. Recently, how-

10) The observed hfs constant of the methyl proton of the toluene anion is positive in sign; E. de Boer and J. P. Colpa, *J. Phys. Chem.*, **71**, 21 (1967).
11) R. W. Fessenden and R. H. Schuler, *J. Chem. Phys.*, **39**, 2147 (1963).
12) T. Yonezawa, H. Nakatsuji, T. Kawamura and H. Kato, This Bulletin, **40**, 2211 (1967).
13) A. Hinchliffe and H. M. Atherton, *Mol. Phys.*, **12**, 89 (1967).
14) J. A. Pople, D. L. Beveridge and P. A. Dobosh, *J. Amer. Chem. Soc.*, **90**, 4201 (1968).

ever, Kochi and Krusic[15] settled this assignment by observing the hfs constants of the methyl-substituted allyl radicals; they proved that the assignment by the present authors[6,12] was correct. Here, we calculated the proton hfs constants of these methyl-substituted allyl radicals. The results are summarized in Table 6. The assignments of the hfs constants of the $H_{3\alpha}$ and $H_{3\beta}$ protons of the cis- and trans-1-methylallyl radicals agree with the experimental results, although the differences in the calculated hfs constants of these two protons are rather small compared with the experimental values. In the 2-methylallyl radical, the methyl-proton hfs constants are calculated to be due only to the SP mechanism and to be negative in sign. The calculated hfs constants of the $H_{1\alpha}$ proton of the cis-form and of the $H_{1\beta}$ proton of the trans-form are too large (absolute value) compared with the experimental values.

Origin of the Angular Dependence. Here, we shall give a molecular orbital description of the angular dependences expressed by Eqs. (2), (3), and (4). For the present purposes the configuration interaction (CI) treatment may be most suitable. As has been shown previously, the UHF wave-function is expressed by the following CI form to a first-order approximation:[7]

$$\Psi_{uhf} = \Psi^{rf} + \sum_i C^{\infty}(ii^*) \ \Psi^{\infty}(ii^*),$$ (6)

where the second term is due to the spin polarization perturbation. Ψ^{rf} is the restricted function composed of the natural orbitals,[16,4b] λ_i and μ, of the UHF wave-function and $\Psi^{\infty}(ii^*)$ represents the normalized singly-excited configuration expressed by the one-electron jump from λ_i to ν_i:

$$\Psi^{rf} = |\lambda_1\alpha \ \lambda_1\beta \cdots \lambda_q\alpha \ \lambda_q\beta\mu\alpha|$$

$$\Psi^{\infty}(ii^*) =$$

$$|\lambda_1\alpha \ \lambda_1\beta \cdots \nu_i\lambda_i \frac{1}{\sqrt{2}} (\alpha\beta + \beta\alpha) \cdots \lambda_q\alpha\lambda_q\beta\mu\alpha| \quad (7)$$

$2q+1$ is the number of electrons in the radical. The natural orbitals, λ, μ, and ν, correspond, respectively, to the doubly-occupied, singly-occupied, and unoccupied orbitals of the restricted function, Ψ^{rf}, and are orthonormal to each other.[16] Note that λ_i and ν_i correspond to the bonding and antibonding partner MO's of the alternant molecular orbital method.[16,4b]

From Eq. (6), the SP and SD contributions to the UHF spin density are given by[16]:

$$(\rho_{uhf})_{SD} = \langle \Psi^{rf}|\rho|\Psi^{rf}\rangle - \mu^2 \quad (8)$$

15) J. K. Kochi and P. J. Krusic, *ibid.*, **90**, 7157 (1968).
16) a) A. T. Amos and G. G. Hall, *Proc. Roy. Soc.*, Ser. A. **263**, 483 (1961). b) T. Amos and L.C. Snyder, *J. Chem. Phys.*, **41**, 1773 (1964).

TABLE 7. UHF NATURAL ORBITALS, λ AND μ OF THE ETHYL RADICAL

AO	λ						μ
	$1(\sigma_1)$	$2(\sigma_2)$	$3(\bar{\pi}_1)$	$4(\pi_1)$	$5(\bar{\pi}_2)$	$6(\sigma_3)$	$7(\pi_2)$
			Configuration[a]				
$Y(1C)$	0.000	0.000	0.310	0.000	−0.341	0.000	0.000
$Z(1C)$	0.000	0.000	0.000	0.038	0.000	0.001	1.000
$Y(2C)$	0.000	0.000	0.340	0.000	0.312	0.000	0.000
$Z(2C)$	−0.001	0.000	0.000	0.458	0.000	0.003	0.013
$h(5H)$	0.167	−0.118	−0.356	−0.307	−0.410	0.082	0.115
$h(6H)$	0.167	−0.118	0.356	−0.307	0.410	0.082	0.115
$h(7H)$	0.161	−0.115	0.000	0.614	0.000	0.089	−0.229
			Configuration[b]				
$Y(1C)$	0.000	0.000	0.310	0.000	−0.341	0.000	0.000
$Z(1C)$	0.000	0.000	0.000	0.038	0.000	0.000	1.000
$Y(2C)$	0.001	0.000	0.340	0.000	0.313	−0.003	0.000
$Z(2C)$	0.000	0.000	0.000	0.458	0.000	0.000	0.013
$h(5H)$	0.163	−0.116	−0.206	−0.531	−0.237	0.086	0.198
$h(6H)$	0.163	−0.116	−0.206	0.531	−0.237	0.086	−0.198
$h(7H)$	0.169	−0.119	0.411	0.000	0.474	0.079	0.000

a) Configuration I
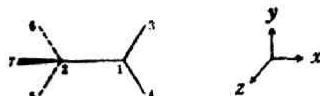
b) Configuration II
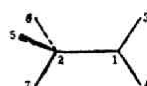
TABLE 8. COEFFICIENTS OF THE SINGLY EXCITED CONFIGURATIONS, $C^{se}(ii^*)$ OF THE ETHYL RADICAL

Geometry[a]	Coefficients, $C^{se}(ii^*)$					
	11^*	22^*	33^*	44^*	55^*	66^*
Configuration I	0.0013	0.0292	0.0043	0.0049	0.0031	0.0130
Configuration II	0.0015	0.0292	0.0042	0.0048	0.0032	0.0130

a) See footnotes a and b of Table 7.

and:

$$(\rho_{uhf})_{SP} = 2\sum_i C^{se}(ii^*) < \Psi^{rf}|\rho|\Psi^{se}(ii^*)>$$

$$= 2\sqrt{2}\sum_i C^{se}(ii^*)\lambda_i\nu_i, \qquad (9)$$

where ρ is the spin-density operator.

Now let us enter upon a description of the angular dependence of the methyl group proton spin density. In Table 7 the natural orbitals, λ and μ, of the ethyl radical, as calculated by the present method, are given for the two rotational configurations, and in Table 8 the coefficients of the singly-excited configurations, $C^{se}(ii^*)$, are summarized.[4] Table 8 shows that the coefficients, $C^{se}(ii^*)$, are almost independent of the rotational angle, θ. Thus, we have only to consider the angular dependence of the AO coefficients of the natural orbitals.

The local-group orbitals constructed from the three hydrogen $1s$ AO's of the methyl group may be written as:

$$\phi_\sigma = h_1 + h_2 + h_3,$$
$$\phi_{\bar{\pi}} = h_1 - h_3, \qquad (10)$$
$$\phi_\pi = h_1 + h_2 - 2h_3.$$

ϕ_σ is totally symmetric about the rotation, while $\phi_{\bar{\pi}}$ and ϕ_π are the quasi-π-orbitals and are perpendicular to each other. Thus, the angular dependence of the coefficients of the one particular hydrogen $1s$ AO, h, in various molecular orbitals (i) may be grouped into the following three types:

$$\sigma\text{-type: } a_i \cdot h,$$
$$\bar{\pi}\text{-type: } b_i \sin\theta \cdot h, \qquad (11)$$
$$\pi\text{-type: } c_i \cos\theta \cdot h,$$

where a_i, b_i, and c_i are the AO coefficients of the molecular orbital, i, at $\theta=90°$ or at $\theta=0°$. In Table 7 the orbitals are divided into the above three groups. For the π-electron radicals, the angular dependence of the coefficient of the methyl hydrogen is, of course, of the π-type. Hence, the

SD contribution to the methyl-proton spin density is given by:

$$(\rho_{uhf})_{SD} = c_\mu^2 \cos^2\theta \cdot \tag{12}$$

From Eqs. (9) and (11) the SP contribution is similarly expressed by:

$$
\begin{aligned}
(\rho_{uhf})_{SP} &= 2\sqrt{2}\,\{\sum_i^\sigma C^{se}(ii^*)\,a_i a_{i^*} \\
&\quad + \sum_i^{\bar{\pi}} C^{se}(ii^*)\,b_i b_{i^*}\sin^2\theta \\
&\quad + \sum_i^\pi C^{se}(ii^*)\,c_i c_{i^*}\cos^2\theta\} \\
&= (\nu_0)_{SP} + (\rho_1)_{SP}\cos^2\theta,
\end{aligned}
\tag{13}
$$

where:

$$(\rho_0)_{SP} = 2\sqrt{2}\,\{\sum_i^\sigma C^{se}(ii^*)\,a_i a_{i^*} + \sum_i^{\bar{\pi}} C^{se}(ii^*)\,b_i b_{i^*}\}$$

$$(\rho_1)_{SP} = 2\sqrt{2}\,\{\sum_i^\pi C^{se}(ii^*)\,c_i c_{i^*} - \sum_i^{\bar{\pi}} C^{se}(ii^*)\,b_i b_{i^*}\}.$$

$\sum^\pi$ denotes the summation over the π-type orbitals. Eqs. (12) and (13), and the sum of them, correspond to Eqs. (4), (3), and (2) respectively.

Note here that the conditions for the local symmetry orbitals expressed by Eq. (10) (the conditions for the definite grouping of MO's by Eq. (11)) are not satisfactorily fulfilled in cases of poor symmetry,[17] and that, in the usual CI treatment, the transitions other than $i \to i^*$ (i and i^* have, of course, the same type of local symmetry) must be included.[18] (Compare this with Eq. (6)). In

these cases, Eqs. (12) and (13) may include types of angular-dependent terms other than $\cos^2\theta$. One example of the poor symmetry is the n-propyl radical, where the curves obtained by Eqs. (2), (3), and (4) deviate slightly from the calculated curves. Nevertheless, the relations (2), (3), and (4) are still good approximations to the angular dependences of the β-proton spin density of the n-propyl radical (See Fig. 2).

The effects of the inclusion of the $i \to j^*$ ($i \neq j$) transitions are not certainly determined numerically by the present study, but they can be estimated as follows. The $i \to j^*$ transitions may be grouped into two groups; one is composed of the transitions where i and j^* have the same local symmetry, and the other is composed of the transitions where i and j^* have different local symmetries. By including the former type of transition, the angular dependence expressed by Eq. (13) is not altered. Only the coefficients may be changed. For the latter type of transition, which may produce types of angular-dependent terms other than $\cos^2\theta$, their CI coefficients, $C^{se}(ij^*)$, can be expected from symmetry considerations to be very small. Thus, the inclusion of the $i \to j^*$ ($i \neq j$) transitions will not much alter the type of angular dependence expressed by Eq. (13).

17) For example, the condition of the local symmetry expressed by Eq. (10) is already broken in the ethyl radical (See Table 7). However, the relations (2), (3) and (4) are very satisfactory as shown in the previous section.

18) A. L. H. Chung, *J. Chem. Phys.*, **46**, 3144 (1967).

PART II, CHAPTER 4

CALCULATION

OF THE FORCE CONSTANT

OF ETHYLENE

Calculation of Force Constants of Ethylene by a Semiempirical ASMO–SCF Method

A semiempirial ASMO–SCF calculation involving all valence electrons was carried out for a number of nuclear configurations of ethylene molecule. From the variation of the ground-state energy on the change of various structure parameters, all the diagonal quadratic force constants in the internal symmetry coordinate system were calculated and compared with those obtained from vibrational spectra. A modification of the Dewar and Klopman's formula including two empirical parameters was used to represent the core repulsion energy. It gave reasonable potential energy curves for the stretching coordinates.

INTRODUCTION

In the SCF molecular orbital theory involving all valence electrons, the relative positions of all nuclei in a molecule are taken into account explicitly on evaluating the multicenter integrals. This theory provides accordingly a general and straightforward procedure to predict the equilibrium structure and the force constants of polyatomic molecules through the calculation of ground-state energies for a variety of nuclear configurations. The rigorous treatment of this sort of calculation requires, however, so much labor even for the smallest molecules that the introduction of more or less approximations is inevitable to reduce the calculation to a tractable size. By using the approximation of the neglect of differential overlaps, Pople et al. have formulated a semiempirical ASMO–SCF theory for all valence electrons of molecules.[1] These authors' method has given, in spite of its simplicity, a fairly successful result in predicting correct valence angles and bending force constants of a number of simple polyatomic molecules.[2,3] The stretching force constants calculated by this method are too large, however, compared to those obtained from experimental data on vibrational spectra.[3,4]

Since there are many ways of approximations in evaluating the atomic integrals involved in the ASMO–SCF theory, further studies seem to be necessary in order to clarify the influence of various approximations on the reliability of the calculated force constants. It is also worthwhile to look for any systematic way of combining the approximations which can predict force constants and other properties of molecules simultaneously. With these points of view, we have carried out a semiempirical ASMO–SCF calculation of force constants of ethylene based on the method of Yonezawa, Kato, and co-workers which has recently given reasonable values of orbital energies, ionization potentials, electronic transition energies, and ESR hyperfine coupling constants[5,6] for molecules similar to those treated by Pople et al. This method is different from that of Pople et al. in adopting the one- and two-center electronic repulsion integrals evaluated semiempirically and in taking account of differential overlaps. In the present paper, the calculated force constants are compared with those obtained from the analysis of vibrational spectra and are discussed.

ATOMIC INTEGRALS

Since the detail of the procedure to evaluate the ground-state energy for a given nuclear configuration has already been reported,[5] we outline here only the evaluation of basic atomic integrals. The overlap integrals, S_{rs}, were taken to be the theoretical values for the Slater AO's, the effective nuclear charges being 1.00 and 3.25 for hydrogen and carbon, respectively. The one-center electron repulsion integrals were calculated by the well-known approximation due to Pariser,[7]

$$(rr \mid rr) = a_r^{-1} = I_r - A_r, \qquad (1)$$

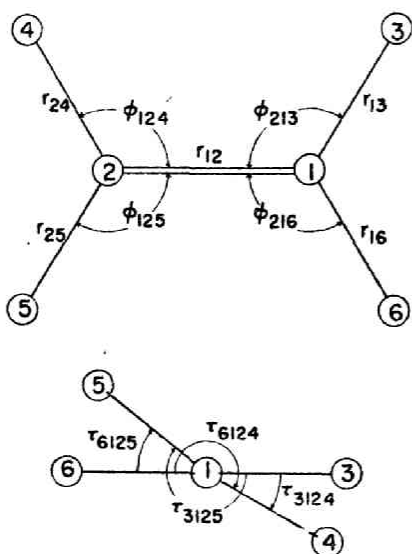where I_r and A_r represent the valence state ionization

FIG. 1. Internal coordinates.

potential and the electron affinity, respectively, of the atomic orbital (AO) r.[8] For the two-center electron repulsion integrals, we used the Ohno approximation,[9]

$$(rr \mid ss) = \tfrac{1}{2}[(a_r^2 + R_{rs}^2)^{-1/2} + (a_s^2 + R_{rs}^2)^{-1/2}], \quad (2)$$

where R_{rs} is the distance between the nuclei on which the AO's r and s are centered. The multicenter electron repulsion integrals were then calculated by the Mulliken approximation,[10]

$$(rs \mid tu) = \tfrac{1}{4} S_{rs} S_{tu}[(rr \mid tt) + (rr \mid uu)$$
$$+ (ss \mid tt) + (ss \mid uu)]. \quad (3)$$

Let N_r be the number of valence electrons on the AO r, and Z_A be the net core charge of the nucleus A. The core Hamiltonian matrix elements were then approximated as

$$H_{rr} - U_{rr} + \sum_{B \neq A} (B \mid rr), \quad (4)$$

$$(B \mid rr) = - \sum_s^B N_s (rr \mid ss), \quad (5)$$

$$U_{rr} = -I_r - (N_r - 1)(rr \mid rr)$$
$$- \sum_{r' \neq r}^A N_{r'}[(rr \mid r'r') - \tfrac{1}{2}(rr' \mid rr')], \quad (6)$$

and

$$H_{rs} = \tfrac{1}{2} S_{rs}[-P(Z_A + Z_B)(rr \mid ss) - (B \mid rr)$$
$$- (A \mid ss) + H_{rr} + H_{ss}], \quad (7)$$

where P is an empirical parameter and is taken to be 1.40.[6] In Eqs. (4)–(7), it is implied that the AO's r and s are centered on the nuclei A and B, respectively, and the superscript on $\sum$ in Eqs. (5) and (6) indicates that the sum is taken only over the AO's centered on that nucleus. The present treatment is different from the previous one[5] in the introduction of the one-center exchange integrals $(rr' \mid rr')$ evaluated according to

Hinze and Jaffe,[11] and in the estimation of the off-diagonal core matrix elements, H_{rs} $(r \neq s)$, for which the previous treatment[5] adopted the approximation by Wolfsberg and Helmholz.[12] Furthermore, in order to use the nonzero $(rr' \mid rr')$ without violating the invariance of the basic integrals on the rotation of the coordinate axes for p orbitals, the one-center integral $(rr \mid r'r')$ for the two different p orbitals centered on the same nucleus, e.g., p_x and p_y, was calculated by

$$(p_x p_x \mid p_y p_y) = (p_x p_x \mid p_z p_z) - 2(p_x p_y \mid p_x p_y). \quad (8)$$

By using the above integrals, the molecular orbital ϕ_i was obtained through the SCF calculation as the linear combination of atomic orbitals χ_r,

$$\phi_i = \sum_r C_r^i \chi_r, \quad (9)$$

and the ground-state electronic energy E_{el} was calculated by

$$E_{el} = \sum_{r,s} P_{rs} H_{rs} + \tfrac{1}{2} \sum_{t,u} P_{rs} P_{tu}[(rs \mid tu) - \tfrac{1}{2}(rt \mid su)], \quad (10)$$

where

$$P_{rs} = 2 \sum_i^{occ} C_r^i C_s^i. \quad (11)$$

The ground-state energy for a given nuclear configuration is then given by

$$E = E_{el} + \sum E^{AB}_{core}, \quad (12)$$

where E^{AB}_{core} represents the core repulsion energy between the nuclei A and B, and the sum is taken over all possible pairs of nuclei in the molecule.

CORE REPULSION ENERGY

There have been several ways of estimating the core repulsion energy in the literature. For the π-electron system, Parr and Pariser interpreted it as due to the positively charged holes vacated by the π electrons and evaluated it by the corresponding two-center electron repulsion integrals.[13] On the other hand, the core is just a nucleus for hydrogen and a nucleus surrounded by a closed 1s shell for carbon in the present treatment, and it seems more reasonable, at first sight, to use simply the point charge approximation,

$$E^{AB}_{core} = Z_A Z_B e^2 / R_{AB}, \quad (13)$$

where e is the electronic charge and R_{AB} is the distance between the nuclei A and B. Segal and Pople et al. adopted this approximation and obtained the equilibrium bond lengths agreeing well with the experiments for a number of molecules.[4] The success of Eq. (13) in these authors' method is, however, based on the use of the one- and two-center electron repulsion integrals evaluated theoretically by the Slater 1s and 2s AO's. Since the semiempirical evaluation by Eqs. (1) and (2) gives much smaller values to these integrals than

TABLE I. Internal symmetry coordinates.

Symmetry	Coordinate	Description	Increment
a_g	$S_1 = (\Delta r_{13} + \Delta r_{24} + \Delta r_{25} + \Delta r_{16})/2$	C–H stretching	± 0.1 Å
	$S_2 = \Delta r_{12}$	C=C stretching	± 0.05 Å
	$S_3 = (\Delta\varphi_{213} + \Delta\varphi_{124} + \Delta\varphi_{125} + \Delta\varphi_{216})/2$	CH$_2$ bending	± 0.1 rad
a_u	$S_4 = (\Delta\tau_{3125} + \Delta\tau_{3124} + \Delta\tau_{6124} + \Delta\tau_{6125})/2$	torsion	0.2 rad
b_{1g}	$S_5 = (\Delta r_{13} - \Delta r_{24} + \Delta r_{25} - \Delta r_{16})/2$	C–H stretching	0.1 Å
	$S_6 = (\Delta\varphi_{213} - \Delta\varphi_{124} + \Delta\varphi_{125} - \Delta\varphi_{216})/2$	CH$_2$ rocking	0.1 rad
b_{1u}	$S_7 = (\Delta\tau_{3125} - \Delta\tau_{6124})/\sqrt{2}$	CH$_2$ wagging	$0.2/\sqrt{2}$ rad
b_{2g}	$S_8 = (\Delta\tau_{3124} - \Delta\tau_{6125})/\sqrt{2}$	CH$_2$ wagging	$0.2/\sqrt{2}$ rad
b_{2u}	$S_9 = (\Delta r_{13} + \Delta r_{24} - \Delta r_{25} - \Delta r_{16})/2$	C–H stretching	0.1 Å
	$S_{10} = (\Delta\varphi_{213} + \Delta\varphi_{124} - \Delta\varphi_{125} - \Delta\varphi_{216})/2$	CH$_2$ rocking	0.1 rad
b_{3u}	$S_{11} = (\Delta r_{13} - \Delta r_{24} - \Delta r_{25} + \Delta r_{16})/2$	C–H stretching	0.1 Å
	$S_{12} = (\Delta\varphi_{213} - \Delta\varphi_{124} - \Delta\varphi_{125} + \Delta\varphi_{216})/2$	CH$_2$ bending	0.1 rad

the theoretical values, the core repulsion energy in the present method must also be smaller than that given by Eq. (13), in order that its change on a nuclear displacement be just canceled by the corresponding change of E_{el} at the equilibrium nuclear distance. From this reason we adopted initially an extended form of the Parr and Pariser's expression,

$$E^{AB}_{core} = \sum_r^A \sum_s^B N_r N_s (rr \mid ss). \quad (14)$$

On the calculation of force constants, the equilibrium structure of ethylene was initially taken from Allen and Plyler's data.[14] From the internal coordinates shown in Fig. 1, the internal symmetry coordinates were constructed in the same way as in the previous analysis of the vibrational anharmonicity.[15] These coordinates are defined to represent the actual changes of the given structural parameters and are therefore related to the Cartesian coordinates curvilinearly. They are listed in Table I together with their symmetries and descriptions.[16] Distorted configurations of the molecule were then constructed by displacing the nuclei from the equilibrium positions successively along each internal symmetry coordinate, in terms of which the increments were taken as given in Table I. From the ground-state energies for these nuclear configurations, the potential energy curve for each coordinate was obtained, and by fitting it to a polynomial of that coordinate, say S_i, by the least squares method, the quadratic diagonal force constant,

$$K_{ii} = \tfrac{1}{2}(\partial^2 E/\partial S_i^2),$$

was evaluated at the minimum of the calculated potential. As the polynomial to be fitted, the quartic function was used in general but the sextic function was also used for the totally symmetric stretching coordinates, S_1 and S_2.

Generally, the force constants are required by their definition to be evaluated for the nuclear configuration corresponding to the true minimum of the potential function in the multidimensional space spanned over all vibrational degrees of freedom. The force constant

obtained by the Taylor expansion of the potential function with respect to a single coordinate satisfies this requirement in the case either when the Taylor expansion is carried out at the calculated equilibrium configuration or when the contribution from interaction force constants to the potential energy is negligibly small. Since we cannot regard the second of these conditions to be a good approximation, the calculated equilibrium configuration is required to agree with the initially assumed one in order that the first condition is satisfied without the complicated transformation of the origin of the coordinate system. On the use of Eq. (14), the calculated potential minimum was found very close to the origin for the a_gCH$_2$ bending coordinate (S_3),[17] whereas the potential functions for the C=C stretching (S_2) and the a_g C–H stretching (S_1) coordinates showed only monotonous increases on the increase of the bond distances within the investigated ranges. In the curvilinear internal coordinate system, the distance between bonded nuclei changes only on the change of stretching coordinates. Accordingly, the success for the S_3 mode and the failure for the S_1 and S_2 modes in predicting the correct equilibrium configuration suggest that the core repulsion energy estimated by Eq. (14) is appropriate for such comparatively large nuclear distances as those between nonbonded nuclei but is too small for such shorter distances as those between bonded nuclei. With the purpose to obtain reasonable core repulsion energies for both the cases of bonded and nonbonded nuclei, we interpolated Eqs. (13) and (14) by a two-parameter function,

$$E^{AB}_{core} = \sum_r^A \sum_s^B N_r N_s (rr \mid ss) + [Z_A Z_B e^2/R_{AB}$$
$$- \sum_r^A \sum_s^B N_r N_s (rr \mid ss)] \exp(-\alpha_{AB} R_{AB}^n), \quad (15)$$

where the parameter n was fixed to 1.0, 1.5, and 2.0 after several trial calculations. When $n=1$, Eq. (15) becomes identical with that proposed by Dewar and Klopman in the calculation of the heats of formation of a number of hydrocarbon molecules.[18] In the semi-
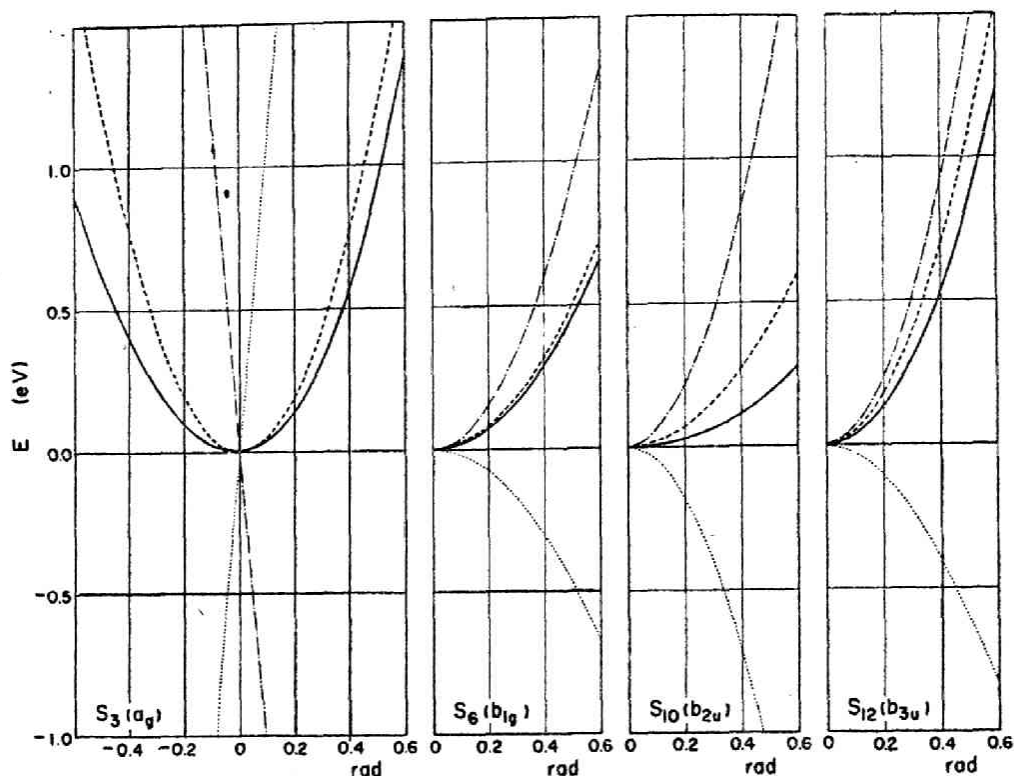
FIG. 2. Potential energy curves for valence angle deformation coordinates: —, E (calculated); - - -, E (experimental); $\cdots$, E_{el}; $\cdot$–$\cdot$, E_{core}.

empirical calculation used in this work, however, reasonable values of the stretching force constants were obtained, as shown in the following, only for the cases where $n \neq 1$. After fixing n to the above values, the parameter α_{AB} was adjusted independently for each of the coordinates S_1 and S_2 to reproduce the correct equilibrium bond distances. On using Eq. (15) with α_{AB} fixed so as to reproduce the equilibrium length of the C–H bond, the contribution from the second term to E^{AB}_{core} was found to be almost negligible at distances larger than 1.5 Å. This result means that the equilibrium H–C–H angle obtained from Eq. (14) is not much changed on the use of Eq. (15) for both the bonded and nonbonded C$\cdots$H distances, and that the difference between Eqs. (14) and (15) is not essential for the latter. Accordingly, by assuming a similar situation for the H$\cdots$H repulsion, we simplified the calculation by using Eq. (14) for E^{AB}_{core} between nonbonded nuclei.

RESULTS AND DISCUSSION

It has been pointed out that the values of force constants calculated by the polynomial fitting of a potential curve are affected seriously by the spacing and the spread of the representative points of the coordinate.[19] In the present calculation, the uncertainty due to this effect is estimated to be 0.1 and 0.05 mdyn/Å for the C=C and the C–H stretching coordinates, respectively, 0.01 mdyn$\cdot$Å/rad^2 for the CH$_2$ bending and the CH$_2$

rocking coordinates, and 0.001 mdyn$\cdot$Å/rad^2 for the CH$_2$ wagging and the torsional coordinates. In Table II, the calculated force constants for the CH$_2$ bending, the CH$_2$ rocking, the CH$_2$ wagging, and the torsional coordinates are shown together with those obtained by the analysis of vibrational spectra.[15] For the in-plane coordinates, the bending force constants K_{33} and $K_{12,12}$ were calculated to be larger than the rocking force constants K_{55} and $K_{10,10}$, as expected from the experiment, but the agreement between the calculated and the experimental values of individual force constants was not so good for K_{33}, $K_{10,10}$, and $K_{12,12}$. From the diagonal force constants for the internal symmetry coordinates in Table II, the interaction force constants connecting the equivalent internal coordinates are obtained by the orthogonal transformation of the coordinates given

TABLE II. Angle deformation force constants (in mdyn$\cdot$Å/rad^2).

Force constant	Experimental[15]	Calculated
K_{33} (a_g CH$_2$ bending)	0.765	0.46
$K_{12,12}$ (b_{3u} CH$_2$ bending)	0.688	0.50
K_{55} (b_{1g} CH$_2$ rocking)	0.319	0.28
$K_{10,10}$ (b_{2u} CH$_2$ rocking)	0.266	0.10
K_{77} (b_{1u} CH$_2$ wagging)	0.0999	0.082
K_{88} (b_{2g} CH$_2$ wagging)	0.0735	0.058
K_{44} (torsion)	0.0685	0.063

97

in Table I. The *trans* and *cis* interaction constants for the C–C–H angles, k_t and k_c, are defined by the terms contributing to the potential energy,

$$k_t(\Delta\phi_{213}\Delta\phi_{125} + \Delta\phi_{124}\Delta\phi_{216}) + k_c(\Delta\phi_{213}\Delta\phi_{124} + \Delta\phi_{125}\Delta\phi_{216}).$$

From the normal coordinate analysis of ethylene molecule,[20] it has been established that k_t is important but k_c is not, and the origin of this *trans* interaction has been an interesting problem for the theoretical prediction of force constants of ethylene. The presently calculated value of k_t (0.07 mdyn·Å/rad²) agrees well with the experimental value (0.065 mdyn·Å/rad²), whereas the calculated k_c (−0.11 mdyn·Å/rad²) is much larger in magnitude than the experimental one (0.012 mdyn·Å/rad²).[15] Thus it seems that any detailed discussion on the interaction force constants requires much more elaborate treatment than the present one.

The force constants for the CH₂ wagging vibrations, K_{77} and K_{88}, were calculated to have reasonable magnitudes with the correct order, and the calculated and the experimental values of the torsional force constant K_{44} agree well with each other. Since the first derivatives of any internuclear distance R_{AB} with respect to the out-of-plane coordinates S_4, S_7, and S_8 vanish for the equilibrium configuration, only the first derivatives of the core repulsion energy with respect to R_{AB} contribute to the force constants K_{44}, K_{77}, and K_{88}, whereas both the first and the second derivatives contribute to the in-plane force constants. In this respect, the satisfactory result obtained presently for the out-of-plane force constants is not surprising because the inadequacy of the functional form of E^{AB}_{core} (R_{AB}) is supposed to be less manifested in the first derivatives than in the second derivatives.

Although the estimation of the cubic and quartic force constants by the polynomial fitting is much more difficult than the case of quadratic constants, the inspection of the energy curves along various coordinates may offer some information on the anharmonicity of a calculated potential function. Figure 2 shows the plot of the calculated potential energy and its components, E_{el} and E_{core}, against the four valence angle deformation coordinates, S_3, S_6, S_{10}, and S_{12}. The corresponding potential energies may be evaluated in the first approximation by multiplying the squares of the coordinates by the quadratic force constants obtained from vibrational spectra.[15] These are also shown in Fig. 2 for the sake of comparison. For the a_g CH₂ bending coordinate, S_3, each of E_{el} and E_{core} changes very steeply near the equilibrium position, but they almost cancel each other to give a reasonable energy curve. As expected from the dominant repulsion between the hydrogen nuclei at the geminal positions, the potential energy curve shows the larger curvature in the first quadrant (closure of the H–C–H angles) than in the second quadrant (opening of the H–C–H angles). Unfortunately, we cannot check the validity of the calculated anharmonicity, since the cubic and the quartic force constants for the valence
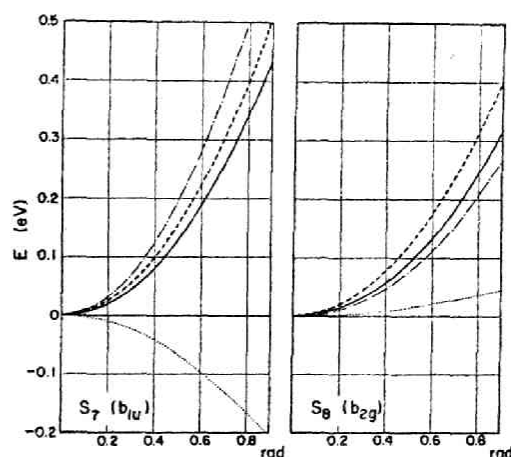

FIG. 3. Potential energy curve for out-of-plane deformation coordinates: —, E (calculated); - - -, E (experimental); ···, E_{el}; —·—, E_{core}.

angle deformation coordinates have not yet been estimated from vibrational spectra. For the nontotally symmetric coordinates, S_6, S_{10}, and S_{12}, it is seen that E_{el} attains the maximum value at the origin, but is overcome by the stabilizing effect of E_{core} to give the symmetrical equilibrium structure. In Fig. 3, the experimental and the calculated potential energies and the components of the latter, E_{el} and E_{core}, are plotted against the CH₂ wagging coordinates S_7 and S_8. Since the quartic force constants for these coordinates were estimated to be very small,[16] we calculated the experimental potential energies in the same way as those in Fig. 2. From the difference in the change of the internuclear distances, it is expected that E_{core} for a given value of S_7 is much larger than that for the same value of S_8, and the former is in fact more than twice the latter. However, the sign of E_{el} is negative for $S_7 \neq 0$ but positive for $S_8 \neq 0$, and the net potential energies calculated for the displacements along these coordinates are not much different from each other in agreement with the experiment.

In contrast to the cases of the valence angle and out-of-plane deformation coordinates discussed above, the potential curve along the torsional coordinate of ethylene has been the subject of a number of theoretical investigations on the electronic structure.[13,21–25] In comparing the theory with the experiment, however, most of the previous authors referred to the torsional force constant obtained only by applying the harmonic approximation to the indirectly estimated fundamental frequency, 1027 cm⁻¹, in the a_u species. We constructed the experimental potential curve in this work by using the quadratic and quartic force constants obtained from the analysis of the vibrational anharmonicity of ethylene[15] as well as the barrier height for the internal rotation obtained from the reaction rate of the *cis–trans* isomerization of 1,2-dideuteroethylene.[26] This barrier height has been referred to by Charney *et al.*

TABLE III. Parameters in core repulsion energy [Eq. (15)] and stretching force constants.[a]

α_{AB} (in Å⁻ⁿ)	Force constant (in mdyn/Å)	Experimental[15]	Calculated		
			$n=1.0$	$n=1.5$	$n=2.0$
α_{CC}			1.900	1.844	1.741
	K_{22} (C=C)	5.861	3.5	4.6	5.8
α_{CH}			2.339	2.525	2.650
	K_{11} (a_g C–H)	2.658	2.15	2.70	3.35
	K_{55} (b_{1g} C–H)	2.777	2.05	2.60	3.25
	K_{99} (b_{2u} C–H)	2.676	1.95	2.50	3.15
	$K_{11,11}$ (b_{3u} C–H)	2.683	2.15	2.75	3.40

[a] The calculated and the experimental bond lengths are: $R_{CC}=1.337$ Å and $R_{CH}=1.086$ Å.

in their analysis of the vibrational structure of the ultraviolet spectrum of ethylene.[27]

The torsional potential of ethylene may be expressed in terms of the coordinate S_4 as

$$E(S_4) = V_1(1- \cos S_4) + V_2(1- \cos 2S_4)$$
$$+ V_3(1- \cos 3S_4)$$
$$= K_{44}S_4^2 + K_{4444}S_4^4. \qquad (16)$$

The force constants K_{44} and K_{4444} and the barrier height B are then related to V_1, V_2, and V_3 by

$$K_{44} = \tfrac{1}{2}(V_1 + 4V_2 + 9V_3),$$
$$K_{4444} = -(V_1/24 + 2V_2/3 + 27V_3),$$

and

$$B = 2(V_1 + V_3).$$

From the numerical values $K_{44}=0.0685$ mdyn·Å/rad², $K_{4444}=-0.0039$ mdyn·Å/rad⁴, and $B=0.4486$ mdyn·A, we obtained V_1, V_2, and V_3 as 0.2239, -0.02253, and 0.0036, respectively, in mdyn·Å. The resulting experimental curve is shown together with the calculated curves for E, E_{el}, and E_{core} in Fig. 4. As indicated by the relative magnitudes of the quadratic and the quartic

force constants, the experimental potential energy curve is quite harmonic except near the top of the barrier, and shows an appreciably smaller curvature at the potential minimum than at the maximum. It is worthwhile to note that the simultaneous fit of the quadratic force constant and the barrier height also requires a potential function which is much less anharmonic than the simple sinusoidal potential which has the same curvature at the minimum and the maximum. On the other hand, the calculated curves for E_{el} and E_{core} appear nearly parabolic and sinusoidal, respectively, and the magnitude of E_{el} increases far more rapidly than that of E_{core} on the increase of the torsional angle. Hence the anharmonicity of the calculated potential function becomes very small, resulting in an excellent agreement between the calculated and the experimental energies over a wide range of the torsional angle. The calculated curve near the top of the barrier is not correct, however, since the interaction between the ground and the excited states is not taken into account in the present treatment.

For the C=C and the C–H stretching coordinates, S_1, S_2, S_5, S_9, and S_{11}, Table III shows the quadratic force constants obtained from the vibrational spectra[16]
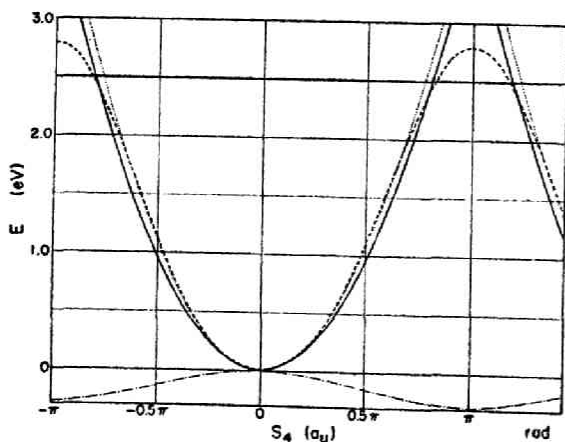

FIG. 4. Potential energy curve for the torsional coordinate: —, E (calculated); - - -, E (experimental); ··· E_{el}; ·—· E_{core}.
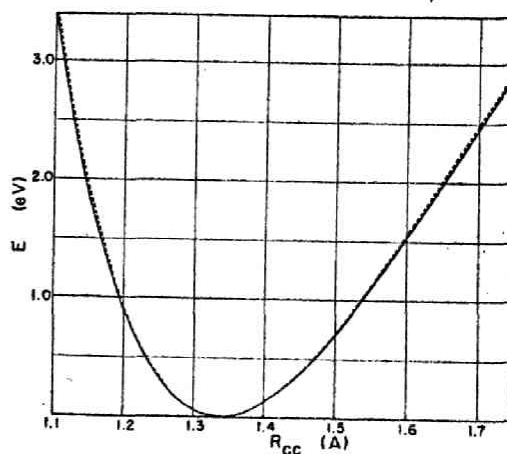

FIG. 5. Potential energy curve for the C=C stretching coordinate: —, E (calculated); - - -, E_z (experimental).

and the corresponding constants calculated in this work. The parameters α_{AB} and n in Eq. (15) are also given in Table III. It is seen that the force constants attain reasonable values when n is 1.5 and 2.0 for the C–H and the C=C bonds, respectively, but the equilibrium bond lengths and the force constants cannot be fitted to the experimental values simultaneously by fixing n for the C=C and the C–H bonds to the same value. The potential curves calculated by using the best values of n are compared with the experimental curves in Figs. 5 and 6 for the C=C stretching and the a_g C–H stretching coordinates, respectively. The experimental curve for the C=C stretching coordinate represents a Morse-type function,

$$E(S_2) = (K_{22}/a^2)[1 - \exp(-aS_2)]^2, \qquad (17)$$

where the parameter a is taken to be 2.0 Å^{-1}. This function has been assumed in estimating the cubic and quartic force constants from the spectroscopic data.[15] The effect of truncating the Taylor expansion of Eq. (17) at the quartic term becomes so large for $S_2 > 0.3$ Å that the curve based on a quartic function is not adequate as the experimental curve to be compared with the calculated. For the a_g C–H stretching coordinate, such the effect of truncation was found to be small in the range -0.6 Å $< S_1 < 0.6$ Å, and the experimental curve in Fig. 6 was calculated by the quartic function ·

$$E(S_1) = K_{11}S_1^2 + K_{111}S_1^3 + K_{1111}S_1^4,$$

where the value of K_{11} was that given in Table III, and according to the previous estimation of the vibrational anharmonicity,[15] K_{111} and K_{1111} were taken to be -2.159 mdyn/Å^2 and 1.007 mdyn/Å^3, respectively.
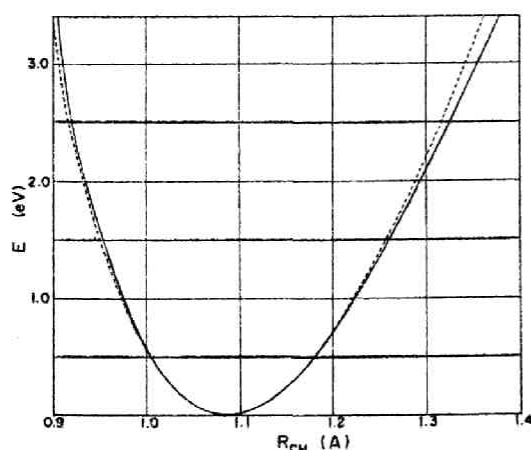

FIG. 6. Potential energy curve for the a_g C–H stretching coordinate: —, E (calculated); - - -, E (experimental).

The agreement between the experimental and the calculated potential energies throughout the investigated range of the bond length indicates that the use of E_{core} including two empirical parameter is fairly successful for predicting the anharmonicity of the bond stretching potential. It may thus be interesting to see if the parameters used for ethylene can fit also the bond lengths and the force constants of other molecules, especially acetylene and ethane.

ACKNOWLEDGMENTS

[1] J. A. Pople, D. P. Santry, and G. A. Segal, J. Chem. Phys. 43, S129, S136 (1965).

[2] J. A. Pople and G. A. Segal, J. Chem. Phys. 44, 3289 (1966); D. P. Santry and G. A. Segal, ibid. 47, 158 (1967); J. A. Pople, D. L. Beveridge, and P. A. Dobosh, ibid. 47, 2026 (1967).

[3] H. Obayashi, H. Takahashi and T. Miyazaki, Symposium on Molecular Structure, Chemical Society of Japan, Sapporo, 1967.

[4] G. A. Segal, J. Chem. Phys. 47, 1876 (1967); J. A. Pople, D. L. Beveridge, and N. S. Ostlund, Intern. J. Quantum Chem. 1, 293 (1967); M. S. Gordon and J. A. Pople, J. Chem. Phys. 49, 4643 (1968).

[5] T. Yonezawa, K. Yamaguchi, and H. Kato, Bull. Chem. Soc. Japan 40, 536 (1967).

[6] H. Kato, H. Konishi, H. Yamabe, and T. Yonezawa, Bull. Chem. Soc. Japan 40, 2761 (1967); T. Yonezawa, H. Nakatzuji, T. Kawamura, and H. Kato, ibid. 42, 2437 (1969).

[7] R. Pariser, J. Chem. Phys. 21, 568 (1953).

[8] For the numerical values, see Ref. 5.

[9] K. Ohno, Theoret. Chim. Acta 2, 219 (1964).

[10] R. S. Mulliken, J. Chim. Phys. 46, 497 (1949).

[11] J. Hinze and H. Jaffe, J. Chem. Phys. 38, 1834 (1963).

[12] M. Wolfsberg and L. Helmholz, J. Chem. Phys. 20, 837 (1952).

[13] R. G. Parr and R. Pariser, J. Chem. Phys. 23, 711 (1955).

[14] H. C. Allen, Jr. and E. K. Plyler, J. Am. Chem. Soc. 80, 2673 (1958).

[15] K. Machida, J. Chem. Phys. 44, 4186 (1966).

[16] The numbering of symmetry coordinates has been revised to follow that of normal coordinates.

[17] The equilibrium H–C–H angle was calculated to be 117°59', agreeing practically with the experimental value, 117°22', by Allen and Plyler.[14]

[18] M. J. S. Dewar and G. Klopman, J. Am. Chem. Soc. 89, 3089 (1967).

[19] J. Gerratt and I. M. Mills, J. Chem. Phys. 49, 1719 (1968).

[20] J. Overend and J. R. Scherer, J. Chem. Phys. 33, 1681 (1960).

[21] R. S. Mulliken and C. C. J. Roothaan, Chem. Rev. 91, 219 (1947).

[22] R. G. Parr and B. L. Crawford, Jr., J. Chem. Phys. 16, 526 (1948).

[23] J. W. Moskowitz and M. C. Harrison, J. Chem. Phys. 42, 1726 (1965).

[24] U. Kaldor and I. Shavitt, J. Chem. Phys. 48, 191 (1968).

[25] R. J. Buenker, J. Chem. Phys. 48, 1368 (1968).

[26] J. E. Douglas, B. S. Rabinovitch, and F. S. Looney, J. Chem. Phys. 23, 315 (1955).

[27] R. McDiarmid and E. Charney, J. Chem. Phys. 47, 1517 (1967).

CHAPTER 5

CONCLUSION

• In Part II of the present thesis, the author aimed to extend
the applicability of the semi-empirical SCF-MO method for valence
electron systems to various molecular properties. From the
studies summarized in Chapter 2 and 3, explicit accounts of σ-elect-
rons (not like in π-electron theory) and of the electron-repulsion
terms (not like in the extended Hückel theory) are shown very impor-
tant. σ-electrons work generally to relax the localization of
charge in carbonium ions; the electrons on protons are found most
important for this role. In the studies of doublet radicals,
the empirical McConnell rule becomes unnecessary and direct calcula-
tion of the hfs constant becomes possible by including σ-electrons;
thus, in allyl radical, different hfs constants are obtained for
the two terminal methylene protons, agreeing with experiment.
The explicit inclusion of the electron repulsion term is important
in carbonium ions, since there, the electron repulsion energy
diminishes by one electron, comparing with the neutral molecules.
This effect is shown most important in the orbital energies and
transition energies. The importance of this term in doublet
radicals is obvious since the spin-polarization mechanism comes
from this term.

From the studies given in Chapter 3, Section 1, the method
proposed in Part I, Chapter 2 to separate the UHF spin densities
into mechanistic contributions is proved useful in the actual
calculations. From this it is shown that the spin-polarization
(SP) mechanism is important even in cases where the spin-delocali-
zation (SD) mechanism has been considered dominant. In methyl

101

and vinyl radicals, their hfs constants and mechanistic contributions are shown to be strongly angular dependent. From the examinations of this dependence and of the potential energy curve, the C-C-H_α angle of vinyl radical is predicted to be nearly 135°. Moreover, for the hydrogenated pyridine, similar treatment predicted its preferable structure to be N-hydrogenated configuration.

From the study given in Chapter 3, Section 2, it is found out that the observed relation, $Q(\theta) = B_0 + B_1 \cos^2\theta$, for the angular dependence of the ß-proton hfs constant is explained as the sum of the following two equations,

$$Q_{SD}(\theta) = (B_1)_{SD} \cos^2\theta ,$$

$$Q_{SP}(\theta) = (B_0)_{SP} + (B_1)_{SP} \cos^2\theta ,$$

where θ is the rotational angle about C-C bond.

From the study given in Capter 4, the present valence electron SCF-MO method is proved applicable also to the calculation of force constant of ethylene by a small modification in the core-repulsion energy. Since the core-repulsion energy becomes infinite when two cores approach, this modification is reasonable. The calculated force constants agree satisfactorily with the experimental values. Note that this method can give reasonable potential curves even for the stretching coordinate.

PART III

THEORETICAL STUDIES ON

THE ANISOTROPY OF THE INDIRECT NUCLEAR

SPIN-SPIN COUPLING CONSTANT

—— PROBLEMS IN THE STRUCTURE DETERMINATION OF

THE MOLECULE DISSOLVED IN A NEMATIC SOLVENT ——

CHAPTER 1

INTRODUCTION

Since the experiment of Saupe and Englart,[1] active investigations of the molecules dissolved in liquid-crystal solvents have been carried out by the nuclear magnetic resonance (NMR) technique. Anisotropy of the indirect nuclear spin-spin coupling constant (J_{aniso}) is one of the informations obtained from the NMR spectra of the molecule dissolved in a nematic solvent. The relation between J_{aniso} and the experimental NMR splitting is illustrated in Fig. 1.

NMR spectra in liquid crystal solvent

$(J_{AB})_{aniso} \propto$ [Total anisotropic coupling]

— [Direct coupling]

sensitive

insensitive   sensitive

Molecular geometry

Possible difference originates from;

(i) gas ⟶ liquid crystal

(ii) molecular vibration

$\langle 1/r^3 \rangle$: NMR

$\langle 1/r^2 \rangle$: microwave

$\langle r \rangle$: electron diffraction
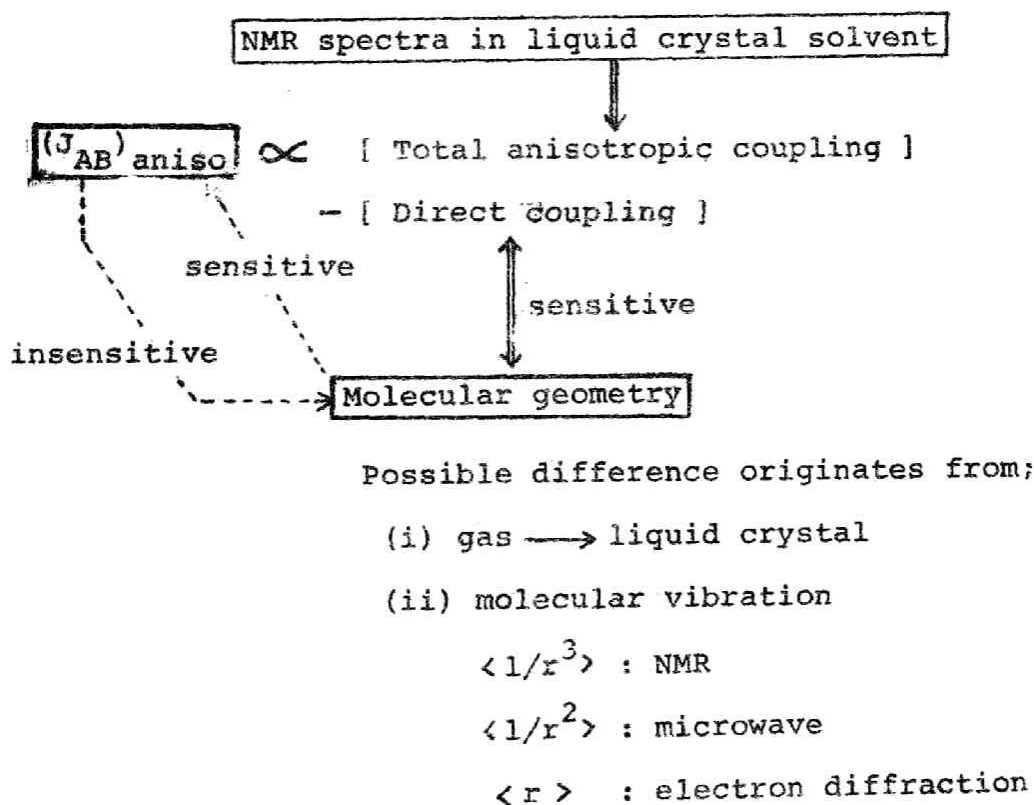
Fig. 1. INFORMATION DIAGRAM

As seen from Fig. 1, the value of $(J_{AB})_{aniso}$ between nuclear pair A and B cannot be determined without the supplemental data on molecular geometry. The reverse of this is also correct. The data of molecular geometry usually used is that determined by the microwave or electron-diffraction method in gas-phase, which may be different from the geometry of the molecule under consideration by the following two points; firstly, the states are different, and secondly, the experimental techniques are different, causing dfferences in the vibrational averaging of the internuclear distance, r.

In Chapter 2, Section 1 (published in Chemical Physics Letters, 4, 607 (1967)), a molecular orbital study of the anisotropy of the indirect nuclear spin-spin coupling constant is given. Since there was no theoretical study on this subject, the author firstly formulated three mechanisms important to J_{aniso} by the usual sum-over-state perturbation method. They are Fermi-spin dipolar cross term, spin dipolar term and orbital term. Relative importance of these mechanisms is investigated.

In Chapter 2, Section 2 (published in Chemical Physics Letters, 6, 541 (1970)), another approach to this problem by the finite perturbation method is reported. Since the nuclear spin-spin coupling is due essentially to the spin-correlation in closed-shell electronic system[2], the finite perturbation method is useful as proved in Part I, Chapter 4. This is also the first application of this method to this problem. From this study, the superiority of the finite perturbation method to the sum-over-state perturbation method is proved in the actual calculations.

In Chapter 3 (to be published in the Bulletin of the Chemical Society of Japan), the order of magnitude of $(J_{AB})_{aniso}$ is exten-

sively calculated for various nuclear pairs, by using INDO-MO's of Pople et al.[3]   From these numerical results and from the experimental examination of the substituent effect on $(J_{CH})_{aniso}$ in CH_3X series,[4] it is concluded that the experimentally estimated value of the ^{13}C-H coupling anisotropy in CH_3F as large as 1890 Hz[5] is erronious and that these values still contain some other more important effects than the electronic one, such as those given in Fig. 1.   The relative importance of these two effects is disscussed by using the relevant data available at present and then, it is concluded that the change in the molecular geometry from gas state to the solute state in nematic solvent is the most natural origin for the differences between the theoretical and 'experimental' values.

REFERENCES

1. (a) A. Saupe and G. Englart, Phys. Rev. Letters, 11, 462 (1963).

   (b) G. Englart and A. Saupe, Z. Naturforsch. 19a, 172 (1964).

2. M. Barfield, J. Chem. Phys. 44, 1836 (1966); 49, 2145 (1968).

3. J. A. Pople, D. L. Beveridge and P. A. Dobosh, J. Chem. Phys. 47, 2026 (1967).

4. I. Morishima, A. Mizuno, H. Nakatsuji and T. Yonezawa, Chem. Phys. Letters, in press.

PART III, CHAPTER 2

MO STUDIES OF

THE ANISOTROPY OF THE INDIRECT NUCLEAR

SPIN-SPIN COUPLING CONSTANT

SECTION 1   TREATMENT BY THE SUM-OVER-STATE PERTURBATION METHOD

SECTION 2   TREATMENT BY THE FINITE PERTURBATION METHOD

ANISOTROPY OF THE INDIRECT NUCLEAR SPIN-SPIN COUPLING CONSTANT

Various contributions to the anisotropy of the indirect nuclear spin-spin coupling constant in nuclear magnetic resonance are examined and order-of-magnitude calculations are reported for hydrocarbons and for methyl fluoride.

1. INTRODUCTION

Recently, Krugh and Bernheim [1] reported the existence of very large anisotropy of the indirect nuclear spin-spin coupling constants of methyl fluoride dissolved in a nematic solvent. Their results show that the anisotropy is especially large for the coupling constants between directly bonded nuclei (C—F and C—H). In the present paper, the origin of the anisotropy in the indirect nuclear spin-spin coupling constant is examined and the orders of magnitude of various contributions are calculated for hydrocarbons and for methyl fluoride with rather crude approximations.

2. ORIGIN OF ANISOTROPY

The Hamiltonian for the indirect nuclear spin-spin coupling in nuclear magnetic resonance spectra is given by the sum of the following four terms [2]:

i) Terms due to the magnetic shielding of the direct interaction of the nuclear spins by electron orbital motion.

$$\mathcal{H}_1^{(a)} = (e\hbar\beta/c) \sum_{A,B,k} \gamma_A \gamma_B r_{kA}^{-3} r_{kB}^{-3} [(I_A \cdot I_B)(r_{kA} \cdot r_{kB}) - (I_A \cdot r_{kB})(I_B \cdot r_{kA})], \tag{1}$$

$$\mathcal{H}_1^{(b)} = (2\beta\hbar/i) \sum_{A,k} \gamma_A r_{kA}^{-3} I_A \cdot (r_{kA} \times \nabla_k). \tag{2}$$

ii) (Electron-spin)-(nuclear-spin) dipolar interaction term.

$$\mathcal{H}_2 = 2\beta\hbar \sum_{A,k} \gamma_A [3(S_k \cdot r_{kA})(I_A \cdot r_{kA}) r_{kA}^{-5} - S_k \cdot I_A r_{kA}^{-3}]. \tag{3}$$

iii) Term due to the Fermi interaction between electron-spins and nuclear-spins.

$$\mathcal{H}_3 = (16\pi\beta\hbar/3) \sum_{A,k} \gamma_A \delta(r_{kA}) S_k \cdot I_A. \tag{4}$$

In the above equations, A and B denote nuclei and k refers to an electron. Since the indirect nuclear spin-spin interaction is a second-order property with respect to the Hamiltonians $\mathcal{H}_1^{(b)}$, $\mathcal{H}_2$ and $\mathcal{H}_3$, the various contributions to the anisotropy may be summarized as shown in table 1. Among these contributions, the Fermi-spin dipolar cross term is expected to be an important source for the anisotropy of the coupling constant between light nuclei, although this contribution is averaged out to zero when the

Table 1
Origin of the anisotropy of the electron-coupled nuclear spin-spin coupling constant

Interaction	Fermi $\mathcal{H}_3$	Spin dipolar $\mathcal{H}_2$	Orbital	
			$\mathcal{H}_1^{(a)}$	$\mathcal{H}_1^{(b)}$
Fermi $\mathcal{H}_3$	isotropic	anisotropic	0	0
Spin dipolar $\mathcal{H}_2$		isotropic and anisotropic	0	0
Orbital $\mathcal{H}_1^{(a)}$			isotropic and anisotropic	---
$\mathcal{H}_1^{(b)}$				isotropic and anisotropic

molecule is rotating randomly. Moreover, table 1 suggests that the anisotropy of the H—H coupling constant should be very small.

Now, it may be useful to develop these contributions in terms of molecular orbital theory, along similar lines to the treatment of Pople and Santry [3]. By resorting to rather crude approximations ((i) use of a single determinant wavefunction, (ii) LCAO MO approximation and (iii) retaining only one-center integrals), the Fermi-spin dipolar cross term is written as

$$\left(K_{AB}^{(2\cdot 3)}\right)_{\alpha\alpha} =$$

$$= -(64\pi\beta^2/15)[(s_A|\delta(r_A)|s_A)\langle r^{-3}\rangle_B \sum_i^{occ} \sum_j^{unocc} (^3\Delta E_{i\to j})^{-1} C_{is_A} C_{js_A}(2C_{ip_{\alpha B}} C_{jp_{\alpha B}} - \sum_\beta' C_{ip_{\beta B}} C_{jp_{\beta B}}) +$$

$$+ (s_B|\delta(r_B)|s_B)\langle r^{-3}\rangle_A \sum_i^{occ} \sum_j^{unocc} (^3\Delta E_{i\to j})^{-1} C_{is_B} C_{js_B}(2C_{ip_{\alpha A}} C_{jp_{\alpha A}} - \sum_\beta' C_{ip_{\beta A}} C_{jp_{\beta A}})], \tag{5}$$

where $p_{\alpha A}$ denote the $2p_\alpha$ atomic orbital (α is x, y or z) of the A atom. $\sum_\beta'$ means the sum over the directions x, y and z except α. The other notations are the same as Pople and Santry's [3]. Further, if the average excitation energy approximation and the assumption of the orthogonality of the basic atomic orbitals are made, one obtains

$$\left(K_{AB}^{(2\cdot 3)}\right)_{\alpha\alpha} = (16\pi\beta^2/15)[(s_A|\delta(r_A)|s_A)\langle r^{-3}\rangle_B(^3\Delta E)^{-1}(2P^2_{s_A p_{\alpha B}} - \sum_\beta' P^2_{s_A p_{\beta B}}) +$$

$$+ (s_B|\delta(r_B)|s_B)\langle r^{-3}\rangle_A(^3\Delta E)^{-1}(2P^2_{s_B p_{\alpha A}} - \sum_\beta' P^2_{s_B p_{\beta A}})], \tag{6}$$

where

$$P_{s_A p_{\alpha B}} = \sum_i^{occ} 2C_{is_A} C_{ip_{\alpha B}}. \tag{7}$$

The other contributions shown in table 1 can also be formulated as above, but they are not given here for want of space. From the above equations and table 1, the Fermi-spin dipolar cross term is expected to make the dominant contribution to the anisotropy of the X—H coupling constant, where X is a nucleus other than a proton.

3. APPLICATIONS

Now it may be necessary to estimate the order of magnitude of each contribution shown in table 1. Although the anisotropies of coupling constants of hydrocarbons are not yet known, these are of basic

Table 2
Results of K_{AB} (cm^{-3} × 10^{20}) for hydrocarbons (directly bonded) [a, b]

| Bond | Isotropic, $(K_{AB})_{iso}$ [c] | | | | Exptl. | Anisotropic. $(K_{\parallel} - K_{\perp})_{AB}$ | | | |
| | Calc. | | | | | Calc. | | | |
	Fermi	Spin dipolar	Orbital	Total		Fermi-spin dipolar	Spin dipolar	Orbital	Total
—C—H	44	0.0	0.0	44	41.8	11	0.0	0.0	11
=C—H	58	0.0	0.0	58	52.3	10	0.0	0.0	10
≡C—H	87	0.0	0.0	87	83.1	7.6	0.0	0.0	7.6
C—C	55	1.3	0.0	56	45.6	29	1.9	0.0	31
C=C	97	1.0	-12.4	86	89.0	34	-1.9	18.7	51
C≡C	219	5.0	0.0	224	225.9	38	-10.1	84.0	112

a) The molecular axis is parallel with the bond.
b) The values of ΔE are 15 eV for Fermi and Fermi-spin dipolar cross terms and 10 eV for the other contributions (see ref. [3]).
c) See ref. [3].

interest from a theoretical standpoint. Some approximate calculations of these are summarized in table 2. In these, we assumed i) homopolar bond, ii) localized sp^3, sp^2 and sp hybrids respectively for carbon in single, double and triple bonds, iii) zero overlap integrals and iv) average excitation energy approximation (eq. (6)). The values of the average excitation energies. ΔE are 15 eV for the excitations concerning s-AO (Fermi and Fermi-spin dipolar cross terms), and 10 eV for the other excitations concerning only 2p-AO's [3]. The one-center integral values are summarized in table 3.

Table 3
One-center integrals (au) [a]

Nucleus	$(s_A \mid \delta(r_A) \mid s_A)$	$\langle r^{-3} \rangle_A$
H	0.550 [b]	0.0
C	2.767	1.692
F	11.966	7.546

a) Ref. [5].
b) Slater orbital with $Z = 1.2$.

Table 2 shows that the Fermi-spin dipolar cross term is a very important source for the anisotropy of the coupling constant, although the orbital contribution becomes important for the coupling between triply-bonded carbons. Furthermore, the anisotropies of the C—H couplings are expected to be small compared to the isotropic couplings. while those of the (singly, doubly, and triply bonded) C—C couplings are comparable in magnitude to their isotropic couplings.

At present, methyl fluoride is the only compound for which the anisotropy of the indirect nuclear spin-spin coupling has been observed [1]. Since the anisotropy in the indirect nuclear spin-spin coupling was obtained by subtracting the direct coupling from the observed total anisotropy, some uncertainty of the experimental value still remains owing to the uncertainty of the geometry and of the anharmonicity in vibration of the methyl fluoride [1]. Thus, an order-of-magnitude calculation of the anisotropy of the indirect nuclear spin-spin coupling constant may be useful. The various contributions to the anisotropy are calculated by using the MO's obtained by the CNDO 2 method [4], without making the average-excitation-energy approximation (eq. (5)). The results are summarized in table 4 with the isotropic coupling constants obtained by the same approximate method.

Table 4 shows that the Fermi-spin dipolar cross term is an important source for the anisotropy. For the C—F coupling constant, both the isotropic and anisotropic couplings are small if compared with experiment. (This is mainly due to the large value of the calculated $^3\Delta E_{i-j}$.) The ratio of

Table 4

Results of K_{AB} (cm^{-3} × 10^{20}) for the methyl fluoride with CNDO/2 method

| A—B | Isotropic, $(K_{AB})_{iso}$ | | | | | Anisotropic, $(K_{\parallel} - K_{\perp})_{AB}$ [a] | | | | |
| | Calcd. | | | | Exptl. [b] | Calcd. | | | | Exptl. [b] |
	Fermi	Spin dipolar	Orbital	Total		Fermi-spin dipolar	Spin dipolar	Orbital	Total	
C—F	-20.6	3.5	-0.9	-18.0	-56.99	37.2	6.1	-1.1	42.2	246 ± 46
C—H	24.4	0.0	0.0	24.4	49.27	-3.6	0.0	0.0	-3.6	626 ± 43
H—F	0.79	0.0	0.0	0.79	4.10	-1.2	0.0	0.0	-1.2	-1.6 ± 4.8
H—H	0.37	0.0	0.0	0.37	-0.80	0.0	0.0	0.0	0.0	0.0

a) The direction of the molecular axis is parallel with the C—F bond.
b) Ref. [1].

$(K_{\parallel} - K_{\perp})_{CF}/(K_{CF})_{iso}$ is -2.3 for the calculated values and -4.3 ± 0.8 for the experimental ones. For the C—H coupling, the calculated anisotropy is too small to compare with experiment. Moreover, within the present approximations, it is expected to be minus in sign if the molecular axis is taken to be parallel to the C—F bond. Thus, at present, it seems necessary to examine more carefully both the approximations introduced in the present calculations (see the next section) and the experimental values. For the coupling constants between non-directly bonded nuclei, the calculated anisotropy is small as may be expected from eq. (6). The anisotropy of the H—H coupling constant is expected to be zero within the present approximations.

4. DISCUSSION

The large anisotropy of the C—H coupling constant of methyl fluoride reported by Krugh and Bernheim [1] cannot be interpreted from the present calculations. Of the previous approximations (section 2), the one-center integral approximation seems most drastic. Then we examined the effect of the two-center integrals of the type, $(2s(C)|\delta(r_H)|s_H)$, $(2p_\sigma(C)|\delta(r_H)|s_H)$ and $(2p_\pi(C)|\delta(r_H)|s_H)$. The correction due to these two-center integrals to the anisotropy of the C—H coupling is only 2% of the one-center contribution.

It should be emphasized that the figures given in table 4 are results which are very sensitive to the approximations introduced in the molecular orbital calculations and are therefore subject to considerable error. It seems necessary to use more reliable molecular orbitals, such as non-empirical molecular orbitals, and a more refined method. Further experimental study, especially for hydrocarbons, would be very valuable from the theoretical standpoint *.

* Experimental values of the anisotropy of ^{13}C—H indirect spin coupling constants in some methyl derivatives have recently been obtained by the present authors. The manuscript is now in preparation.

REFERENCES

[1] T. R. Krugh and R. A. Bernheim, J. Am. Chem. Soc. 91 (1969) 2385.
[2] N. F. Ramsey, Phys. Rev. 91 (1953) 303.
[3] J. A. Pople and D. P. Santry, Mol. Phys. 8 (1964) 1.
[4] J. A. Pople and G. A. Segal, J. Chem. Phys. 44 (1966) 3289.
[5] J. A. Morton, Chem. Rev. 64 (1964) 453.

ANISOTROPY OF THE INDIRECT NUCLEAR SPIN-SPIN COUPLING CONSTANT.
II. TREATMENT BY THE FINITE PERTURBATION METHOD *

The finite perturbation method is applied to the calculation of the anisotropy of the indirect nuclear spin-spin coupling constants. For CH_3F, all the elements of the calculated coupling tensors become larger than those reported in Paper I of this series. However, for the C-H coupling anisotropy, the calculated value is still too small to compare with the experimentally estimated value as large as 1890 Hz. It seems that the effects other than the electronic one is important.

The finite perturbation method (FPM), theoretically equivalent to the coupled Hartree-Fock perturbation method, has only been used for the calculation of the electrical polarizabilities [2,3] and shielding factors [4] of atoms and molecules. However, more recently, Pople and his co-workers applied this method to the calculation of the isotropic nuclear spin-spin coupling constant, stressing many important advantages of this method [5]. We have investigated the possibility of applying it to the calculation of the other properties of atoms and molecules. In this communication, the FPM is applied to the calculation of the anisotropy in the indirect nuclear spin-spin coupling constant which has attracted attention because of the experimental studies of high resolution nuclear magnetic resonance (NMR) spectra in nematic solvents [6].

The theory of the indirect nuclear spin-spin coupling constant, originally formulated by Ramsey [7] is based on the three types of interaction:

i) an electron orbital-nuclear dipole interaction

$$\mathcal{H}_1^{(a)} = (e\hbar\beta/c) \sum_{A,B,k} \gamma_A \gamma_B r_{kA}^{-3} r_{kB}^{-3} [(I_A \cdot I_B)(r_{kA} \cdot r_{kB}) - (I_A \cdot r_{kB})(I_B \cdot r_{kA})],$$

$$\mathcal{H}_1^{(b)} = (2\beta\hbar/i) \sum_{A,k} \gamma_A r_{kA}^{-3} I_A \cdot (r_{kA} \times \nabla_k).$$

ii) a magnetic dipole interaction

$$\mathcal{H}_2 = 2\beta\hbar \sum_{A,k} \gamma_A [3(S_k \cdot r_{kA})(I_A \cdot r_{kA}) r_{kA}^{-5} - S_k \cdot I_A r_{kA}^{-3}].$$

iii) a Fermi contact interaction

$$\mathcal{H}_3 = (16\pi\beta\hbar/3) \sum_{A,k} \gamma_A \delta(r_{kA}) S_k \cdot I_A.$$

These one electron operators may be grouped into two classes: a spin independent operator, $\mathcal{H}_1$, and spin linear operators, $\mathcal{H}_2$ and $\mathcal{H}_3$. In the FPM, when the perturbation belongs to the former type, we use the restricted Hartree-Fock (RHF) wavefunction since $\Psi^{rf}(SCF)$ is expressed to first order as a sum of the unperturbed wavefunction Ψ_0^{rf} and the singly excited singlet wavefunctions [eq. (1)]. This point may easily be understood from the Brillouin's theorem.

___

$$\Psi^{\text{rf}}(\text{SCF}) = \Psi_0^{\text{rf}} + \sum_{i,k} C_{ik} |S_{ik}\rangle, \qquad |S_{ik}\rangle \quad |\dots \varphi_i \varphi_k \frac{1}{\sqrt{2}}(\alpha\beta - \beta\alpha)\dots|. \tag{1}$$

On the other hand, when the perturbation belongs to the latter type, the singlet wavefunction for the ground state gets mixed with the singly excited triplet wavefunctions. As shown by our previous study [8], the same can be done more easily by using the unrestricted Hartree-Fock (UHF) method, since

$$\Psi^{\text{uhf}} - \Psi_0^{\text{rf}} + \sum_i C_i |T_i\rangle + \dots, \qquad |T_i\rangle = |\dots \lambda_i \nu_i \frac{1}{\sqrt{2}}(\alpha\beta + \beta\alpha)\dots|, \tag{2}$$

where $|T_i\rangle$ is the triplet function. Thus the UHF method is applicable to the perturbation of the latter type.

The origins for the anisotropy of the indirect nuclear spin-spin coupling constants have already been studied in the previous report of this series. (See table 1 of paper L) Among those sources, we formulate here the Fermi-spin dipolar interaction term rather fully along the line of the FPM. Taking the fixed magnetic dipoles μ_A and μ_B oriented along the z direction, the total hamiltonian is given by

$$\mathcal{H} = \mathcal{H}_0 + \mu_A \mathcal{H}_A + \mu_B \mathcal{H}_B. \tag{3}$$

where

$$\mathcal{H}_A = 2\beta \sum_k [3(S_k r_{kA})Z_{kA} r_{kA}^{-5} - S_{kz} r_{kA}^{-3}], \tag{4}$$

$$\mathcal{H}_B \quad (16\pi\beta/3) \sum_k \delta(r_{kB})S_{kz}. \tag{5}$$

In the FPM, the zz-component of the reduced coupling constant tensor K_{AB} (the coupling constant per unit magnetic moments) can be written as

$$(K_{AB})_{zz} = \left[\frac{\partial}{\partial \mu_A} \langle \Psi(\mu_A, 0) | \mathcal{H}_B | \Psi(\mu_A, 0) \rangle \right]_{\mu_A=0}, \tag{6}$$

where $\Psi(\mu_A, 0)$ is the wavefunction when only the spin dipolar perturbation is present at nucleus A and can be calculated by means of the UHF method. The Fock operator for $\Psi(\mu_A, 0)$ is

$$F(1) = h^{\text{core}}(1) + \mu_A \mathcal{H}_A(1) + \sum_{j=1}^N \langle x_j(2) | r_{12}^{-1}(1 - P_{12}) | x_j(2) \rangle. \tag{7}$$

where x_j is the UHF spin orbital. On practical calculation, we adopted the one-center integral approximation for the atomic orbital (AO) matrix elements of $\mathcal{H}_A$ and $\mathcal{H}_B$. Then we obtain from eq. (6) the following;

$$(K_{AB})_{zz} = (16\pi/15)\beta^2 \langle r^{-3} \rangle_A s_B^2(0) \left[\frac{\partial}{\partial h_A} \rho_{s_B s_B}(h_A) \right]_{h_A=0}. \qquad h_A = (2/5)\beta \mu_A \langle r^{-3} \rangle_A. \tag{8}$$

The spin density at the s_B AO, $\rho_{s_B s_B}(h_A)$ is calculated by adding the small quantity h_A to the diagonal $2p_{x_A}$, $2p_{y_A}$ and $2p_{z_A}$ elements of the F^α matrix in the ratio of $-1 : -1 : 2$, respectively and at the same time, by subtracting the same quantities from the corresponding elements of F^β. The physical meaning of eq. (8) is that adding the perturbation h_A at nucleus A, the orbitals of atom A are spin-polarized and this effect propagates to nucleus B, resulting in the induced spin density at nucleus B, and the coupling is calculated by taking the derivative of the spin density $\rho_{s_B s_B}(h_A)$ with respect to the added perturbation h_A. The xx-, yy- components of the coupling tensor K_{AB} are derived similarly by rotating the x, y, z suffixes. Note that the same interaction can be obtained by interchanging the terms $\mu_A \mathcal{H}_A$ and $\mu_B \mathcal{H}_B$ in the above treatment. In this case, the result becomes

$$(K_{AB})_{zz} = (16/15)\pi\beta^2 \langle r^{-3} \rangle_A s_B^2(0) \left[\frac{\partial}{\partial h_B} \left(2\rho_{z_A z_A}(h_B) - \rho_{x_A x_A}(h_B) - \rho_{y_A y_A}(h_B) \right) \right]_{h_B=0},$$

$$h_B \quad (8/3)\pi\beta\mu_B s_B^2(0), \tag{9}$$

where h_B is added to the diagonal s_B element of the F^α matrix and is subtracted at the same time from the corresponding β-element.

The other sources of the coupling constant tensor can easily be formulated as above by means of the FPM, and we give here only the resultant formulae. The spin dipolar contribution to the $\xi\xi$ element of K_{AB} is given by,

$$(K_{AB})_{\xi\xi} = (9/25)\beta^2 \langle r^{-3}\rangle_A \langle r^{-3}\rangle_B \left[\frac{\partial}{\partial h_{A1}} \rho_{\eta_B \xi_B}(h_{A1})\right]_{h_{A1}=0}$$

$$+ (9/25)\beta^2 \langle r^{-3}\rangle_A \langle r^{-3}\rangle_B \left[\frac{\partial}{\partial h_{A2}} \rho_{\zeta_B \xi_B}(h_{A2})\right]_{h_{A2}=0}$$

$$+ (4/25)\beta^2 \langle r^{-3}\rangle_A \langle r^{-3}\rangle_B \left[\frac{\partial}{\partial h_{A3}} \left(2\rho_{\xi_B \xi_B}(h_{A3}) - \rho_{\eta_B \eta_B}(h_{A3}) - \rho_{\zeta_B \zeta_B}(h_{A3})\right)\right]_{h_{A3}=0}, \qquad (10)$$

$$h_{A1} = h_{A2} = (3/5)\beta\mu_A \langle r^{-3}\rangle_A, \qquad h_{A3} = (2/5)\beta\mu_A \langle r^{-3}\rangle_A,$$

where the suffixes (ξ, η and ζ) appearing in the right-hand side of eq. (10) correspond to ($2p_x$, $2p_y$ and $2p_z$). Practically, the above three terms in eq. (10) are calculated separately. That is, $\rho_{\eta_B \xi_B}(h_{A1})$ is calculated by adding h_{A1} ($-h_{A1}$) to the $F^\alpha_{\eta_A \xi_A}$ and $F^\alpha_{\eta_A \eta_A}$ ($F^\beta_{\eta_A \xi_A}$ and $F^\beta_{\eta_A \eta_A}$) elements, $\rho_{\zeta_B \xi_B}(h_{A2})$ by adding h_{A2} ($-h_{A2}$) to the $F^\alpha_{\zeta_A \xi_A}$ and $F^\alpha_{\zeta_A \zeta_A}$ ($F^\beta_{\zeta_A \xi_A}$ and $F^\beta_{\zeta_A \zeta_A}$) elements, and the third term, $2\rho_{\xi_B \xi_B}(h_{A3}) - \rho_{\eta_B \eta_B}(h_{A3}) - \rho_{\zeta_B \zeta_B}(h_{A3})$ is calculated in the same way as in the Fermi-spin dipolar cross term [eq. (8)]. For the orbital term, the RHF method is employed and h_A becomes imaginary [9].

$$(K_{AB})_{\xi\xi} = 16\beta^2 \langle r^{-3}\rangle_A \langle r^{-3}\rangle_B \left[\frac{\partial}{\partial h_A} \text{Im}\left(\sum_i C^*_{i\eta_B} C_{i\zeta_B}(h_A)\right)\right]_{h_A=0}, \qquad h_A = 2\beta\mu_A \langle r^{-3}\rangle_A i,$$

where h_A is added to $F_{\zeta_A \eta_A}$ and $-h_A$ to $F_{\eta_A \zeta_A}$.

In the present communication, the above treatment is applied to the calculation of the coupling constants of CH_3F and the results are summarized in table 1. In these we used the INDO method of Pople et al. [10], and the values of integrals introduced by perturbation are the same as those given in table 3 of paper I. The values in parentheses are those calculated by the method reported in paper I. As can be seen from this table, the Fermi and the Fermi-spin dipolar cross terms make the dominant contributions to the isotropic and anisotropic couplings respectively. Note however that, for the C-F coupling, the other terms make 10-15% contribution to the total isotropic and anisotropic coupling constants and are not negligible. As shown by Pople, McIver and Ostlund [5], the agreement of the calculated isotropic C-H coupling constant with the experimental value becomes fairly satisfactory in this FPM treatment.

Table 1
Results of J_{AB} [a] (Hz) for the directly bonded nuclei in CH_3F with INDO MO's

Isotropic $(J_{AB})_{iso}$

A-B	Fermi	Spin dipolar	Orbital	Total	Exptl. [b]
C-H	147(75)	0(0)	0(0)	145(75)	148.8
C-F	- 97(-99)	15(9.4)	-15(-6.3)	97(- 96)	-161.9

Anisotropic $(J_\parallel - J_\perp)_{AB}$ [c]

A-B	Fermi Spin dipolar	Spin dipolar	Orbital	Total	Exptl. [b]
C-H	- 19(-11)	0(0)	0(0)	19(- 11)	1500 ± 130
C-F	208(94)	26(16.2)	27(4.5)	261(115)	700 ± 130

a) $J_{AB} = (h/2\pi)\gamma_A \gamma_B K_{AB}$.
b) Ref. [6].
c) The axis is chosen to be parallel with the molecular symmetry axis.

113

However, for the anisotropy of the C-H couplings, the disagreement between theory and experiment is still extraordinary even in the present FPM treatment as in the previous one reported in paper I. A similar discrepancy was also reported by Barfield by means of the valence-bond method [11]. It seems that these discrepancies between theory and experiment are far beyond the accuracy of the calculated values. Since the anisotropy of the indirect coupling was obtained experimentally by subtracting the direct coupling anisotropy, calculated with the gas phase microwave geometry, from the observed total anisotropy, some uncertainty may still remain owing to the neglect of the vibrational effects and of the change in molecular geometry from the gas state to the solute state in nematic solvent [12]. Thus, at present we believe that this discrepancy may suggest that the experimental values of the coupling anisotropy still contain some important effects other than the electronic one. In fact, the substituent effect to the C-H coupling anisotropies of the methyl derivatives, obtained from the NMR spectra by using gas phase microwave geometry [12], was extraordinarily large to interpret only from the electronic effect, and then a possibility of change of molecular geometry in nematic solvent from that in gas phase was suggested previously [12]. For the C-F coupling constant considerably large anisotropy can be expected from the present calculation although it is still small to compare with experiment.

Now, compare the present results with those calculated by the method reported in paper I: the signs of coupling constants obtained by these two methods are the same, but the absolute values obtained by the FPM are about 1-5 times as large as the ones obtained by the method reported in paper I. Since the FPM is equivalent to the coupled Hartree-Fock perturbation method in the small perturbation limit, and since the previous method is almost equivalent to the alternative uncoupled Hartree-Fock perturbation method of Langhoff et al. [13], this refinement in the FPM may be attributed to the inclusion of the self-consistency requirement for the calculation of the coupling constant. In fact, a similar trend was also seen in the model calculations [13] of the properties which lay stress on the electron distribution near the nucleus, as the present coupling constant does.

More details of the present method and fuller examinations of the coupling anisotropy will be published in the near future.

REFERENCES

[1] H. Nakatsuji, H. Kato, I. Morishima and T. Yonezawa, Chem. Phys. Letters 4 (1970) 607.
[2] H. D. Cohen and C. C. J. Roothaan, J. Chem. Phys. 43 (1965) S 34;
    H. D. Cohen, J. Chem. Phys. 43 (1965) 3558; 45 (1966) 10.
[3] A. Schweig, Chem. Phys. Letters 1 (1967) 163, 195.
[4] R. E. Watson and A. J. Freeman, Phys. Rev. 131 (1963) 250.
[5] J. A. Pople, J. W. McIver Jr. and N. S. Ostlund, J. Chem. Phys. 49 (1968) 2960, 2965;
    G. E. Maciel, J. W. McIver Jr., N. S. Ostlund and J. A. Pople, J. Am. Chem. Soc. 92 (1970) 1, 11.
[6] T. R. Krugh and R. A. Bernheim, J. Am. Chem. Soc. 91 (1969) 2385.
[7] N. F. Ramsay, Phys. Rev. 91 (1953) 303.
[8] H. Nakatsuji, H. Kato and T. Yonezawa, J. Chem. Phys. 51 (1969) 3175.
[9] A. C. Blizzard and D. P. Santry, Chem. Commun. (1970) 87.
[10] J. A. Pople, D. L. Beveridge and P. A. Dobosh, J. Chem. Phys. 47 (1967) 2026.
[11] M. Barfield, Chem. Phys. Letters 4 (1970) 518.
[12] I. Morishima, A. Mizuno, H. Nakatsuji and T. Yonezawa, Chem. Phys. Letters, to be published.
[13] P. W. Langhoff, M. Karplus and R. P. Hurst, J. Chem. Phys. 44 (1966) 505.

PART III, CHAPTER 3

FULLER EXAMINATIONS OF

THE ANISOTROPY OF THE INDIRECT NUCLEAR

SPIN-SPIN COUPLING CONSTANT

—— PROBLEMS IN THE STRUCTURE DETERMINATION OF

THE MOLECULE DISSOLVED IN A NEMATIC SOLVENT ——

Anisotropy of the Indirect Nuclear Spin-Spin Coupling Constant
III. Problems in the Structure Determination of the Molecule
Dissolved in the Nematic Solvent.

Introduction

Since the experiment of Saupe and Englart,[1,2] active
investigations of the molecules dissolved in the liquid-crystal
solvents have been carried out by the nuclear magnetic resonance
(NMR) technique.[3-5] In these, the chemically fundamental data
such as the molecular motion and the molecular geometry in
liquid phase are now more and more accumulated, in addition to
the more detailed knowledges of the NMR parameters than those
available by the usual NMR measurements in isotropic liquid
phase. However, some troubles exist in the determination of
molecular geometry. Namely, in order to calculate molecular
geometry (more strictly, ratios of the geometrical parameters)
from spectral splittings one needs the value of the anisotropy
of the indirect nuclear spin-spin coupling constant (J),[3,6]
and the most frequent assumption has been to neglect the
anisotropy of the indirect coupling constant. However, the
molecular geometries obtained under this assumption have sometimes
differed slightly from those obtained by the other measurements of

115

gas phase molecules (e.g. electron diffraction method, microwave method etc.).[6,7] On the other hand, if one assumes that the geometry obtained by the other measurements in gas phase can be used without any corrections, one may calculate the anisotropy of the indirect coupling from the spectral splittings. This treatment, however, has sometimes given extremely large anisotropy.[8]

To settle these situations, one must clarify the following problems. (1) Is the assumption that the anisotropy of the indirect coupling is nearly zero valid? (2) If this assumption is valid, why the geometry obtained by the NMR in liquid crystal solvent differs from those given by the other measurements in gas phase such as the electron diffraction or microwave techniques?

The main purpose of this series of investigation[9,10] is to settle the first problem above from the theoretical standpoint. In Paper I of this series,[9] possible origin of the anisotropy of the indirect coupling constant has been examined with the molecular orbital (MO) method. Among these, Fermi-spin dipolar cross term is shown to be an important source of the coupling anisotropy between singly-bonded nuclei. For doubly and triply bonded nuclei, orbital term is also found to make important contribution. However, for the directly bonded ^{13}C-H coupling in CH_3F, the calculated anisotropy was too small to compare with the experimentally estimated value as large as 1890 Hz, obtained by assuming the microwave geometry.[8a] Similar results were also obtained in Paper II of this series[10] by the more refined treatment, by Barfield[11] with the valence-bond method and more recently, by Buckingham and Love[12] by the similar molecular orbital treatment.

116

In the present paper, we examine further the above problems (1) and (2). In the next section, the theoretical background of the coupling anisotropy is described briefly and then it is applied to the various molecules by using the INDO MO's of Pople et al..[13] Especially for the directly bonded ^{13}C-H coupling anisotropy, the substituent effect in the ^{13}CH$_3$X series[14] will be fully discussed. From this a conclusion about the ^{13}C-H coupling anisotropy will be deduced. Another important aspect invoked experimentally is the coupling anisotropy between F-F nuclei.[8b-8d] Then we turn to this problem at the end of this section. In the last section, we examine the above problem (2). The implication of this problem is twofold; the vibrational effect and the effect due to the structural change from gas phase to the solute state in a nematic solvent. The relative importance of these two possible effects is examined.

Theoretical Background

The important part of the theory of the anisotropy of the indirect nuclear spin-spin coupling has already given in Paper I of this series and more recently by Buckingham and Love[12] with the similar molecular orbital treatment. Then we only summarize here the important aspects relevant to the following discussions.

As shown in Paper I, the anisotropy of the indirect coupling originates from the three mechanisms: Fermi-spin dipolar cross term, spin dipolar term and orbital term. In these, the Fermi-spin dipolar cross term is averaged out to zero when a molecule is ran-

domly rotating.[15] These contributions can be developed in terms
of the molecular orbital theory, along similar lines to the treat-
ment of Pople and Santry[16]. For notational convenience, we intro-
duce a reduced coupling constant $\mathbb{K}_{AB}$ defined by

$$\mathbb{K}_{AB} = (2\pi/\hbar \gamma_A \gamma_B) \, J_{AB} \qquad\qquad (1)$$

First we set the following three approximations (Level A approxima-
tion). (1) We use the sum-over-state perturbation method, making
the single Slater determinant built up from the SCF MO's as zero-th
order wavefunction. An improvement over this sum-over-state
perturbation method may be achieved by using the finite perturbation[17]
(coupled Hartree-Fock[18]) method, which was the content of Paper II
of this series. (2) LCAO-MO approximation. Actually the INDO
SCF-MO's expanded by all the valence atomic orbitals (AO's) will
be used. (3) One-center integral approximation. This approxi-
mation may be crude especially for the coupling tensor between
directly bonded nuclei. However, since all the Hamiltonians
considered here (Eqs. (1)-(4) of Paper I) lay stress on the electronic
structure in the vicinity of nuclei, and since we use the INDO MO's
based on the zero-differential overlap approximation (theoretically
based on the orthogonalized AO's[19]), this approximation may be
approved.[9] Note that under this approximation, the anisotropy
of the coupling constant between two protons becomes zero, which
may be justified from the study of Barfield.[11]

The elements of the coupling tensor obtained under the
Level A approximation are given, for example, for the Fermi-spin
dipolar cross term as;

$$(\mathbb{K}_{AB}{}^{(2,3)})_{\alpha\alpha} = -(64\pi\beta^2/15)S_A(0)\langle r^{-3}\rangle_B \sum_i^{occ}\sum_j^{vac}({}^3\Delta E_{i\to j})^{-1}C_{iS_A}C_{jS_A}$$

$$\times(2C_{iP_{\alpha B}}C_{jP_{\alpha B}} - \sum_{\delta(\neq\alpha)}' C_{iP_{\delta B}}C_{jP_{\delta B}}) \quad + [\text{interchange term of A and B}]$$

$$(2\text{-}a)$$

$$(\mathbb{K}_{AB}{}^{(2,3)})_{\substack{\alpha\beta \\ (\alpha\neq\beta)}} = -(32\pi\beta^2/5)S_A(0)\langle r^{-3}\rangle_B \sum_i^{occ}\sum_j^{vac}({}^3\Delta E_{i\to j})^{-1}C_{iS_A}C_{jS_A}$$

$$\times(C_{iP_{\alpha B}}C_{jP_{\beta B}} + C_{iP_{\beta B}}C_{jP_{\alpha B}}) \quad\quad\quad +[\text{interchange term of A and B}]$$

$$(2\text{-}b)$$

The other contributions are summarized in Appendix. In Eq. (2),
$S_A(0) = (S_A|\delta(\mathbf{r}_A)|S_A)$, S_A and $P_{\alpha A}$ are the s-type AO and $2p_\alpha$ AO
(α is x, y or z) centered on the atom A. $\sum_{\delta(\neq\alpha)}'$ means the sum over
the directions x, y and z except α. The other notations are
the same as Pople and Santry's.[16]

In the following applications we use the equations obtained
under the Level A approximation. However, it is sometimes
convenient to set further approximations, which enables us to
image simplified "chemical picture" about the mechanisms of the
coupling interactions. These further approximations added to
the Level A approximation are as follows.
(4) Average excitation energy (ΔE) approximation.[20,21]
(5) Zero-differential overlap (ZDO) approximation.
Hereafter we call this level of approximation as Level B
approximation, where the elements of the coupling tensor for the
Fermi-spin dipolar cross term becomes

$$(\mathbb{K}_{AB}{}^{(2,3)})_{\alpha\alpha} = (16\pi\beta^2/15)S_A(0)\langle r^{-3}\rangle_B ({}^3\Delta E)^{-1}(2P_{S_A P_{\alpha B}}^2 - \sum_{\delta(\neq\alpha)}' P_{S_A P_{\delta B}}^2)$$

$$+ [\text{interchange term of A and B}]$$

$$(3\text{-}a)$$

$$(\text{IK}_{AB}{}^{(2,3)})_{\alpha\beta} = (16\pi\beta^2/5)\, s_A{}^2(0)\langle r^{-3}\rangle_B\, (3\Delta E)^{-1}\, P_{s_A P_{\alpha B}}\, P_{s_A P_{\beta B}}$$

$(\alpha \neq \beta)$

+ [interchange term of A and B]

(3-b)

The other contributions are summarized in Appendix. In Eq. (3),

$P_{s_A P_{\alpha B}}$ denotes the bond order between s_A and $2P_{\alpha B}$ AO's.

$$P_{s_A P_{\alpha B}} = \sum_i 2 C_{i s_A}\, C_{i P_{\alpha B}} \tag{4}$$

When the localized AO's illustrated in Fig. 1 are introduced, the chemical picture of the coupling mechanisms becomes clear. Namely, each contribution to the $\sigma\sigma$-element of the coupling tensor, $(J_{AB})_{\sigma\sigma}$ becomes proportional to the following (sums of) squares and/or products of the AO bond orders.

[Fermi term] $\propto P_{ss'}^2$

[Fermi-spin dipolar cross term] $\propto P_{s\sigma'}^2$ + [interchange term]

[Spin dipolar term] $\propto 8 P_{\sigma\sigma'}^2 + 2(P_{\pi\pi'}^2 + P_{\bar\pi\bar\pi'}^2) + 9 P_{\sigma\sigma'}(P_{\pi\pi'} + P_{\bar\pi\bar\pi'})$

[Orbital term] $\propto P_{\pi\pi'}\, P_{\bar\pi\bar\pi'}$
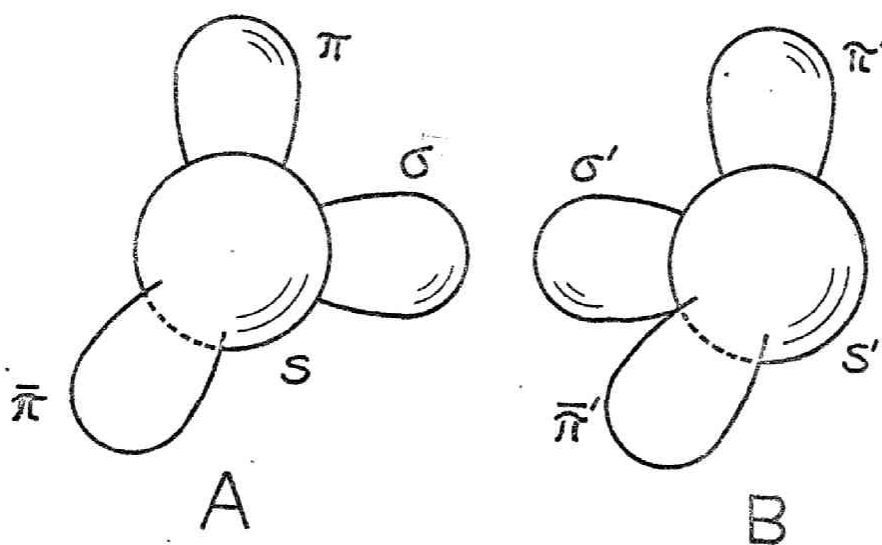
Fig. 1. Localized AO model.

These equations may be considered as showing the "paths" and their "width" along which two nuclear moments interact. Note, however, that although this chemical picture is very intuitive, it sometimes leads to the erronious results, especially for the coupling constants between nuclei in polar bond.[15]

Thus, in the following applications, we use the Level A approximation. The basic MO's are calculated by the INDO method of Pople and his co-workers. In Table 1 , the values of the one-center integrals, $s_A(0)$ and $\langle r^{-3}\rangle_A$ used in the calculations are summarized.

Table 1 . One-center integrals (a.u.)[a]

Nucleus	$s_A(0)$	$\langle r^{-3}\rangle_A$
H	0.550[b]	0.0
C	2.767	1.692
N	4.770	3.101
F	11.966	7.546

[a] J. R. Morton, Chem. Revs. 64, 453 (1964).
[b] Slater orbital with Z=1.2.

Results and Discussions

X-H Couplings

In this section, we discuss the results obtained for the X-H couplings, where X is the nucleus other than the proton. As seen from Eqs. (2), (A-1)-(A-3), the sources of the isotropic

and anisotropic couplings between X and H nuclei are only Fermi and Fermi-spin dipolar cross terms respectively, under the one-center integral approximation.

To begin with, it may be useful to see the general trends in the coupling tensors of the C-H bonds. In Table 2 the

Table 2 Directly bonded ^{13}C-H coupling tensors (Hz) calculated for methane, ethylene and acetylene[a]

Molecule	Fermi[b]	Fermi-spin dipolar	Total	$J_{\parallel} - J_{\perp}$
Methane	64.6	$\begin{bmatrix} 22.0 & 0. & 0 \\ 0 & -11.0 & 0 \\ 0 & 0 & -11.0 \end{bmatrix}$	$\begin{bmatrix} 86.5 & 0 & 0 \\ 0 & 53.6 & 0 \\ 0 & 0 & 53.6 \end{bmatrix}$	33.0
Ethylene	80.1	$\begin{bmatrix} 16.4 & -0.8 & 0 \\ -0.8 & -8.1 & 0 \\ 0 & 0 & -8.1 \end{bmatrix}$	$\begin{bmatrix} 96.6 & -0.8 & 0 \\ -0.8 & 72.0 & 0 \\ 0 & 0 & 72.0 \end{bmatrix}$	24.5
Acetylene	141.9	$\begin{bmatrix} 12.0 & 0 & 0 \\ 0 & -6.0 & 0 \\ 0 & 0 & -6.0 \end{bmatrix}$	$\begin{bmatrix} 153.9 & 0 & 0 \\ 0 & 135.9 & 0 \\ 0 & 0 & 135.9 \end{bmatrix}$	18.0

[a] The x-axis of tensor is parallel with the C-H bond. In ethylene, the molecular plane is on the xy-plane.

[b] The experimental values of the isotropic coupling constants are 125.0, 156.2 and 249.0 Hz respectively for methane, ethylene and acetylene.

122

coupling tensors of the directly bonded ^{13}C-H nuclei in methane, ethylene and acetylene are summarized. The X axes of these tensors are all parallel with the C-H bonds. From Table 2 , we find the followings: 1) The sequence of change from methane to acethylene reflects those expected from changes in hybridization for both Fermi and Fermi-spin dipolar cross terms. This agrees with the previous results in Paper I calculated with the Level B approximation by using the localized AO model. 2) For the isotropic couplings, the calculated values are almost the halves of the experimental values. This disagreement may be due to the too large value of the excitation energy calculated by the INDO method and to the neglect of the self-consistency requirement[22] in the present perturbation treatment. An improvement of the latter defect can be achieved by using the finite perturbation method, as shown by Pople, McIver and Ostlund[17] and as discussed in Paper II of this series.

In Table 3 , the calculated isotropic and anisotropic coupling constants between X-H nuclei in CH$_3$Y (Y = H, CH$_3$, F, I, CN, NC and OH) are summarized. As seen from this table, the calculated coupling anisotropies between non-bonded nuclei are very small in magnitude, comparing with those between directly bonded nuclei. This is not always true as will be seen later for the F-F couplings. Note that in the present approximation the coupling anisotropy between two protons becomes zero.

As seen in Paper I and II of this series, the present result of the ^{13}C-H coupling anisotropy of CH$_3$F is also too small to compare with the experimentally estimated value,[8a] obtained by using its gas phase microwave geometry in the

Table 3 . X-H couplings in the methyl derivatives.

Molecule	Nuclei[a]	$(J_{XH})_{iso}$		$(J_{XH})_{aniso.}$		S_{zz}
		Exptl.	Calcd	Exptl.	Calcd	
C_2H_6	^{13}C-H	124.9[b]	57.8	---	-8.7	
	(^{13}C-H)		0.3	---	0.3	
CH_4	^{13}C-H	125.0[b]	64.6	---	-9.9	---
CH_3CN	^{13}C-H	136.0[c]	58.9	-50[d]	-8.7	0.1009[d]
	(^{15}N-H)	-1.75[c]	-0.2	---	2.1	
	(^{13}C-H)	-10.0[c]	1.4	---	1.1	
CH_3OH	^{13}C-H	141.0[b]	68.9	---	-10.7[e]	0.0050[d]
CH_3NC	^{13}C-H	145.2[f]	64.7	-108[g]	-9.8	0.0997[g]
	(^{13}C-H)		-0.1		-1.8	
	(^{15}N-H)	3.8[f]	-0.6	$\left(\begin{array}{c}-401\\+142\end{array}\right)$[h]	-0.5	
CH_3F	^{13}C-H	148.8[i]	75.2	1890[i] +130	-11.0	0.0166[i]
	(^{19}F-H)	46.3[i]	7.3	-18[i] +54	-9.0	
CH_3I	^{13}C-H	151.4[j]	---	555[k]	---	0.0323[k]

[a] The nuclei in parentheses are non-bonding.

[b] N. Muller and D. E. Pritchard, J. Chem. Phys. 31, 768, 1471 (1959).

[c] W. McFarlane, Mol. Phys. 10, 603 (1966): G. Englart and A. Saupe, Mol. Cryst. 8, 233 (1969).

[d] A. Saupe, G. Englart and A. Povh, Adv. Chem. Ser. 63, 51 (1967).

[e] Free rotation about the C-O bond is assumed.

[f] W. McFarlane, J. Chem. Soc. 1967, 1660.

[g] H. Spiesecke, Z. Naturforsch. 23a, 467 (1968).

Table 3, continued

h) C. S. Yannoni, J. Chem. Phys. 52, 2005 (1970).

i) T. R. Krugh and R. A. Bernheim, J. Am. Chem. Soc. 91, 2385 (1969).

j) S. L. Miller, L. C. Aamodt, G. Dousmanis, C. H. Townes, and J. Kraitchman, J. Chem. Phys. 20, 1112 (1952).

k) I. Morishima, A. Mizuno, H. Nakatsuji, and T. Yonezawa, Chem. Phys. Letters, to be published.

l) $J_{aniso} = J_{\parallel} - J_{\perp}$, where $\parallel$ means the molecular symmetry axis.

analysis of the NMR spectrum. Similar results to ours were also obtained by Barfield[11] and by Buckingham and Love[12]. These discrepacies between theories and experiments seem to be far beyond the accuracy of these calculated values. Moreover, fuller examinations of this discrepancy are now possible, since the substituent effects to the directly bonded $^{13}C-H$ coupling anisotropies in the methyl derivatives are obtained by analysing their NMR spectra with exactly the same way as in CH_3F.[14] They are also given in Table 3.

First, let's examine the substituent effect on the isotropic $^{13}C-H$ couplings, $(J_{CH})_{iso}$. From the experimental values of the isotropic coupling constants, we can estimate the order of magnitude of the change in the electron distribution near the C-H bond induced by the substituent change. It is 2-6%. The same order of change is also reproduced by the INDO MO's, although their absolute values are rather small and the details of the sequence are erroneous. On the other hand, the order of magnitude of the substituent effect on the coupling anisotropy, $(J_{CH})_{aniso}$ estimated from the experimental analyses is extraordinarily large and is far beyond the usual concept of the substituent effect on

the electronic structure. In fact, in order to *explain* this substituent effect, extraordinarily large change in the electronic structure near the C-H bond must be supposed to accompany ~~with~~ the substituent change. However, this contradicts clearly to the above order of change seen in the substituent effect on the isotropic couplings. Whereas, the calculated substituent effect on the coupling anisotropy is the same order as those on the experimental and calculated isotropic couplings.

From the above discussions, we reached to the conclusions that the experimentally estimated values of the ^{13}C-H coupling anisotropy given in Table 3 still contain some other more important effects than the electronic one and therefore that the experimentally assumed ^{13}C-H coupling anisotropy of CH_3F as large as 1890 Hz[8a] is erronious. Then, the next problem is "what are the more important effects?" This problem will be examined in the next section. Note lastly that the substituent effect to the experimentally assumed values of the coupling anisotropy is _{almost} parallel with that to the orientation parameters S_{zz} in the nematic solvent.

X-X' Couplings

In this paragraph we discuss the results obtained for the X-X' couplings, where all the terms can contribute to the coupling tensor. The calculated values of these contributions for the C-C coupling tensors of ethane, ethylene and acethylene are summarized in Table 4. The principal x-axis is parallel with the C-C bond. From this table, we find the followings: 1) For anisotropy, the Fermi-spin dipolar cross term contribute almost

126

Table 4. Calculated ^{13}C-^{13}C coupling tensors (Hz) of ethane, ethylene and acetylene[a].

Molecule	Fermi	Fermi-spin dipolar			Spin dipolar			Orbital			Total			$(J_{CC})_{iso}$
		xx	yy	zz	xx	yy	zz	xx	yy	zz	xx	yy	zz	Exptl.[b]
Ethane	6.6	8.4	-4.2	-4.2	0.9	0.2	0.2	0.2	-1.3	-1.3	16.1	1.3	1.3	34.6
		0.0[c]	(12.7)[d]		0.4	(0.7)		-0.8	(1.5)		6.2	(14.8)		
Ethylene	20.8	9.6	-4.8	-4.8	0.0	1.3	3.0	1.6	-16.3	-1.5	32.0	1.0	17.5	67.6
		0.0	(14.4)		1.4	(-2.2)		-5.4	(8.9)		16.8	(22.7)		
Acetylene	56.1	9.5	-4.7	-4.7	0.2	6.4	6.4	34.9	-8.3	-8.3	100.6	49.5	49.5	171.5
		0.0	(14.2)		4.2	(-6.2)		6.1	(43.2)		66.5	(51.1)		

a) The tensors are diagonal, where one of the principal axes (x-axis) is chosen parallel with the C-C bond. In ethylene, the molecular plane is on the xy-plane.

b) R. M. Lynden-Bell and N. Sheppard, Proc. Roy. Soc. A269, 385 (1962).

c) The contribution to the isotropic coupling constant.

d) The contribution to the anisotropy, $J_{xx} - (J_{yy} + J_{zz})/2$.

(faded)ly for these three molecules, while the orbital contribution
becomes important rapidly from ethane to acetylene. Thus, Fermi-
spin dipolar cross term is dominant in ethane, both Fermi-spin
dipolar cross term and orbital term are equally important in
ethylene, and orbital term is dominant in acetylene. This
point may easily be understood from the chemical picture
obtained by the Level B approximation. 2) Different from the
cases of the $C-H$ bonds, the magnitudes of the anisotropic
couplings are comparable to those of the isotropic couplings in
these $C-C$ bond cases. 3) Although the calculated isotropic
couplings are small comparing with the experimental values
(this is mainly due to the too large values of $\Delta E_{i \to j}$), note
that even for the isotropic couplings, orbital contributions
are not negligible for ethylene and acetylene.

In Table 5, the calculated isotropic and anisotropic
couplings between X-X' nuclei in the C_{3v}-symmetry molecules are
summarized. For the couplings between directly bonded nuclei,
the above mentioned features seen in the C-C couplings apply
without exceptions. However, the calculated value of the
$^{13}C-F$ coupling anisotropy is still small comparing with the
experimental value,[8a] although the value of 207 Hz is obtained
in Paper II[10] by the finite perturbation method. For the
coupling constants between non-bonded nuclei, their anisotropies
are very small comparing with those between directly bonded
nuclei for the compounds shown in Table 5. However, this is
not always true especially for the F-F couplings, which are the
content of the next paragraph.

128

Table 5. X-X' coupling constants in the methyl derivatives (Hz).

Molecule	X-X'	Isotropic, $(J_{XX'})_{iso}$ Calcd				Exptl.	Anisotropic, $(J_{XX'})_{aniso}$ Calcd.				Exptl.
		Fermi	Spin dipolar	Orbital	Total		Fermi-spin dipolar	Spin dipolar	Orbital	Total	
C_2H_6	$^{13}C-^{13}C$	6.6	0.4	-0.7	6.2	34.6[a]	12.7	0.7	1.5	14.8	---
CH_3F	$^{13}C-^{19}F$	-99.2	9.4	-6.3	-96.0	-161.9[b]	93.5	16.2	4.6	114.2	700 ± 130[b]
CH_3CN	$^{13}C\equiv^{15}N$	1.8	-1.9	-0.2	-0.3	-17.5[c]	-11.0	3.7	-27.7	-35.1	---
	$^{13}C-^{13}C$	15.3	0.3	-0.5	15.2	57.3[d]	16.7	0.1	1.9	18.7	---
	$(^{13}C-^{15}N)$[e]	0.0	-0.2	0.0	-0.2	---	-0.6	-0.2	0.8	0.0	---
CH_3NC	$^{15}N\equiv^{13}C$	10.5	-1.7	-0.3	8.5	±5.8[f]	-10.5	3.4	-25.5	-32.6	---
	$^{13}C-^{15}N$	-2.3	-0.3	0.4	-2.2	-10.7[g]	-9.2	-0.3	-1.0	-10.5	---
	$(^{13}C-^{13}C)$	1.2	0.0	0.1	1.3	---	1.1	0.3	1.1	2.5	---

a) R. M. Lynden-Bell and N. Sheppard, Proc. Roy. Soc. A269, 385 (1962).

b) T. R. Krugh and R. A. Bernheim, J. Am. Chem. Soc. 91, 2385 (1969).

c) W. McFarlane, Mol. Phys. 10, 603 (1966).

Table 5, continued

d) K. Frei and H. J. Bernstein, J. Chem. Phys. 38, 1216 (1963).

e) The nuclei in parenthesis are non-bonding.

f) I. Morishima, T. Yonezawa, and K. Goto, to be published.

g) W. McFarlane, J. Chem. Soc. 1967A, 1660.

h) $J_{13_C 14_N} = - 0.713 J_{13_C 15_N}$

Coupling tensors of the Molecules Including Fluorine Nuclei
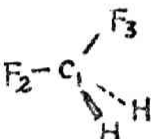
In the previous section, we saw that the coupling anitropies between non-bonded nuclei are very small in magnitude comparing with those between directly bonded nuclei. However, this is not generally true. Experimentally, Snyder and Anderson[8d] pointed out that the anisotropy of the fluorine coupling in hexafluorobenzene might be considerably large. Similar suggestions were also given for symm-tetrafluorobenzene,[8b] for 1,3,5-trifluorobenzene,[8b] for 1,1-difluoroethylene[8f] and for tetrafluoroethylene.[8g]

Thus we calculated here the coupling anisotropy of the several fluorine containing molecules and found that the F-F coupling anisotropy is indeed large inasmuch as they are non-bonding and interestingly that the orbital term is the very important mechanism and in some cases makes decisive contribution. Moreover, the orbital and spin dipolar terms are very important even to the isotropic F-F couplings.

First, let's consider the coupling tensors of CH_3F and CH_2F_2, which are given in Table 6 . The following points are remarkable: 1) For the C-F couplings, the anisotropy becomes large (absolute value) by the fluorine substitution from CH_3F to CH_2F_2 chiefly due to the increase in the orbital contribution. 2) The F-F coupling anisotropy is very large comparing with the H-F coupling anisotropy in CH_3F shown in Table 4 . This is mainly due to the extremely large contribution of the orbital term. 3) Even in the calculations of the isotropic couplings, the spin dipolar and orbital terms can never be omitted in these cases.[23] In fact, the change in the isotropic C-F coupling constants from CH_3F to CH_2F_2 cannot be explained without orbital contributions. Moreover, the experimental positive sign of the F-F coupling constant of CH_2F_2 cannot be understood until both of the spin dipolar and orbital contributions are included.

Next, let's compare the calculated coupling tensors of the various difluoroethylenes shown in Table 6 , from which we notice the followings: 1) For the C-C couplings, the isotropic Fermi contribution becomes very large comparing with that of ethylene given in table 4. This point may be understood from the s-electron donating power of the fluorine atom. The other contributions are essentially the same in magnitude as those in ethylene. 2) For the F-F coupling tensors, the orbital contributions are indeed very large. Note furthermore that the spin dipolar contribution is also important in the geminal F-F coupling in 1,1-difluoroethylene. The importance of these mechanisms is proved by comparing the calculated and experimental isotropic coupling constants. Namely, the sign of the geminal F-F coupling

131

Table 6. Calculated coupling tensors (Hz) of the fluoromethanes and difluoroethylenes[a]

CH$_3$F, C–F[b], Fermi = −99.1

Fermi-spin dipolar:
$$\begin{bmatrix} 62.3 & 0 & 0 \\ 0 & -31.1 & 0 \\ 0 & 0 & -31.1 \end{bmatrix} \quad 0.0\ (93.5)$$

Spin dipolar:
$$\begin{bmatrix} 20.3 & 0 & 0 \\ 0 & 4.1 & 0 \\ 0 & 0 & 4.1 \end{bmatrix} \quad 9.5\ (16.2)$$

Orbital:
$$\begin{bmatrix} -3.2 & 0 & 0 \\ 0 & -7.7 & 0 \\ 0 & 0 & -7.7 \end{bmatrix} \quad -6.2\ (4.6)$$

Total:
$$\begin{bmatrix} -19.8 & 0 & 0 \\ 0 & -133.9 & 0 \\ 0 & 0 & -133.9 \end{bmatrix} \quad -95.8\ (114.2)$$

J_{iso} Exptl. = −161.9[c]

CH$_2$F$_2$, C$_1$–F$_2$, Fermi = −95.3

Fermi-spin dipolar:
$$\begin{bmatrix} 67.1 & 11.8 & 0 \\ 11.8 & -32.2 & 0 \\ 0 & 0 & -34.2 \end{bmatrix} \quad 0.0\ (100.3)$$

Spin dipolar:
$$\begin{bmatrix} 12.5 & -1.1 & 0 \\ 0.4 & 1.1 & 0 \\ 0 & 0 & 2.8 \end{bmatrix} \quad 5.4\ (10.6)$$

Orbital:
$$\begin{bmatrix} -0.4 & -2.6 & 0 \\ -0.7 & -1.4 & 0 \\ 0 & 0 & -39.9 \end{bmatrix} \quad -13.9\ (20.3)$$

Total:
$$\begin{bmatrix} -16.1 & 8.1 & 0 \\ 11.4 & -127.7 & 0 \\ 0 & 0 & -167.4 \end{bmatrix} \quad -103.7\ (131.5)$$

J_{iso} Exptl. = −234.8[d]

(Structure diagram: F$_2$–C with F$_3$ and two H atoms)

F$_2$–F$_3$, Fermi = −103.9

Fermi-spin dipolar:
$$\begin{bmatrix} 32.3 & -0.7 & 0 \\ -0.7 & 32.3 & 0 \\ 0 & 0 & -65.1 \end{bmatrix} \quad 0.0\ (48.7)$$

Spin dipolar:
$$\begin{bmatrix} 53.9 & 3.6 & 0 \\ 18.6 & 46.0 & 0 \\ 0 & 0 & 9.2 \end{bmatrix} \quad 36.4\ (26.3)$$

Orbital:
$$\begin{bmatrix} -24.4 & 11.6 & 0 \\ 7.1 & -31.0 & 0 \\ 0 & 0 & 286.1 \end{bmatrix} \quad 76.9\ (-152.0)$$

Total:
$$\begin{bmatrix} -42.1 & 14.5 & 0 \\ 24.9 & -56.6 & 0 \\ 0 & 0 & 126.4 \end{bmatrix} \quad 9.2\ (-77.0)$$

J_{iso} Exptl. = +(150)[e]

1,1-C₂H₂F₂

C=C 31.8

$$\begin{bmatrix} 10.7 & 0 & 0 \\ 0 & -5.4 & 0 \\ 0 & 0 & -5.4 \end{bmatrix}\; 0.0(15.1) \qquad \begin{bmatrix} 0 & 0 & 0 \\ 0 & 1.0 & 0 \\ 0 & 0 & 2.5 \end{bmatrix}\; 1.2(-1.8) \qquad \begin{bmatrix} 2.0 & 0 & 0 \\ 0 & -10.7 & 0 \\ 0 & 0 & -1.2 \end{bmatrix}\; -3.3(8.0) \qquad \begin{bmatrix} 44.6 & 0 & 0 \\ 0 & 16.7 & 0 \\ 0 & 0 & 27.7 \end{bmatrix}\; 29.7(22.4) \qquad ---$$

C_1–F_3 −59.2

$$\begin{bmatrix} -16.4 & 42.4 & 0 \\ 42.2 & 53.7 & 0 \\ 0 & 0 & -37.3 \end{bmatrix}\; 0.0(-24.6) \qquad \begin{bmatrix} 3.0 & 4.8 & 0 \\ 1.9 & 4.7 & 0 \\ 0 & 0 & -1.3 \end{bmatrix}\; 2.3(1.3) \qquad \begin{bmatrix} -15.1 & 12.2 & 0 \\ 12.4 & -11.8 & 0 \\ 0 & 0 & -25.6 \end{bmatrix}\; -17.4(3.6) \qquad \begin{bmatrix} -87.7 & 59.1 & 0 \\ 56.5 & -12.6 & 0 \\ 0 & 0 & -123.3 \end{bmatrix}\; -74.6(-19.8) \qquad -87.0^{\,d)}$$

F_3–F_4 −34.3

$$\begin{bmatrix} -19.0 & 0 & 0 \\ 78.4 & 0 & 0 \\ 0 & 0 & -59.3 \end{bmatrix}\; 0.0(-28.6) \qquad \begin{bmatrix} 23.4 & -2.0 & 0 \\ 2.0 & 51.0 & 0 \\ 0 & 0 & -3.4 \end{bmatrix}\; 25.7(5.6) \qquad \begin{bmatrix} -79.0 & 0.1 & 0 \\ -0.1 & -36.3 & 0 \\ 0 & 0 & 174.0 \end{bmatrix}\; 19.6(-147.9) \qquad \begin{bmatrix} -92.9 & -2.0 & 0 \\ 2.0 & 68.7 & 0 \\ 0 & 0 & 87.0 \end{bmatrix}\; 20.9(-170.3) \qquad -36.4^{\,f)}$$

trans-C₂H₂F₂

C_1=C_2 35.5

$$\begin{bmatrix} 9.4 & -1.8 & 0 \\ -1.8 & -4.6 & 0 \\ 0 & 0 & -4.8 \end{bmatrix}\; 0.0(14.1) \qquad \begin{bmatrix} 0.9 & 0.7 & 0 \\ -1.5 & 1.0 & 0 \\ 0 & 0 & 2.4 \end{bmatrix}\; 1.1(-1.7) \qquad \begin{bmatrix} -1.5 & 0.1 & 0 \\ -11.7 & 1.0 & 0 \\ 0 & 0 & -1.0 \end{bmatrix}\; -3.9(7.3) \qquad \begin{bmatrix} 45.3 & -3.6 & 0 \\ -3.2 & 20.1 & 0 \\ 0 & 0 & 32.1 \end{bmatrix}\; 32.7(19.7) \qquad ---$$

C_1–F_3 −65.4

$$\begin{bmatrix} -5.4 & 56.6 & 0 \\ 56.6 & 47.0 & 0 \\ 0 & 0 & -41.7 \end{bmatrix}\; 0.0(-3.1) \qquad \begin{bmatrix} 4.2 & 6.2 & 0 \\ 3.8 & 7.5 & 0 \\ 0 & 0 & -1.9 \end{bmatrix}\; -3.3(1.4) \qquad \begin{bmatrix} -11.4 & 0.1 & 0 \\ -1.0 & -10.4 & 0 \\ 0 & 0 & -7.5 \end{bmatrix}\; -9.8(-2.5) \qquad \begin{bmatrix} -78.0 & 62.9 & 0 \\ 59.4 & -21.3 & 0 \\ 0 & 0 & -115.4 \end{bmatrix}\; -71.9(-9.2) \qquad ---$$
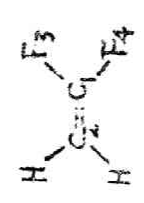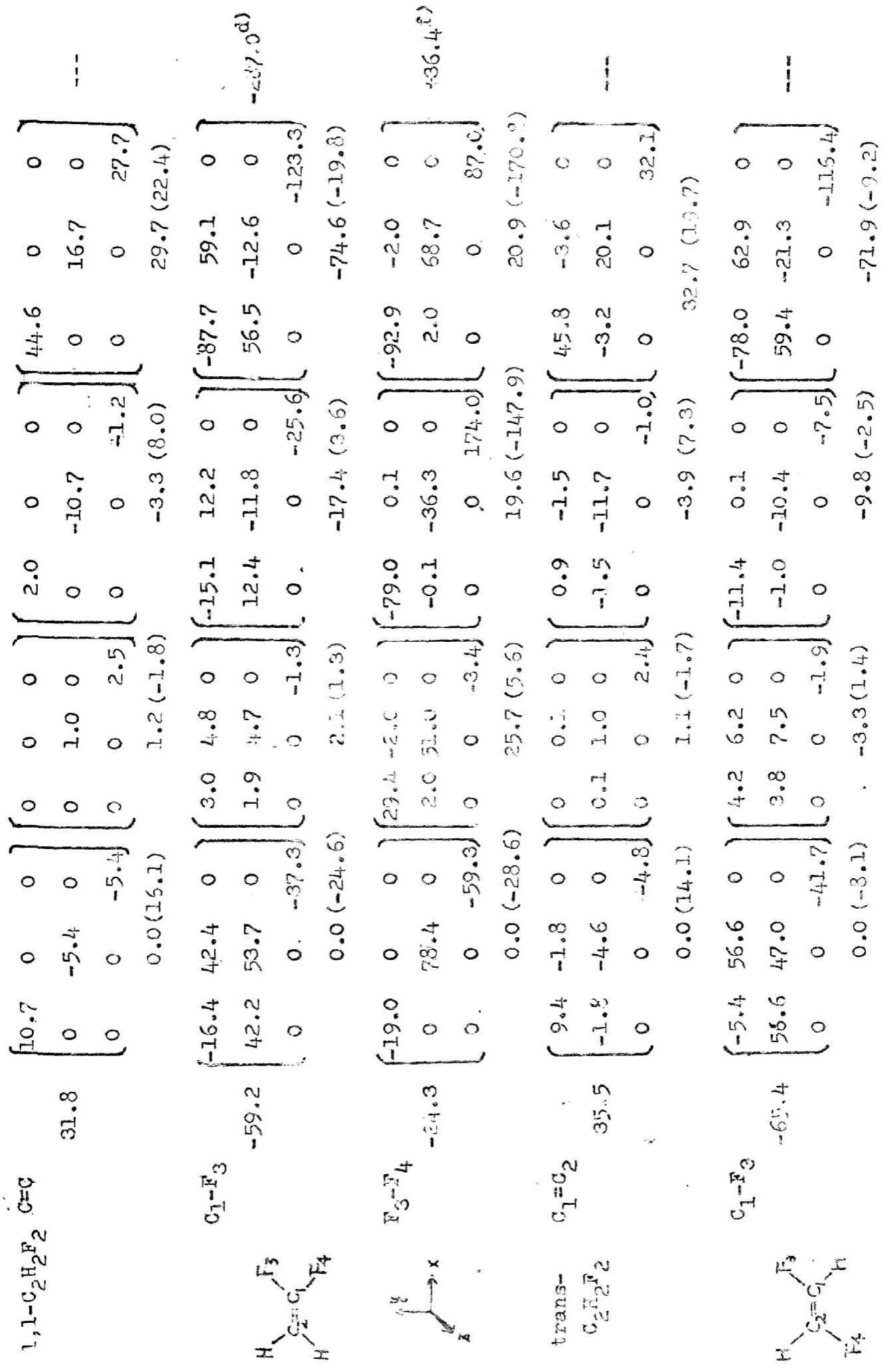
(molecular structure diagrams and y–x–z axis reference shown)

133

F_3-F_4

$$13.4 \quad \begin{bmatrix} 12.1 & 35.5 & 0 \\ 35.5 & 11.8 & 0 \\ 0 & 0 & -23.8 \end{bmatrix} \begin{bmatrix} 9.2 & -3.4 & 0 \\ -0.8 & 7.7 & 0 \\ 0 & 0 & -4.2 \end{bmatrix} \begin{bmatrix} -92.7 & 95.6 & 0 \\ 95.6 & -118.2 & 0 \\ 0 & 0 & -7.7 \end{bmatrix} \begin{bmatrix} -58.1 & 127.8 & 0 \\ 130.3 & -85.3 & 0 \\ 0 & 0 & -22.3 \end{bmatrix} \quad -124.8^{\delta)}$$

0.0 (18.1)   4.2 (7.5)   -72.9 (-29.8)   -55.2 (-4.3)

cis-$C_2H_2F_2$ $C_1=C_2$

$$30.6 \quad \begin{bmatrix} 10.2 & 0 & 0 \\ 0 & -5.0 & 0 \\ 0 & 0 & -5.2 \end{bmatrix} \begin{bmatrix} 0 & -0.1 & 0 \\ 0.1 & 1.0 & 0 \\ 0 & 0 & 2.6 \end{bmatrix} \begin{bmatrix} 1.7 & -2.1 & 0 \\ 2.1 & -10.7 & 0 \\ 0 & 0 & -0.8 \end{bmatrix} \begin{bmatrix} 42.5 & -2.2 & 0 \\ 2.2 & 15.9 & 0 \\ 0 & 0 & 27.2 \end{bmatrix} \quad ---$$

0.0 (15.3)   1.2 (-1.8)   -3.3 (7.5)   28.5 (21.0)

C_1-F_3

$$-70.7 \quad \begin{bmatrix} -5.9 & 48.6 & 0 \\ 48.6 & 41.9 & 0 \\ 0 & 0 & -36.0 \end{bmatrix} \begin{bmatrix} 5.0 & 7.1 & 0 \\ 3.6 & 7.9 & 0 \\ 0 & 0 & -1.8 \end{bmatrix} \begin{bmatrix} -12.6 & 1.0 & 0 \\ 0.6 & -10.9 & 0 \\ 0 & 0 & -7.5 \end{bmatrix} \begin{bmatrix} -84.2 & 56.6 & 0 \\ 52.7 & -31.8 & 0 \\ 0 & 0 & -115.9 \end{bmatrix} \quad ---$$

0.0 (-8.9)   3.7 (2.0)   -10.3 (-3.4)   -77.3 (-10.4)

(structure diagram: F_4, F_3; $C_2=C_1$; H, H)

F_3-F_4

$$49.0 \quad \begin{bmatrix} -27.9 & 0 & 0 \\ 0 & 46.4 & 0 \\ 0 & 0 & -18.5 \end{bmatrix} \begin{bmatrix} -1.0 & -3.7 & 0 \\ 3.7 & -6.5 & 0 \\ 0 & 0 & 11.2 \end{bmatrix} \begin{bmatrix} -54.2 & -42.1 & 0 \\ 42.1 & 11.9 & 0 \\ 0 & 0 & 39.7 \end{bmatrix} \begin{bmatrix} -34.0 & -45.8 & 0 \\ 45.8 & 100.8 & 0 \\ 0 & 0 & 81.4 \end{bmatrix} \quad -18.7^{\delta)}$$

0.0 (-41.9)   1.2 (-3.4)   -2.6 (-80.0)   47.6 (-125.1)
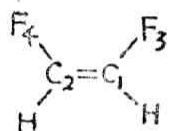
a) The notation of the tensor elements is as follows;

$$J_{AB} = \begin{bmatrix} (J_{AB})_{xx} & (J_{AB})_{xy} & (J_{AB})_{xz} \\ (J_{AB})_{yx} & (J_{AB})_{yy} & (J_{AB})_{yz} \\ (J_{AB})_{zx} & (J_{AB})_{zy} & (J_{AB})_{zz} \end{bmatrix}$$

The value given under each tensor is the contribution to the isotropic coupling constant, and the value given in parentheses is the contribution to the coupling anisotropy defined by

$$J_{xx} - \frac{1}{2}(J_{yy} + J_{zz}).$$

b) The C-C axis is parallel with the x-coordinate axis.

c) P. R. Krugh and R. A. Bernheim, J. Am. Chem. Soc. 91, 2385 (1969).

d) N. Muller and D. T. Carr, J. Phys. Chem. 67, 112 (1963).

e) Assumed from the observed coupling constants of the substituted ethanes: J. W. Emsley, J. Feeney and L. H. Sutcliffe, "High Resolution Nuclear Magnetic Resonance", Pergamon Press, pp886 (1966),

f) G. W. Flynn and J. D. Baldeschwieler, J. Chem. Phys. 38, 226 (1963).

g) G. W. Flynn, M. Matsushima and J. D. Baldeschwieler, J. Chem. Phys. 38, 2295 (1963); Y. Kanazawa, J. D. Baldeschwieler and N. C. Craig, J. Mol. Spect. 16, 325 (1965).

cannot be understood until both of the spin dipolar and orbital contributions are included. This was also seen in CH_2F_2 above. Thus, this point may be generalized to the F-F couplings in $C\!\!<^F_F$ fragment. Likewise, in trans-$C_2H_2F_2$, the orbital term is the dominant mechanism, which gives large negative contribution surpassing the small positive contributions due to the Fermi and spin dipolar mechanisms. In cis-$C_2H_2F_2$, the calculated contributions to the isotropic F-F coupling due to the spin dipolar and orbital terms are very small and almost cancell to each other, resulting the positive coupling constant due chiefly to the Fermi contact term. However, in this case, the calculated sign contradicts to the experimental negative sign. For the F-F coupling anisotropies, orbital term is the most important mechanism, although Fermi-spin dipolar cross term is still important. The spin dipolar term seems less important in this case. Among the isomeric $C_2H_2F_2$, the calculated anisotropy is large for cis- and 1,1-difluoroethylene. That of the trans-$C_2H_2F_2$ is small by cancellation.

Lastly in Table 7 , we summarized the coupling tensors obtained for mono- and di-fluoroacetylene. The following points are remarkable: 1) For the C-C couplings, the isotropic Fermi contribution increases from acetylene (Table 4) to mono- and di-fluoroacetylene. This is due to the s-electron donating power of the fluorine atom. The other contributions are essentially the same in magnitude as those in acetylene. 2) For the directly bonded C-F coupling anisotropies, the Fermi-spin dipolar cross term is the dominant mechanism, while for the non-bonded C-F coupling anisotropies, orbital term is the most important mechanism. 3) For the F-F coupling, the orbital term is the

Table 7 . Calculated coupling tensors^a (Hz) of the mono- and di-fluoroacetylene.

Molecule	Nuclei^b	Fermi	Fermi-spin dipolar		Spin dipolar		Orbital		Total		J_{iso}	J_{aniso}
			xx	yy^c	xx	yy^c	xx	yy^c	xx	yy^c		
C_2HF	C-C	71.4	9.7	-4.8	0.4	5.6	30.3	-5.5	111.7	66.6	81.7	45.1
	C-F	-64.8	127.5	-63.8	9.1	-1.6	-16.1	-12.5	55.8	-142.6	-76.5	198.4
	C-H	153.7	10.7	-5.3	0.0	0.0	0.0	0.0	164.4	148.4	153.7	16.0
	(C-F)	-18.1	6.0	-3.0	-1.2	8.4	50.0	-22.1	36.7	-34.8	-10.9	71.5
C_2F_2	C-C	101.3	8.1	-4.0	0.6	5.5	29.3	-4.0	139.2	98.8	112.3	34.4
	C-F	-69.9	146.8	-73.4	9.6	-1.3	-17.3	-6.6	69.2	-151.2	-77.7	220.3
	(C-F)	-21.2	15.2	-7.6	0.2	7.9	43.6	-11.3	37.8	-32.3	-8.9	70.1
	(F-F)	17.7	-1.3	0.6	-30.6	-4.1	76.6	-173.6	62.5	-159.3	-85.4	221.8

^{a} The molecular axis is parallel with the x-coordinate.

^{b} The nuclei in parenthesis are non-bonding.

^{c} $J_{zz} = J_{yy}$.

dominant mechanism for <u>both</u> isotropic and anisotropic couplings, as was seen in the F-F coupling of trans-$C_2H_2F_2$.

Although too much confidence cannot lay on the details of the numerical values to this level of approximation, it may safely be concluded for the molecules studied here that the anisotropies of the F-F coupling constants are exceptionally large inasmuch as they are non-bonding, and that the orbital term is the most important mechanism, although the Fermi-spin dipolar cross term is still important. Note furthermore that the orbital and spin dipolar terms are very important even to the <u>isotropic</u> F-F couplings, and in some cases, they (especially the orbital term) make the dominant contributions over the Fermi term as exemplified above.[24]

The Implication of the Discrepancy between Theory and Experiment

Now, we return to the ^{13}C-H coupling anisotropy. From the above section, it becomes clear that the experimentally estimated anisotropies of the ^{13}C-H couplings of the methyl derivatives still contain some other more important effects than the electronic one. Then, what are the more important effects? To examine the implication of this problem is the purpose of this section.

First, let's examine how the experimental value of the anisotropy of the indirect coupling constant is determined. It is calculated from the spectral splitting $(\Delta\nu)_{CH}$ obtained

by the NMR measurement in nematic solvent by using the following formula for the C_{3v}-symmetry molecules;[3]

$$(J_{CH})_{aniso} = \left\{ (\Delta\nu)_{CH} - (J_{CH})_{iso} - D_{CH} \right\} / (\tfrac{2}{3} S_{zz}), \qquad (5)$$

where S_{zz} is the orientation parameter of the molecular z-axis with respect to the applied magnetic field (z-axis is parallel with the molecular symmetry axis) and D_{CH} is the anisotropy due to the direct coupling through nuclear-spin dipole-dipole interaction. To obtain S_{zz} for the compounds listed in Table 3 , one assumes that the anisotropies of the indirect couplings between non-bonded protons are zero.[6,7] This is fully justified from the present study and from that of Barfield.[11] Moreover, Krugh and Bernheim[25] examined the effects on the isotropic coupling constant, $(J_{CH})_{iso}$ due to the solvent change and to the solvent phase change from the nematic to the isotropic phases and they reached to the conclusion that these effects should not be major factors influencing their final results. Then, the most important should be the value of D_{CH}, on which the value of the ^{13}C-H coupling anisotropy depends sensitively through Eq. (5).[25,14] To obtain the values of $(J_{CH})_{aniso}$ given in Table 3 , D_{CH} values were calculated from the gas phase molecular geometries determined by the microwave technique. However, since the NMR measurements of these molecules were carried out in their solute states in the nematic solvents, the D_{CH} values in Eq. (5) must correspond to this state and to this method of measurement, and then some corrections to the microwave geometries should be necessary. Now designate this correction as Δ_M (the suffix M means a special molecule M), which is given by,

$\Delta_M = [$NMR geometry in the solute state in nematic solvent$]$

$\quad - [$Microwave geometry in the gas phase$]$ $\qquad$ (6)

Then, the "apparent" substituent effect on $(J_{CH})_{aniso}$ given in Table 3 is now reconsidered as representing the substituent effect essentially on Δ_M. Possible origins of Δ_M are twofold: (a) The effect due to the molecular (harmonic and anharmonic) vibrations.[7d, 8a, 25] In NMR, the measured value is approximately, say, $\ll 1/r^3 \gg$, while in the microwave spectroscopy, it is approximately $\ll 1/r^2 \gg$.[26a] Thus the effect (a) may become important.[26] (r is the internuclear distance and $\ll$ $\gg$ means the statistical average.)[27] (b) The effect due to the change in its molecular geometry (more rigorously the change in the molecular potential function) from its gas state to its solute state in nematic solvent.[7a,7c] In the following we examine the relative importance of each effect above.

First, let's examine the effect (a) above. If we assume that the orientation parameter S_{zz} is independent of the internal molecular vibration,[6] and that the anisotropy of the indirect H-H coupling constant is negligible, then we obtain the following equation for methyl derivatives;[28]

$$(T_{CH})_{zz} = \frac{(\gamma_C \gamma_H \hbar/2\pi)(\langle r^2_{HH}/r^5_{CH} \rangle - 2\langle 1/r^3_{CH} \rangle) + \frac{2}{3}(J_{CH})_{aniso}}{(\gamma^2_H \hbar/2\pi)\langle 1/r^3_{HH} \rangle} (T_{HH})_{zz},$$

(7)

where $(T_{CH})_{zz}$ and $(T_{HH})_{zz}$ are the total anisotropic couplings obtained from the NMR spectra in nematic solvent. r_{CH} and r_{HH} are the distances between two nuclei and $\langle \rangle$ means the vibrational average.[27,6] Since the values of $(J_{CH})_{aniso}$ given in Table 3 are calculated by using the r_0 structure determined by the

140

microwave technique, it is convenient to introduce the notation;[26a]

$$r_n = \langle r^n \rangle^{1/n}.$$

As a special case, r_{-2} is approximately the r_0 structure obtained by the microwave technique.[26a] Ibers and Stevenson[26a] gave the expansion of r_n;

$$r_{\pm n} = r_e \left[1 + \frac{\langle x \rangle}{r_e} - \frac{(1 \mp n)}{2 r_e^2} \langle x^2 \rangle + \cdots \cdots \right], \tag{8}$$

where r_e is the equilibrium distance and x is the displacement coordinate ($x = r - r_e$). From Eq. (12), we obtain

$$r_{-3} = r_{-2} - \frac{1}{2} \langle x^2 \rangle / r_e + \cdots \cdots$$
$$\simeq r_0 (m.w.) - \frac{1}{2} \langle x^2 \rangle / r_e + \cdots \cdots , \tag{9}$$

which shows that, when we use the r_0 structure determined by the microwave technique in Eq. (7), the main correction due to the molecular vibration comes only from the harmonic one, and thus we can eliminate the effect of anharmonicity to first approximation. Note that the value of r_{-3} is always shorter than that of r_{-2}.

For polyatomic molecules the displacement coordinate x_i introduced above is given by a linear combination of the normal coordinates Q_K;[26b]

$$x_i = \sum_K L_{ik} Q_K ,$$

By virtue of the separability of normal coordinates in the harmonic oscillator treatment, the mean-square amplitude, $\langle x_i^2 \rangle$ is given by,[26b]

$$\langle x_i^2 \rangle = \sum_K L_{ik}^2 \langle Q_K^2 \rangle , \tag{10}$$

where the mean-square amplitude of a normal vibration, $\langle Q_k{}^2 \rangle$ is given by[26b]

$$\langle Q_K{}^2 \rangle = \frac{h}{8\pi^2 c\nu_K} \coth \frac{hc\nu_K}{2\kappa T} \qquad (11)$$

$$\longrightarrow \frac{h}{8\pi^2 c\nu_K} \quad (T \longrightarrow 0; \text{ zero-point vibration}).$$

In Eq. (11) ν_k is the wave number given in cm^{-1} unit, T the absolute temperature. The values of L_{ik}, ν_K of the methyl halides were summarized by Overend and his coworkers.[29]

Now let's consider the effect of harmonic C-H stretching and H-C-H bending vibrations separately.[29] By including these correction terms given in Eq. (9) to Eq. (7), we find that the value of the first term (D_{CH} part) in numerator becomes smaller and the value of the denominator becomes larger. (Note that both of these denominator and numerator of Eq. (7) are positive.) Then, both of these corrections make the resultant value of $(J_{CH})_{aniso}$ larger than the uncorrected one.[30] Thus, the effect of harmonic vibration does not interpret the discrepancy between theory and experiment seen in CH_3F and CH_3I. Moreover, this effect cannot explain the substituent effect to $(J_{CH})_{aniso}$ given in Table 3 . In fact, since the value of ν_{HCH} (ν_2) is more sensitive than that of ν_{CH} (ν_1) to the substituent change,[29] we can expect that the most important change induced by the substitution is the change in the correction term to $\langle 1/r_{HH}^3 \rangle$ in the denominator of Eq. (7). From the values of the wave number,[29] this correction term (positive) is larger in CH_3I than in CH_3F, and then the resultant correction (positive) to the value of $(J_{CH})_{aniso}$ is larger in CH_3I than in CH_3F. This is reverse to the substituent effect shown in Table 3 .

The effect of anharmonicity in molecular vibration is not so clear as that of the harmonic vibration, since the experimental anharmonicity constants are not fully known, at present, for these compounds. However, since we can eliminate this effect approximately in the above treatment, and since the values of the "apparent" anisotropies of the ^{13}C-H coupling constants of the methyl derivatibes given in Table 3 are most sensitive to the change in the H-C-H angle,[25,26] the effect of anharmonicity and the substituent effect to it will not be so large as to be able to explain the large change shown in Table 3 . Thus, we believe that the effect (a) cannot interpret the discrepancy between theory and experiment shown in Table 3 . Similar opinion was also reported by Sackmann[7b] in his recent NMR study of the molecular structure of allene in a nematic solvent. He stated that the shortness of the C-C bond relative to the C-H bond in comparison with the electron diffraction value cannot be completely explained on the basis of the molecular vibration.

Next, we enter the examination of the second effect (b) above. It should be noted first that the essentially important chemical and/or physical solvent-solute interactions must exist in the solute state of the methyl derivatives in nematic solvent. This is obvious from the fact that these molecules are oriented on an average with their symmetry axes parallel with the longitudinal axes of the nematic solvent molecules. Namely, the orientation parameter S_{zz} indicate essentially the strength of the solvent-solute interaction. Upon this, we find in Table 3 an approximate parallelism between the values of the "apparent" anisotropy (essentially proportional to Δ_M above) and the values

143

of S_{zz}.[14] At present, the experiments showing this kind of parallellism[31] are so few that we cannot stress too much to this finding. However, if this finding is true more generally, it will give a positive support to the importance of the effect (b). Thus, from the above finding and from the discussions given hitherto, we believe that the effect (b) should be the most natural origin of Δ_M above. There are further supports to the above conclusion: Snyder and Meiboom[32] found the distortion of molecular geometry in a nematic solvent for neopentane and tetramethylsilane, and similar result was also found for teramethyltin.[33] There are some experimental results showing that the molecular geometries change from their gas phases to their molecular crystal phases. For example, the I-As-I valence angle in AsI_3 is $100.2° \pm 0.4°$ (electron diffraction)[34] in its gas phase and is $102.0° \pm 0.1°$ (X-ray)[35] in its crystal phase. Similar differences are also found for $AsBr_3$,[36] $SbCl_3$[37] and SbI_3.[38] The rotational potential curves of haloethanes change from gas state to liquid state,[39] and in biological systems it is well known that the conformation of high polymer changes from solvent to solvent. For methyl derivatives, the most probable change in molecular geometry from gas state to the solute state in nematic solvent may be a change in the H-C-H valence angle,[14] since this change is most sensitive[40] to the value of the "apparent" anisotropy shown in Table 3, and since the energy necessary to this *order of* change will easily be compensated[41] by the van der Waals forces and by the other interaction energies. [7a,7c]

If the above conclusion is correct, the next step will be the fuller examination of the implications of the effect (b)

above. This will lead us to clarify the relationship between the molecular geometry in a solvent and the nature of the solvent-solute interaction.[42-44] This is certainly an interesting field to chemists and physicists.

APPENDIX

Hereafter we abbreviate $2p_{\alpha A}$ AO as α_A ($\alpha = x$, y or z), since only the 2p AO's appear in the following equations.

(i) Spin dipolar term

(a) Level A approximation

$$(K_{AB}^{(2)})_{\alpha\alpha} = -(4\beta^4/25)\langle r^{-3}\rangle_A \langle r^{-3}\rangle_B \sum_i^{occ} \sum_j^{vac} (^3\Delta E_{i\to j})^{-1} \left[4\left(2C_{i\alpha_A}C_{j\alpha_A}\right. \right.$$

$$\left. -\sum_{\delta(\neq\alpha)}' C_{i\delta_A}C_{j\delta_A}\right)\left(2C_{i\alpha_B}C_{j\alpha_B} - \sum_{\delta(\neq\alpha)}' C_{i\delta_B}C_{j\delta_B}\right) +$$

$$\left. +9\sum_{\delta(\neq\alpha)}' \left(C_{i\alpha_A}C_{j\delta_A} + C_{i\delta_A}C_{j\alpha_A}\right)\left(C_{i\delta_B}C_{j\alpha_B} + C_{i\alpha_B}C_{j\delta_B}\right)\right] \quad (A.1-a)$$

$$(K_{AB}^{(2)})_{\alpha\beta} = -(12\beta^2/25)\langle r^{-3}\rangle_A \langle r^{-3}\rangle_B \sum_i^{occ} \sum_j^{vac} (^3\Delta E_{i\to j})^{-1} \left[\left(4C_{i\alpha_A}C_{j\alpha_A}\right.\right.$$
$$(\alpha\neq\beta)$$

$$\left. -2\sum_{\delta(\neq\alpha)}' C_{i\delta_A}C_{j\delta_A}\right)\left(C_{i\alpha_B}C_{j\beta_B} + C_{i\beta_B}C_{j\alpha_B}\right) + \left(C_{i\alpha_A}C_{j\beta_A}\right.$$

$$\left. + C_{i\beta_A}C_{j\alpha_A}\right)\left(4C_{i\beta_B}C_{j\beta_B} - 2\sum_{\delta(\neq\beta)}' C_{i\delta_B}C_{j\delta_B}\right) + 3\left(C_{i\alpha_A}C_{j\delta_A}\right.$$

$$\left.\left. + C_{i\delta_A}C_{j\alpha_A}\right)\left(C_{i\beta_B}C_{j\delta_B} + C_{i\delta_B}C_{j\beta_B}\right)\right] . \quad (A.1-b)$$

(b) Level B approximation

$$(K_{AB}^{(2)})_{\alpha\alpha} = (2\beta^2/25)\langle r^{-3}\rangle_A \langle r^{-3}\rangle_B (^3\Delta E)^{-1}$$

$$\times \left[2\left(4P_{\alpha_A\alpha_B}^2 + P_{\beta_A\beta_B}^2 + P_{\delta_A\delta_B}^2\right) + 9P_{\alpha_A\alpha_B}\left(P_{\beta_A\beta_B} + P_{\delta_A\delta_B}\right) - 2\left(2P_{\alpha_A\beta_B}^2\right.\right.$$

$$\left. + 2P_{\alpha_A\delta_B}^2 + 2P_{\beta_A\alpha_B}^2 + 2P_{\delta_A\alpha_B}^2 - P_{\beta_A\delta_B}^2 - P_{\delta_A\beta_B}^2\right) + 9\left(P_{\alpha_A\beta_B}P_{\beta_A\alpha_B} + P_{\alpha_A\delta_B}P_{\delta_A\alpha_B}\right)\right]$$

$$(A.2-a)$$

$$(K_{AB}^{(2)})_{\alpha\beta} = (6\beta^2/25)\langle r^{-3}\rangle_A \langle r^{-3}\rangle_B (^3\Delta E^{-1})\left[4\left(P_{\alpha_A\alpha_B}P_{\alpha_A\beta_B} + P_{\beta_A\beta_B}P_{\alpha_A\beta_B}\right)\right.$$
$$(\alpha\neq\beta)$$

$$+ 3\left(P_{\alpha_A\beta_B}P_{\delta_A\delta_B} + P_{\alpha_A\delta_B}P_{\delta_A\beta_B}\right) - 2\left(P_{\alpha_A\alpha_B}P_{\beta_A\alpha_B} + P_{\beta_A\beta_B}P_{\beta_A\alpha_B}\right.$$

$$\left.\left. + P_{\alpha_A\delta_B}P_{\beta_A\delta_B} + P_{\delta_A\alpha_B}P_{\delta_A\beta_B}\right)\right] \quad (A.2-b)$$

145

(ii) Orbital term

Under the one-center integral approximation, the contribution coming from $\mathcal{H}_1^{(a)}$ of Eq. (1) of Paper I becomes zero, and then we have only to consider the contribution coming from $\mathcal{H}_1^{(b)}$ of Eq. (2) of Paper I.

(a) Level A approximation

$$(lK_{AB}^{(lb)})_{\alpha\alpha} = l6\beta^2 \langle r^{-3} \rangle_A \langle r^{-3} \rangle_B \sum_{i}^{occ} \sum_{j}^{vac} ('\Delta E_{i \to j})^{-1} (C_{i\gamma_A} C_{j\beta_A} - C_{i\beta_A} C_{j\gamma_A})$$
$$\times (C_{i\beta_B} C_{j\gamma_B} - C_{i\gamma_B} C_{j\beta_B}) \tag{A.3-a}$$

$$(lK_{AB}^{(lb)})_{\alpha\beta} = l6\beta^2 \langle r^{-3} \rangle_A \langle r^{-3} \rangle_B \sum_{i}^{occ} \sum_{j}^{vac} ('\Delta E_{i \to j})^{-1} (C_{i\gamma_A} C_{j\beta_A} - C_{i\beta_A} C_{j\gamma_A})$$
$$\times (C_{i\gamma_B} C_{j\alpha_B} - C_{i\alpha_B} C_{j\gamma_B}) \tag{A.3-b}$$

(b) Level B approximation

$$(lK_{AB}^{(lb)})_{\alpha\alpha} = 8\beta^2 \langle r^{-3} \rangle_A \langle r^{-3} \rangle_B ('\Delta E)^{-1} (P_{\beta_A\beta_B} P_{\gamma_A\gamma_B} - P_{\beta_A\gamma_B} P_{\gamma_A\beta_B}) \tag{A.4-a}$$

$$(lK_{AB}^{(lb)})_{\alpha\beta} = 8\beta^2 \langle r^{-3} \rangle_A \langle r^{-3} \rangle_B ('\Delta E)^{-1} (P_{\beta_A\gamma_B} P_{\gamma_A\alpha_B} - P_{\beta_A\alpha_B} P_{\gamma_A\gamma_B}) \tag{A.4-b}$$

Note that, although the tensor due to the Fermi-spin dipolar cross term is symmetric, those due to the spin dipolar and orbital terms are not necessarily symmetric. For isotropic Fermi contribution, its tensor is diagonal and is given in Eqs. (3.3) and (3.6) of Pople and Santry's paper[16] for the Level A and Level B approximations, respectively.

146

REFERENCES

[1] A. Saupe and G. Englert, Phys. Rev. Letters, 11, 462 (1963).

[2] G. Englert and A. Saupe, Z. Naturforsch. 19a, 172 (1964).

[3] A. D. Buckingham and K. A. McLauchlan, "Progress in nuclear magnetic resonance spectroscopy", ed. J. W. Emsley, J. Feeney and L. H. Sutcliffe, Pergamon Press, New York, Vol. 2 (1967)

[4] G. R. Luckhurst, Quart. Rev. 22, 179 (1968).

[5] A. Saupe, Angew. Chem. internat. Edition 7, 107 (1968)

[6] L. C. Snyder, J. Chem. Phys. 43, 4041 (1965).

[7] a) G. Englert and A. Saupe, Mol. Cryst. 8, 233 (1969).

b) E. Sackmann, J. Chem. Phys. 51, 2984 (1969).

c) A. Saupe, G. Englert, and A. Povh, Advan. Chem. Ser. 63, 51 (1967).

d) A. D. Buckingham, E. E. Burnell, C. A. de Lange, and A. J. Rest, Mol. Phys. 14, 105 (1968).

e) L. C. Snyder and S. Meiboom, J. Chem. Phys. 47, 1480 (1967).

f) D. N. Silverman and B. P. Dailey, J. Chem. Phys. 51, 655 (1969).

g) G. Englert, A. Saupe and J. -P. Weber, Z. Naturforsch. 23a, 152 (1968).

h) G. Englert and A. Saupe, Mol. Cryst. 1, 503 (1966).

i) P. Diehl, C. L. Khetrapal, and U. Lienhard, Canad. J. Chem. 46 2645 (1968).

j) A. D. Buckingham, E. E. Burnell and C. A. de Lange, Mol. Phys. 16, 521 (1969); 17, 205 (1969).

[8] a) T. R. Krugh and R. A. Bernheim, J. Am. Chem. Soc. 91, 2385 (1969).

b) J. Bulthis, J. Gerritsen, C. W. Hilbers, and C. MacLean, Rec. Trav. Chim. 87, 417 (1968).

c) W. Bovée, C. W. Hilbers, and C. MacLean, Mol. Phys. 17, 75 (1969).

d) L. C. Snyder and E. W. Anderson, J. Chem. Phys. 42, 3336 (1965); J. Am. Chem. Soc. 86, 5023 (1964).

e) C. S. Yannoni, J. Chem. Phys. 52, 2005 (1970).

f) A. D. Buckingham, E. E. Burnell and C. A. de Lange, Mol. Phys. 16, 299 (1969).

g) Private communication from Prof. H. Spiesecke.

9) H. Nakatsuji, H. Kato, I. Morishima and T. Yonezawa, Chem. Phys. Letters, 4, 607 (1970), hereafter, called Paper I.

10) H. Nakatsuji, K. Hirao, H. Kato and T. Yonezawa, Chem. Phys. Letters, 6, 541 (1970). Hereafter, called Paper II.

11) M. Barfield, Chem. Phys. Letters 4, 518; 5, 316 (1970).

12) A. D. Buckingham and I. Love, J. Magnetic Resonance, 2, 338 (1970).

13) J. A. Pople, D. L. Beveridge and P. A. Dobosh, J. Chem. Phys. 47, 2026 (1967).

14) I. Morishima, A. Mizuno, H. Nakatsuji and T. Yonezawa, Chem. Phys. Letters, to be published.

15) N. F. Ramsey, Phys. Rev. 91, 303 (1953).

16) J. A. Pople and D. P. Santry, Mol. Phys. 8, 1 (1964).

17) J. A. Pople, J. W. McIver, Jr., and N. S. Ostlund, J. Chem. Phys. 49, 2960, 2965 (1968). See also, G. E. Maciel, J. W. McIver, Jr., N. S. Ostlund and J. A. Pople, J. Am. Chem. Soc. 92, 1, 11 (1970).

18) H. D. Cohen and C. C. J. Ro... ..... an, J. Chem. Phys. 43, 534

(1965); R. E. Watson and A. J. Freeman, Phys. Rev. 131, 250 (1963).

19) P. -O. Löwdin, J. Chem. Phys. 18, 365 (1950).

20) M. Barfield, J. Chem. Phys. 44, 1836 (1966); 49, 2145 (1968).

See also, M. Karplus, Rev. Mod. Phys. 32, 455 (1960).

21) H. M. McConnell, J. Chem. Phys. 24, 460 (1956).

22) P. W. Langhoff, M. Karplus and R. P. Hurst, J. Chem. Phys. 44,

505 (1966).

23) J. N. Murrell, P. E. Stevenson and G. T. Jones, Mol. Phys. 12,

265 (1967).

24) Very recently, the importance of the orbital term in the

isotropic F-F coupling constants has been stressed by Blizzard

and Santry. (A. C. Blizzard and D. P. Santry, Chem. Communi-

cations, 1970, 87.)

25) T. R. Krugh and R. A. Bernheim, J. Chem. Phys. 52, 4942 (1770).

26) a) J. A. Ibers and D. P. Stevenson, J. Chem. Phys. 28, 929

(1958).

b) S. J. Cyvin, Molecular Vibrations and Mean Square Amplitudes

(Elsevier Pub. Co. N. Y., 1968).

27) In the solute state in a nematic solvent, $\langle\!\langle \ \rangle\!\rangle$ means the

statistical average in its state. However, if the molecular

potential function in this state is not so different from

that in the gas state, we can use the vibrational average in

its gas state to $\langle\!\langle 1/r^3 \rangle\!\rangle$ to first approximation. The order of

difference of the potential functions in the gas and liquid

states may be expected from the infra-red spectral data.

(See, for example, G. Herzberg, Molecular Spectra and Molecular

Structure (D. van Nostrand Co. Inc. 1945), Vol. III, pp534.)
See also the discussions given above Eq. (7).

28) The dependence of the "true" value of $(J_{CH})_{aniso}$ on the molecular vibration is negligible.

29) The values of $\nu_1(a_1)$ and $\nu_2(a_1)$ are respectively 2995 and 1493 cm^{-1} for CH_3F, and 3048 and 1279 cm^{-1} for CH_3I. (S. Reichman and J. Overend, J. Chem. Phys. 48, 3095 (1968).) Since the matrix $\{L_{ik}^2\}$ is almost diagonal for the totally symmetric a_1 vibrations, ν_1 and ν_2 represent approximately the C-H stretching and H-C-H angular displacement frequencies, respectively. The values of L_{11}^2 and L_{22}^2 are respectively 1.0167 and 1.9251 for CH_3F. (J. W. Russell, C. D. Needham and J. Overend, J. Chem. Phys. 45, 3383 (1966).)

30) Krugh and Bernheim obtained the same result by considering the harmonicity in the C-H stretching vibration (Ref. 25).

31) Buckingham, Burnell, de Lange and Rest studied the structure of 3,3,3-trifluoropropylene dissolved in the different nematic solvents at various temperatures (Ref. 7d). Their results show the parallelism between S_{zz} and the molecular structures calculated by neglecting the anisotropies of the indirect F-F couplings. Since the anisotropy of the geminal F-F coupling is expected to be large   (see Table 6), the molecular structure determined by them may have some uncertainty. However, the above parallelism will not be changed by this correction.

32) L. C. Snyder and S. Meiboom, J. Chem. Phys. 44, 4057 (1966).

33) K. Hayamizu and O. Yamamoto, Symposium on Nuclear Magnetic Resonance, 8, 88 (1969). (Written in Japanese.)

34) Y. Morino, T. Ukaji and T. Ito, Bull. Chem. Soc. Jap. 39, 71 (1966).

35) J. Trotter, Z. Krist. 121, 81 (1965).

36) a) Gas phase; K. Hedberg, Trans. Am. Cryst. Assocn. 2, 79 (1966).

b) Crystal phase; J. Trotter, Z. Krist. 122, 230 (1966).

37) a) Gas phase; P. Kisliuk, J. Chem. Phys. 22, 86 (1954).

b) Crystal phase; I. Lindqvist and A. Niggli, J. Inorg. Nucl. Chem. 2, 345 (1956).

38) a) Gas phase; S. M. Swingle, quoted by P. W. Allen and L. E. Sutton, Acta Cryst. 3, 46 (1950).

b) Crystal phase; J. Trotter and T. Zobel, Z. Krist. 123, 67 (1966).

39) S. Mizushima, Structure of Molecules and Internal Rotation (Academic Press, New York, 1954).

40) For CH_3F, the increase in the H-C-H angle about 1° is necessary in order to settle the discrepancy between theory and experimental estimation. For CH_3I, it is about 20'. For the molecules for which the values of the $(J_{CH})_{aniso}$ in Table 3 are negative, the decrease in the H-C-H angle is necessary. (Ref. 14).

41) The energy necessary to the above order of change in the H-C-H angle is less than $20 \sim 20$ calories.

42) Saupe, Englert and Povh (Ref. 7a, 7c, 7h) studied the molecular geometry of CH_3CN dissolved in the three nematic solvents and observed slight differences in the H-C-H angle. They interpleted these differences as due to the differences of the protonating abilities of these solvents.

43) In the study of the molecular structure of CH_3CN dissolved in the nematic solvents, Englert and Saupe (Ref. 7a) obtained the C-N bond length considerably shorter than its microwave geometry, and they suggested a possibility that this change might be caused by the solvent-solute interaction such as the interaction of the polar C-N bond with the electric reaction field induced by the nematic solvent molecules.

44) From this standpoint, the change of moledular geometry from gas phase to the molecular crystal phase is very interesting. However, the data which enable us to examine fully the nature of the intermolecular interaction from this point of view are very limied at present. (Private communication from K. Osaki, Professor of Pharmaceutical Science, Kyoto Univ..)

CHAPTER 5

CONCLUSION

The investigation summarized in Part III makes a stage in the growing current of the NMR studies of the molecules dissolved in nematic solvents.

From the studies given in Part III, the impotant mechanisms to the anisotropy of the indirect nuclear spin-spin coupling constant is firstly clarified; Fermi-spin dipolar cross term is found important for every nuclear pairs studied, orbital term is important for the multiply bonded nuclear pairs such as C≡C in acetylene, and for the fluorine-fluorine coupling constants, and spin dipolar term is less important.

From the comparative calculations by the sum-over-state perturbation method and by the finite perturbation method, the superiority of the finite perturbation method is proved in the actual calculations of the isotropic indirect nuclear spin-spin coupling constants. This is a natural consequence of the study given in Part I, Chapter 4.

However, both of these calculations cannot explain the extraordinarily large ^{13}C-H coupling anisotropy of CH_3F as large as 1890 Hz obtained experimentally by Krugh and Bernheim. Then, in Chapter 3, is examined the substituent effect on the anisotropy of the ^{13}C-H couplings in CH_3X series. From this, it is concluded that the experimentally estimated values of the ^{13}C-H coupling anisotropy in CH_3X series are erronious and that these values still contain some other more important effects than the electronic one. The implication of these important effects is analyzed and examined

by using the relevant data available at present, and then it is deduced that the change in the molecular geometry from gas state to the solute state in nematic solvent is the most natural origin for the defferences between theoretical and 'experimental' values.

For the directly bonded C-X couplings (X is C, N or F), their anisotropies are not always negligible. They are in the same order in magnitude as their isotropic couplings. The coupling anisotropies between the non-bonded C-X nuclei seems negligible in magnitude.

For the F-F couplings, their anisotropies are exceptionally large inasmuch as they are non-bonding and the orbital term is a very important source of anisotropy. Furthermore, even to the isotropic F-F couplings, the orbital and spin dipolar terms are very important and sometimes make decisive contributions over Fermi contact term.

GENERAL CONCLUSION

In the studies summarized in this thesis, the author have intended to have some insights on the electronic phenomena in atoms and molecules from theoretical standpoint.

From the studies given in Part I, the interconnections of the orbital theories for open-shell electronic systems; the unrestricted Hartree-Fock theory, the projected unrestricted Hartree-Fock theory and the spin-extended Hartree-Fock theory, are clarified in conjunction with the first-order sum-over-state perturbation method starting from the restricted Hartree-Fock wavefunction. The spin-correlation effects included in these theories are compared by using their first-order spin densities. The accuracy of these wavefunctions in the calculation of the expectation values of the one-electron operators is also investigated for both closed and open-shell electronic systems. These results mean physically that the orbital model in open-shell electronic systems distorts to some extent the real spin-correlation correction, in order to include effectively the correlation correction due essentially to the two-electron correlation phenomena. Since both of the spin-correlation and the two-electron correlation corrections are important in the open-shell electronic systems, it seems necessary for the theories of spin-correlation to include both of these correlation effects explicitly in a reasonable framework, or to exclude reasonably the effect due to the two-electron correlation corrections. This seems to provide a key to the future theoretical study on the spin-correlation phenomena in open-shell electronic systems.

In the course of this study, the author found a simple method to separate the UHF or PUHF spin density into the mechanistic contributions due to spin-polarization (SP) and spin-delocalization (SD) mechanisms. By using this method, more profound understandings than before on the nature of spin density may be obtained because of the physical simplicity and visuality of each mechanism. This is exemplified in actual applications given in Part II, Chapter 3. The author also believes that this general treatment may put an end to the previous confusions seen on this subject.

From the studies given in Part II, a semi-empirical SCF-MO method for valence electron systems developed in the laboratory to which the author belongs is proved to be useful in the studies of the electronic structures of carbonium ions and doublet radicals, and even to the calculation of force constants of ethylene after small modifications in core-repulsion energy. The importance of the explicit inclusions of σ-electrons and of the electron repulsion terms are found for these subject. Furthermore, the theoretical results obtained in Part I are successfully applied in the study of the hfs constants of doublet radicals, and threw a new light on this subject. For example, it is shown that the SP mechanism is important even in the cases where the SD mechanism has been considered dominant. The angular dependence of these mechanisms is also clarified.

From the studies given in Part III, the important mechanisms to the anisotropy of the indirect nuclear spin-spin coupling constant are firstly clarified; Fermi-spin dipolar cross term is found important for every nuclear pairs studied, orbital term is important for the multiply bonded nuclear pairs and for the

fluorine-fluorine couplings, and spin dipolar term is less important. Secondly, from the comparative calculations by the two methods, namely by the sum-over-state perturbation method and by the finite perturbation method, the superiority of the finite perturbation method is proved in the actual calculation of the isotropic indirect coupling constants. This is a natural consequence of the theoretical study given in Part I, Chapter 4. However, both of these calculations cannot explain the extraordinarily large ^{13}C-H coupling anisotropy of CH_3F as large as 1890 Hz obtained experimentally by Krugh and Bernheim. After the detailed examinations of the substituent effects on the anisotropy in CH_3X series and of the geometries used in evaluating the 'experimental' anisotropy, it is suggested that the molecular geometry may differs slightly between in its gas state and in its solute state in nematic solvent. From this study, it is expected that by means of the NMR study of the molecule dissolved in a nematic solvent, one may obtain the molecular geometry corresponding to that state. This is certainly an interesting point in the future study on the nature of the solvent-solute interactions in liquid.